Determinants for mRNP Remodeling at the Cytoplasmic Face of the Nuclear Pore Complex

By

Rebecca Lynn Adams

Dissertation

Submitted to the Faculty of the

Graduate School of Vanderbilt University

in partial fulfillment of the requirements

for the degree of

DOCTOR OF PHILOSOPHY

in

Cell and Developmental Biology

May, 2015

Nashville, Tennessee

Approved:

Susan R. Wente, Ph.D.
Kathleen L. Gould, Ph.D. (Chair)
Katherine L. Friedman, Ph.D.
Ian G. Macara, Ph.D.
Sandra S. Zinkel, Ph.D.

I dedicate this thesis to my two favorite people: my husband, Josh Adams, and my twin sister, Beth Bowman. Beth, you are the reason I am here, I have always looked up to you as an inspiration, and life is better when you are around. Josh, you are my support and my sanity, I am happy every minute I am with you because you make life fun, and I am so proud of you. I have loved experiencing life's journey with you, and I love you both so much.

ACKNOWLEDGEMENTS

This work was possible thanks to funding by the National Institutes of Health, both through a M.E.R.I.T. grant awarded to Susan Wente, Ph.D. (R37 GM051219-19) and through the Program in Developmental Biology (PDB) training grant (T32 HD007502-14) under which I was fortunate to be a trainee.

My time at Vanderbilt has been one of the richest experiences in my life, and I have grown immensely both professionally and personally as a consequence of the fantastic training I have received. Recruitment into the BRET IGP program during my first year was instrumental in helping me learn important concepts required for graduate school. Jim Patton and Roger Chalkley have developed an incredible program, and I will forever be indebted to Michelle Grundy for suggesting that I rotate in the Wente lab. Being a member of the PDB has added tremendously to my scientific critical thinking skills, and I believe it is unequaled in its emphasis on student learning. Chris Wright is foundational in maintaining this atmosphere (and I admire his continual desire to provide "outside the box" learning experiences), and my time working with David Bader during the Bootcamp course was fantastically fun and educational. I have had the pleasure of calling the department of Cell and Developmental Biology (CDB) my graduate school "home". Because it is such a collaborative and supportive department, I have felt comfortable honing my thinking skills during seminars by asking questions, and there are several members of the department whom I have admired as model scientists. I have also benefited from working with Melanie Ohi and her lab for a period on one of my projects. The administrators of the CDB and PDB, particularly Elaine Caine, Kim Kane, Susan Walker, and Carol Johnson have been unsung heroes by providing the support in navigating graduate school smoothly. I look forward to continued relationships with fellow graduate students and post-docs with whom I have developed relationships during my time here.

I truly appreciate the thoughtful, rigorous members of my committee. Because of their guidance, I have become more excited about learning things that used to intimidate me. I am honored to have their signatures on the front of this document.

I was lucky beyond measure to have rotated in Susan Wente's lab. I became immediately aware that Susan's lab would provide an environment where I was surrounded by talented trainees. I am particularly grateful to Andrew Folkmann, whose constant questioning has made me a better thinker; Laura Terry, who generously took me under her wing as she was preparing to move on to her post-doc; Amanda Lloyd, who has been my companion throughout the my entire time at Vanderbilt; and Barbara Natalizio, Kristen Noble, Aditi, Chris Lord, Laura Burns, Li-En Jao, Tim Bolger, Sean Minaker, and Michelle Lazarus who have all been wonderful friends and mentors. Renee Dawson has also been fundamental to my success in the Wente lab; her levelheaded guidance will always be appreciated.

Finally, I can still sometimes not believe that I have been lucky enough to work with Susan Wente. She is an enduring role model in countless ways: as a scientist, mentor, leader, mother, and multi-tasker. I have particularly enjoyed how our relationship has matured, and I don't think I will ever stop learning from her. It has been my greatest honor to be a member of her lab.

TABLE OF CONTENTS

LIST OF TABLES

LIST OF FIGURES

ABBREVIATIONS

Δ	deletion
5-FOA	5-fluororotic acid
ADP	adenosine di-phosphate
AMP	adenosine mono-phosphate
APO	no nucleotide
ATP	adenosine tri-phosphate
CTD	carboxy-terminal domain
CTE	constitutive transport element
EJC	exon junction complex
EM	electron microscopy
ET	electron tomography
FG	phenylalanine glycine
FRET	fluorescence resonance energy transfer
FxFG	phenylalanine any amino acid phenylalanine glycine
GFP	green fluorescent protein
GLFG	glycine leucine phenylalanine glycine
GST	glutathione-S-transferase
h	human
hnRNP	heterogeneous ribonucleoprotein particle
His_6	six histidine epitope tag
IP_6	inositol hexakisphosphate
Kap	karyopherin
kDa, MDa	kiloDalton, megaDalton
LCEA	last common eukaryotic ancestor
lnRNA	long non-coding RNA
MBP	maltose binding protein
miRNA	microRNA
mRNA	messenger RNA
ncRNA	noncoding RNA
NE	nuclear envelope
NES	nuclear export signal
NLS	nuclear localization signal
NPC	nuclear pore complex
NTD	amino-terminal domain
Nup	nucleoporin
$poly(A)^+$	poly-adenylated
RNP	ribonucleoprotein particle
rRNA	ribosomal RNA
snRNA	small nuclear RNA
tRNA	transfer RNA
S.c.	*Saccharomyces cerevisiae*
SR protein	serine arginine rich RNA binding protein

CHAPTER I:

Introduction to mRNA Export

Subcellular compartmentalization in eukaryotic cells has allowed evolution of cellular specialization such that even though humans, for example, are vastly more complex than the single-celled yeast *Saccharomyces cerevisiae*, the same basic principles of life are shared. Indeed, the human genome contains only ~21,000 protein coding genes (ENCODE 2012), only 3.5-fold more than *S. cerevisiae* (GOFFEAU *et al.* 1996). The evolution of the nucleus both allowed separation of the nuclear transcription material from cytoplasmic translation machinery and necessitated specific transport mechanisms to maintain distinct compartments. It is this separation that has permitted the huge amount of transcriptional and post-transcriptional regulation that is essential in complex organisms. Central to this process is coordinated transport between the nuclear and cytoplasmic compartments of the eukaryotic cell. From control of transcription by subcellular localization of transcription factors to directed export of fully mature spliced mRNPs, there are countless interconnected nuclear and cytoplasmic processes that regulate gene expression. It is this complexity that allows the more diverse utilization of the genome needed to generate the distinct repertoire of functional macromolecules within each cell of a multicellular individual. Therefore, regulated nuclear transport and gene expression are intimately connected, essential processes for eukaryotic life.

Essential for regulated nuclear transport is the nuclear pore complex (NPC). This highly conserved complex penetrates the nuclear envelope to allow specific

transport across the double lipid bilayer and is thought to have been present in the last common eukaryotic ancestor (LCEA) (DEGRASSE *et al.* 2009; NEUMANN *et al.* 2010). In *S. cerevisiae* and humans, it is composed of ~30 different proteins (known as nuclear pore proteins, nucleoporins, Nups) which fall into three categories (Figure II.1) (reviewed in ADAMS and WENTE 2013). Pore membrane proteins (Poms) anchor the NPC at the pore membrane, which is where the inner nuclear membrane (INM) and outer nuclear membrane (ONM) fuse; scaffold Nups support the curvature of the pore membrane and provide binding sites for other proteins; and FG Nups are the functional class of NPC proteins which generate the permeability barrier. The NPC permeability barrier allows diffusion of molecules smaller than 5 nm or 40 kDa, but above this size, the rate of diffusion is decreases (reviewed in WENTE and ROUT 2010). In general, for a larger molecule to transport or for any molecule to accumulate against its concentration gradient, it must be ferried across the NPC in an active transport process by soluble molecules known as transport receptors. Thus, regulated transport across the NPC maintains nuclear compartmentalization and is essential for molecules to access distinct compartments in eukaryotic cells.

Part 1: Regulated mRNA nuclear export

The export of transcripts from the nucleus to access cytoplasmic translational machinery is essential for eukaryotic gene expression. This process is mediated by associating binding proteins. Transcripts exist in the cell as messenger ribonucleoprotein particles (mRNPs), and the associating proteins direct the function and fate of the RNP (MULLER-MCNICOLL and NEUGEBAUER 2013). Specifically, associating proteins direct localization of transcripts (e.g. export from the nucleus or specific localization within a cell) and also protect the RNA from degradation. Transcripts undergo dynamic "molecular wardrobe" changes throughout their life cycle as associating proteins are removed, added, or exchanged during different mRNP processing steps (KELLY and CORBETT 2009). For example, a fully mature mRNP must bind a transport receptor to cross the NPC, and the receptor is removed after export.

Most mRNPs are exported by the conserved heterodimer Mex67-Mtr2 (vertebrate TAP-p15; NXF1-NXT1) (SEGREF *et al.* 1997; SANTOS-ROSA *et al.* 1998; KATAHIRA *et al.* 1999; BRAUN *et al.* 2001). The Mex67-Mtr2 dimer associates with proteins of the NPC, thus allowing transport of bound mRNP cargo (SEGREF *et al.* 1997; SANTOS-ROSA *et al.* 1998; KATAHIRA *et al.* 1999; STRASSER *et al.* 2000). Although TAP was first identified by virtue of its direct interaction with the structured constitutive transport element (CTE) RNA of type D simian retroviruses (GRUTER *et al.* 1998), Mex67-Mtr2 and TAP-p15 bind to cellular RNAs through adaptor proteins (reviewed in NATALIZIO and WENTE 2013). Specifically, early experiments suggested that although TAP is the rate-limiting factor for CTE export, there are additional factors required for splicing-dependent mRNA export (GRUTER *et al.* 1998). Furthermore, the current

model is that Mex67-Mtr2/TAP-p15 association with RNA *in vitro* is too weak to sufficiently account for export *in vivo* (SANTOS-ROSA *et al.* 1998; KATAHIRA *et al.* 1999; ZENKLUSEN and STUTZ 2001), and the region of TAP that associates with CTE RNA instead has a conserved interaction with adaptor proteins (BACHI *et al.* 2000; LIKER *et al.* 2000; STUTZ *et al.* 2000; ZENKLUSEN *et al.* 2002). Importantly, only fully processed transcripts are exported as Mex67 association is limited to spliced mRNA (TUCK and TOLLERVEY 2013; BAEJEN *et al.* 2014), and adaptor proteins ensure appropriate Mex67-Mtr2/TAP-p15 recruitment.

Journey to the pore: coordinated mRNP processing for efficient export

The multiple processing steps that a transcript undergoes are not discrete events but rather coordinated, often concurrent and synergistic processes such that an mRNA quickly becomes export-competent upon transcription. As an example, mRNAs are co-transcriptionally capped and spliced, and nascent transcripts are quickly polyadenylated after 3' cleavage. Factors involved in these processes are recruited to transcripts by association with the CTD of the large subunit of RNA Polymerase (PolII CTD) (MCCRACKEN *et al.* 1997). The PolII CTD is composed of highly conserved repeats of the heptad sequence YSPTSPS, each residue of which can be post-translationally modified. Importantly phosphorylation of serine residues 2, 5 or 7 is correlated with stages of transcription (initiation, elongation, termination), and the current model is that the PolII phosphorylation status serves as a code for recruitment of processing factors involved at each of these steps (EGLOFF *et al.* 2012; BAEJEN *et al.* 2014). In addition to coordination of transcription and RNA processing, these processes are also coupled to

mRNA export. This coordination is mediated through complexes that function in these processes and also recruit Mex67-Mtr2, and some of these complexes also promote physical proximity of gene loci to NPCs. Furthermore, quality control mechanisms are linked to each step in the RNA lifecycle (reviewed in PARKER 2012). Thus, transcription and RNA processing are highly coordinated to ensure efficient maturation and export.

Transcription- and processing-coupled Mex67-Mtr2/TAP-p15 adaptors

The conserved THO complex is also recruited to transcripts by association with the PolII CTD (Figure I.1A) (MEINEL *et al.* 2013). In *S.c.*, the THO complex contains 5 subunits (Tho2, Hpr1, Tex1, Mft1, and Thp2) and is a general regulator of transcription elongation (CHAVEZ and AGUILERA 1997; CHAVEZ *et al.* 2000; STRASSER *et al.* 2002; MASON and STRUHL 2005), particularly through GC-rich sequences (GOMEZ-GONZALEZ *et al.* 2011). Importantly, the THO complex in *S.c.* and mammals has been linked to mRNA export (STRASSER *et al.* 2002; MASUDA *et al.* 2005), and work from several labs has provided a model for the linear recruitment of Mex67-Mtr2 to transcripts via the THO complex (Figure I.1). Specifically, Hpr1 recruits two other conserved proteins, Sub2 (UAP56) and Yra1 (Aly/REF) to form the TREX (transcription-coupled export) complex (STRASSER *et al.* 2002; ZENKLUSEN *et al.* 2002), with Yra1 serving an essential conserved role as an adaptor for Mex67-Mtr2/TAP-p15 (STRASSER and HURT 2000; STUTZ *et al.* 2000; ZENKLUSEN *et al.* 2001). Therefore, the THO complex functions to coordinate transcription and mRNA export.

Yra1 also functions with the poly-A binding protein Nab2 in recruitment of Mex67-Mtr2 (Figure I.1) (IGLESIAS *et al.* 2010). Nab2 is required for proper transcript

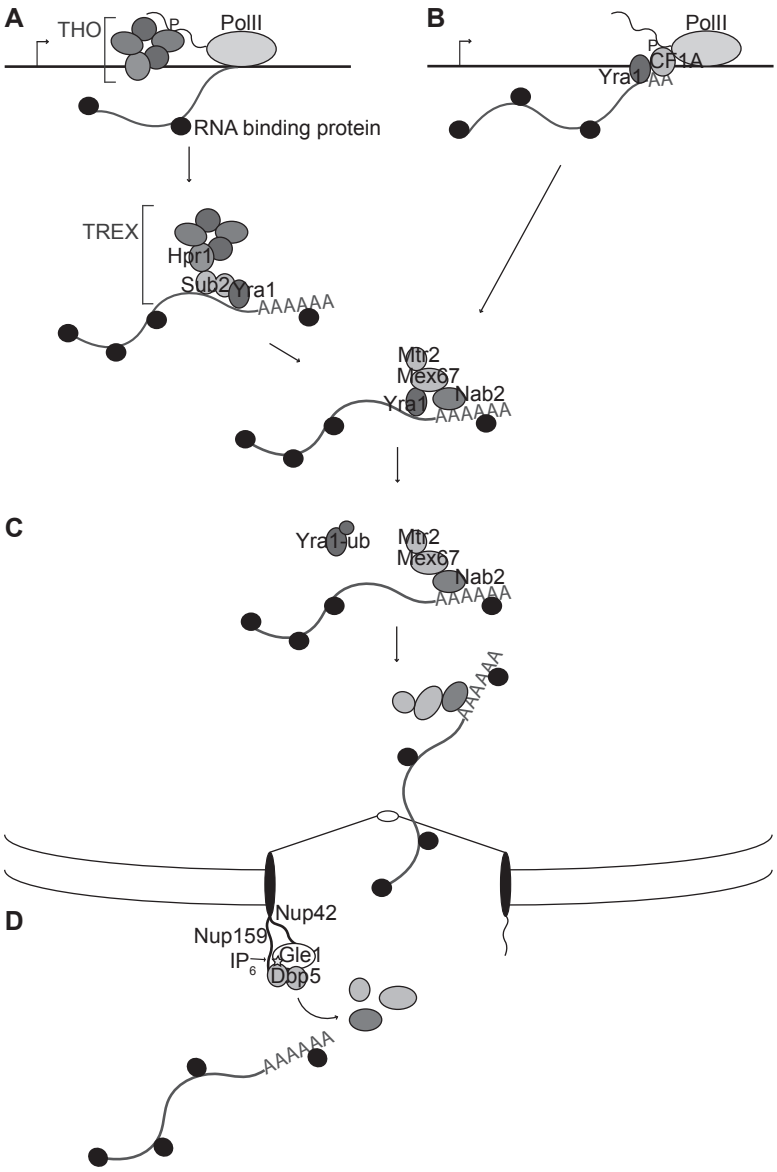

Figure I.1. Model for Mex67-Mtr2 recruitment via Yra1 and mRNP remodeling. (A) THO/TREX recruitment of Mex67-Mtr2. Hpr1 of the THO complex recruits Sub2 to transcripts (ZENKLUSEN *et al.* 2002). Sub2 is a member of the DEAD-box group of RNA-dependent ATPases (STRASSER and HURT 2001) and it is therefore likely that Sub2-mediated RNA rearrangements are required for association of Yra1 or other proteins with the transcript. The Yra1 binding sites for Sub2 and Mex67 overlap suggesting that Mex67-Mtr2 association with Yra1 releases Sub2 (STRASSER and HURT 2001). Yra1 interaction with Nab2 enhances Mex67 recruitment (IGLESIAS *et al.* 2010). (B) Alternate method of Yra1 recruitment. Yra1 directly associates with the mRNA cleavage and polyadenylation complex CF1A, and this association is sufficient for Yra1 recruitment to transcripts (JOHNSON *et al.* 2009). (C) Yra1 is ubiquitylated by Tom1 for release before mRNA export (IGLESIAS *et al.* 2010). (D) At the cytoplasmic face of the NPC, Dbp5, in conjunction with Gle1 and IP_6 remodel the mRNP for Nab2 and Mex67-Mtr2 release and subsequent recycling (LUND and GUTHRIE 2005; TRAN *et al.* 2007).

polyadenylation as mutants of *NAB2* result in hyperadenylated transcripts (HECTOR *et al.* 2002). Thus, a model is that Nab2 detects properly adenylated transcripts for export. Importantly, Nab2 is the only Mex67-Mtr2 adaptor that has been demonstrated to transport through NPCs for removal at the cytoplasmic face (Figure I.1D) (TRAN *et al.* 2007; see Part 3). In contrast, Yra1 is removed through ubiquitination prior to export (Figure I.1C). Thus, the function of the TREX complex as a Mex67 adaptor may be through recruitment of Nab2 to mRNPs. However, these proteins (Tho2, Hpr1, Sub2, Yra1, Nab2, Mex67) have distinct global binding patterns to mRNA (BAEJEN *et al.* 2014), which indicates Nab2 and/or Mex67 are recruited by other factors.

Directly linking transcription and mRNA export is the conserved TREX-2 complex, composed of Thp1, Sac3, Sus1, and Cdc31 in *S.c.* (GONZALEZ-AGUILERA *et al.* 2008; JANI *et al.* 2012). Sus1 is also shared with the SAGA histone acetylase complex, and is thought to recruit TREX-2 to active gene loci via interaction with PolII (RODRIGUEZ-NAVARRO *et al.* 2004; PASCUAL-GARCIA *et al.* 2008). Furthermore, Sac3 directly interacts with Mex67, and may serve to recruit Mex67-Mtr2 to transcripts (FISCHER *et al.* 2002). Finally, TREX-2 is localized at NPCs via an interaction with Nup1, which is localized at the nuclear face of the NPC (FISCHER *et al.* 2002), and is suggested to serve as a physical bridge between transcripts/gene loci to NPCs for efficient export.

Another group of proteins, the SR RNA binding proteins, play conserved roles linking transcription, splicing, export, and translation. In *S.c.*, the SR protein Npl3 binds to the PolII CTD and stimulates transcription by inhibiting mRNA cleavage (DERMODY *et al.* 2008). Furthermore, Npl3 functions in recruitment of splicing factors (KRESS *et al.*

2008). This is similar to mammalian SR proteins, which function in regulation of alternative splicing (LONG and CACERES 2009; SHEPARD and HERTEL 2009). Additionally, Npl3 and mammalian SR proteins serve as Mex67-Mtr2/TAP-p15 adaptors (LEE *et al.* 1996; HUANG *et al.* 2003; GILBERT and GUTHRIE 2004). After nuclear export, Npl3 continues to associate with mRNPs where it functions in translation. Specifically, Npl3 functions in recruitment of 60S subunit to 43S-mRNA complex (BAIERLEIN *et al.* 2013), but has also been implicated in repression of translation (WINDGASSEN *et al.* 2004). Npl3 release from transcripts and subsequent nuclear import is mediated through phosphorylation by Sky1 (GILBERT *et al.* 2001; GILBERT and GUTHRIE 2004). Thus, SR proteins couple nuclear and cytoplasmic mRNA functions.

Early biochemical studies revealed the link between mRNA splicing and export. In particular, after injection into *Xenopus* nuclei, transcripts that are spliced are exported more quickly than unspliced counterparts (LUO and REED 1999). This has been attributed to the deposition of exon junction complexes (EJCs) just upstream of splicing locations. EJCs enhance export by recruitment of REF (the Yra1 homolog) and TAP-p15 (KIM *et al.* 2001; LE HIR *et al.* 2001). Also in mammals, the THO complex is recruited to spliced transcripts rather than being co-transcriptionally loaded as in *S.c.* (MASUDA *et al.* 2005). Whether such a bias toward export of spliced transcripts exists in *S.c.* has not been determined; only a small percentage of transcripts are spliced in *S.c.* (~5%). However, quality control mechanisms exist in *S.c.* to ensure unspliced transcripts are not exported (GALY *et al.* 2004). Therefore, splicing serves as an essential prerequisite for export of transcripts originally containing introns.

The discovery of multiple Mex67-Mtr2/TAP-p15 adaptors leads to the question of whether a single transcript uses multiple adaptors concurrently and how many are required for export of a single mRNP. RNPs are packaged such that the long RNA thread is compacted by binding proteins (reviewed in MULLER-MCNICOLL and NEUGEBAUER 2013). Many RNA binding proteins associate to generate higher order RNP structure; an RNA "nucleosome" like structure has even been proposed to direct splicing in mammals by the hnRNPC tetramer (KONIG *et al.* 2010), and similar compaction has been proposed to be mediated through EJCs and SR proteins (SINGH *et al.* 2012). Structural examination of export competent RNPs in *S.c.* (isolated by Nab2-TAP) by negative stain EM revealed a globular proteinaceous ribbon-like structure 5-7nm wide x 20-30nm long, with particle length correlating with transcript length (Figure I.5B) (BATISSE *et al.* 2009). Potentially, multiple Mex67-Mtr2/TAP-p15 adaptors are required to coat the length of the particle for efficient export through the NPC. Ribosome subunits, which are also large RNP particles, concurrently use multiple transport receptors which bind at defined regions of the subunit, suggesting that multiple factors are required to guide the large RNP cargo through the NPC (KOHLER and HURT 2007, see Appendix B). Furthermore, meta-analysis of mRNA binding sites has demonstrated that mRNP adaptors bind different regions along RNAs, with preference toward the 5' or 3' end of the ORF, but Mex67 associates homogenously throughout the ORF (TUCK and TOLLERVEY 2013; BAEJEN *et al.* 2014). This result indicates that Mex67-Mtr2/TAP-p15 may be associated with transcripts at multiple points along the transcript via different adaptors. However, these adaptors have preferences for binding shorter or longer transcripts, and there was a very limited correlation between transcripts that

bound Yra1, Nab2, or Npl3 (BAEJEN *et al.* 2014). Unlike ribosomal subunits, which assemble into a canonical structure, thousands of distinct RNPs must assemble into structures to allow transport, and transport receptor binding must accommodate the distinct configurations of these particles. The existence of multiple transport receptor binding sites thus implies that the mechanism for Mex67-Mtr2 removal after transport through the NPC must be permissive for the multiple possible configurations of its association. Finally, study of one or more distinct RNP particles rather than a genome-wide analysis should provide insight into general mechanisms used for mRNA export.

Other mRNA export mechanisms

It should be noted that although Mex67/TAP is essential for export of most mRNA, some transcripts are exported by alternative mechanisms. A major alternative RNA transport receptor is the protein export receptor Crm1. As with Mex67-Mtr2/TAP-p15, Crm1 requires adaptors to associate with cellular transcripts (reviewed in NATALIZIO and WENTE 2013). These adaptor proteins are usually RNA binding proteins that also contain a nuclear export signal (NES), directly recognized by Crm1. Additionally, ribosomal subunit RNPs (reviewed in ZEMP and KUTAY 2007) and the signal recognition particle RNP (CIUFO and BROWN 2000) are exported by Crm1. Other small functional RNAs such as miRNAs and tRNAs are directly recognized by their specific export receptors once they have been properly cleaved and matured (COOK *et al.* 2009; OKADA *et al.* 2009). In general for mRNA, specialized adaptors are recruited by cis regulatory elements of the RNA, of which several have been identified (reviewed in NATALIZIO and WENTE 2013). For example, in mammalian cells, one class of RNAs contain a 50-

nucleotide eIF4E-sensitivity element that interacts with a protein (LRPPRC) that mediates recruitment of eIF4E for Crm1-mediated export (CULJKOVIC *et al.* 2006; TOPISIROVIC *et al.* 2009). Additionally, AU-rich RNAs are bound by HuR, which interacts with NES-containing proteins pp32 and APRIL for export by Crm1 (BRENNAN *et al.* 2000). An NPC-independent mRNP export route has also been identified. Specifically, Wnt signaling in neurons promotes export of transcripts encoding synaptic proteins through nuclear egress, or membrane budding from the INM, through the NE lumen to the ONM (SPEESE *et al.* 2012), an export mechanism that completely bypasses the NPC and has been shown to be used by herpes virus capsids (METTENLEITER *et al.* 2013).

The use of multiple transport receptors may influence how cells regulate RNA function, affecting development and disease progression. For instance, as stated above, the recruitment of Mex67-Mtr2/TAP-p15 is limited to mature transcripts. However, direct binding of TAP to the structured constitutive transport element (CTE) of simian type D viral RNA permits export of unspliced messages (GRUTER *et al.* 1998). Additionaly, Crm1-mediated export of eIF4E-bound transcripts is linked to cancer progression (SIDDIQUI and BORDEN 2012). During *C. elegans* neuronal development, usage of different transport receptors for a single transcript affects downstream processes. Specifically, the sex-determining *tra-2* transcript is normally exported by Crm1 though binding of the adaptor TRE. Altering this process so that *tra-2* is exported by TAP results in increased translation of the transcript and aberrant feminization of the germline (KUERSTEN *et al.* 2004). Therefore, distinct export pathways have profound impacts on cellular RNA metabolism and cell fate.

From gene loci to NPCs

Once transcribed at the location of the gene, mRNPs must travel through the nucleus to reach the nuclear periphery and NPCs for transport. Data from single-molecule live-cell experiments suggest that the packaging of transcripts into particles aids in diffusion through the nucleus. Specifically, diffusion of large transcripts (14kb) is only ~4-fold slower than smaller messages (1.7kb) (MOR *et al.* 2010). The compaction of chromatin also impacts transcript export (MOR *et al.* 2010). Most transcripts sample a limited volume of the nucleus and instead travel through chromatin-free channels. Altering nuclear structure by exposing cells to a hyperosmolar medium to increase DNA compaction caused messages to sample a larger volume of the nucleus before export. Finally, one of the rate-limiting steps of the transport process is finding the "right" NPC to transport through. Transcripts can sample several different NPCs before a successful transport event occurs (GRUNWALD and SINGER 2010; KAMINSKI *et al.* 2013), but the causes for this phenomenon are unclear. Therefore, exit from the nucleus is an important factor in the rate of gene expression.

One mechanism for limiting the time between transcription and export from the nucleus may be the relative location between the gene and NPCs. Indeed, in *S.c.*, genes that are highly expressed have increased association with nuclear pore proteins (CASOLARI *et al.* 2004), and several inducible gene loci have been demonstrated to re-localize from the nuclear interior to the nuclear periphery at NPCs upon induction and may remain associated for several hours (reviewed in SOOD and BRICKNER 2014). Importantly, this re-localization is dependent on transcription factors (CABAL *et al.* 2006; LUTHRA *et al.* 2007; BRICKNER *et al.* 2012), NPC proteins (LIGHT *et al.* 2010), and

transcripts themselves (CASOLARI *et al.* 2005). Specifically, the SAGA and TREX-2 complexes are essential for gene re-localization and for maintenance of that localization after induction (CABAL *et al.* 2006; LUTHRA *et al.* 2007). Thus, the functional connection between transcription and export described above can also be a physical connection. Association of a gene locus with the NPC has been proposed to enhance gene expression (TADDEI *et al.* 2006), limit diffusion of the gene locus (CABAL *et al.* 2006), provide an epigenetic transcriptional memory so that cells can respond more quickly to a stimulus (BRICKNER *et al.* 2007; TAN-WONG *et al.* 2009), and promote association with post-translational modifiers that are also localized to NPCs (TEXARI *et al.* 2013). Finally, the interaction between activated genes and nuclear pore proteins is conserved in higher organisms, where Nups that have dynamic association with the NPC have been demonstrated to associate with active chromatin within the nucleus (CAPELSON *et al.* 2010; KALVERDA *et al.* 2010; LIANG *et al.* 2013; LIGHT *et al.* 2013). Therefore, the overall architecture of the nucleus and proximity of genes to NPCs and/or asymmetric cytoplasmic elements may serve as a "gene gating" mechanism for epigenetic control of expression (BLOBEL 1985).

QC of RNA: coordinated processes to inhibit decay

Because it is an essential intermediary in the process of gene expression, mRNA is subject to a variety of quality control steps. RNA is a very labile species in the cell: 5' to 3' exonucleases and the exosome, which is a complex that contains 3' to 5' exonuclease and endonuclease activity, are abundant and available to target any RNA (reviewed in PARKER 2012). In addition to helping fulfill functionality of RNAs, binding

proteins also protect transcripts from the degradation machinery. For example, binding to the polyA binding protein PABP dramatically increases stability of poly-adenylated transcripts (BERNSTEIN *et al.* 1989). *In vivo*, RNA processing and RNA turnover are competitive pathways a transcript takes: a delay in processing leads to decay rather than buildup at a particular biogenesis step. Indeed, deletion of the gene encoding the nuclear subunit of the RNA exosome, *RRP6*, enhances the growth defects of several RNA processing and export mutants, most likely due to buildup of mis-processed transcripts (ZENKLUSEN *et al.* 2002; SCARCELLI *et al.* 2008; KALLEHAUGE *et al.* 2012).

Furthermore, RNA processing is highly integrated where feedback mechanisms exist to inhibit earlier processes when a downstream process is perturbed. For example, inhibiting RNA export using a variety of mutants results in accumulation of transcripts at the site of transcription and a global down regulation in gene expression (JENSEN *et al.* 2001; LIBRI *et al.* 2002). Interestingly, this feedback is also partially mediated by the nuclear exosome, as transcripts are released from their site of transcription in *rrp6Δ* mutants (HILLEREN *et al.* 2001). Therefore, the coupling of steps in mRNA biogenesis not only serves to increase the efficiency of gene expression, it is essential to prevent inappropriate degradation of messages.

Feedback along the steps of RNA maturation may be partly attributable to auto regulation of RNA processing factors themselves. For example, Yra1 levels are controlled through its non-canonical splice site, which causes inefficient splicing and subsequent degradation (PREKER *et al.* 2002; RODRIGUEZ-NAVARRO *et al.* 2002; PREKER and GUTHRIE 2006). Proper control of Yra1 protein levels is essential as overexpression of an unspliced transcript is detrimental to viability. Due to the conserved role of the

THO complex in splicing (ABRUZZI *et al.* 2004; MASUDA *et al.* 2005), self-regulation of the associated Yra1 protein serves as an important barometer and central regulation point for control of gene expression. Furthermore, Nab2 (ROTH *et al.* 2005) and Npl3 (LUND *et al.* 2008) have been reported to also auto-regulate their own expression, though by a different mechanism.

The cell also contains important quality control checkpoints both in and outside of the nucleus to ensure only properly processed transcripts are translated. At the nuclear face of the NPC, a structure termed the nuclear basket contains proteins, Mlp1 and Mlp2 (vertebrate Tpr), that prevent the export of unspliced transcripts (GALY *et al.* 2004). In the cytoplasm, incorrectly spliced transcripts, transcripts with premature stop codons codons, transcripts without stop codons, and transcripts with stem loops or poly-lysine or arginine-coding tracts that slow translation are detected by a variety of mechanisms associated with the pioneer round of translation (reviewed in DOMA and PARKER 2007). Therefore, quality control steps exist throughout the RNA lifecycle.

Importantly, the coupled processing steps and quality control mechanisms not only ensure proper RNA fidelity, they also are essential for proper genome maintenance. Mutations in or depletion of many transcription and export factors, including THO (WELLINGER *et al.* 2006; DOMINGUEZ-SANCHEZ *et al.* 2011; GOMEZ-GONZALEZ *et al.* 2011), TREX-2 (GONZALEZ-AGUILERA *et al.* 2008; SANTOS-PEREIRA *et al.* 2014a), Npl3 (SANTOS-PEREIRA *et al.* 2014b), Sub2, Yra1, and Mex67 (JIMENO *et al.* 2002), and Nups (PALANCADE *et al.* 2007) lead to DNA hyper-recombination and increased sensitivity to DNA damage inducing drugs in *S.c.* and mammalian cells. These defects are associated with increased presence of R-loops (RNA-DNA hybrids)

which arise as a result of gene transcription. Thus DNA damage may accumulate from altered RNA maturation and increased susceptibility to mutation or improper targeting of DNA damage response factors to transcription sites (reviewed in AGUILERA and GAILLARD 2014). Therefore, efficient RNA processing due to coupling of maturation and export steps is required to prevent this transcription-mediated DNA damage.

Part 2: mRNA export through the NPC

In general, nuclear mRNA export is the final step before a transcript has access to the cytoplasmic translational machinery. Therefore, it serves an important point of regulation in the gene expression pathway. Under some conditions, export of mRNA is globally altered to aid in quickly changing a cell's proteome. For example, most mRNA is retained in the nucleus after heat shock or treatment with high ethanol concentrations in *S.c.*, allowing specific export of heat shock-induced transcripts (SAAVEDRA *et al.* 1996). This process is correlated with a change in the localization of Nab2, Yra1 and Mlp1, suggesting that altered association with mRNA adaptors and export factors mediates nuclear retention (CARMODY *et al.* 2010). mRNA export can also be regulated at specific points during development of multicellular organisms. In sea urchin eggs, maternal histone transcripts are specifically retained in the nucleus until after nuclear envelope breakdown during cell division after fertilization (SHOWMAN *et al.* 1982; DELEON *et al.* 1983). Additionally, viruses hijack the cellular export machinery to inhibit endogenous mRNA export (BELTZ and FLINT 1979, reviewed in YARBROUGH *et al.* 2014). Therefore, mRNA export is an essential, regulatable step during gene expression.

General properties of NPC transport

The NPC is a very busy place. It has been estimated that the biogenesis of ribosomes required for HeLa cell doubling every 24 hours requires the import of 100 ribosomal proteins and export of 3 ribosomal subunits for each of the ~2600 NPCs per minute (GORLICH and MATTAJ 1996). In *S.c.*, which divide roughly every 100 minutes and contain only ~150 NPCs, it has been suggested that 1000 ribosomal proteins and

24 assembeled subunits must transport every minute per NPC (WARNER 1999). Kinetic analysis of nuclear accumulation of the transport receptor Ntf2 in permeabilized cells revealed that each NPC can transport up to 2500 molecules per second (RIBBECK and GORLICH 2001), although this likely represents an upper limit of NPC transport capacity since permeabolizing the cells removes competing factors, concentrations of cargo were at saturation, and larger molecules transported more slowly. A more representative estimation of *in vivo* cargo transport comes from cytoplasmic microinjection of Ran, which requires Ntf2 for import, because the experiment is done in the context of intact cell (SMITH *et al.* 2002). In this experiment, it was estimated that 120 Ran molecules can transport per NPC per second when injected at half-saturating concentrations. NPC transport is so efficient that it is not the rate-limiting step of protein import. Instead, the interaction between a cargo and its transport receptor is limited by diffusion and non-specific interactions in the cytoplasm and represents the limiting step of import (TIMNEY *et al.* 2006). During mRNA export, interactions at the nuclear and cytoplasmic face of the NPC, but not the transport step itself are rate-limiting (GRUNWALD and SINGER 2010). Thus, movement through the NPC is very fast, and the coupling of mRNA biogenesis to recruitment of transport receptors bypasses the rate-liming step for protein transport.

In addition to the large capacity of NPCs for transport, they are highly selective for a wide range of cargo sizes. For similarly sized molecules smaller than the diffusion limit, transport receptors are imported 120x faster than a non-specific protein in permeabilized cells (Ntf2 vs GFP) (RIBBECK and GORLICH 2001). In addition to inhibiting import of small proteins, the NPC allows the transport of extremely large cargo. This

includes import of virus capsids (reviewed in COHEN *et al.* 2011) and partially assembled proteasomes (reviewed in ENENKEL 2014), and export of large mRNP complexes such as ribosomal subunits (reviewed in ZEMP and KUTAY 2007) and the Balbiani ring mRNP in *C. tentans* salivary glands (reviewed in DANEHOLT 2001). Indeed, gold particles coated with an NLS-containing protein or importins were permitted to import with a functional radius up to 39nm (26nm gold + additional volume contributed by the conjugated protein) when injected into the cytoplasm of *Xenopus laevis* oocytes (PANTE and KANN 2002). Thus, the nature of NPC transport is flexible enough to specifically accommodate a variety of transporting cargo.

It is possible that association of specific NPC proteins alters NPC functionality and that specialized NPCs allow specific transport. It is well-established that cell-specific expression of transport receptors, particularly importin-α isoforms, alters cargo selection (reviewed in SANGEL *et al.* 2014), but differences in NPC composition have only recently been identified. Targeted mass spectroscopic analysis of NPC proteins from different tissues revealed although core NPC components are similarly expressed, several peripheral proteins (gp210, Tpr, Nup50, Pom121, Nup214, Aladin) have varying expression (ORI *et al.* 2013). Tissue-specific expression has been validated for several Nups (GUAN *et al.* 2000; OLSSON *et al.* 2004; CHO *et al.* 2009), with distinct requirements for some during differentiation (LUPU *et al.* 2008; D'ANGELO *et al.* 2012; BUCHWALTER *et al.* 2014). It is also likely that different NPCs within a single cell have differing capacity for transport. For example, in *S.c.*, the Mlp proteins involved in mRNA export are located at NPCs that are not adjacent to the nucleolus, suggesting the possibility for usage of distinct NPCs for mRNA or ribosome export (GALY *et al.* 2004). The fact that a

transcript samples several NPCs before export further suggests differing capacities for transport among NPCs within a cell (GRUNWALD and SINGER 2010). Despite this potential for specialization, immuno-EM experiments have demonstrated that a single NPC is capable of bi-directional transport of different cargo (FELDHERR *et al.* 1984).

FG Nups are the molecular workhorses of the NPC

A class of Nups, the FG Nups, is responsible for generating the selective permeability barrier of the NPC. In *S.c.*, 11 of the 30 Nups are FG Nups, which are thus named because they contain domains enriched in phenylalanine-glycine (FG) repeats (Figure I.2). These FG repeats are separated by stretches of 10-20 charged and polar residues, which make FG domains highly hydrophilic (reviewed in TERRY and WENTE 2009). Because of these properties, FG domains do not adopt a secondary structure, but are rather intrinsically disordered (DENNING *et al.* 2002; DENNING *et al.* 2003). In addition to FG domains, FG Nups contain structured regions that anchor the protein at a particular location in the NPC, either with bias toward the nuclear or cytoplasmic face or an equal distribution on both sides of the pore (reviewed in TERRY and WENTE 2009). Some FG Nups contain additional structured regions that perform specialized functions. Because of the flexible nature of FG domains, they location within the pore is dynamic within the pore such that though an FG Nup is anchored at one location in the NPC, the distal end of the FG domain can be located at the other side (PAULILLO *et al.* 2005). Immuno-EM experiments have suggested that FG domain topology is altered based on transport status, suggesting that the dynamic nature of these domains is important in

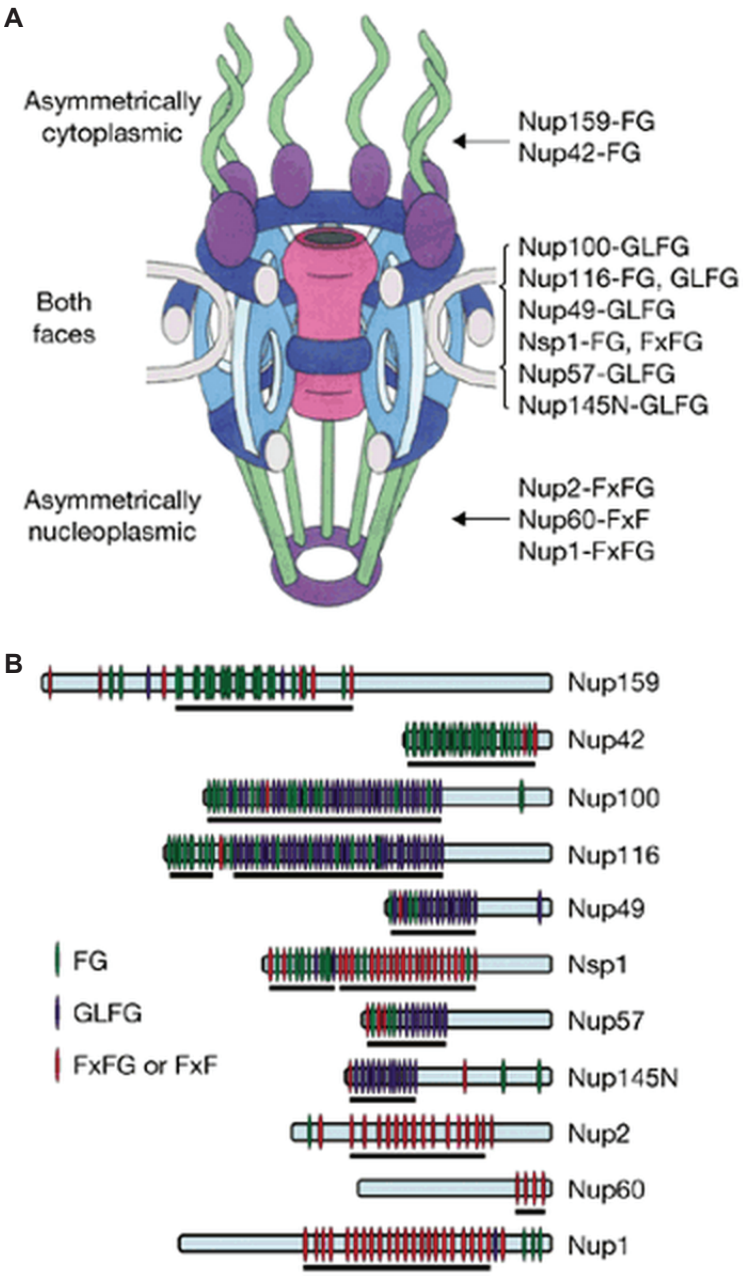

Figure I.2. *S.c.* FG domain type and distribution.
(A) Anchor site of FG domains as determined in (ROUT *et al.* 2000). Reprinted from (STRAWN *et al.* 2004). (B) FG repeat distribution in *S.c.* Nups. Each FG repeat is colorized based on type and displayed with reference to primary sequence of each Nup. Reprinted from (STRAWN *et al.* 2004).

the transport process (PAULILLO *et al.* 2005). Therefore, our current understanding of NPC structure is that of a core scaffold ring composed of structural Nups that anchor FG Nups such that their FG domains extend into the center of the NPC to inhibit non-specific transport (Figure II.1).

In vitro studies have demonstrated that individual FG domains are sufficient for generating a size-dependent permeability barrier that can be overcome by transport receptors (FREY and GORLICH 2007; JOVANOVIC-TALISMAN *et al.* 2009). Furthermore, several studies have demonstrated that FG domains are necessary for barrier function and active transport. Among the first studies performed demonstrated that active transport can be disrupted by treatment with WGA, a lectin that binds O-glycosylated FG domains in mammals, or antibodies that react with FG domains (DAVIS and BLOBEL 1987; FINLAY *et al.* 1987; HOLT *et al.* 1987; DABAUVALLE *et al.* 1988; FEATHERSTONE *et al.* 1988). Additionally, the FG domain of Nup98 is required for maintenance of the permeability barrier in a cell-extract system (HULSMANN *et al.* 2012). *In vivo* deletion of the FG domain of the Nup98 homologs in *S.c.*, Nup116, Nup145, and Nup100, results in "leaky" pores (LORD *et al.* 2015), and deletion of additional FG domains disrupts active transport processes (STRAWN *et al.* 2004; TERRY and WENTE 2007). Thus, FG domains constitute the functional players of the NPC for selective transport.

Transport receptors and directionality

Soluble factors termed transport receptors are required for molecules to traverse the NPC. Transport receptors allow macromolecule passage by interacting with cargo as well as FG domains (reviewed in WENTE and ROUT 2010). Protein and small RNA

molecules use a class of transport receptors termed karyopherins (Kaps), also called importins/exportins. These proteins share a common C- or S-shaped superhelical structure that arises from alpha solenoid HEAT repeats (Figure I.3B, reviewed in CONTI *et al.* 2006). The outer convex surface of Kaps contains FG domain binding sites, and the inner concave surface binds to cargo and/or the small GTPase Ran (Figure I.3C). Through its nucleotide bound state, Ran is the mediator of directional Kap transport (reviewed in GORLICH and KUTAY 1999). The Ran guanine nucleotide exchange factor (GEF, Prp20 in *S.c.*) is nuclear localized and the Ran GTPase activating protein (GAP, Rna1 in *S.c.*) is cytoplasmic, resulting in an asymmetric distribution of Ran-GTP in the nucleus and Ran-GDP in the cytoplasm. For transport into the nucleus, an importin binds cargo directly or indirectly (using importin-α) via a nuclear localization signal (NLS), ferries it through the NPC transport tunnel, and interacts with Ran-GTP, causing allosteric cargo release (Figure I.3A, reviewed in CONTI *et al.* 2006; XU *et al.* 2010). Conversely, exportins transport nuclear exit signal (NES)-containing cargo as a trimeric complex, bound to both cargo and Ran-GTP. Upon reaching the cytoplasm, Rna1 induces Ran GTPase activity, and Ran-GDP and cargo are released from the exportin. An unrelated transport receptor, Ntf2, then re-imports Ran (MOORE and BLOBEL 1994; RIBBECK *et al.* 1998; SMITH *et al.* 1998). Thus, for Kap mediated transport, the energy dependence is due to a requirement for GTP in the process.

The soluble proteins involved in mRNA export and directionality are distinct from Kap-mediated export. The general mRNA export receptor dimer, Mex67-Mtr1/TAP-p15 is structurally and evolutionarily unrelated to Kaps. Instead, the domains involved in NPC transport are related to the Ran importer, Ntf2

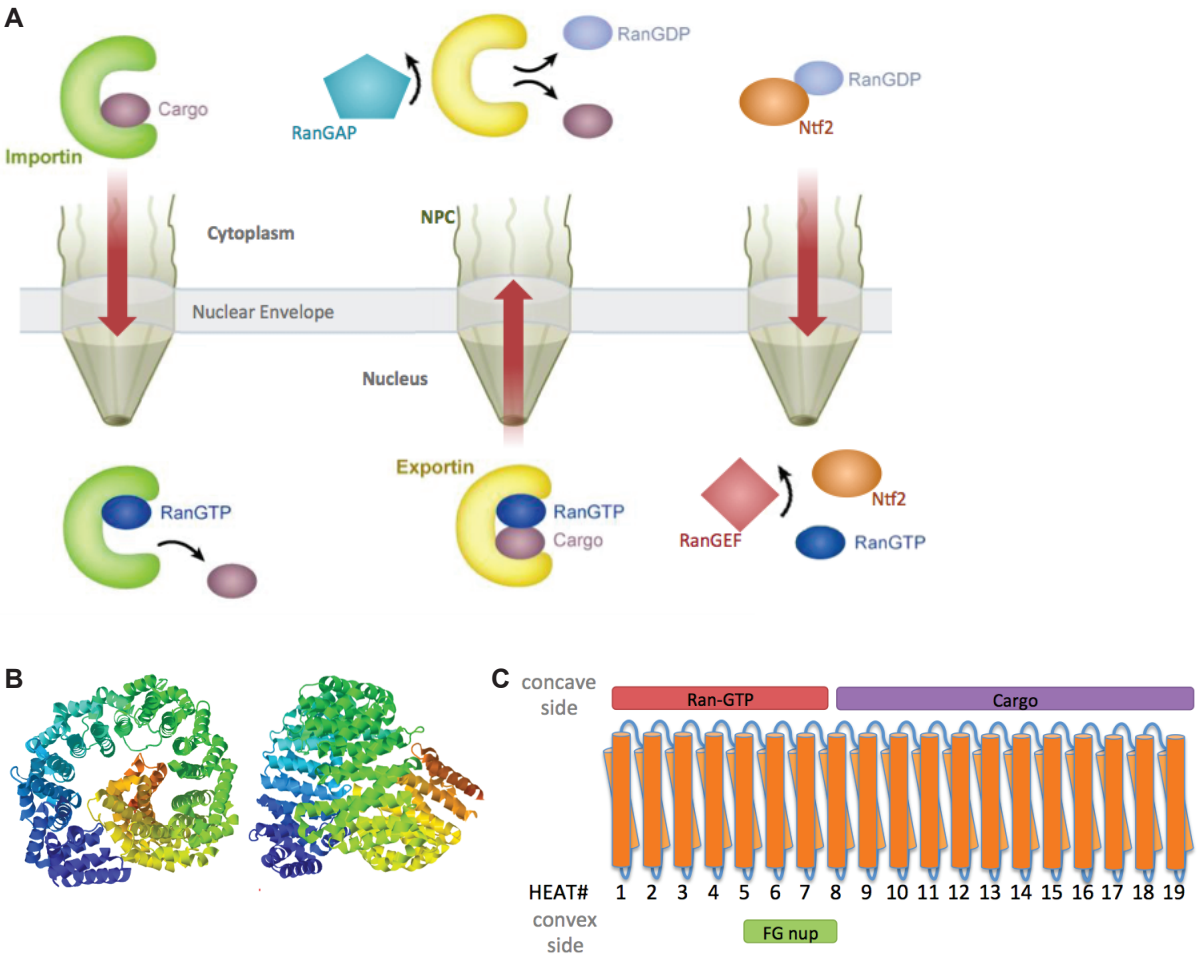

Figure I.3. Protein transport across the NPC.
(A) Protein transport mediated by Kaps as detailed in text. Figure adapted from CONTI *et al.* 2006). (B) Super-helical structure of *S.c.* Kap95 (importin-β). Amino-terminus, blue; carboxy-terminus, red. Adapted from (PDB3ND2 FORWOOD *et al*. 2010). (C) HEAT-repeat organization of Kap95, displaying binding sites as described in (CONTI *et al.* 2006).

(FRIBOURG *et al.* 2001; FRIBOURG and CONTI 2003). However, Mex67 and Mtr2 do not interact with Ran; rather, they are released from the mRNP at the cytoplasmic face of the NPC by the conserved RNA-dependent ATPase Dbp5 (Figure I.1; see Part 3) and subsequently recycle back into the nucleus for additional rounds of mRNA export (reviewed in FOLKMANN *et al.* 2011). Other RNA species also use Mex67-Mtr2 for export. The telomerase RNA species, *TLC1*, exports from the nucleus before association with telomerase protein subunits for re-import and nuclear function. It has recently been reported that *TLC1* export requires Mex67 and Dbp5 (WU *et al.* 2014). Additionally, both the large and small ribosome subunits have been reported to depend on Mex67-Mtr2 for export (YAO *et al.* 2007; FAZA *et al.* 2012). Interestingly, ribosome subunits and *TLC1* also have a requirement for the major protein export receptor Crm1 during export (WU *et al.* 2014, reviewed in PANSE and JOHNSON 2010), and this dual requirement likely serves to integrate mRNA and Kap-mediated export.

Aspects of transport

Despite the presence of different classes of transport receptors, they share common features for NPC transport. First, transport receptors contain multiple FG binding sites. For mRNA export, Mex67 and Mtr2 each contain an FG binding site, and the requirement for this dimer can be bypassed by engineering two FG binding sites on Mex67 alone (STRASSER *et al.* 2000). The importin for classic NLS-containing cargo, importin-β, contains at least four FG binding sites along its surface (BAYLISS *et al.* 2000; BEDNENKO *et al.* 2003). Finally, Ntf2, the Ran importer, is a homodimer that provides two identical FG binding sites (BAYLISS *et al.* 2002a). It is thought that these multiple

binding sites are required so that the transport receptor can “walk” along FG domains within the transport channel via sequential interaction with phenylalanine residues. Single molecule experiments have demonstrated that transport receptor movement through the NPC is not directional. Instead, protein and mRNA cargo move through the NPC in Brownian motion (YANG *et al.* 2004; KUBITSCHECK *et al.* 2005; LOWE *et al.* 2010; MOR *et al.* 2010; PARK *et al.* 2014) with removal of the transport receptor from the cargo defining transport directionality.

Second, the interaction between transport receptors and FG domains is relatively weak. The FG binding interface on transport receptors consists of a small surface-accessible hydrophobic pocket which interacts with phenylalanine residues of FG repeats (BAYLISS *et al.* 2000; BAYLISS *et al.* 2002b; GRANT *et al.* 2003; LIU and STEWART 2005). Measured dissociation constants range between K_D ~1uM-100nM (BEN-EFRAIM and GERACE 2001; PYHTILA and REXACH 2003), but the fact that transport receptors contain multiple FG binding sites, and FG domains consist of numerous FG repeats makes it difficult to accurately measure the affinity of these interactions. It has been suggested that the measured affinity is too high to account for the fast transport rates and that transport receptor-FG binding is modulated *in vivo* by non-specific competition from other cytosolic proteins and solutes (TETENBAUM-NOVATT *et al.* 2012). It is likely that *in vitro* and *in vivo*, the multivalent FG interactions result in a high avidity between these proteins (reviewed in TERRY and WENTE 2009), but individual interactions are highly transient. Furthermore, the conformational flexibility of FG domains likely contributes to a high off-rate for transport receptors (FORMAN-KAY and MITTAG 2013). Importantly, low affinity, transient interactions are necessary for the large amount of

transport across the NPC, as stronger interactions and decreased off-rates would likely clog the NPC (RIBBECK and GORLICH 2001). Indeed, mutants of *NTF2* that result in higher Ntf2 affinity for FG domains create a dominant negative effect on multiple transport pathways (LANE *et al.* 2000; QUIMBY *et al.* 2001). Therefore, the current model is that transport receptors transport via sequential weak interactions with FG repeats during movement across the NPC.

Models of NPC transport

Despite the understanding of the functional proteins involved in the transport process, a consensus for the mechanism of selective transport has not been agreed upon. Specifically, the nature of the permeability barrier and how transport receptors overcome it remains hotly debated. Several models have been proposed, each with its own level of experimental evidence to support it.

The Gorlich lab proposed the selective phase model over 10 years ago (Figure I.4A) (RIBBECK and GORLICH 2001). This model proposes that phenylalanine residues of FG domains interact with transport receptors, and they also have inter- and intra-domain hydrophobic interactions. These F-F interactions cause FG domains to generate a gel-like phase that forms a physical barrier for non-specific transport. Transport receptors overcome this barrier by interacting with phenylalanine residues, thus outcompeting the F-F interactions and either melting the gel or dissolving into the phase is they move through. The first pieces of evidence that led to this proposal were that the permeability barrier is formed by hydrophobic interactions

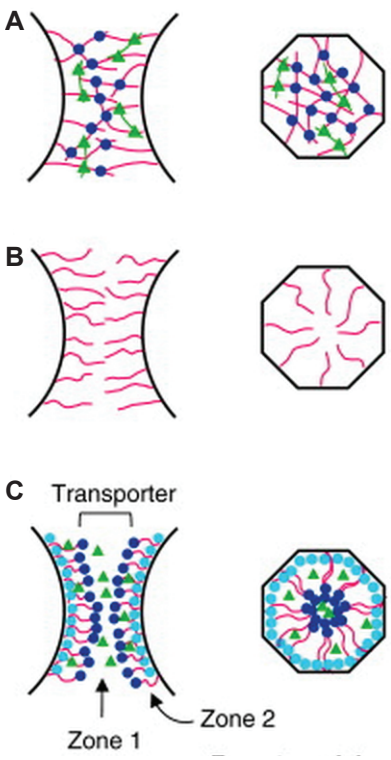

Figure I.4. Models of NPC transport.
(A) Selective Phase model. (B) Entropic Barrier model. (C) Forrest Model. Models elaborated in text. Figure adapted from (WALDE and KEHLENBACH 2010).

(RIBBECK and GORLICH 2002). Treatment of permeabilized cells with 1,2-hexanediol reversibly disrupts the barrier and allows non-specific import. The Gorlich lab also had the surprising finding that recombinant *S.c.* Nsp1 FG domain can form a gel-like substance when dialyzed from denaturing to non-denaturing conditions (FREY *et al.* 2006; FREY and GORLICH 2007). Interestingly, this gel is much more permeable to transport receptors than non-specific molecules. Finally, altering phenylalanine residues within this domain to tyrosine disrupted Kap interaction by *in vitro* pull-down experiments but still formed a gel and restored the function of the FG domain *in vivo*, suggesting that hydrophobic interactions between FG domains are sufficient for barrier function (FREY *et al.* 2006). Subsequent analysis using a cell extract system to generate NEs with NPCs found that depletion of the Nup98 FG domain alone disrupted the permeability barrier, suggesting that a single domain is necessary for barrier formation (HULSMANN *et al.* 2012). However, several FG domains have been shown to be capable of forming a selective gel, with glycosylation of FG domains fine-tuning the barrier (FREY and GORLICH 2009; LABOKHA *et al.* 2013).

The interactions between unstructured proteins to generate a separate phase has been observed with other proteins that have similar biophysical properties (TORETSKY and WRIGHT 2014). Specifically, diverse kinds of RNP granules (processing bodies, stress granules, P-granules, germ granules) are enriched for proteins that contain intrinsically disordered or low complexity regions (TORETSKY and WRIGHT 2014). For example, the low complexity region of FUS, an RNA-binding protein found in RNA granules, can form a hydrogel *in vitro* that interacts specifically with other proteins that contain low complexity domains found in RNA granules (KATO *et al.* 2012). These

phase separations formed by such proteins have been termed assemblages, and they are thought to provide a way to separate functions in a cell without the requirement for membrane bound organelles. Thus, it is possible that the NPC transport channel is a distinct phase that molecules must traverse to access different cellular compartments.

The entropic barrier model was suggested by the Rout lab when proteomic analysis of NPC components did not uncover conventional molecular motors or ATPases found in simpler membrane channels like the sodium potassium pump. This model proposes that the FG domains extend from the NPC as filaments, and rapid Brownian movement of these filaments forms an energetic barrier (Figure I.4B) (ROUT *et al.* 2000; ROUT *et al.* 2003). The attractive forces between transport receptors and FG domains exceeds the repulsive forces of these mobile FG domains, and rather than dissolving through a physical barrier as suggested by the selective phase model, transport receptors bypass the FG "virtual gate". Although there is little direct evidence for this model, it remains a popular possibility for the transport mechanism due to the flexible nature of FG domains.

Although the selective phase and entropic barrier models are seemingly opposite in how FG domains generate a barrier (inter-domain interaction or not), a third model has proposed a combination of the two. The Forest model was proposed by the Rexach lab after uncovering differing biophysical properties between FG domains (Figure I.4C) (YAMADA *et al.* 2010). The bead halo assay, in which a soluble fluorophore-tagged molecule is tested for accumulation around a bead conjugated with another molecule, was developed to qualitatively assess the weak interactions between transport proteins (PATEL *et al.* 2007; PATEL and REXACH 2008). This assay uncovered

differences in the ability of FG domains to interact with each other, classifying centrally anchored FG domains as cohesive and peripheral FG domains as non-cohesive (PATEL *et al.* 2007). Importantly, deletion of central or peripheral FG domains caused an increased permeability defect when cells were treated with 1,6-hexanediol, suggesting that both cohesive and non-cohesive FG domains contribute to the permeability barrier (PATEL *et al.* 2007). Expanding on the model, the Rexach lab uncovered distinct levels of compaction of individual FG domains due to intra-domain interaction, identifying FG regions as extended coils or collapsed coils (trees or shrubs) (PATEL *et al.* 2007). For some FG domains, collapsed coils exist at the proximal end of extended coils and fill the center of the NPC, leading to the presence of peripheral channels along the side of the NPC (Zone 2) where the majority of active transport occurs. Passively-transporting molecules pass through the middle of the NPC channel (Zone 1). Immuno-EM and real-time studies have demonstrated that transporting molecules are enriched at the periphery of the NPC, supporting this aspect of the Forest model (FISEROVA *et al.* 2010; MA *et al.* 2012; MA *et al.* 2013a).

The above models predict that transport receptors move across the NPC channel by Brownian motion in a 3D environment, and visualization of single protein and mRNA transport events support this mechanism (GRUNWALD and SINGER 2010; LOWE *et al.* 2010). However, two models propose alternate methods of movement through the pore. The polymer brush or highway model, an expansion of the entropic barrier model, suggests that the multiple interaction sites between transport receptors and FG domains causes the extended FG domains to collapse upon interaction with a transport receptor (SCHOCH *et al.* 2012). Evidence for this model has come from atomic force microscopy

where a probe detects the repulsive height of a molecular brush containing FG domains conjugated to a surface at one terminus. Addition of transport receptors results in a decreased FG brush height, though the mass of the brush has been increased (LIM *et al.* 2007). Expanding on this model, it has been suggested that FG domain collapse allows the FG domain to pull the transporting molecule into the NPC pore. Finally, this model further proposes that a population of transport receptors stably associate with the NPC, and these transport receptors are required for maintenance of the permeability barrier (SCHOCH *et al.* 2012). Transport-dependent changes in the topology of the Nup153 FG domain support dynamic conformations of FG domains that are regulated by the presence of transport receptors (PAULILLO *et al.* 2005; LIM *et al.* 2007). The reduction of dimensionality model proposes that FG repeats interact at the periphery of the NPC channel to generate a hydrophobic surface, and spacer sequences between FG repeats extend into the pore lumen (PETERS 2009). Transport receptors then slide along the FG repeats in a two-dimensional walk, and this reduction in dimensionality (from 3D movement to 2D movement) explains the bias of transport receptors to cross the NPC. This model also suggests the possibility that transport receptors cycle within an individual NPC, picking up and releasing cargo at the nuclear or cytoplasmic face. Imaging movement of Kap-coated beads on an FG domain brush has uncovered 2D diffusion, demonstrating that FG domains can limit the range of diffusion of soluble molecules (SCHLEICHER *et al.* 2014), but whether movement is constricted in the context of an intact NPC is known. Thus, there have been proposed a range of possibilities for how specific NPC transport occurs. Higher temporal and spatial resolution of transport events is likely to help resolve these disputes.

Although informative of the biochemical and biophysical properties of FG domains, there are several aspects of *in vivo* NPC transport that *in vitro* studies do not take into account. First, the NPC is full of dynamically associating transport receptors and cargo. Considering the models, can a gel form under these complex conditions, or are FG domains collapsed in the presence of these molecules? The selective phase model proposes that the FG gel can self heal after a transport receptor passes through, and the presence of transport receptors increases the stringency of transport (FREY and GORLICH 2009), but these experiments were done outside the context of a cell. Thus, the abundance of empty and cargo-containing transport receptors is likely to influence how a molecule navigates within an NPC.

Second, these models should consider the differing levels of association that FG Nups have with the NPC. Some of the peripheral Nups are only transiently associated with the NPC, having residence times of seconds (RABUT *et al.* 2004). In fact, Npap60/Nup50, an FG Nup that is located at the NPC basket at steady state, has been suggested to accompany importin-β-importin-α-NLS cargo into the NPC (LINDSAY *et al.* 2002) in addition to its role in protein export (GUAN *et al.* 2000). Other FG Nups associate for very long periods of time, having an NPC association of hours (RABUT *et al.* 2004), and scaffold Nups are among the longest-lived proteins in cells and are thought to remain associated with NPCs once assembeled (SAVAS *et al.* 2012; TOYAMA *et al.* 2013). Thus, even some Nups are dynamic components of the NPC.

Third, it is very likely that FG domains serve specialized functions during transport. Only the Forest model has considered distinct properties of FG domains that arise from sequence differences (YAMADA *et al.* 2010). When FG domains were

originally identified in *S.c.*, they were classified into three different types based on the repeats present in its domain: FG domains with phenylalanine-glycine repeats, GLFG repeats with glycine-leucine-phenylalanine-glycine repeats, and FxFG with phenylalanine-any-phenylalanine-glycine repeats (ROUT and WENTE 1994). Additionally, each of these types of FG repeats have distinct residues enriched in the spacer sequences. Interestingly, the different types of FG repeat domains are vectorally distributed in the *S.c.* NPC, with FxFG domains at the nuclear face, GLFG and FxFG domains anchored on both faces, and FG domains at the cytoplasmic face. These different residues (type of FG repeat or spacer sequences) likely contribute to specific functions, either pertaining to formation of the barrier or specific transport. Indeed, GLFG domains are cohesive with other GLFG domains, whereas others aren't (PATEL *et al.* 2007), leading to the suggestion that these repeats are important for forming the permeability barrier, as has been shown for the Nup98 GLFG domain (HULSMANN *et al.* 2012). FG domains have also been shown to have variable affinity for transport receptors (ALLEN *et al.* 2001; BEN-EFRAIM and GERACE 2001; PYHTILA and REXACH 2003, as examples), most notable of which is the affinity of importin-β/Kap95 for FxFG domains (BAYLISS *et al.* 2000). However, FxFG and GLFG repeats bind to the same site on Kap95, and spacer sequences contribute to the FxFG-Kap95 interaction suggesting that these spacers contribute to specialized binding to transport receptors (BAYLISS *et al.* 2000; BAYLISS *et al.* 2002b). *In vivo* evidence suggests that transport receptors use distinct FG domains as they move through the NPC: deletion of different combinations of FG domains results in defective transport of distinct transport receptor cargo (STRAWN *et al.* 2004; TERRY and WENTE 2007). Furthermore, comparison of FG

domain sequences among yeast species has uncovered “hot spots” of sequence conservation surrounding FG repeats, which may represent functionally important interfaces (DENNING and REXACH 2007). Therefore, it is likely that although FG domains share common features, each plays specialized roles during export, and *in vivo* studies of transport should preferentially inform transport models.

Based on *in vivo* results (STRAWN *et al.* 2004; TERRY and WENTE 2007), our lab favors a model where transport receptors utilize specialized pathways dictated by preferred interaction with FG repeats and/or potentially surrounding sequences in FG domains during NPC transport (reviewed in TERRY and WENTE 2009). However, it is unclear what characteristics of individual FG domains result in these pathways. It is likely that a combination of preferred interaction sites and where those sites dynamically exist in the NPC dictate transport pathways. Potentially, specialized transport pathways organize the vast amount of molecules crossing the NPC. Or possibly, transport of one kind of molecule alters FG domain topology to affect transport of another. These are complicated questions due to the flexibility and redundancies that exist between FG domains. Furthermore, in addition to the canonical transport paradigms described above, additional layers of complexity (reviewed in ADAMS and WENTE 2013) and regulation (reviewed in TERRY *et al.* 2007) are present to affect transport, and some of these factors are elaborated in Chapter II. In order to further understand specialized FG domain function during transport, we have used mRNA export as a model, and we have uncovered an important function during terminal steps of transport, when Mex67-Mtr2 is removed from the mRNP (Chapter III). It is likely that similar specialized FG domain functions exist throughout the transport process.

Part 3: mRNP remodeling: removal of specific proteins at the cytoplasmic face of the NPC

The structure that an RNA molecule adopts is highly correlated with its functionality, and there is a cross-talk between RNA structure and associating proteins, such that each can affect the other. For example, some transcripts contain local RNA structures that promote interaction with certain RNA binding proteins that recognize these structural elements. Examples include interaction of She2 with an extended hairpin structure found in transcripts that are asymmetrically localized in daughter buds of *S.c.* (NIESSING *et al.* 2004), direct binding of TAP-p15 to CTE RNA hairpin in viral RNA mentioned above (TEPLOVA *et al.* 2011), and direct recognition of IRES-containing RNA for translation (JACKSON 2013). Whereas these local RNA structural elements permit specialized RNA functionality through recruitment of interaction partners, global alterations in mRNA structure accompany each phase of an RNA lifecycle (Figure I.5). During transcription, the long RNA thread compacts into a RNP particle. EM images of *C. tentans* Balbiani ring RNAs beautifully demonstrate this compaction: the large transcript (nearly 40 kbp long) folds into a round particle that is 50nm in diameter, and this structure is adopted coincidently with the transcription process (Figure I.5A, reviewed in DANEHOLT 2001). Visualization of the Balbiani ring transcription site has been compared to the Christmas tree morphology observed during transcription of ribosomal RNA from the nucleolus (MILLER and BEATTY 1969), where the 5' end of the RNA appears as a compact circle at the end of a thread with increasing length along the gene. For nuclear export, the mRNP must adopt a structure that enables it to cross the NPC efficiently. The large Balbiani ring mRNA undergoes dramatic structural

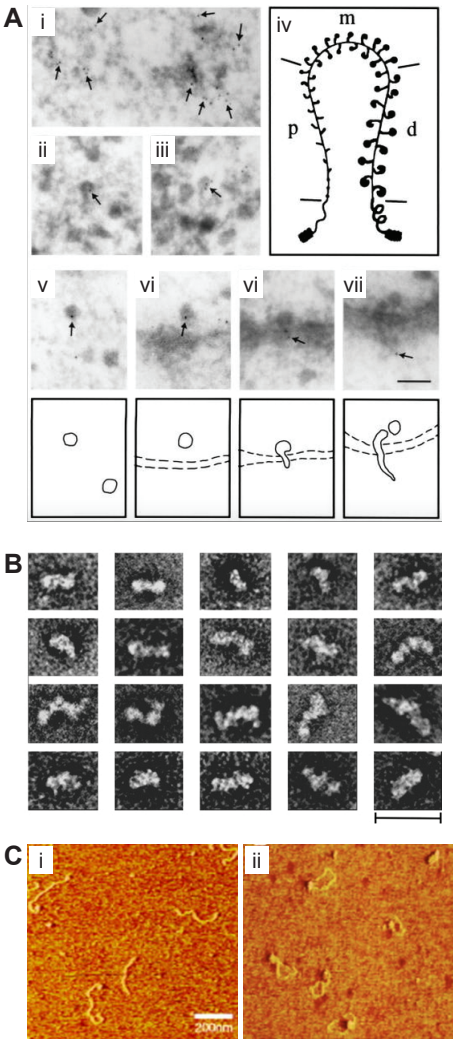

Figure I.5. Global mRNP structure.
(A) EM of Balbiani ring mRNPs. Arrows indicate position of nuclear cap binding protein Cbp20 as determined by immumo-EM. i-iv: transcription of Balbiani ring mRNA (p, proximal; m, middle; d, distal portions of the gene). v-viii: nuclear transport and export across the NPC Scale bar=100nm. Reprinted from (DANEHOLT 2001). (B) Structure of exporting mRNPs. mRNPs isolated from cells by Nab2 purification followed by resolving and fixing using a GraFix sucrose gradient, detected by single particle negative stain EM. Scale bar=30nm. Reprinted from (BATISSE *et al.* 2009). (C) Circularized mRNPs. Model transcripts (~1400nt with synthetic cap and poly-A tail) incubated without (i) or with (ii) with eIF4E, eIF4G, and Pab1 were detected by atomic force microscopy. Scale bar=200nm. Reprinted from (WELLS *et al.* 1998).

alterations as it unfolds from a circular structure to an elongated particle that exports 5' to 3' (Figure I.5A, reviewed in DANEHOLT 2001). Additionally, biochemically isolated nuclear and exporting transcripts from *S.c.* cells adopt an elongated structure (Figure I.5B) (BATISSE *et al.* 2009). After export, the RNA becomes accessible to translation machinery (potentially analogous to de-compaction of DNA during transcription), and it forms a circular species connected at the 5' and 3' ends with multiple associated translating ribosomes (polysomes) (Figure I.5C) (WELLS *et al.* 1998). Correct RNA folding is particularly challenging because it is a single-stranded nucleic acid, and base-pairing is promiscuous. A class of enzymes known as DEAD-box proteins function during the maturation of multiple classes of RNA (rRNA, mRNA, lncRNA, miRNA) to both promote RNA to adopt the correct structure and affect the association of RNA binding proteins (reviewed in FAIRMAN-WILLIAMS *et al.* 2010). During mRNA export, a DEAD-box protein, Dbp5, plays an essential role in altering mRNA structure to remove specific proteins and impose transport directionality.

The DEAD-box family

DEAD-box proteins are a group of conserved ATPases (37 in humans, 26 in S. cerevisiae, and 4 in E coli) that bind RNA and alter its structure through their ATPase cycle (reviewed in FAIRMAN-WILLIAMS *et al.* 2010). In addition to the eponymous DEAD motif (aspartic acid, glutamic acid, alanine, aspartic acid), DEAD-box proteins share up to 12 conserved sequence motifs that are embedded in a common core structure: two very similar globular domains connected by a flexible linker (Figure I.6, reviewed in LINDER and JANKOWSKY 2011; HENN *et al.* 2012; RUSSELL *et al.* 2013). The globular

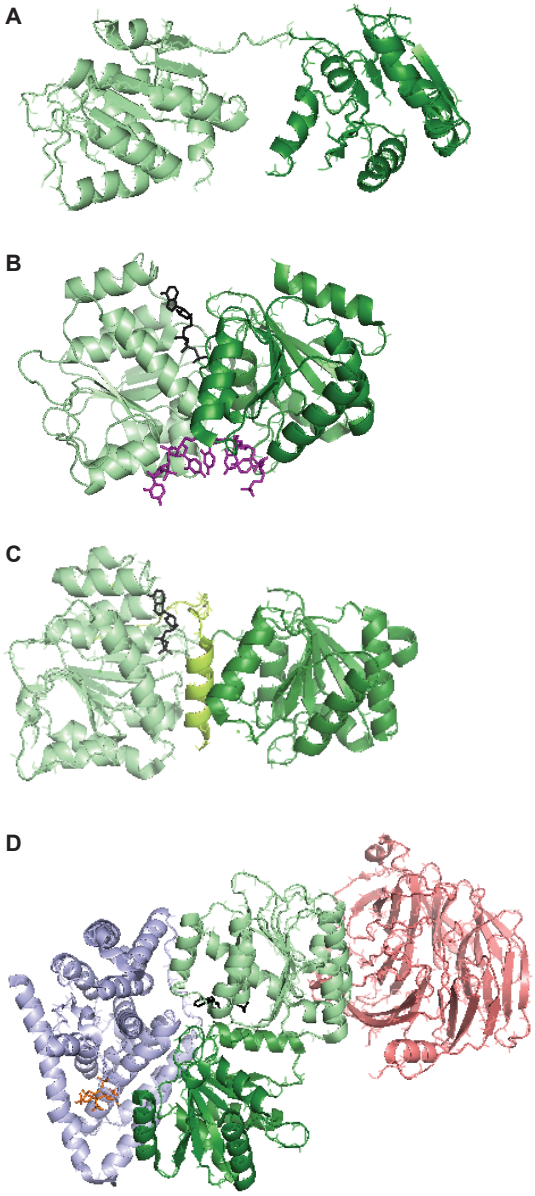

Figure I.6. Dbp5 structural changes upon nucleotide binding.
(A-D) Dbp5, green; Dbp5NTD, light green; Dbp5CTD, dark green; Dbp5 N-terminal helix, lime green; nucleotide (ADP/ADP-BeF_3), black; RNA (poly-U), purple; IP_6, orange; Gle1, blue; Nup159NTD, pink. (A) *S.p.* Dbp5-APO. Adapted from (FAN *et al.* 2009). (B) *S.c.* Dbp5-ATP-RNA. Adapted from (MONTPETIT *et al.* 2011). (C) *H.s.* Dbp5-ADP. Adapted from (COLLINS *et al.* 2009). (D) *S.c.* Dbp5-ADP-IP_6-Gle1-Nup159. Adapted from (MONTPETIT *et al.* 2011).

regions are structurally similar to the RecA bacterial DNA recombinase, which consists of a β-sheet surrounded by α-helices, and are thus termed RecA domains. The conserved motifs function in nucleotide (ATP/ADP) binding, RNA binding, or allosteric communication between these interfaces. For most proteins tested in this family, ATP and RNA binding are cooperative, and RNA promotes ATP hydrolysis. This cooperative binding is due to DEAD-box proteins structural rearrangements that accompany interaction with RNA and ATP. ATP binds at the interface of the RecA domains, promoting a "closed" state, and the RNA interaction spans across both domains in this conformation (FigureI.6B) (SENGOKU *et al.* 2006). This RNA interface includes 5-6 single-stranded nucleotides with the DEAD-box protein contacting the phosphate backbone of the RNA. Interaction with the nucleic acid backbone provides specificity for RNA over DNA, but because the protein does not interact with bases, it is a sequence-independent interaction. Importantly, when bound to the DEAD-box protein in this manner, the RNA is in a kinked conformation that is incompatible with helical base-pairing (SENGOKU *et al.* 2006). Indeed, the first DEAD-box protein was identified as an RNA helicase capable of unwinding short helices (RAY *et al.* 1985; ROGERS *et al.* 1999). Since their initial characterization, the known functions associated with DEAD-box proteins have drastically increased, likely attributable to small structural differences and/or association with different binding proteins. However, biochemical and structural data from a number of DEAD-box proteins has uncovered a common ATPase/RNA binding cycle, and studies of a few well-characterized members have been used to infer mechanistic features across the family.

In the absence of nucleotide (APO), the DEAD-box protein RecA domains are flexible in solution, and crystal structures of multiple DEAD-box protein cores demonstrate an open, extended "dumbbell" conformation (Figure I.6A) (CARUTHERS *et al.* 2000; STORY *et al.* 2001; ZHAO *et al.* 2004a; CHENG *et al.* 2005; SUN *et al.* 2014), which has been confirmed with the *S. pombe.* Dbp5 core (FAN *et al.* 2009). Upon ATP and RNA binding, the RecA domains of Dbp5 and other DEAD-box proteins close with a change in the relative orientation such that both domains contact the nucleotide and RNA (Figure I.6B) (ANDERSEN *et al.* 2006; BONO *et al.* 2006; SENGOKU *et al.* 2006; VON MOELLER *et al.* 2009; MONTPETIT *et al.* 2011; SUN *et al.* 2014). For another DEAD-box protein (Mss116), structures with multiple ATP analogs depicted similar structural conformations, suggesting that ground state ATP and transitional ADP-P structures are similar (DEL CAMPO and LAMBOWITZ 2009). Phosphate release triggers a conformational change: ADP bound DEAD-box proteins retain an open structure in solution (THEISSEN *et al.* 2008). This leads to RNA release, since the affinity for RNA is much lower in the presence of ADP (LORSCH and HERSCHLAG 1998a). For hDbp5 complexed with ADP, the amino-terminal helix was found to bind at the interfaces of the two RecA domains (Figure I.6C) (COLLINS *et al.* 2009). Biochemical analysis uncovered an inhibitory function for this amino-terminal extension: deletion results in increased RNA-independent ATPase activity *in vitro*. However, deletion of this region in *yDBP5* does not result in growth or mRNA export defects, suggesting that this is not a rate-limiting function *in vivo* or other factors compensate (HODGE *et al.* 1999). It is possible that this region is important for regulating ADP release from Dbp5, since Nup159 binds the amino-terminal RecA domain of Dbp5 for ADP release (Figure I.6D) (NOBLE *et al.* 2011),

and DEAD-box proteins generally have a higher affinity for ADP compared to ATP in the absence of RNA (LORSCH and HERSCHLAG 1998a). Several biochemical approaches have suggested that that ADP and APO structures are distinct in solution (LORSCH and HERSCHLAG 1998b; NOBLE *et al.* 2011), suggesting possible functional conformational changes upon ADP release. Thus, the nucleotide bound state of DEAD-box proteins serves as important regulatory steps in their function.

Because DEAD-box proteins interact with a few RNA bases and release RNA after ATP hydrolysis, they only locally alter RNA structure. This method of action is distinct from other helicases, which processively move along DNA or RNA, and it has been termed "local strand separation" (YANG *et al.* 2007). DEAD-box helicase activity decreases with increasing duplex length, but decreasing duplex stability allows activity on longer substrates (ROGERS *et al.* 1999). Furthermore, on these short substrates, only ATP binding but not ATPase activity is required for duplex unwinding, suggesting that ATP hydrolysis is only necessary for RNA release and enzyme recycling (CHEN *et al.* 2008; LIU *et al.* 2008). Thus, this class of enzymes serves as short-range RNA interactors whose binding is modulated by ATP hydrolysis. This functionality allows the DEAD-box core to serve as a module that can be used in a variety of ways as determined either by divergent amino- or carboxy-terminal extensions or association of binding partners. In many cases, these divergent extensions or binding partners have been shown to modulate ATPase activity and/or direct activity to a particular substrate, leading to a wide variety of functions for this class of proteins (KOSSEN *et al.* 2002; MALLAM *et al.* 2011; YOUNG *et al.* 2013). Indeed, many DEAD-box proteins function in dynamic multi-protein RNP complexes such as the spliceosome or maturing ribosomal

subunits. Having activity limited to a short RNA region is important for precise modulation of RNA structure so as not to disrupt other interactions along the RNA.

DEAD-box protein function

The variety of ways that DEAD-box protein function has been specialized demonstrates the flexible nature of the DEAD-box core. As the first characterized, *S. c.* eIF4A is the "godfather" of DEAD-box proteins (reviewed in ROGERS *et al.* 2002; ANDREOU and KLOSTERMEIER 2013). eIF4A serves an essential function during translation initiation in eukaryotes, where it is thought to unwind structures in the 5' end of the transcript to allow 43S pre-initiation complex binding (RAY *et al.* 1985; SVITKIN *et al.* 2001). eIF4A contains minimal extensions from the DEAD-box core and its activity is directed by binding partners in the eIF4F translation initiation complex. eIF4B stimulates eIF4A activity, and different regions of eIF4G stimulate or inhibit eIF4A (reviewed in ROGERS *et al.* 2002; ANDREOU and KLOSTERMEIER 2013). Because of the early studies of eIF4A, RNA helicase activity is considered the canonical DEAD-box protein function. For some enzymes, helicase activity is directed by extensions from the DEAD-box core. An RRM in *Bacillus subtilis* YxiN directly binds to a hairpin of ribosomal RNA (KOSSEN and UHLENBECK 1999; WANG *et al.* 2006), and the carboxy-terminal extension of *S.c.* Mss116 aids in RNA structural distortion (DEL CAMPO and LAMBOWITZ 2009). Despite the classical characterization of DEAD-box proteins as helicases, it was previously unknown how these proteins specifically detect double-stranded RNA. Recent biochemical and structural data of Mss116 has demonstrated that the carboxy-terminal RecA domain has a higher affinity for double-stranded RNA

than the full-length protein, and the amino-terminal RecA domain alone can bind ATP (MALLAM *et al.* 2012). These observations led to the model that the two RecA domains individually recognize substrates promoting subsequent structural rearrangements for RNA inter-domain interactions. This mechanism of independent ATP and RNA interactions may be generalizable to other members of the DEAD-box family, and may contribute to our understanding of Dbp5 activity at the NPC.

Other DEAD-box proteins have been shown to alter protein association with an RNA molecule. This function was originally suggested from studies of the spliceosome (STALEY and GUTHRIE 1998), where cold-sensitive mutants of DEAD-box proteins could be bypassed by mutating or deleting other spliceosomal protein-encoding genes (STRAUSS and GUTHRIE 1991; CHEN *et al.* 2001; KISTLER and GUTHRIE 2001). The first biochemical demonstration of this activity was displacement of U1A from its cognate RNA hairpin structure by the DEAD-box protein Ded1 (FAIRMAN *et al.* 2004; BOWERS *et al.* 2006). *In vivo*, Dbp5 has been demonstrated to remove Mex67-Mtr2 and Nab2 from RNA, the latter being confirmed biochemically (LUND and GUTHRIE 2005; TRAN *et al.* 2007). This activity is stimulated at the NPC by Gle1, but the mechanism of removal of specific proteins has not been uncovered (see below). In the nucleus, another DEAD-box protein, Dbp2, alters RNA structure to load proteins including Yra1, Nab2, and Mex67 onto transcripts (MA *et al.* 2013b). Interestingly, Yra1 inhibits Dbp2 activity and likely serves as a checkpoint that limits Dbp2 helicase activity toward the RNA once it is properly assembled. By performing these functions, DEAD-box proteins generally function as mRNP modifiers to chaperone correct assembly and promote dynamic association of binding proteins.

Another DEAD-box protein, eIF4AIII, functions as an RNA clamp in the exon junction complex (EJC) (BALLUT *et al.* 2005; ANDERSEN *et al.* 2006; BONO *et al.* 2006). Here, Y14-MAGOH inhibits eIF4AIII ATP hydrolysis, locking it onto the RNA, where it can serve as a platform for the assembly of other EJC components (PALACIOS *et al.* 2004; SHIBUYA *et al.* 2004; BALLUT *et al.* 2005). This complex associates co-transcriptionally with spliced transcripts in mammals, ~20 nucleotides upstream of the splice site in a sequence-independent manner, and most of its components travel with the mRNA to the cytoplasm, where they are removed during the pioneer round of translation (DOSTIE and DREYFUSS 2002; LEJEUNE *et al.* 2002; SHIBUYA *et al.* 2004). The mechanism of eIF4AIII interaction with RNA was surprising due to the transient association between other DEAD-box proteins and RNA in the presence of ATP, highlighting the drastic ways in which associating proteins can regulate DEAD-box protein function. *In vitro* experiments with other DEAD-box proteins have uncovered similar long-lived protein-RNA interactions in the presence of ATP analogues, but different proteins have distinct capabilities for these persistent interactions, suggesting distinct structural conformations in the presence of these nucleotides (LIU *et al.* 2014).

Finally, some DEAD-box proteins have demonstrated RNA annealing activity, but the *in vivo* implications of this activity is unknown (ROSSLER *et al.* 2001; YANG and JANKOWSKY 2005; HALLS *et al.* 2007). Additionally, some DEAD-box proteins have been suggested to function as energy sensors in cells, as AMP inhibits the activity of a subset of these proteins (PUTNAM and JANKOWSKY 2013). Thus, the DEAD-box proteins have evolved from a common core structure to perform a variety of functions in cells.

Dbp5 removes specific proteins at the NPC for directional mRNA export

Dbp5 was coincidently identified in *S.c.* by two labs: one characterizing new DEAD-box proteins in *S.c.*, and the other identifying temperature-sensitive *S.c.* mutants that result in nuclear mRNA accumulation at the non-permissive temperature (SNAY-HODGE *et al.* 1998; TSENG *et al.* 1998). Subsequent studies identified the conserved human homologue, hDbp5 (Ddx19), which is also required for mRNA export (SCHMITT *et al.* 1999; HODGE *et al.* 2011, Aditi and Wente, personal communication). Dbp5 is localized to the cytoplasmic face of the NPC via a conserved interaction with Nup159 (hNup214), which is anchored at this location via a predicted coiled-coil domain at its carboxy-terminus (DEL PRIORE *et al.* 1997; HODGE *et al.* 1999; SCHMITT *et al.* 1999), see Figure III.11). When it was originally identified, Dbp5 was characterized as a poor helicase, and based on its localization and mRNA export function, it was postulated that Dbp5 removes proteins from nascently-exported transcripts (SNAY-HODGE *et al.* 1998; TSENG *et al.* 1998). This function was demonstrated several years later, when it was shown that Dbp5 removes Mex67-Mtr2 and Nab2 from transcripts in a process termed mRNP remodeling (LUND and GUTHRIE 2005; TRAN *et al.* 2007). It had been proposed that these factors are removed shortly after mRNA export based on several pieces of data: Nab2 is localized to the nucleus at steady state, but it accumulates in the cytoplasm when nuclear import is inhibited indicating that it shuttles between the nucleus and cytoplasm (DUNCAN *et al.* 2000; GREEN *et al.* 2002), Mex67 is localized to the nuclear rim at steady state (SEGREF *et al.* 1997), and neither protein is present in polysomes (WINDGASSEN *et al.* 2004).

Biochemical studies have provided some insight into potential structural changes in Dbp5 that mediate Nab2 remodeling. Specifically, Dbp5 releases Nab2 from a 25-base poly-A RNA oligonucleotide, as indicated using an electro-mobility shift assay (TRAN *et al.* 2007). Interestingly, ATP and ADP, but not AMP-PNP, permits this activity. This indicates that a structural change as Dbp5 transitions to the ADP bound form permits remodeling. In fact, structure for the ADP bound form of Dbp5 that is distinct from APO- and ATP-binding has been suggested based on circular dichroism and limited protease results, and it was proposed that this structural conformation change occurs upon ATP hydrolysis or ADP binding (TRAN *et al.* 2007; NOBLE *et al.* 2011). Dbp5 also remodels Pab1 from poly-A RNA *in vitro*, but *in vivo*, Pab1 remains on the transcript in the cytoplasm for circularization during translation, among other functions (WELLS *et al.* 1998; TRAN *et al.* 2007) indicating that specificity for which proteins are remodeled is not an inherent property of Dbp5 but is determined by *in vivo* factors. However, it is unknown which proteins are remodeled by Dbp5 and how these proteins are selected. Most likely, the proteins are those used for mRNA export such that their removal confers export directionality. Indeed, mutants of *DBP5* result in re-import of transcripts that have successfully exported (Weis, personal communication), and Mex67 steady state localization is not altered in *dbp5* mutants, suggesting that it and potentially the mRNPs it is bound to remain at the NPC (LUND and GUTHRIE 2005). Furthermore, diffusion of the transcript away from the NPC may serve as a method for terminating Dbp5-mediated remodeling, serving as a kind of remodeling checkpoint. Additionally, Mex67, which binds to the RNA via adaptor proteins, is likely remodeled as a consequence of removal of the adaptors. Thus, in the context of an mRNP coated with

many proteins, the question remains of how Mex67 and its adaptors are specified for mRNP remodeling by Dbp5.

Modulation of Dbp5 by interaction partners at the NPC

Dbp5 activity is modulated by binding partners located at the cytoplasmic face of the NPC. In combination with the small molecule inositol hexakisphosphate (IP_6), Gle1 enhances the RNA-dependent ATPase and the Nab2-RNA remodeling activity of Dbp5 (ALCAZAR-ROMAN *et al.* 2006; WEIRICH *et al.* 2006; TRAN *et al.* 2007). Gle1 was originally identified in a screen for mutants synthetically lethal with deletion of gene encoding the GLFG Nup Nup100 where it was described as an essential mRNA export factor (MURPHY and WENTE 1996). Additionally, other labs reported isolation of Gle1 in genetic screens related to mRNA maturation and export (DEL PRIORE *et al.* 1996; NOBLE and GUTHRIE 1996). A second genetic screen uncovered the surprising link between inositol phosphorylation and Gle1 function during mRNA export (YORK *et al.* 1999), and subsequent reports revealed that this is due to the role for IP_6 in mediating the Gle1-Dbp5 interaction (Figure I.6D) (ALCAZAR-ROMAN *et al.* 2006; WEIRICH *et al.* 2006; ALCAZAR-ROMAN *et al.* 2010). The conserved human Gle1 (hGle1) is also required for mRNA export (WATKINS *et al.* 1998) and the *hGle1* transcript is differentially spliced to yield hGle1A and hGle1B proteins (KENDIRGI *et al.* 2005). hGle1A exhibits a pan-cellular localization when expressed in the presence of endogenous hGle1, and hGle1B contains a carboxy-terminal extension that interacts with the cytoplasmically-oriented Nup hCG1 resulting in enrichment of hGle1B at the NPC (STRAHM *et al.* 1999; KENDIRGI *et al.* 2005). Both hGle1A and hGle1B interact with hNup155 at their amino-terminus,

and this interaction is also required for enrichment of hGle1 at the NE (RAYALA *et al.* 2004). Interestingly, only hGle1B is required for mRNA export, suggesting that differential splicing regulates the functionality of Gle1 through modulation of its localization (FOLKMANN *et al.* 2013). *S.c.* Gle1 interacts with the hCG1 homologue, Nup42, and is located at the cytoplasmic fibrils of the NPC (Figure I.1D) (STRAHM *et al.* 1999). Both yGle1 and hGle1 self-associate to form a large disk-shaped homo-oligomer *in vitro*, and self-association is required for Gle1 function during mRNA export (FOLKMANN *et al.* 2013). Additionally, at least partly due to this self-association, Gle1 is stably localized to the NPC (Andrew Folkmann, personal communication). Thus, Gle1 serves to spatially activate Dbp5 at the NPC cytoplasmic face, potentially by activating multiple Dbp5 molecules for multiple rounds of mRNP remodeling.

Although structural data has revealed the nature of the Gle1-IP_6-Dbp5 interaction (Figure 1.6D, Figure A.1A), the mechanism of ATPase stimulation is not agreed upon (FOLKMANN *et al.* 2011; MONTPETIT *et al.* 2011). Gle1 is an alpha-solenoid HEAT-repeat containing protein that interacts with both RecA domains of Dbp5, supporting a "half-open" conformation (Figure A.1A). Interaction with one of the RecA domains is relatively strong and contains the IP_6 binding pocket, while the other interface has a weak interaction (MONTPETIT *et al.* 2011). Importantly, disruption of either binding site is detrimental for mRNA export (DOSSANI *et al.* 2009; MONTPETIT *et al.* 2011). This interaction is very similar to the interaction between eIF4G and eIF4A, where eIF4G stimulates eIF4A ATPase activity and supports a similar orientation of eIF4A RecA domains in crystal structures (OBERER *et al.* 2005; SCHUTZ *et al.* 2008). It has been suggested that eIF4G serves as a "conformational guide" for eIF4A, where the stronger

interface anchors the protein-protein interaction with the weaker interface positioning the RecA domain for modulation of nucleotide binding (HILBERT *et al.* 2011). The Weis lab has suggested that by separating the RecA domains of Dbp5, Gle1 functions to release ADP (MONTPETIT *et al.* 2011). However, we have proposed an alternate model (see below). Interestingly, eIF4AIII has recently been demonstrated to interact with NOM1, which is highly homologous to eIF4G, suggesting that multiple DEAD-box proteins may have similar HEAT-repeat containing ATPase activators (ALEXANDROV *et al.* 2011).

Nup159 localizes Dbp5 to the NPC via a beta-propeller at its amino-terminus, and deletion of this region results mislocalization of Dbp5 at steady state and a temperature-sensitive mRNA export defect that can be rescued by overexpression of Dbp5 (Figure I.1D) (DEL PRIORE *et al.* 1997; HODGE *et al.* 1999; SCHMITT *et al.* 1999; VON MOELLER *et al.* 2009). While the mRNA export defect was thought to be due to mislocalization of Dbp5 activity, it has been determined that Nup159 functions to release ADP from Dbp5, and this function is important for proper mRNA export (NOBLE *et al.* 2011). Indeed, a mutant allele of *DBP5* that efficiently releases ADP but does not localize to the NPC, $dbp5^{RR}$, bypasses the temperature-sensitivity of *nup159ΔN* (NOBLE *et al.* 2011). However, localized Dbp5 activity is important for proper mRNP remodeling as deletion of *NUP42*, which results in altered Gle1 localization (STRAHM *et al.* 1999), in combination with expression of $dbp5^{RR}$ results in a temperature-sensitive mRNA export defect (NOBLE *et al.* 2011). This function of Nup159 in ADP release from Dbp5 was the first reported nucleotide release factor for a DEAD-box protein, adding an additional point at which the activity of this class of enzymes can be modulated. Additionally,

structural studies have demonstrated that the hDbp5 binding sites for Nup214 (the Nup159 homolog) overlap with the RNA binding site, and Nup214 and RNA compete for interaction with hDbp5 (VON MOELLER *et al.* 2009). This suggests that Nup214/Nup159 bind Dbp5 after the RNA has unbound, leading to ADP release after this step.

FRAP analysis of yDbp5 (recovery half-time <1sec HODGE *et al.* 2011), and single-molecule studies of *C. tentans* Dbp5 (residence time 50ms KAMINSKI *et al.* 2013), have demonstrated that Dbp5 is dynamically associated with the NPC, whereas Nup214 has a residence time of approximately 44 hours (RABUT *et al.* 2004), indicating a dynamic interaction between Dbp5 and Nup159/Nup214. While the Dbp5-Nup159 interaction has been reported to be strongest in the absence of nucleotide (SCHMITT *et al.* 1999), the structural basis for this is not immediately clear. Only the amino-terminal RecA domain of Dbp5 contacts Nup159 (VON MOELLER *et al.* 2009), suggesting that altered inter-domain conformation cannot account for the reported nucleotide-dependent changes in interaction. *In vivo*, ATP binding is required for Dbp5 to localize to the nuclear rim as demonstrated by mutational analysis and energy depletion (HODGE *et al.* 2011). This indicates that an ATP-dependent step potentially exists before Dbp5 can bind Nup159.

Based on biochemical and genetic data, our lab has developed a model for the Dbp5 ATPase cycle at the NPC (reviewed in FOLKMANN *et al.* 2011). A major contribution to this model was the identification of a mutation in *DBP5* (*DBP5*^{R369G}) that results in a dominant growth an mRNA export defect with overexpressed (HODGE *et al.* 2011). Furthermore, Dbp5^{R369G} inhibits Gle1-stimulated Dbp5 ATPase activity *in vitro*. Dbp5^{R369G} is defective in binding to RNA, and its dominance can be rescued by

increased levels of Gle1 both *in vivo* and *in vitro*. Additionally, combining this mutant with a mutation which disrupts interaction with Gle1 results in a loss of the growth defect when overexpressed *in vivo*. This indicates that binding to RNA is required for Gle1 release, putting the Gle1-Dbp5 interaction upstream of the RNA-Dbp5 interaction. Biochemical data supports a function for Gle1 in ATP loading, as Dbp5 ATP binding is increased 2-4 fold in the presence of Gle1, likely accounting for the 5-6-fold stimulation of ATPase activity (NOBLE *et al.* 2011), and non-hydrolyzable AMP-PNP increases IP_6 binding to Dbp5-Gle1, suggesting an increased affinity between these molecules in the presence of ATP (ALCAZAR-ROMAN *et al.* 2010). Additionally, whereas the *dbp5*^{RR} mutant with reduced ADP affinity rescues *nup159* mutants, it results in enhanced growth defects when combined with mutants that affect *gle1* function, indicating that ADP release does not bypass the requirement for *GLE1* (NOBLE *et al.* 2011). We therefore propose that Gle1 serves as a platform to activate Dbp5 by aiding in ATP binding through modulating the conformation of the Dbp5 RecA domains.

Thus, our model is as follows (Figure I.7): 1: A mature mRNP gains access to the NPC for transport. 2: The mRNP crosses the NPC, reaching the cytoplasmic face. 3&4: Gle1 loads ATP onto Dbp5. 5: ATP-bound Dbp5 binds RNA across the RecA domains, causing simultaneous Gle1 release. 6: Dbp5 hydrolyzes ATP and phosphate release triggers conformational change that results in RNP remodeling and release. 7. Dbp5 binds Nup159 for ADP release and enzyme recycling. 8. Removed proteins are re-imported by their cognate Kap for additional rounds of mRNA export.

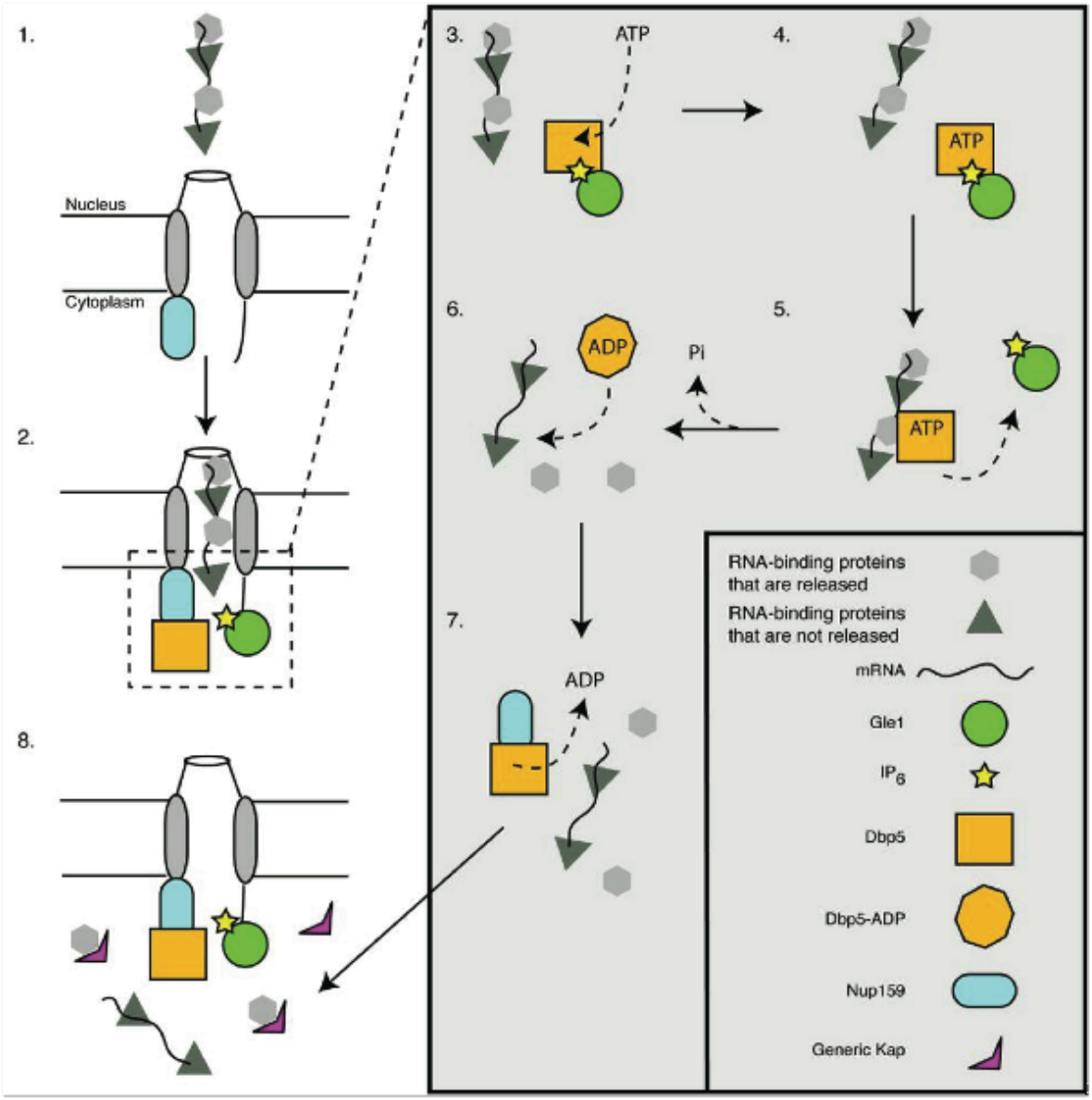

Figure I.7. Model for order of events during mRNP remodeling.
Details listed in text. Figure reprinted from (FOLKMANN *et al.* 2011).

For the homologous eIF4A-eIF4G interaction, eIF4G enhances the closed state of eIF4A as measured by single-molecule FRAP (HILBERT *et al.* 2011; ANDREOU and KLOSTERMEIER 2014; HARMS *et al.* 2014), and eIF4G has been shown to increase ATP binding of eIF4A (MARINTCHEV *et al.* 2009). Finally, we propose that local enzyme recycling by Nup159 and simultaneous activation of multiple Dbp5 molecules through Gle1 oligomers are required during mRNA export to allow for multiple rounds remodeling of the large mRNPs.

In addition to their roles at the NPC, both Gle1 and Dbp5 function at other points along the gene expression pathway. Analysis of Dbp5 association with Balbiani ring RNPs by immuno-EM localization has demonstrated that Dbp5 is associated with nuclear and cytoplasmic RNPs (ZHAO *et al.* 2002). In *S.c.*, Dbp5 accumulates in the nucleus of *MEX67* mutants and when transcription is halted (HODGE *et al.* 1999), and the growth of transcription initiation mutants is exacerbated when *DBP5* is mutated (ESTRUCH and COLE 2003; ESTRUCH *et al.* 2012). This data has lead to the proposal that Dbp5 either has a nuclear function during mRNA biogenesis or is loaded onto mRNPs co-transcriptionally for mRNP remodeling at the cytoplasmic face of the NPC (or a combination of the two). In the cytoplasm, Dbp5 is associated with polysomes and potentially remodels the mRNA for proper recognition of the stop codon (GROSS *et al.* 2007). To localize this activity, Dbp5 interacts with translation release factor eRF1, and its activity is required for eRF3 association with eRF1 and the translating ribosome for cleavage of the polypeptide from the ribosome (GROSS *et al.* 2007). Furthermore, a genetic screen with a *dbp5* mutant uncovered links to P-body components, and Dbp5 localizes to cytoplasmic granules when its function is altered in mutants (SCARCELLI *et*

al. 2008). Thus, Dbp5 interacts with additional proteins for nuclear and cytoplasmic functions, but whether the same Dbp5 molecule travels with the mRNA or different pools of Dbp5 perform these functions remains unknown. Furthermore how Dbp5 activity is modulated during these roles has not been determined.

It is likely that Gle1 stimulates Dbp5 during is role in translation termination. This is because Gle1 interaction with IP_6 is required for proper translation termination, and it directly interacts with eRF1 and is also required for eRF3 association with polysomes (BOLGER *et al.* 2008; ALCAZAR-ROMAN *et al.* 2010). Surprisingly, Gle1 also functions during translation initiation, but this role is independent of IP_6 (BOLGER *et al.* 2008). Instead, Gle1 inhibits the ATPase activity of another DEAD-box protein, Ded1, for proper mRNA start site selection (BOLGER and WENTE 2011). In a similar fashion, a related HEAT-repeat protein, CWC22, inhibits the RNA binding and ATPase activity of eIF4III (BARBOSA *et al.* 2012). Structural analysis uncovered a surprising mechanism for this inhibition, where CWC22 is anchored at eIF4AIII by one RecA domain similar to the stronger Gle1-Dbp5 interface, and contacts the other RecA domain so that the ATP binding interfaces do not face each other (BUCHWALD *et al.* 2013). Thus, Gle1 is a multifunctional regulator of different DEAD-box proteins, and it will be interesting to determine whether it can promote distinct conformations of these proteins. Gle1 also shuttles between the nucleus and cytoplasm, and this shuttling is essential for mRNA export, but a distinct nuclear function and whether IP_6 is required have not been uncovered (KENDIRGI *et al.* 2003). Because Gle1 is alternately spliced in humans, different isoforms likely contribute to different DEAD-box protein regulation. Indeed, hGle1B, but not hGle1A, is sufficient for mRNA export (FOLKMANN *et al.* 2013).

Although hGle1 and hDbp5 are required for mRNA export in human cells, it remains to be determined whether the mechanism of hGle1 stimulation of hDbp5 activity is conserved. Expression of hDbp5^{R372G}, which is homologous to the dominant negative yDbp5^{R369G}, results in an mRNA export defect (HODGE *et al.* 2011). Considering the mechanism of how this alteration affects mRNA export in *S.c.*, by sequestering Gle1, we anticipate that hGle1 stimulation of hDbp5 is conserved. It was also anticipated that these proteins play a general, essential function during mRNA export for all cells, so it was surprising when the tissue-specific motor neuron defects associated with Lethal Congenital Contracture Syndrome (LCCS1) and the related Lethal Arthrogrtposis with Anterior Horn Cell Disease were found to be caused by mutations in *GLE1* (NOUSIAINEN *et al.* 2008). Modeling of this disease by *GLE1* knockdown in zebrafish resulted in similar phenotypes, and it was determined that although motor neuron defects are among the most prominent, decreased Gle1 function generally affects highly proliferative cell types (JAO *et al.* 2012). Thus, Dbp5 and Gle1 are thought play essential, conserved roles in mRNA export across cell types in humans, and mechanistic features of mRNP remodeling by these factors uncovered in *S.c.* are likely to inform human functionality.

CHAPTER II:

Uncovering Nuclear Pore Complexity with Innovation

Published, Rebecca L. Adams, Laura J. Terry, and Susan R. Wente, *Cell*, March, 2013; reprinted with permission: license #: 3544390293928

Abstract

Recent technological advances in imaging and reductionist approaches are providing a high-resolution understanding of nuclear pore complex structure and transport. This work reveals unexpected mechanistic complexities based on nucleoporin functions and specialized import and export pathways.

Introduction

First impressions can be misleading. Nearly 60 years ago, pioneering transmission electron microscopy approaches first revealed the presence of a structure within the eukaryotic nuclear envelope (NE): the nuclear pore complex (NPC) (GALL 1954) (Figure II.1A). The original views are striking yet deceptively simple, with the large ~100 MDa proteineacous NPC assembly spanning the NE to provide a straightforward passageway between the nucleus and cytoplasm. Over time, insights into NPC structure and function have revealed unexpected complexities.

The NPC pathways for nucleocytoplasmic transport are based on the type of cargo. Diffusion through NPCs is inhibited for molecules greater than ~40kDa, and facilitated transport is required for larger macromolecules and/or accumulation against a concentration gradient (reviewed in AITCHISON and ROUT 2012). RNAs synthesized in

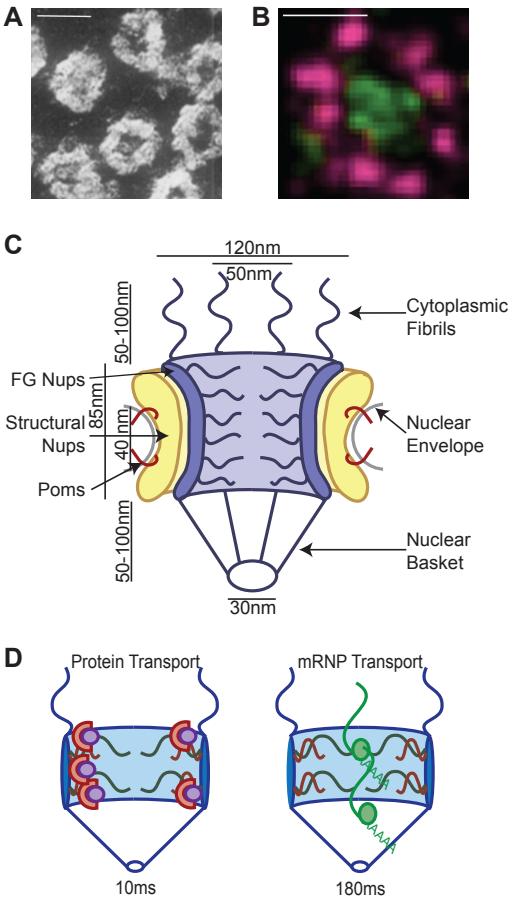

Figure II.1. Observing NPC structure and transport at high resolution.
(A) Early EM image of the NPC cytoplasmic face in a salamander (*Triturus viridescens*) oocyte NE. Reprinted with permission from (GALL 1954). Scale bar, 100nm. (B) 8-fold symmetry of the NPC in the NE plane resolved by dSTORM microscopy. Localizations of the lumenal domain of the transmembrane Nup gp210 (magenta, by indirect immunofluorescence, X222 antibody) and the FG Nups (green, by ATTO520-conjugated WGA staining) were resolved in a *Xenopus laevis* oocyte NE. Reprinted with permission from (LOSCHBERGER *et al.* 2012). Scale bar, 100nm. (C) Schematic representation of NPC architecture. Measurements indicate dimensions for the human NPC from cryoET (MAIMON *et al.* 2012). (D) Cartoon of different transport pathways through the NPC, with distinct FG Nup requirements for Kap transport versus mRNA export (reviewed in TERRY and WENTE 2009). Protein transport occurs in approximately 10ms (YANG and MUSSER 2006), whereas mRNA export takes 180ms (GRUNWALD and SINGER 2010). Transport cargo sizes are approximately to scale with NPC: protein cargo as ~80kDa globular shape, and mRNP size potentially proportional to the transcript length (indicated by expanded shading) including the 5' Cap-binding protein complex (CBP) (star) and other RNA binding proteins (circles).

the nucleus are actively exported for function in the cytoplasm. Nuclear import is required for proteins made in the cytoplasm during interphase. Increased knowledge of the eukaryotic proteome and RNA repertoires has expanded the complexity in terms of the range and bulk of macromolecules that require facilitated transport through NPCs. Moreover, based on this plethora of physiological needs for proper gene expression, the NPC must be a robust and selective portal.

A common operating principle has been that all NPCs in a given cell and all transport pathways in a given NPC essentially function the same. Recently, however, unanticipated layers of complexity combined with simplicity of design in NPC structure and function have been uncovered. High-resolution imaging advances have allowed dynamic visualization of NPC transport events. In addition, NPC-wide analysis and reductionist approaches have pinpointed how both complex and simple components potentially contribute to transport pathway specialization. It is intriguing to consider how such specialization might contribute to the transport mechanism and high cargo load capacity. This innovative work also sets the stage for future studies taking into account possible heterogeneity between NPCs and within NPCs.

Insights gained from high-resolution NPC structural analysis

The original electron microscopy (EM) views of the NPC documented a structure of elegant simplicity with an apparent 8-fold rotational symmetry in the plane of the NE. Additional details of cytoplasmic filaments and a nuclear basket structure were further defined by scanning EM (reviewed in AITCHISON and ROUT 2012). The basic features of the current structural model are shown in Figure II.1C. The most recent leaps in

structural resolution have come from a combination of both high-resolution cryo-electron tomography (cryo-ET) of NPCs in intact NEs and x-ray crystallography studies of NPC proteins (nucleoporins, Nups) (reviewed in BILOKAPIC and SCHWARTZ 2012); the cryo-ET work yielded a 6.6nm resolution image of the human NPC (MAIMON *et al.* 2012). In the future, coupling this technology with the strategies to individually pinpoint different Nups might allow the crystal structures of components to be modeled into the entire NPC. Tour de force analysis of virtually all the yeast *S. cerevisiae* Nups (termed "NPC-wide") by parallel structural and biochemical approaches also enabled *in silico* computational modeling, and generated new insights into the potential NPC molecular architecture (ALBER *et al.* 2007).

Importantly, while previous low-resolution studies showed a general conservation of structure between human and other eukaryotes, high-resolution cryo-ET allowed the visualization of subtle differences in particular structures of these divergent NPCs. Specifically, variations were noted in the cavities near the periphery of the central transport channel, suggesting that there might be functional divergence in this part of the NPC (MAIMON *et al.* 2012). These distinctions might arise from the few noted NPC protein composition differences across species, and recent innovations in super-resolution light microscopy should allow Nup localization to be examined at a resolution previously only afforded by EM. For example, these methods have already permitted visualization of the 8-fold symmetry of Nups in fixed cells (LOSCHBERGER *et al.* 2012) (Figure II.1B), and direct live cell observations of the asymmetric nuclear-cytoplasmic distribution of Nups in NPCs (HAYAKAWA *et al.* 2012). Further such studies could be

employed to map Nups to particular NPCs, and allow conclusions to be drawn regarding how specific Nup subcomplexes are oriented in NPCs.

Functional complexity revealed by NPC-wide analysis

Most of the proteins that constitute the *S. cerevisiae* and human NPC were identified over a decade ago. The ~30 different proteins are grouped into three simple functional classes (reviewed in TERRY and WENTE 2009): transmembrane Nups that anchor the NPC in the NE, also known as pore membrane proteins (Poms); structural Nups that are thought to stabilize the NE curvature at nuclear pores and provide scaffolding for assembling other peripheral Nups; or FG Nups that contribute both to the permeability barrier for nonspecific transport and to facilitated movement as direct binding sites for transport receptors. Strikingly, there are a limited variety of structural folds that these Nups adopt with the majority of the structures in the NPC as either beta-propeller, alpha solenoid, or FG domains (reviewed in AITCHISON and ROUT 2012; BILOKAPIC and SCHWARTZ 2012). It has been suggested that parts of this simple structural assembly reflect the Nups' ancestral relationship with proteins in vesicle coat complexes. Thus, this complex machine derives its function through surprisingly simple structural elements.

The complexity in NPC function comes from several elements. First, different Nups are associated with NPCs for different time periods. Recent work revealed that the structural Nups are among the most stable proteins in a cell, capable of persisting for months or years in a non-dividing cell (SAVAS *et al.* 2012); and these proteins remain stably NPC-associated once assembled into the NPC (RABUT *et al.* 2004). In contrast,

FG Nups are highly dynamic (RABUT *et al.* 2004), with residence times as low as seconds to minutes in the NPC. How this dichotomy in association times for different components might affect the transport mechanism is unknown. Second, the NPC cargo load can alter the transport mechanism. Single molecule microscopy studies demonstrated that increasing concentrations of the importin beta transport receptor altered the transport time of both its cargo and molecules that passively diffuse (YANG and MUSSER 2006). Together, it is intriguing to consider that the environment of a given transport channel might be temporally impacted due to either cargo load or the specific FG Nups that are associated.

Third, diversity in function among the FG Nups is illuminated by several key NPC-wide studies. Traditionally, the FG Nups have been considered interchangeable and of uniform function due to their common attributes. The FG Nups contain motifs enriched in phenylalanine (F) and glycine (G) repeats, such as FXFG and GLFG (L, leucine; X, any amino acid); the spacer sequences between FG repeats consist of ~5-30 residues typically enriched in polar amino acids. All analysis to date indicates that the FG domains are unstructured and occupy the central NPC channel (summarized in TERRY and WENTE 2009; YAMADA *et al.* 2010; AITCHISON and ROUT 2012). Although these FG domains constitute roughly 12% of the mass of the NPC, they are not resolved in high-resolution structures apparently due their inherent flexibility. Immuno-EM analysis indicated that a single FG domain type occupies multiple topologies within an NPC (FAHRENKROG *et al.* 2002). Thus, all FG Nups seem to share an unexpected structural flexibility as a defining feature.

Despite shared structural characteristics, several notable distinctions are defined amongst the FG domains. NPC-wide analysis of the biochemical and biophysical properties of individual FG domains or subdomains showed differences in cohesive properties in terms of self- and inter-FG interactions, and in levels of compaction (collapsed versus random coil) (YAMADA *et al.* 2010). Furthermore, *in vivo* evidence revealed that the FG domains have distinct functions. In an NPC-wide analysis of FG domain deletion mutants, *S. cerevisiae* viability required only specific combinations of FG domains: all were individually dispensable with only a few strictly required in double or triple mutant combinations (reviewed in TERRY and WENTE 2009). More importantly, different FG domain deletion mutants were defective in specific nuclear transport pathways. For example, a FG deletion mutant defective in Kap121 import was competent for mRNA export, and vice versa (reviewed in TERRY and WENTE 2009). Most recently, using an immuno-depletion/add-back approach with *Xenopus* oocyte nuclear assembly extracts, the FG Nup Nup98 was necessary for generation of the permeability barrier that inhibits diffusion of macromolecules (HULSMANN *et al.* 2012). In the absence of the Nup98 FG domain, only substitution with another cohesive FG domain restored the barrier. It is striking that the permeability barrier function could be attributed to one specific FG Nup and provides additional assertive evidence that all FG Nups are not the same and are not interchangeable.

A final layer of complexity stems from reports of Nup post-translational modifications. It has long been appreciated that vertebrate FG Nups are O-linked glycosylated, and recent studies suggested this might play a role in the vertebrate NPC permeability barrier (LABOKHA *et al.* 2013). In addition, Nup98 phosphorylation is an

important initial step in the breakdown of the NPC during open mitosis (LAURELL *et al.* 2011). This phosphorylation lead to increased permeability of the NPC, whether through altering the conformation of the Nup98 GLFG domain or inducing Nup98 dissociation from NPCs. This finding is consistent with the essential role of Nup98 in generating the permeability barrier (HULSMANN *et al.* 2012). More recently, NPC-wide analysis of ubiquitylation was carried out in *S. cerevisiae* (HAYAKAWA *et al.* 2012), and this modification was discovered on almost all Nups. Interestingly, proper nuclear migration during mitosis required Nup159 ubiquitylation. Further work will be required to understand how these layers of complexity impact nuclear transport function.

Dynamic and diverse transport pathways uncovered within NPCs

The NPC translocation mechanism is well characterized by basic concepts of docking, translocation and release steps for cargo complexes (reviewed in depth elsewhere, (AITCHISON and ROUT 2012). Briefly, a protein must display a nuclear localization sequence (NLS) for entry or nuclear export sequence (NES) for exit. These motifs provide binding sites for transport receptors (Kaps, importins, exportins, transportins). RNA transport receptors either recognize the RNA directly (tRNA, miRNA) or interact with an RNA-binding adaptor protein (in the mRNA ribonucleoprotein (mRNP) complex). In addition to cargo interactions, transport receptors also contain hydrophobic pockets that bind the phenylalanine residues of FG domains (reviewed in TERRY and WENTE 2009).

Several alternative models for how transport receptor-FG interactions mediate NPC translocation are currently under investigation (see below). However, the

understanding of how transport directionality is dictated has been fairly well agreed upon. For the Kap family, accumulation of cargo against its concentration gradient and recycling of the transport receptor is based on localized control of Ran GTPase activity (favoring the GTP state in the nucleus, and GDP in the cytoplasm). Specifically, the importin-cargo complex binding to Ran-GTP in the nucleus causes cargo release. In contrast, a RanGTP-exportin-cargo complex disassembles in the cytoplasm with GTP hydrolysis (reviewed in AITCHISON and ROUT 2012). An analogous, though quite distinct, non-RanGTP mechanism exists for mRNA export by the NXF1 receptors (*S. cerevisiae* Mex67), wherein ATP/ADP cycling of a RNA-dependent DEAD-box ATPase (Dbp or DDX) localized on the NPC cytoplasmic filaments is necessary for directional transport (reviewed in FOLKMANN *et al.* 2011). Overall, directional facilitated translocation is dictated by spatially controlled, nucleotide-dependent switches at the exit sites.

The distinct requirements of different FG Nups for specific transport receptors underscores the potential for multiple preferential pathways existing in an NPC (Figure II.1D) (reviewed in TERRY and WENTE 2009). However, whether the active and passive transport pathways are both functionally and spatially distinct in the NPC central channel has been debated. Recently, new microscopy technologies have enabled documentation of real-time single translocation events (notable examples are (YANG and MUSSER 2006; GRUNWALD and SINGER 2010; LOWE *et al.* 2010; MA and YANG 2010; MOR *et al.* 2010). These are based on both high spatial resolution (as low as 6nm) and temporal parameters (in the ms range), coupled with single molecule innovations for specific protein cargo labeling (for example, thiol-reactive Alexa fluor dyes (YANG and MUSSER 2006) and large quantum dots (LOWE *et al.* 2010)). NPC interaction times

during facilitated protein transport were measured as approximately 10ms, with a reported range between 2-34ms (YANG and MUSSER 2006), and RanGTP provided a critical role for the release of large cargo from the NPC (LOWE *et al.* 2010). Most recently, the three-dimensional pathways for importin beta cargo were found to be more peripheral to that for diffusive cargo (Figure II.1D) (MA *et al.* 2012).

Single mRNAs have also been observed moving across the NPC by engineering sequence specific RNA stem-loops into endogenous or inducible transcripts and co-expressing fluorescently-tagged MS2 RNA stem-loop binding proteins (GRUNWALD and SINGER 2010; MOR *et al.* 2010). Using this system, the observed time frame for mRNA transport through the pore was between 180ms (GRUNWALD and SINGER 2010) and 500ms (MOR *et al.* 2010), with two rate-limiting steps: one at the nuclear and one at the cytoplasmic face (GRUNWALD and SINGER 2010). Presumably, the rate-limiting interval at the cytoplasmic face was due to mRNP remodeling to promote directionality. Although both fast and slow (>800ms) transport rates were observed for a single type of mRNA (GRUNWALD and SINGER 2010), mRNP translocation through the NPC occurred 15-fold faster than diffusion through the nucleus (MOR *et al.* 2010), in keeping with the mode of facilitated transport.

By comparing the transport of protein and mRNA, there are some clear differences. Specifically, mRNA transport across the NPC is of longer duration. This might be due to the size differences in the respective protein versus mRNP cargos (Figure II.1D). mRNA export also has a rate-limiting step at the NPC entry site that is not detected for protein transport, and might be attributed to the mRNA quality control and surveillance mechanisms prior to export. For both protein and mRNA transport

single molecule experiments, a striking common conclusion is that cargo entered the NPC and explored the channel in a diffusive or subdiffusive manner with back and forth movements often observed. This suggests that there is no straight path through the NPC and that movement itself is not inherently directional. In addition, it is remarkable that the transport events were most often unsuccessful (15-50% success rate) (YANG and MUSSER 2006; GRUNWALD and SINGER 2010) – meaning that cargo entered, explored, and returned to the original entry face. This raises the question of how the NPC accommodates not only a large amount of successful transport events but also an even larger number of unsuccessful events.

Models impacted by nuclear pore complexity and heterogeneity

Because of the NPC's inherent complexity, reductionist approaches have been required to gain molecular insights into the transport mechanism. Notable innovations have been in the development of *in vitro* nanopores and hydrogels for testing the selective barrier properties with transport receptors and cargo. In a nanopore approach, recombinant FG domains were coupled to a small nanopore (30nm holes in a polycarbonate membrane) (JOVANOVIC-TALISMAN *et al.* 2009). In contrast, the hydrogels self-formed under experimentally determined conditions with recombinant FG domains (for example, (LABOKHA *et al.* 2013). These strategies have been critical in demonstrating that FG domains are sufficient for allowing selective passage of transport receptors. Importantly, the most recent hydrogel study characterized individual FG domains of *Xenopus laevis* on an NPC-wide level and found that the resulting hydrogels had different capacities for selective transport (LABOKHA *et al.* 2013). To become more

effective mimics of the heterogeneous and dynamic whole NPC environment, these systems will require constructing single nanopores and hydrogels with multiple different FG domains included. Because of the now known complexity, one component (one FG domain type) cannot necessarily be considered in isolation, nor can all FG domains be considered the same.

Potentially reflective of divergent FG domain properties, several different models have been proposed for the mechanism of NPC translocation. The most discussed include the entropic barrier and selective phase models. These models differ in how the intermolecular interactions between FG domains contribute to facilitated transport and a selective barrier (reviewed in TERRY and WENTE 2009; AITCHISON and ROUT 2012; HULSMANN *et al.* 2012). The entropic barrier model suggests that the unstructured FG domains function to exclude non-interacting molecules. Alternatively, the selective phase model proposes that inter-domain hydrophobic interactions form a gel-like meshwork which is locally "dissolved" by transport receptor interactions. For both models, continued work is needed to account for the heterogeneity of FG domain properties both *in vivo* and *in vitro*. Due to this heterogeneity, a hybrid model is also quite appealing wherein functions for cohesive (for permeability barrier) and noncohesive (for entropic bristles) interactions are both considered (YAMADA *et al.* 2010). These unexpected complexities in resolving the translocation mechanism provide an exciting challenge for further investigations.

Perspective

From the work to date, a single mechanism of nuclear transport across the NPC likely does not exist; rather, layers of complexity lead to multiple specialized pathways in a given NPC. Whether different transport pathways allow multiple transport events to take place within a single NPC is still unresolved. Classic immuno-EM experiments demonstrated that an individual NPC is capable of carrying out both import and export (FELDHERR *et al.* 1984); however, it has not been tested directly whether such can be simultaneous. Tracking single mRNA transcripts revealed transient association with multiple NPCs before exit (GRUNWALD and SINGER 2010). This might be due to the inherent properties of stochastic cargo movement with the NPC (see above). Alternatively, it is possibly more likely this could reflect a full cargo load for a given NPC inhibiting entry and new translocation events. Other mechanisms at work might involve the absence of specific factors/Nups at a given NPC or quality control mechanisms detecting incomplete processing of the transcript. To directly address questions of simultaneous transport, a future challenge will be to monitor single molecule facilitated transport of different cargoes at the same time within one cell/NPC.

Although it is clear that specialized transport pathways exist within the heterogenous environment of the NPC, it remains to be seen whether different NPCs in a single cell are specialized for distinct types of transport. Distinct differences might exist in the architecture of each NPC as a result of dynamic Nup associations, post-translational or conformational changes in the Nups, and even temporal changes in Nup expression. There is substantive evidence for differential NPC function in specific animal tissues and at different times in cellular differentiation. A recent study found that

a transmembrane Nup (gp210) was absent in proliferating myoblasts, but its expression was required for differentiation into neuroprogenitors (D'ANGELO *et al.* 2012). Using genome-wide RNA-sequencing, the expression of gp210 caused differential regulation of a subset of transcripts without global perturbations on NPC transport. How a transmembrane Nup has these effects is unclear; however, NPC function is evidently altered by differential Nup association. Continued advances in imaging and NPC-wide, or genome wide, approaches will be needed to further analyze NPC mechanisms of specialization on cellular and organism levels.

Finally, the complexity of Nups extends beyond roles at the NPC, as transport-independent and NPC-independent functions have been uncovered for some Nups (reviewed in RAICES and D'ANGELO 2012). Taken together, a full understanding of nuclear pore complexity is needed to strongly position the field in evaluating the molecular mechanisms underlying *nup* mutants linked to human developmental diseases (reviewed in RAICES and D'ANGELO 2012). Based on the wealth of innovations over more than half a century, NPC structure and function has been unveiled as much more complex than anticipated at first glance.

Acknowledgements

We thank Joe Gall (Carnegie Institution for Science) and Markus Sauer (Julius-Maximilians-University Wurzburg) for permission to reprint the images in Figure II.1A and B, respectively; and members of the Wente laboratory and Elizabeth Bowman for discussion. Due to space constraints, we regret not being able to cite all primary

references. The authors were supported by grants from the National Institute of Health (R37GM051219 (S.R.W.) and T32HD007502 (R.L.A.).

CHAPTER III:

Nucleoporin FG Domains Facilitate mRNP Remodeling at the Cytoplasmic Face of the Nuclear Pore Complex

Published, Rebecca L. Adams, Laura J. Terry, and Susan R. Wente, *Genetics*, August, 2014

Abstract

Directional export of mRNA-protein particles (mRNPs) through nuclear pore complexes (NPCs) requires multiple factors. In *Saccharomyces cerevisiae,* the NPC proteins Nup159 and Nup42 are asymmetrically localized to the cytoplasmic face and have distinct functional domains: a phenylalanine-glycine (FG) repeat domain that docks mRNP transport receptors, and domains that bind the DEAD-box ATPase Dbp5 and its activating cofactor Gle1, respectively. We speculated that the Nup42 and Nup159 FG domains play a role in positioning mRNPs for the terminal mRNP remodeling steps carried out by Dbp5. Here we find that deletion (Δ) of both the Nup42 and Nup159 FG domains results in a cold-sensitive poly(A)$^+$ mRNA export defect. The *nup42ΔFG nup159ΔFG* mutant also has synthetic lethal genetic interactions with *dbp5* and *gle1* mutants. RNA crosslinking experiments further indicate that the *nup42ΔFG nup159ΔFG* mutant has a reduced capacity for mRNP remodeling during export. To further analyze the role of these FG domains, we replaced the Nup159 or Nup42 FG domains with FG domains from other Nups. These FG “swaps” demonstrate that only certain FG domains are functional at the NPC cytoplasmic face. Strikingly, fusing the Nup42 FG domain to the carboxy-terminus of Gle1 bypasses the need for the

endogenous Nup42 FG domain, highlighting the importance of proximal positioning for these factors. We conclude that the Nup42 and Nup159 FG domains target the mRNP to Gle1 and Dbp5 for mRNP remodeling at the NPC. Moreover, these results provide key evidence that character and context play a direct role in FG domain function and mRNA export.

Introduction

In eukaryotes, mRNA export from the nucleus is an essential process that is highly regulated, with events sequentially coordinated to ensure proper RNA processing and cytoplasmic fate (reviewed in MOORE 2005; MULLER-MCNICOLL and NEUGEBAUER 2013). In general, transcripts exit the nucleus through nuclear pore complexes (NPCs), large (60 MDa in *S.c.*, 100 MDa in vertebrates) proteinaceous structures that provide an aqueous channel for ions, metabolites, proteins, and ribonuclear protein complexes (RNPs) to cross the nuclear envelope (WENTE and ROUT 2010; BILOKAPIC and SCHWARTZ 2012). For molecules >40kDa, transport through the NPC is facilitated via transport receptors (TRs) which bind both the cargo and NPC proteins (nucleoporins, Nups). For mRNA, binding to TRs is carefully coordinated to allow export only after the message is fully processed in the nucleus (reviewed in MULLER-MCNICOLL and NEUGEBAUER 2013).

A key aspect of NPC function involves different NPC structures performing specific roles to ensure efficient transport. During NPC translocation, TRs interact with a class of Nups known as phenylalanine-glycine (FG) Nups (reviewed in WENTE and ROUT 2010). Each FG Nup has an unstructured domain enriched with FG, glycine-leucine-

phenylalanine-glycine (GLFG), or phenylalanine-any amino acid-phenylalanine-glycine (FxFG) repeats, which are flanked by characteristic polar spacer sequences (DENNING *et al.* 2003; TERRY and WENTE 2009). Each FG Nup is anchored in a specific NPC substructure via non-FG domains that interact with scaffold Nups (Figure I.2). In *S. cerevisiae*, the 11 FG Nups are located either symmetrically or asymmetrically (on the nuclear or cytoplasmic face) in the NPC (ROUT *et al.* 2000; ALBER *et al.* 2007). FG Nups are required for the NPC permeability barrier (HULSMANN *et al.* 2012), and TRs overcome this barrier by interacting with phenylalanine residues of the FG domains (reviewed in WENTE and ROUT 2010). Using a large-scale genetic approach in *S. cerevisiae*, we previously generated a collection of FG deletion mutants in higher order combinations amongst the 11 different FG Nups. This work defined the minimal, functionally important FG domains, and revealed functionally distinct FG pathways used by different TRs (STRAWN *et al.* 2004; TERRY and WENTE 2007; FISEROVA *et al.* 2010).

Importantly, NPC structures involved in the terminal steps of the protein import and export pathways are critical for the action of TRs in the Ran-dependent karyopherin (Kap) family. For example, in addition to their FG repeat domains that bind Kaps, Nups localized asymmetrically at the nuclear NPC face contain key binding sites for coordinated Kap-import cargo disassembly (GILCHRIST *et al.* 2002; GILCHRIST and REXACH 2003; MATSUURA *et al.* 2003; MATSUURA and STEWART 2005; SUN *et al.* 2013). Additionally, at the cytoplasmic NPC face, the mammalian FG Nup358 (RanBP2) functions as a multi-subunit SUMO E3 complex that coordinates SUMO ligase activity, export cargo disassembly through binding the RanGAP, and Kap binding (WERNER *et al.* 2012). Also at the cytoplasmic face, the conserved FG Nups, Nup42 (*S.c.*)/hCG1

(vertebrate) and Nup159 (*S.c.*)/Nup214 (vertebrate) provide important binding sites for the Kap protein export receptor, Crm1 (FLOER and BLOBEL 1999; SABRI *et al.* 2007; ROLOFF *et al.* 2013). Thus, within individual Nups, juxtaposed binding sites for TRs and TR-cargo release factors function to integrate terminal transport steps of transport. It has not been directly investigated whether proximal positioning of binding sites for TRs and cargo release factors is required for mRNP cargo disassembly. We speculate that an mRNP might require combinatorial interactions between Nups, TRs, and mRNP remodeling factors for at the NPC cytoplasmic face.

The mRNA export cargo is defined as an mRNA-protein (mRNP) complex that contains the TR heterodimer Mex67-Mtr2 (Tap-p15 in vertebrates), which is bound through adaptor proteins, such as the poly(A)$^+$ RNA binding protein Nab2 (reviewed in RODRIGUEZ-NAVARRO and HURT 2011; NATALIZIO and WENTE 2013). When the mRNP reaches the NPC cytoplasmic face, it undergoes mRNP remodeling where a subset of RNP proteins, including Mex67 and Nab2, are selectively removed (LUND and GUTHRIE 2005; TRAN *et al.* 2007). The conserved DEAD-box ATPase Dbp5 (DDX19B in vertebrates) catalyzes this mRNP remodeling in a manner that is dependent upon Gle1 and the small molecule inositol hexakisphosphate (IP_6) (ALCAZAR-ROMAN *et al.* 2006; WEIRICH *et al.* 2006; TRAN *et al.* 2007). Dbp5/DDX19B is localized to the NPC cytoplasmic face through interaction with Nup159/Nup214 (HODGE *et al.* 1999; SCHMITT *et al.* 1999; WEIRICH *et al.* 2004), and Gle1 interacts with Nup42/hCG1 (MURPHY and WENTE 1996; HODGE *et al.* 1999; SCHMITT *et al.* 1999; STRAHM *et al.* 1999; WEIRICH *et al.* 2004; KENDIRGI *et al.* 2005). The cycling of interactions between Dbp5, Gle1-IP_6, Nup159, and RNA has been investigated in depth (FOLKMANN *et al.* 2011; HODGE *et al.*

2011; MONTPETIT *et al.* 2011; NOBLE *et al.* 2011). Additionally, we recently discovered that Gle1 self-associates via a conserved coiled-coil domain in its amino-terminal region, and this self-association is required during mRNA export (FOLKMANN *et al.* 2013). However, it is unknown how mRNP remodeling selectivity is dictated, wherein Mex67-Mtr2, Nab2, and potentially other mRNP components are specifically targeted for remodeling.

In addition to having binding sites for the mRNP remodeling factors Dbp5 and Gle1-IP_6, Nup159 and Nup42 also contain FG domains (GORSCH *et al.* 1995; KRAEMER *et al.* 1995; STUTZ *et al.* 1995). These FG domains bind Mex67 *in vitro* (STRASSER *et al.* 2000). Therefore, we hypothesized that the Nup159 and Nup42 FG domains serve to position the mRNP for remodeling by Dbp5, and potentially target the TR Mex67-Mtr2 for release. Using a combination of genetic and biochemical approaches, we have uncovered a role during mRNP remodeling for these FG domains at the cytoplasmic NPC face.

Materials And Methods

Yeast Strains and Growth

Table III.1 lists the yeast strains used in this study. Yeast genetic methods including mating, sporulation, dissection, and transformations were conducted according to standard procedures (SHERMAN 1986). Yeast strains were grown at indicated temperatures in either YPD (2% peptone, 2% dextrose, 1% yeast extract) or selective minimal media lacking appropriate amino acids and supplemented with 2%

Strain	Genotype	Source
SWY2283	*MATa ade2-1::ADE2 ura3-1 his3-11,15 leu2-3,112 lys2 can1-100*	(STRAWN *et al.* 2004)
SWY5703	*MATα ade2-1 ura3-1 his3-11,15 leu2-3 lys2 can1-100*	This Study
SWY2832	*MATα ade2-1::ADE2 ura3-1 his3-11,15 leu2-3,112 lys2 can1-100 HA-LoxP-nup42ΔFG*	(STRAWN *et al.* 2004)
SWY2808	*MATa ade2-1::ADE2 ura3-1 his3-11,15 leu2-3,112 lys2 can1-100 myc-LoxP-nup159ΔFG*	(STRAWN *et al.* 2004)
SWY2846	*MATa ade2-1::ADE2 ura3-1 his3-11,15 leu2-3,112 lys2 can1-100 myc-LoxP-nup159ΔFG HA-LoxP-nup42ΔFG*	(STRAWN *et al.* 2004)
SWY5701	*MATa ade2-1 ura3-1 leu2-3,112 his3-11,15 can1-100 myc-LoxP-nup159ΔFG HA-LoxP-nup42ΔFG*	This Study
SWY5825	*MATa ade2-1::ADE2 ura3-1 his3-11,15 leu2-3,112 lys2 can1-100 myc-LoxP-nup159ΔFG HA-LoxP-nup42ΔFG-GFP:HIS3*	This Study
SWY5826	*MATa ade2-1::ADE2 ura3-1 his3-11,15 leu2-3,112 lys2 can1-100 myc-LoxP-nup159ΔFG-GFP:HIS3 nup42ΔFG*	This Study
SWY5334	*MATa ura3 leu2 his3 rat8-2 (dbp5) +pCA5005*	This Study
SWY4301	*MATa ura3 leu2 his3 trp1 myc-LoxP-nup159ΔFG rat8-2 (dbp5) +pCA5005*	This Study
SWY5542	*MATα ura3 leu2 his3 HA-LoxP-nup42ΔFG rat8-2 (dbp5) +pCA5005*	This Study
SWY4320	*MATα ura3 leu2 his3 trp1 nup42ΔFG myc-LoxP-nup159ΔFG rat8-2 (dbp5) +pCA5005*	This Study
SWY5209	*MATα ura3-1 leu2-3,112 his3-11 trp1-1 gle1-4 +pSW410*	This Study
SWY5208	*MATα ura3-1 leu2-3,112 his3-11 trp1-1 lys2 myc-LoxP-nup159ΔFG gle1-4 +pSW410*	This Study
SWY5206	*MATα ura3-1 leu2-3,112 his3-11 trp1-1 lys2 HA-LoxP-nup42ΔFG gle1-4 +pSW410*	This Study
SWY5207	*MATα ura3-1 leu2-3,112 his3-11 trp1-1 lys2 HA-LoxP-nup42ΔFG myc-LoxP-nup159ΔFG gle1-4 +pSW410*	This Study
Mex67 shuffle	*MATa ade2 his3 leu2 trp1 ura3 mex67::HIS3 +pRS316-MEX67*	(SEGREF *et al.* 1997)
SWY5204	*MATα ade2 his3 leu2 trp1 ura3 HA-LoxP-nup42ΔFG myc-LoxP-nup159ΔFG mex67::HIS3 +pRS316-MEX67*	This Study
SWY5697	*MATα ade2-1 ura3-1 leu2-3,112 his3-11,15 trp1-1 can1-100 gle1::HIS +pSW3345*	This Study
SWY5698	*MATα ade2-1 ura3-1 leu2-3,112 his3-11,15 trp1-1 can1-100 myc-LoxP-nup159ΔFG HA-LoxP-nup42ΔFG gle1::HIS +pSW3345*	This Study
SWY5236	*MATa ura3-1 his3-11,15 leu2-3,112 trp1-1 nab2::HIS3 +pAC717*	This Study

SWY5237	*MATa ura3-1 his3-11,15 leu2-3,112 trp1-1 nab2::HIS3 +pSW3298*	This Study
SWY5238	*MATa ura3-1 his3-11,15 leu2-3,112 trp1-1 HA-LoxP-nup42ΔFG myc-LoxP-nup159ΔFG nab2::HIS3 +pAC717*	This Study
SWY5239	*MATa ura3-1 his3-11,15 leu2-3,112 trp1-1 HA-LoxP-nup42ΔFG myc-LoxP-nup159ΔFG nab2::HIS3 + pSW3298*	This Study
SWY3826	*MATα ade2-1 ura3-1 his3-11,15 leu2-3,112 trp1-1 gle1::HIS3 +pSW399*	(ALCAZAR-ROMAN *et al.* 2010)
SWY4908	*MATα ade2-1 ura3-1 his3-11,15 leu2-3,112 trp1-1 gle1::HIS3 +pSW3743*	(FOLKMANN *et al.* 2013)
SWY4909	*MATα ade2-1 ura3-1 his3-11,15 leu2-3,112 trp1-1 gle1::HIS3 +pSW3742*	(FOLKMANN *et al.* 2013)
SWY4961	*MATα ade2-1 ura3-1 his3-11,15 leu2-3,112 trp1-1 gle1::HIS3 +pSW3760*	(FOLKMANN *et al.* 2013)
SWY5878	*MATα ade2-1 ura3-1 his3-11,15 leu2-3,112 trp1-1 gle1::HIS3 +pSW3936*	This Study
SWY5879	*MATα ade2-1 ura3-1 his3-11,15 leu2-3,112 trp1-1 gle1::HIS3 +pSW3981*	This Study
SWY5880	*MATα ade2-1 ura3-1 his3-11,15 leu2-3,112 trp1-1 gle1::HIS3 +pSW3982*	This Study
SWY5881	*MATα ade2-1 ura3-1 his3-11,15 leu2-3,112 trp1-1 gle1::HIS3 +pSW3983*	This Study
SWY5875	*MATα ura3-1 his3-11,15 leu2-3,112 nup42::KAN^R gle1::HIS3 +pSW410*	This Study
SWY5882	*MATα ura3-1 his3-11,15 leu2-3,112 nup42::KAN^R gle1::HIS3 +pSW399*	This Study
SWY5883	*MATα ura3-1 his3-11,15 leu2-3,112 nup42::KAN^R gle1::HIS3 +pSW3742*	This Study
SWY5885	*MATα ura3-1 his3-11,15 leu2-3,112 nup42::KAN^R gle1::HIS3 +pSW3936*	This Study
SWY5887	*MATα ura3-1 his3-11,15 leu2-3,112 nup42::KAN^R gle1::HIS3 +pSW3982*	This Study
nup42Δ	*MATα his3Δ1 leu2Δ0 lys2Δ0 ura3Δ1 nup42::KAN^R*	(WINZELER *et al.* 1999)
SWY2114	*MATa ade2-1 ura3-1 his3-11,15 trp1-1 leu2-3,112 ipk1::KAN^R nup42::HIS3*	(MILLER *et al.* 2004)
SWY4303	*MATa ura3-1 his3-11,15 trp1-1 leu2-3,112 nup159::KAN^R +pLG4*	This Study

Table III.1 Strain Table

dextrose and 5-fluoroorotic acid (5-FOA; United States Biological) as needed at 1.0 mg/mL.

Vector Construction

Table III.2 lists the vectors used in this study. Vector cloning was performed according to standard molecular biology strategies. FG swap vectors were generated by amplifying a wild type (wt) *NUP* vector to replace the FG domain with a unique restriction site. Swapping FG domains were then amplified with compatible cohesive restriction sites and cloned into the *nupΔFG* vector, with DNA sequencing to confirm the construct.

In Situ Hybridization, Immunofluorescence, and Live Cell Microscopy

Yeast strains were grown to mid-log phase (OD_{600} ~0.5) in YPD media at the indicated temperatures. For live cell imaging, cultures were collected, re-suspended in synthetic complete media, and imaged. For *in situ* hybridization, yeast were processed as described (WENTE and BLOBEL 1993), hybridized with 1ng/μL Cy3-conjugated oligo d(T), stained with 0.1mg/mL DAPI to visualize the nucleus as described in (FOLKMANN *et al.* 2013). For indirect immunofluorescence, yeast were processed as above and labeled as in (HO *et al.* 2000a). Briefly, samples were incubated with anti-Nup159 mouse MAbs (Mab 165C10, (KRAEMER *et al.* 1995) for 16 hrs at 4° followed by incubation with anti-Nup116-C rabbit antibodies (WU600, (IOVINE *et al.* 1995) for 1hr at RT. Bound primary antibodies were detected with Alexa Flour 594-conjugated goat anti-rabbit and 488-conjugated goat anti-mouse IgG (1:200, Molecular Probes) and samples were stained

Plasmid	Description	Source
pSW3801	*NUP42/CEN/LEU2*	This study
pSW3802	*NUP42/CEN/TRP1*	This study
pSW3645	*nup42ΔFG/CEN/LEU2*	This study
pSW3657	*nup42ΔFG/CEN/TRP1*	This study
pSW3662	*nsp42-s-FG^{nup42}/CEN/TRP1*	This study
pSW3658	*nsp42-s-GLFG^{nup57}/CEN/TRP1*	This study
pSW3659	*nsp42-s-FxFG^{nsp1}/CEN/TRP1*	This study
pSW3660	*nsp42-s-GLFG$_{1-12}$ ^{nup116}/CEN/TRP1*	This study
pSW3661	*nsp42-s-GLFG$_{22-33}$ ^{nup116}/CEN/TRP1*	This study
pSW3841	*nsp42-s-FG^{nup159}/CEN/TRP1*	This study
pLG4	*NUP159/URA*	(GORSCH *et al.* 1995)
pSW3647	*NUP159/CEN/TRP1*	This study
pSW3648	*nup159ΔFG/CEN/TRP1*	This study
pSW3692	*nsp159-s-FG^{nup159}/CEN/TRP1*	This study
pSW3693	*nsp159-s-GLFG^{nup57}/CEN/TRP1*	This study
pSW3695	*nsp159-s-FxFG^{nsp1}/CEN/TRP1*	This study
pSW3694	*nsp159-s-FG^{nup42}/CEN/TRP1*	This study
pCA5005	*DBP5/CEN/URA3*	(TSENG *et al.* 1998)
pSW410	*GLE1/CEN/URA3*	(MURPHY and WENTE 1996)
pSW399	*GLE1/CEN/LEU2*	(MURPHY and WENTE 1996)
pSW3345	*gle1$^{K377Q/K378Q}$/CEN/LEU2*	(ALCAZAR-ROMAN *et al.* 2010)
pSW3743	*gle1-136^^{PFQ}/CEN/LEU2*	(FOLKMANN *et al.* 2013)
pSW3742	*gle1-149^^{PFQ}/CEN/LEU2*	(FOLKMANN *et al.* 2013)
pSW3760	*gle1-157^^{PFQ}/CEN/LEU2*	(FOLKMANN *et al.* 2013)
pSW3936	*gle1-FG^{nup42}*	This study
pSW3981	*gle1-FG^{nup42}-136^^{PFQ}/CEN/LEU2*	This study
pSW3982	*gle1-FG^{nup42}-149^^{PFQ}/CEN/LEU2*	This study
pSW3983	*gle1-FG^{nup42}-157^^{PFQ}/CEN/LEU2*	This study
pRS316-MEX67	*MEX67/CEN/URA3*	(SEGREF *et al.* 1997)
pRS314-MEX67	*MEX67/CEN/TRP1*	(SEGREF *et al.* 1997)
pRS314-mex67-5	*Mex67-5/CEN/TRP1*	(SEGREF *et al.* 1997)
pAC717	*NAB2/CEN/LEU2*	(MARFATIA *et al.* 2003)
pSW3298	*nab2-C437S/CEN/LEU2*	(TRAN *et al.* 2007)

Table III.2 Vector Table

with 0.1mg/mL DAPI. Wide-field images were acquired using a microscope (BX50; Olympus) equipped with a motorized stage (Model 999000, Ludl), Olympus 100× NA1.3 UPlanF1 objective, and digital charge coupled device camera (Orca-R2; Hamamatsu). Images were processed with ImageJ (NIH) or Adobe Photoshop CS6.

UV Crosslinking and Immunoblotting

UV crosslinking was performed essentially as described (ANDERSON *et al.* 1993; TRAN *et al.* 2007). 100mL cultures were grown to late-log phase (OD_{600} ~0.8) at the indicated temperatures, crosslinked using a UV Stratalinker (Stratagene) with 254-nm UV light for 2×2.5min, lysed by bead-beating, and poly(A)$^+$ RNA was purified by antisense chromatography using oligo d(T) resin (Applied Biosystems, Foster City, CA) and the manufacturer's protocol. After RNase treatment, samples were separated by SDS-PAGE and immunoblotting was conducted with affinity-purified rabbit anti-Nab2 (ASW 44, TRAN *et al.* 2007) and affinity-purified rabbit anti-Cbp80 (GORLICH *et al.* 1996) antibodies. Enriched protein was quantitated by densitometry and reported as the amount of protein bound to RNA versus the total in lysate. This ratio was normalized between strains with wt set to 1.0.

For whole-cell lysate immunoblotting, cells were grown to mid-log phase, and equal OD_{600} units of cell numbers were collected by centrifugation. Cells were re-suspended in SDS loading buffer (20% glycerol, 4%SDS, 50mM Tris-HCl pH 6.8, 100mM DTT, 0.01% bromophenol blue), lysed by vortexing with glass beads, and boiled 5min. Lysates were then separated by SDS-PAGE and blotted using affinity-purified guinea pig anti-Gle1 (ASW 43.2 (ALCAZAR-ROMAN *et al.* 2010), affinity-purified chicken

anti-Nup159-NTD (ASW 55), or anti-yPgk1 (Invitrogen). The anti-Nup159-NTD antibody was generated against purified His_6-Nup159-NTD (NOBLE *et al.* 2011) and affinity purified using the same antigen. Alexa Flour 650- or 700-conjugated secondary antibodies (1:5000, Molecular Probes) were visualized with the Li-Cor Odyssey scanner (Lincoln, NE).

Quantitative PCR

Q-PCR was performed as described in (BURNS and WENTE 2014). Indicated strains were grown to OD_{600} 0.5-1.0 at 30° or 16°, and total RNA was extracted using the hot acidic phenol method. RNA was DNase treated and reverse transcribed using MultiScribe Reverse Transcriptase (Invitrogen). cDNA levels were quantified with real-time PCR using iQ SYBR green PCR master mix and a CFX96 Quantitative PCR Thermocycler (Biorad). Levels of transcripts from the poly-adenylated transcripts *PGK1* and *ACT1* were normalized to the non-poly-adenylated RNA *SCR1*, and this ratio was normalized between strains with wt set to 1.0. Primers used: *ACT1 Fo: CTCCACCACTGCTGAAAGAGAA, ACT1 Re: CGAAGTCCAAGGCGACGTAA, PGK1 Fo: TTCTCTGCTGATGCCAACAC, PGK1 Re: ATTCGAAAACACCTGGTGGA, SCR1 Fo: AACCGTCTTTCCTCCGTCGTAA, SCR1 Re: CTACCTTGCCGCACCAGACA*.

Assay for Heat Shock Protein Production

The [^{35}S]methionine incorporation assay was performed as described (CARMODY *et al.* 2010). Briefly, strains were grown to early-log phase (OD_{600} ~0.2) in synthetic complete medium lacking methionine and leucine (SC -Met -Leu) at 25°, collected and re-suspended in 500µL SC -Met -Leu. The sample was split in half, and 250µL SC -Met -Leu at 59° was added to one tube that was then incubated for 15min at 42° (heat

shocked sample), and 250µL SC -Met -Leu at 25° was added to the other tube and incubated at room-temperature for 15min (control sample). The samples were then radiolabeled by addition of 50µCi of [^{35}S]methionine, and incubated an additional 15min at the indicated temperature before harvesting by centrifugation at 4°. The cells were washed with 4° SC -Met -Leu and lysed in 25µl SDS loading buffer at 100° for 5min. Samples were separated by SDS-PAGE, and the resulting gel was dried and exposed to autoradiography film.

Results

FG domains at the NPC cytoplasmic face function in mRNP remodeling

Previous studies reported that a *nup42ΔFG nup159ΔFG* double mutant lacking the FG domains of both Nup159 and Nup42 is viable (STRAWN *et al.* 2004; ZEITLER and WEIS 2004). We carefully analyzed the growth of this mutant and observed cold-sensitivity, but no growth defects at higher temperatures (Figure III.1A). In liquid culture at 16°C, the *nup42ΔFG nup159ΔFG* strain displayed a significantly longer doubling time compared to either single mutant or a wild type (wt) strain (Figure III.2A). To analyze whether this growth defect corresponds to an mRNA export defect, we performed *in situ* analysis for poly(A)$^+$ localization after growth at 30° or shifting to 16° for 12 hours. At 16°, we observed a reproducible mRNA export defect in *nup42ΔFG nup159ΔFG* compared to wt (Figure III.2B). Specifically, poly(A)$^+$ RNA localized to puncta within the nucleus (as judged by localization relative to DAPI signal) in approximately 25% of the cells. This phenotype correlates with other reported mRNA export defects in *nup* mutants, e.g. *nup60D* (POWRIE *et al.* 2011). Importantly, this increase in nuclear signal

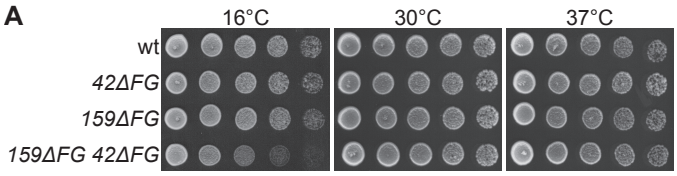
A
16°C
30°C
37°C
wt
42ΔFG
159ΔFG
159ΔFG 42ΔFG

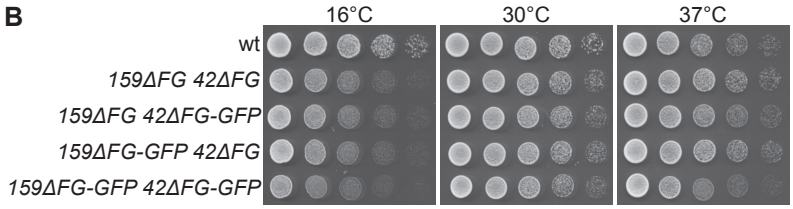
B
16°C
30°C
37°C
wt
159ΔFG 42ΔFG
159ΔFG 42ΔFG-GFP
159ΔFG-GFP 42ΔFG
159ΔFG-GFP 42ΔFG-GFP

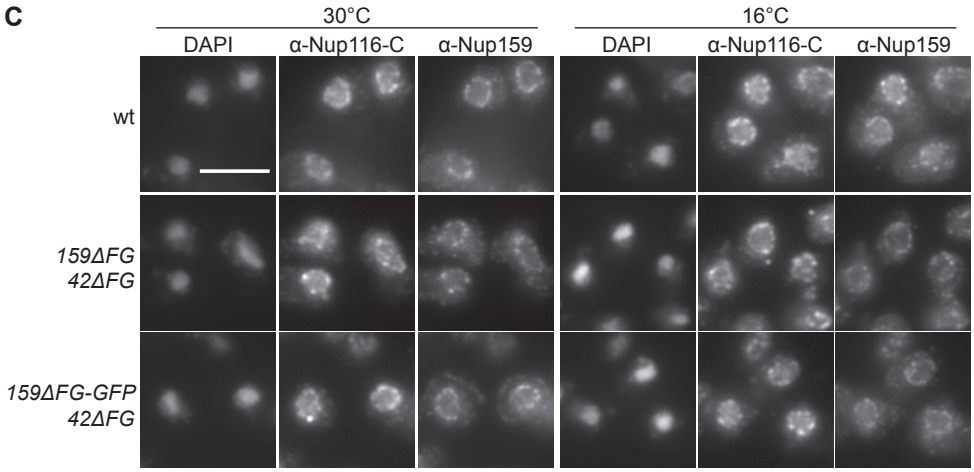
C
30°C
16°C
DAPI
α-Nup116-C
α-Nup159
DAPI
α-Nup116-C
α-Nup159
wt
159ΔFG
42ΔFG
159ΔFG-GFP
42ΔFG

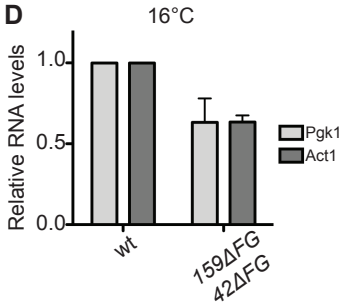
D
16°C
Relative RNA levels
1.0
0.5
0.0
Pgk1
Act1
wt
159ΔFG
42ΔFG

Figure III.1. The cold-sensitive mRNA export defect of *nup42ΔFG nup159ΔFG* is not due to mislocalized or non-functional nup42 and nup159 proteins or altered poly(A)$^+$ RNA levels.
(A) Deletion of both Nup42 and Nup159 FG domains results in a growth defect at cold temperatures. Yeast strains were grown at 30° and five-fold serially diluted on YPD plates for growth at the indicated temperature. (B) GFP fusions of nup42ΔFG and nup159ΔFG do not result in enhanced growth defects. Yeast strains were grown at 30° and five-fold serially diluted on YPD plates for growth at the indicated temperature. (C) nup159ΔFG and nup159ΔFG-GFP localize to the nuclear envelope at the permissive and restrictive temperatures. Indicated strains were grown at 30°, shifted to 16° or 30° overnight, and processed for immunofluoresence using the indicated antibodies. DAPI staining marks the nucleus. Scale bar, 5μm. (D) Steady-state levels of poly-adenylated transcripts are decreased in *nup42ΔFG nup159ΔFG*. Indicated strains were grown at 30°, shifted to 16° or 30° overnight, and total RNA was isolated. Q-PCR analysis of the resulting cDNA was performed for Pgk1, and Act1, and normalized to the non-poly-adenylated Scr1 RNA. Wt levels were set to 1.0, and error bars indicate SEM of triplicate biological replicates. Levels are likely decreased due to feedback mechanisms that reduce transcription in mRNA export mutants.

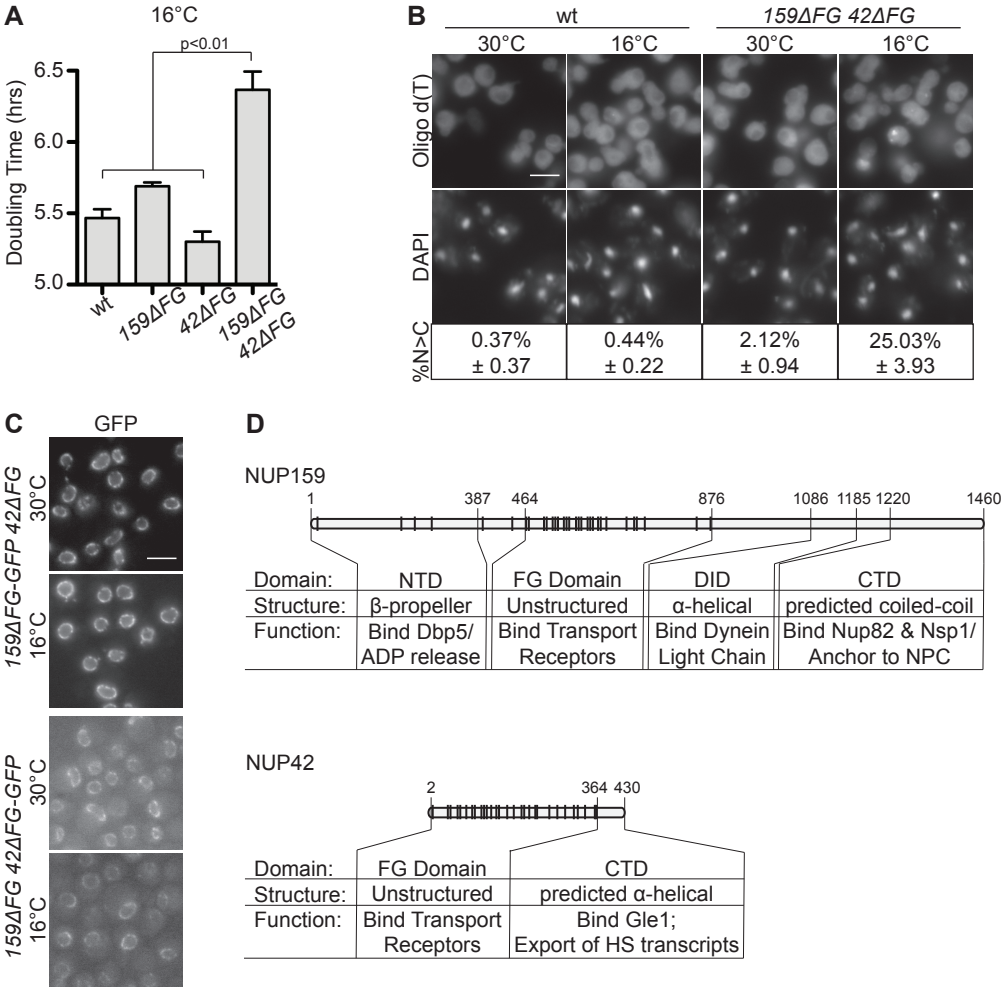
A
16°C
p<0.01
Doubling Time (hrs)
6.5
6.0
5.5
5.0
wt
159ΔFG
42ΔFG
159ΔFG 42ΔFG
B
wt
159ΔFG 42ΔFG
30°C
16°C
30°C
16°C
Oligo d(T)
DAPI
%N>C
0.37% ± 0.37
0.44% ± 0.22
2.12% ± 0.94
25.03% ± 3.93
C
GFP
159ΔFG-GFP 42ΔFG
30°C
16°C
159ΔFG 42ΔFG-GFP
30°C
16°C
D
NUP159
1
387
464
876
1086
1185
1220
1460
Domain: NTD FG Domain DID CTD
Structure: β-propeller Unstructured α-helical predicted coiled-coil
Function: Bind Dbp5/ ADP release Bind Transport Receptors Bind Dynein Light Chain Bind Nup82 & Nsp1/ Anchor to NPC
NUP42
2
364
430
Domain: FG Domain CTD
Structure: Unstructured predicted α-helical
Function: Bind Transport Receptors Bind Gle1; Export of HS transcripts

Figure III.2. Deletion of FG domains on the cytoplasmic face of the NPC results in a cold-sensitive mRNA export defect.
(A) *nup42ΔFG nup159ΔFG* has a cold-sensitive growth defect. The indicated strains were grown to early log phase (OD_{600} ~0.2) at 16°, with OD_{600} measurements taken every 3hrs and normalized to time=0, and doubling times were determined. Graph displays average of three independent experiments, and error bars indicate SEM. (B) *nup42ΔFG nup159ΔFG* has an mRNA export defect at 16°. In situ hybridization with an oligo d(T) probe for poly(A)$^+$ RNA localization was conducted on indicated mutants after growth at 30° and shifting to 16° or 30° overnight. DAPI staining marks the nucleus. Scale bar, 5μm. Quantification of three independent experiments of >100 cells for each strain is shown below images. %N>C indicates the percentage of cells with increased nuclear poly(A)$^+$ signal (as puncta or diffuse nuclear signal). Uncertainty (+/-) indicates SEM. (C) nup42ΔFG-GFP and nup159ΔFG-GFP are localized at the NPC. Cells were grown at 30°, shifted to 16° or 30° for 12hrs, and imaged by wide-field live-cell direct fluorescence microscopy. Scale bar, 5μm. (D) Diagram depicting functional and structural domains of Nup159 and Nup42 as determined by prior studies (DEL PRIORE et al. 1997; SAAVEDRA et al. 1997; STUTZ et al. 1997; BELGAREH et al. 1998; HURWITZ et al. 1998; SCHMITT et al. 1999; STRAHM et al. 1999; BAILER et al. 2000; VAINBERG et al. 2000; DENNING et al. 2003; STRAWN et al. 2004; WEIRICH et al. 2004; STELTER et al. 2007; NOBLE et al. 2011; YOSHIDA et al. 2011), to scale according to primary structure. NTD, amino-terminal domain; DID, dynein-interacting domain; CTD, carboxy-terminal domain.

of poly(A)$^+$ RNA was not due to increased transcription as quantitative PCR showed transcript levels in *nup42ΔFG nup159ΔFG* compared to wt cells were actually lower (Figure III.1D). This decrease in transcript levels is likely due to feedback between the inhibition in mRNA export with transcription and nuclear mRNA decay (reviewed in RODRIGUEZ-NAVARRO and HURT 2011). These results suggested that the Nup159 and Nup42 FG domains perform a function, though not essential, during mRNA export.

Others have shown that the temperature-sensitive mRNA export defect in a *nup159* mutant (*rat7-1*) is due to loss of Nup159 association with the NPC and its subsequent degradation (DEL PRIORE *et al.* 1996). Therefore, as controls, the sequence encoding GFP was fused to either *nup42ΔFG* or *nup159ΔFG* to determine whether Nup localization was altered. At either the permissive or non-permissive growth temperature (30° or 16°), nup42ΔFG-GFP and nup159ΔFG-GFP localized to the nuclear envelope rim (Figure III.2C). This observation is concordant with the fact that domains outside of the FG region are sufficient for NPC localization (Figure III.2D) (DEL PRIORE *et al.* 1997; STUTZ *et al.* 1997). Furthermore, addition of the GFP tags did not alter the function of these proteins, as minimal enhanced growth defects were observed with tagged strains (Figure III.1B). As determined by immunofluorescence microscopy (Figure III.1C), GFP-tagged and untagged nup159ΔFG proteins also localized similarly to wt Nup159 (Figure III.1C). Therefore, we concluded that the *nup42ΔFG nup159ΔFG* growth defect is due to loss of function of the FG domains.

Roles for Nup159 and Nup42 in mRNA export were previously attributed to their respective binding of Dbp5 and Gle1 at the NPC (reviewed in FOLKMANN *et al.* 2011). The regions that interact with Dbp5 and Gle1 are adjacent to the FG domains in Nup159

and Nup42 (Figure III.2D). Therefore, we tested for genetic interactions between the *nup42ΔFG nup159ΔFG* mutant and mutants linked to factors involved in mRNA export. Synthetic lethality was observed when *nup42ΔFG nup159ΔFG* was combined with a temperature-sensitive *dbp5* mutant, *rat8-2* (Figure III.3A) (SNAY-HODGE *et al.* 1998), and when *nup42ΔFG* alone was combined with the *gle1-4* temperature sensitive mutant (Figure III.3B) (MURPHY and WENTE 1996). Notably, synthetic lethality was not observed when *nup42ΔFG nup159ΔFG* was combined with *mex67-5*, where mRNA export is perturbed prior to NPC docking (Figure III.3C) (SEGREF *et al.* 1997; SANTOS-ROSA *et al.* 1998).

We also observed an enhanced growth defect when we combined the *nup42ΔFG nup159ΔFG* mutant with the $gle1^{KK>QQ}$ mutant in which the IP_6 binding sites on Gle1 are altered (Figure III.3D) (ALCAZAR-ROMAN *et al.* 2010). We next tested whether this growth defect correlated with an increased mRNA export defect at 30°. After shifting to 30° for 3 hours, there was an increased mRNA export defect in *nup42ΔFG nup159ΔFG* $gle1^{KK>QQ}$ (57%) relative to $gle1^{KK>QQ}$ alone (22%) (Figure III.3E). Notably, triple mutant cells appeared larger and differently-shaped, likely due to sickness caused by the mRNA export defect. Therefore, deletion of the Nup159 and Nup42 FG domains contributed to an mRNA export defect and resulted in lethality when combined with mutations in genes encoding factors involved in mRNP remodeling at the NPC cytoplasmic face.

Given that the Nup42 and Nup159 FG domains are adjacent to binding sites for mRNP remodeling factors (Gle1-IP_6 and Dbp5 respectively), and our observed genetic interactions with these same mRNP remodeling factors, we hypothesized that the FG

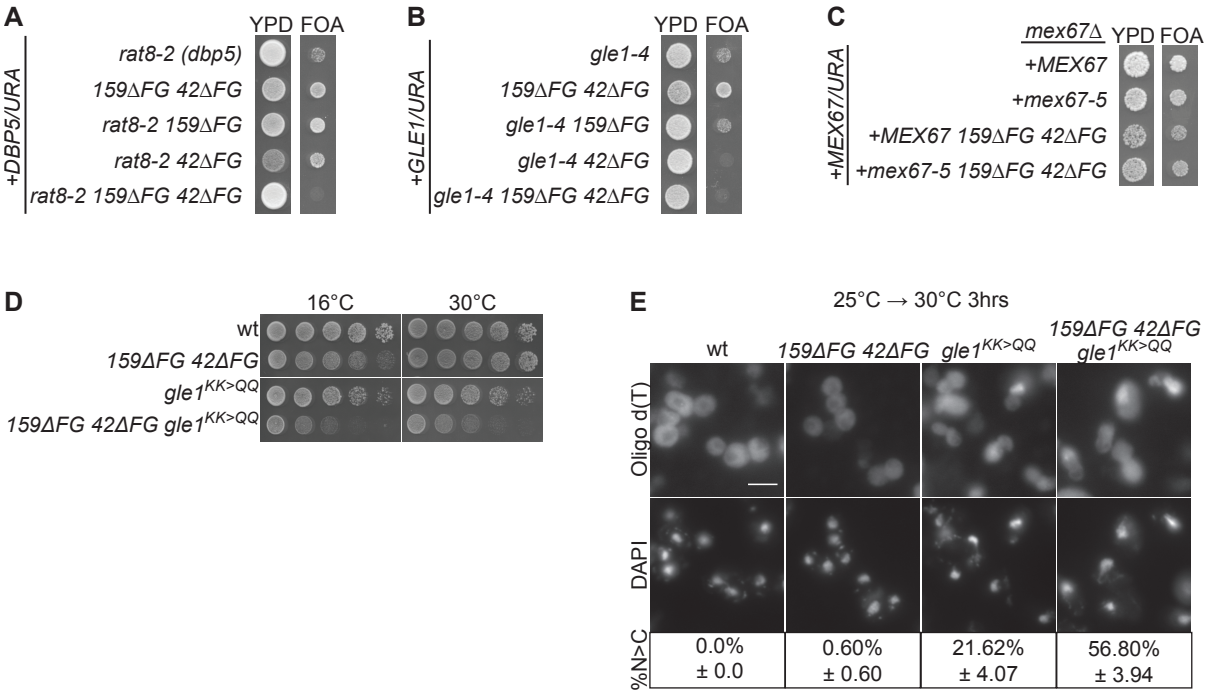

Figure III.3. *nup42ΔFG nup159ΔFG* exhibits genetic interactions with mRNP remodeling mutants.
(A) *nup42ΔFG nup159ΔFG* is synthetically lethal with *rat8-2* (dbp5). Strains bearing the indicated alleles in addition to a *DBP5/URA* vector were spotted onto YPD or 5-FOA at 25°. Failure to grow on 5-FOA indicates synthetic lethality. (B) *nup42ΔFG* is synthetically lethal with *gle1-4*. Strains bearing the indicated alleles, in addition to a *GLE1/URA* vector, were spotted onto YPD or 5-FOA at 25°. (C) *nup42ΔFG nup159ΔFG* is not synthetically lethal with *mex67-5*. Strains bearing the indicated alleles in addition to a *MEX67/URA* vector were spotted onto YPD or 5-FOA at 25°. (D) *nup42ΔFG nup159ΔFG gle1$^{KK>QQ}$* has an enhanced growth defect. Yeast strains were grown at 25° and five-fold serially diluted on YPD plates for growth at the indicated temperature. (E) *nup42ΔFG nup159ΔFG gle1$^{KK>QQ}$* has an enhanced mRNA export defect. *In situ* hybridization with an oligo d(T) probe for poly(A)$^+$ RNA localization was conducted on indicated mutants after growth at 25° and shifting to 30° for 3hrs. DAPI staining marks the nucleus. Scale bar, 5μm. Quantification of three independent experiments of >100 cells for each strain is shown below images. %N>C indicates the percentage of cells with increased nuclear poly(A)$^+$ signal. Uncertainty (+/-) indicates SEM.

domains at the cytoplasmic NPC face function in mRNP remodeling. If so, since Nab2 is a target of Dbp5 remodeling *in vivo*, these mutants should show increased levels of Nab2 association with mRNA. A UV crosslinking and poly(A)$^+$ mRNP isolation procedure was used to analyze the level of Nab2 bound to mRNA in *nup42ΔFG nup159ΔFG* cells after growth at 16° for 12 hours. Cbp80 was used as a control for a protein that is removed after the Dbp5 mRNP remodeling process (with displacement occurring during the pioneer round of translation (ISHIGAKI *et al.* 2001)). An approximately two-fold increased association of Nab2 with poly(A)$^+$ RNA was observed in *nup42ΔFG nup159ΔFG* relative to wt (Figure III.4A, B). Importantly, the levels of Cbp80 associated with poly(A)$^+$ RNA did not change in the *nup42ΔFG nup159ΔFG* mutant compared to wt. If the increased levels of Nab2 associated with poly(A)$^+$ RNA reflected a defect in mRNP remodeling, we speculated that the *nup42ΔFG nup159ΔFG* cold-sensitivity should be rescued by decreasing the stability of the mRNP. The *nab2-C437S* mutant alters one of the Nab2 zinc finger motifs and results in decreased affinity for RNA and a less-stable mRNP, which allows partial rescue of the *rat8-2* (*dbp5*) phenotype (TRAN *et al.* 2007; BROCKMANN *et al.* 2012). We found that expression of *nab2-C437S* also partially rescued the cold-sensitivity of *nup42ΔFG nup159ΔFG*, indicating that the growth defect was due at least in part to defective mRNP remodeling (Figure III.4C).

FG domains have intrinsically distinct functions

Because the Nup159 and Nup42 FG domains were essential in combination with the *rat8-2 (dbp5)* mutant, we used the *rat8-2 (dbp5) nup42ΔFG nup159ΔFG* triple

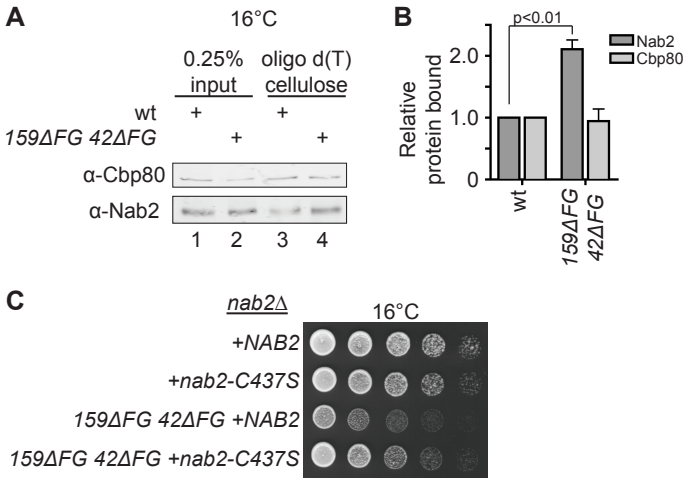

Figure III.4. Deletion of the FG domains on the cytoplasmic face of the NPC results in an mRNP remodeling defect in vivo.
(A & B) *nup42ΔFG nup159ΔFG* has increased Nab2 association with poly(A)$^+$ RNA. The association of Nab2 and Cbp80 proteins with poly(A)$^+$ RNA was assessed by shifting strains to 16° overnight, crosslinking with 254-nm UV light, isolation of RNA by antisense chromatography, and immunoblotting after treatment with RNase. (A) Representative immunoblot. (B) The level of Nab2 and Cbp80 bound is indicated as a ratio of protein bound to poly(A)$^+$ RNA relative to total cellular protein in each strain, with the wt ratio normalized to 1. Graph indicates the average of three independent experiments, and error bars indicate SEM. (C) *nab2-C437S* partially rescues the cold-sensitivity of *nup42ΔFG nup159ΔFG*. Yeast strains were grown at 30° and five-fold serially diluted on YPD plates for growth at 16°.

mutant to analyze whether other FG domains can functionally compensate when anchored to the same location in the NPC. A series of “FG swap” expression vectors were generated in which the endogenous FG domain was replaced with an FG domain from another Nup (Figure III.5A). We tested the normally symmetrically localized Nup57-GLFG and Nsp1-FXFG domains as well as the Nup42-FG and Nup159-FG domains. Expression of all of the FG swap constructs was validated genetically and/or by immunoblotting (Figure III.6). As expected, vectors expressing only *nup42ΔFG* or *nup159ΔFG* did not rescue the synthetic lethality of *rat8-2 (dbp5) nup42ΔFG nup159ΔFG* (Figure III.5B, C). This result indicates that the defect in this strain was not due to the HA/myc and LoxP sites that remain from generation of the chromosomal FG deletions in the *nup42ΔFG nup159ΔFG* mutant, as we had observed with one FG deletion strain (*nup49ΔGLFG*; (TERRY and WENTE 2007). Moreover, when the endogenous FG domain was swapped in, lethality was rescued (Figure III.5B, C). Interestingly, when the Nup42 FG domain was swapped into Nup159, the lethality was rescued. However, when the Nup159 FG domain was swapped into Nup42, the lethality was not rescued. Additionally, the Nup57 GLFG domain only rescued when swapped into Nup42, and the FXFG domain of Nsp1 did not rescue when swapped into either Nup. These results reinforced our previous conclusion that FG domains are functionally distinct (TERRY and WENTE 2007). Furthermore, these results demonstrated that although the FG domains at the cytoplasmic NPC face perform partially redundant functions, they also have distinct features as evidenced by the differential rescue.

Based on the distinct results with the Nup57-GLFG and Nsp1-FXFG swaps, we further tested for rescue with the Nup116 GLFG domain that shows preferential binding

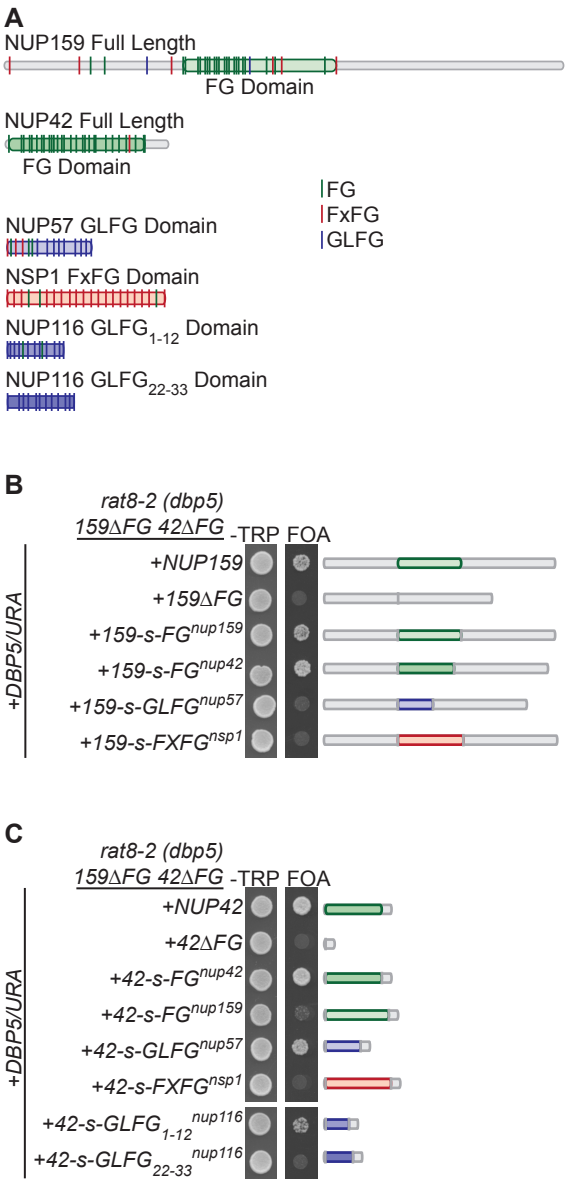

Figure III.5. FG swaps reveal specificity of FG domain function.
(A) Diagram depicting type and location of FG repeats for indicated FG domains. The FG domain is shown as delineated by (STRAWN et al. 2001) (for nup116GLFG$_{1-12}$ and nup116GLFG$_{22-33}$) and (STRAWN et al. 2004). Diagram is to scale according to primary structure. (B) The Nup42 FG domain can functionally compensate for the Nup159 FG domain. *rat8-2 (dbp5) nup42ΔFG nup159ΔFG* mutants containing *nup159-s-FG/TRP* FG swap vectors in addition to a *DBP5/URA* vector were spotted onto -Trp synthetic media or 5-FOA at 25°. Growth on 5-FOA indicates functional complementation. (C) The Nup57 GLFG domain and a Nup116 GLFG subdomain that bind Mex67 can functionally compensate for the Nup42 FG domain. *rat8-2 (dbp5) nup42ΔFG nup159ΔFG* mutants containing *nup42-s-FG/TRP* FG swap vectors in addition to a *DBP5/URA* vector were spotted onto -Trp synthetic media or 5-FOA at 25°.Growth on 5-FOA indicates functional complementation.

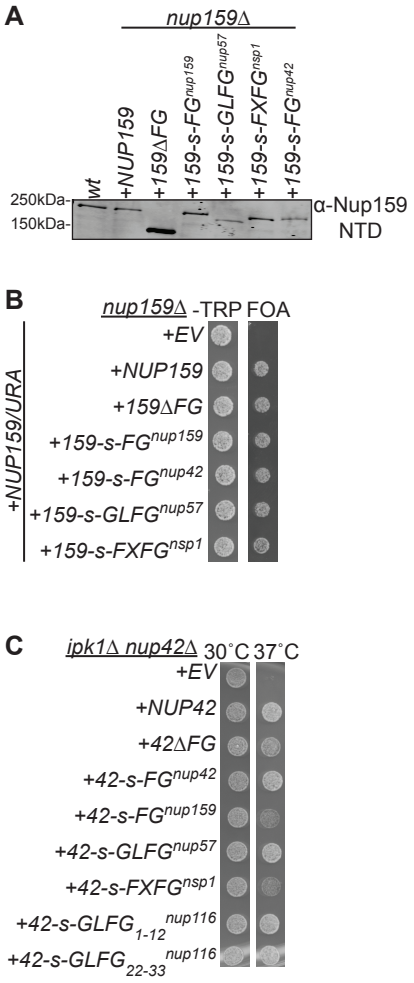

Figure III.6. FG swap constructs are expressed and functional.
(A) *nup159-s-FG* constructs are expressed. Lysates from a wt strain or *nup159Δ* mutants expressing *nup159-s-FG* vectors were separated by SDS-PAGE and immunoblotted using an α-Nup159-NTD antibody. (B) *nup159-s-FG* constructs are functional. *nup159Δ* strains containing empty vector (*EV*) or *nup159-s-FG/TRP* vectors were spotted onto -TRP synthetic media or 5-FOA at 25°. Growth on 5-FOA indicates functional complementation. (C) *nup42-s-FG* constructs are functional. *nup42Δ ipk1Δ* mutants containing empty vector (*EV*) or *nup42-s-FG/TRP* vectors were spotted onto -TRP synthetic media at the indicated temperature. Growth at 37° indicates functional complementation.

in different regions for specific TRs. Yeast two hybrid analysis has shown that the amino-terminal GLFG repeat region of Nup116, $GLFG_{1\text{-}12}$, interacts with Mex67, and the carboxy-terminal repeat region, $GLFG_{22\text{-}33}$, interacts with Kap95 (STRAWN *et al.* 2001). We swapped these subdomains into Nup42 to analyze whether each domain could rescue the synthetic lethality of the *rat8-2 (dbp5) nup42ΔFG nup159ΔFG* mutant. Importantly, *nup42-s-*$GLFG_{1\text{-}12}^{nup116}$ rescued lethality, but *nup42-s-*$GLFG_{22\text{-}33}^{nup116}$ did not (Figure III.5C), suggesting that FG binding to Mex67 was potentially critical in this mutant.

A gle1-FG fusion bypasses the requirement for the endogenous Nup42 FG domain

The carboxy-terminal, non-FG domain (CTD) of Nup42 is required for heat shock mRNA export and in part for localization of Gle1 to the NPC (STUTZ *et al.* 1995; SAAVEDRA *et al.* 1997; STUTZ *et al.* 1997). We recently uncovered an essential function for Nup42 when Gle1 self-association is perturbed by insertion of PFQ residues in the Gle1 coiled-coil region after residues 136 or 149 (designated *gle1*$^{\wedge PFQ}$ mutants) (FOLKMANN *et al.* 2013). As we reported, the *nup42Δ gle1-136*$^{\wedge PFQ}$ mutant is synthetically lethal, the *nup42Δ gle1-149*$^{\wedge PFQ}$ has fitness defects, and the *nup42Δ gle1-157*$^{\wedge PFQ}$ mutant serves as a control with no enhanced defects. To analyze which domain of Nup42 is important in the *nup42D gle1-136*$^{\wedge PFQ}$ mutant, vector complementation studies were conducted. Although expression of full-length *NUP42* rescued the synthetic lethality of *nup42Δ gle1-136*$^{\wedge PFQ}$, *nup42ΔFG* did not (Figure III.7B). This indicated that the FG domain of Nup42 is essential when Gle1 self-association is perturbed.

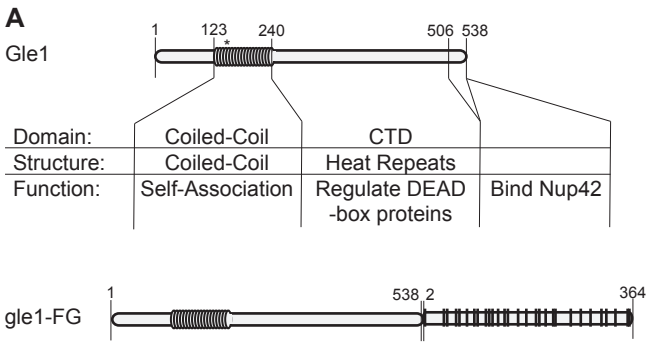
A
Gle1
1
123
240
506
538
Domain:
Coiled-Coil
CTD
Structure:
Coiled-Coil
Heat Repeats
Function:
Self-Association
Regulate DEAD -box proteins
Bind Nup42
gle1-FG
1
538
2
364

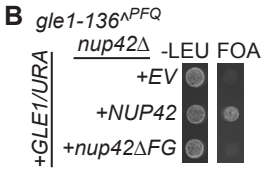
B
gle1-136^PFQ
nup42Δ
-LEU
FOA
+GLE1/URA
+EV
+NUP42
+nup42ΔFG

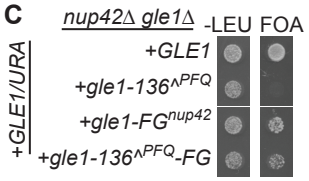
C
nup42Δ gle1Δ
-LEU
FOA
+GLE1/URA
+GLE1
+gle1-136^PFQ
+gle1-FG^nup42
+gle1-136^PFQ-FG

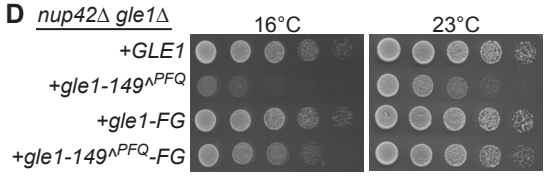
D
nup42Δ gle1Δ
16°C
23°C
+GLE1
+gle1-149^PFQ
+gle1-FG
+gle1-149^PFQ-FG

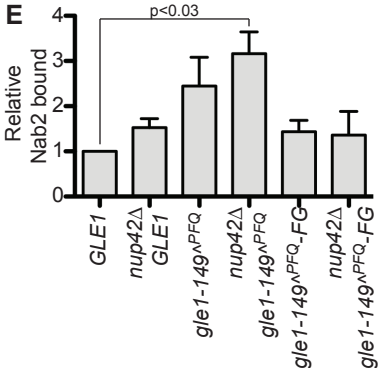
E
p<0.03
Relative Nab2 bound
0
1
2
3
4
GLE1
nup42Δ GLE1
gle1-149^PFQ
nup42Δ gle1-149^PFQ
gle1-149^PFQ-FG
nup42Δ gle1-149^PFQ-FG

Figure III.7. A *gle1-FG* chimera complements *nup42Δ gle1* mutants.
(A) Diagram depicting functional and structural domains of Gle1, to scale according to primary structure, and a diagram of the gle1-FG fusion. Asterisk indicates location of PFQ insertions. (B) The Nup42 FG domain is essential when Gle1 self-association is perturbed. *nup42Δ gle1-136^^{PFQ}* mutants containing a *GLE1/URA* vector in addition to an empty vector (*EV*) or *nup42/TRP* vectors were spotted onto -Trp synthetic media or 5-FOA at 25°. Growth on 5-FOA indicates functional complementation. (C) *gle1-136^^{PFQ}-FG* rescues synthetic lethality of *nup42Δ gle1-136^^{PFQ}*. *nup42Δ gle1Δ* mutants containing a *GLE1/URA* vector in addition to *gle1-136^^{PFQ}/LEU* vectors without or with carboxy-terminal FG fusions were spotted onto -Leu synthetic media or 5-FOA at 25°. (D) *gle1-149^^{PFQ}-FG* partially rescues the synthetic growth defect of *nup42Δ gle1-149^^{PFQ}*. *nup42Δ gle1Δ* mutants containing *gle1-149^^{PFQ}/LEU* vectors without or with carboxy-terminal FG fusions were spotted onto YPD plates to grow at the indicated temperatures. (E) *gle1-149^^{PFQ}-FG* rescues the mRNP remodeling defect of *nup42Δ gle1-149^^{PFQ}*. The association of Nab2 protein with poly(A)$^+$ RNA was assessed by shifting strains to 16° for 3hrs, UV crosslinking, isolation of RNA by antisense chromatography, and immunoblotting after treatment with RNase. The level of Nab2 bound is indicated as a ratio of Nab2 bound to poly(A)$^+$ RNA relative to total cellular protein in each strain, with the GLE1 ratio being normalized to 1. Graph indicates the average of three independent experiments, and error bars indicate SEM.

Taken together, we hypothesized that Nup159 and Nup42 serve as a scaffold to allow coincident, adjacent binding of the exporting mRNP with remodeling factors. To investigate this further, we generated a construct expressing a fusion between Gle1 and the FG domain of Nup42, *gle1-FG* (Figure III.7A). We first tested whether this fusion rescued the synthetic lethality of *nup42Δ gle1-136^PFQ*, because this lethality is due to the loss of the Nup42 FG domain. We next tested the effect of inserting PFQ residues after amino acid residues 136, 149, or 157 in the *gle1-FG*, generating *gle1-136^PFQ-FG*, *gle1-149^PFQ-FG*, and *gle1-157^PFQ-FG* constructs. All *gle1-FG* constructs were expressed and rescued a *gle1Δ* mutant with minimal growth defects (Figure III.8). Importantly, *nup42Δ gle1-136^PFQ-FG* was not synthetically lethal, whereas *nup42Δ gle1-136^PFQ* was (Figure III.7C). We also observed that although *nup42Δ gle1-149^PFQ* was not synthetically lethal, it did result in an enhanced growth defect, particularly at cold temperatures (Figure III.7D). Fusing the Nup42 FG domain to gle1-149^PFQ rescued the *nup42Δ gle1-149^PFQ* enhanced growth defect (Figure III.7D). Using the UV crosslinking assay, the level of Nab2 bound to poly(A)$^+$ RNA was measured in the *gle1-149^PFQ* mutant strains. At 16°, *nup42Δ gle1-149^PFQ* had approximately three-fold more Nab2 bound to transcripts than the *GLE1* wt strain (Figure III.7E, column 4 & 1, respectively; Figure III.9). However, *nup42Δ gle1-149^PFQ-FG* had a decreased level of Nab2 bound which was not statistically different from wt levels (Figure III.7E, column 6). We concluded that the interaction between Gle1 and the Nup42-CTD, at least in part, serves to scaffold the Nup42 FG domain adjacent to Gle1 and this positioning is important for mRNP remodeling.

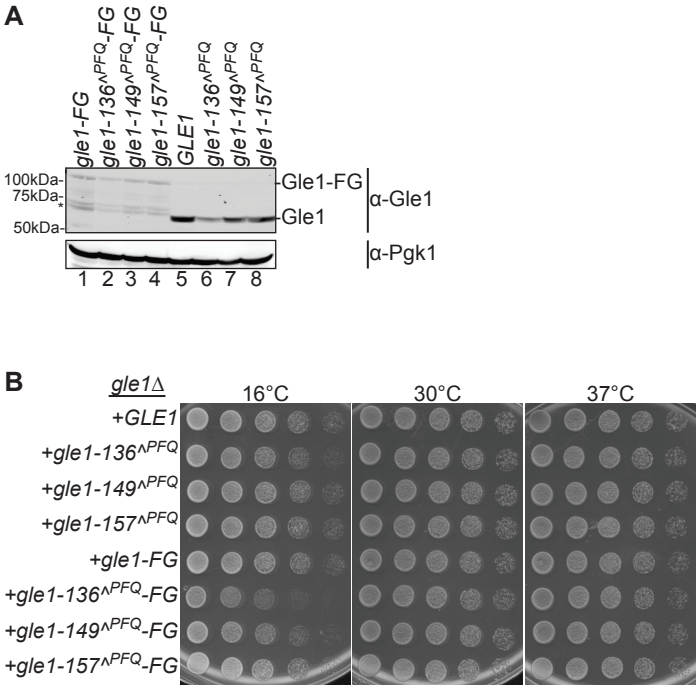

Figure III.8. *gle1-FG* constructs are expressed and show minimal growth defects. (A) *gle1-FG* fusions are expressed. Lysates from *gle1Δ* strains covered by the indicated vectors were separated by SDS-PAGE and immunoblotted using an α-Gle1 antibody. Pgk1 was used as a loading control. (*) Degradation products from the Nup42 FG domain. (B) *gle1^PFQ-FG* constructs display minimal growth defects. *gle1Δ* strains covered by the indicated vectors were grown at 30° and five-fold serially diluted on YPD plates for growth at the indicated temperatures.

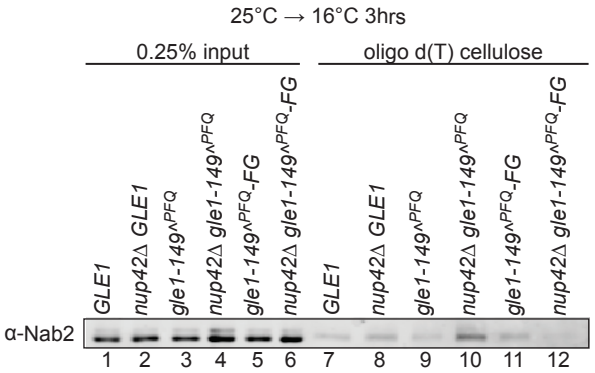

Figure III.9. Representative immunoblot from Figure III.7E: Fusion of the Nup42 FG domain to the carboxy-terminus of Gle1 rescues the mRNP remodeling defect of *nup42Δ gle1-149^PFQ*. The association of Nab2 protein with poly(A)$^+$ RNA was assessed by shifting strains to 16° for 3hrs, UV crosslinking, isolation of RNA by antisense chromatography, and immunoblotting after treatment with RNAse.

To test whether the *gle1-FG* fusion rescued other defects associated with Nup42 and to analyze whether the FG domain and CTD had distinct functions, we transformed the *gle1-FG* construct into a variety of mutants with distinct requirements for these domains. Clearly, the FG domain of Nup42 was essential when combined with *rat8-2 (dbp5)* and *nup159ΔFG* mutants (Figure III.3). Expression of *gle1-FG* rescued this synthetic lethality (Figure III.10A). Thus, the essential function of the Nup42 FG domain was linked with its adjacent positioning to Gle1.

Others have published functions for the Nup42 CTD that are independent from the FG domain. Specifically, Nup42 CTD is required for export of heat shock protein transcripts (*hsp*) after heat shock and for function in a *ipk1Δ* mutant (lacking IP_6 production) (STUTZ *et al.* 1997; STUTZ *et al.* 1995; (MILLER *et al.* 2004). We tested whether *gle1-FG* rescued this defect by monitoring for new protein synthesis using an [^{35}S]methionine incorporation assay. Whereas expression of *NUP42* and *nup42ΔFG* resulted in heat shock protein production and rescued the *nup42Δ* phenotype (Figure III.10B, lanes 4 and 6), expression of *gle1-FG* did not (Figure III.10B, lane 10). This indicated that nuclear export of *hsp* transcripts is inhibited in the *gle1-FG nup42Δ* cells. Expression of *gle1-FG* also did not rescue the *nup42Δ ipk1Δ* growth defect (Figure III.10C). Therefore, we concluded that the Nup42 CTD has a separate function in addition to positioning the FG domain in proximity to Gle1.

Discussion

From this work, we conclude that the Nup159 and Nup42 FG domains at the NPC cytoplasmic face function in mRNP remodeling. Further, we have identified a

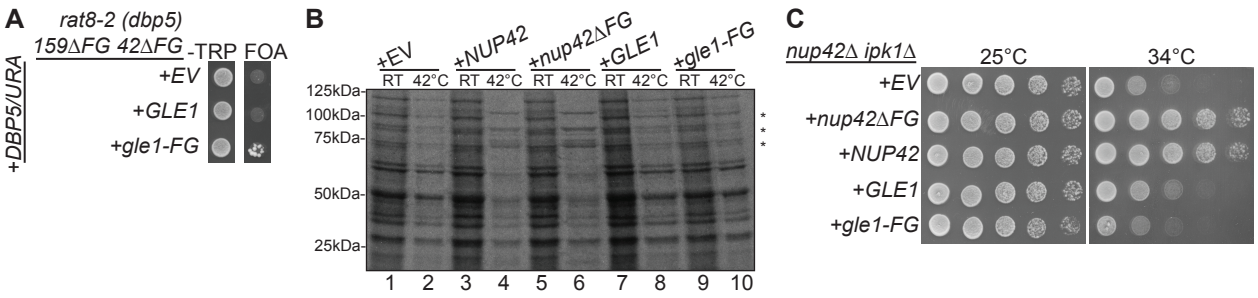

Figure III.10. The Nup42 FG domain and CTD have distinct functions.
(A) *gle1-FG* rescues synthetic lethality due to loss of the Nup42 FG domain. *rat8-2 (dbp5) nup42ΔFG nup159ΔFG* containing empty vector (*EV*) or *gle1/LEU* vectors were spotted onto -Leu synthetic media or 5-FOA at 25°. Growth on 5-FOA indicates functional complementation. (B) *gle1-FG* does not rescue the heat shock mRNA export defect of *nup42Δ* mutants. *nup42Δ* strains containing empty vector (*EV*), *nup42/LEU*, or *gle1/LEU* vectors were grown at 25° to early-log phase, kept at 25° or shifted to 42° for 15min, labeled with [^{35}S]methionine for an additional 15min, and lysed. Lysates were separated by SDS-PAGE, and proteins were visualized by autoradiography. The positions of Hsp proteins, induced upon heat shock, are indicated by asterisks. (C) *gle1-FG* does not rescue temperature-sensitivity of *nup42Δ ipk1Δ*. *nup42Δ ipk1Δ* containing empty vector (*EV*), *nup42/LEU*, or *gle1/LEU* vectors were spotted onto -Leu synthetic media at the indicated temperatures.

requirement for the proximal positioning of remodeling factors and FG domains in this process. Given the conservation of the general domain structures of the vertebrate orthologues of Nup159 and Nup42, respectively Nup214 and hCG1 (KRAEMER *et al.* 1994; STRAHM *et al.* 1999), we predict that FG domains at the NPC cytoplasmic face play roles in mRNP remodeling across eukaryotes. Others have previously used a FG swap approach to investigate the cytoplasmic and nuclear asymmetric FG domains (i.e., exchanging the cytoplasmic Nup159 and nuclear Nup1 FG domains), and concluded that changing the location of these FG domains in the NPC does not dominantly affect bulk transport (ZEITLER and WEIS 2004). In contrast, here we analyzed whether FG swaps could rescue a defect due to loss of the FG domains. The differential rescue observed in this study indicates an inherent specificity to a given FG domain. Moreover, given the function of a gle1-FG fusion protein, these studies reveal a previously undefined step in the mRNA export mechanism, wherein mRNPs are recruited to the FG domains on the NPC cytoplasmic face for remodeling.

The differential rescue by FG swaps uncovers an inherent specialization of FG domain function. This specialization might be due to the different type of FG repeats (FG, GLFG, or FxFG) enriched in the respective domains, or it might be due to the distinct biochemical and biophysical properties that are governed by the spacer sequences between the FG repeats. For example, due to the high content of charged residues in the Nup159 FG domain, it forms a non-cohesive extended coil, whereas the Nup42 FG domain is a cohesive collapsed coil (YAMADA *et al.* 2010). The Nup57 GLFG domain is also a collapsed coil, and this characteristic may partially explain why it can functionally replace the Nup42 FG domain and not the Nup159 FG domain. The Nsp1

FxFG domain is an extended coil, and it did not compensate for either FG domain, suggesting that this property alone is not sufficient for function. Indeed, using a directed approach by swapping in FG domains with distinct binding capabilities, we determined that binding to Mex67 is likely the important function of the Nup42 FG domain. Therefore, we speculate that the combination of biophysical properties (determined by spacer sequences) and preferences for TR binding (determined by type of FG repeat and adjacent residues) underlie the specificity of FG domain function.

In addition to mRNA export roles for FG domains on the cytoplasmic NPC face, these cytoplasmic FG domains also function in Kap (Crm1)-mediated export (FLOER and BLOBEL 1999; SABRI *et al.* 2007; ROLOFF *et al.* 2013) and it is postulated that SAFGxPSFG repeats on Nup159 and Nup42 provide specialized binding sites for Crm1 (DENNING and REXACH 2007). It is established that structured regions on the FxFG Nups located at the nuclear NPC face contribute to import cargo disassembly (GILCHRIST *et al.* 2002; GILCHRIST and REXACH 2003; MATSUURA *et al.* 2003; MATSUURA and STEWART 2005; SUN *et al.* 2013). These structured domains are located adjacent to the FxFG domains that bind importing Kaps (PYHTILA and REXACH 2003). Thus, although the asymmetric FG domains are not strictly required for NPC transport (STRAWN *et al.* 2004; ZEITLER and WEIS 2004), these domains likely play a general function in placing TRs at the optimal locale for cargo disassembly. Based on these roles at both the nuclear and cytoplasmic NPC faces, FG Nups do not simply function as a cargo permeability barrier but also are actively involved in providing spatial context to the transport mechanism through providing specialized binding sites.

There are several potential models for the molecular function of the FG domains during mRNP remodeling. The schematic in Figure III.11 summarizes several of these possible steps. First, the FG domains potentially act in docking the mRNA at the cytoplasmic face of the NPC until Mex67-Mtr2 has been remodeled off (Figure III.11Ai). Real-time single molecule experiments show that steps at the nuclear and cytoplasmic face of the NPC are rate-limiting during the mRNA export process (GRUNWALD and SINGER 2010). These FG domains potentially provide important binding sites during this process, and possibly facilitate multiple rounds of mRNP remodeling. DEAD-box proteins are not processive enzymes, and there is evidence that flexible extensions outside of the helicase core on other DEAD-box proteins aid in allowing additional rounds of activity of the enzyme toward a substrate (MALLAM *et al.* 2011). We speculate that the FG domains at the NPC cytoplasmic face might have a similar role during mRNA export; wherein, if multiple Mex67-Mtr2 dimers associate with an mRNP, the FG repeats could interact with multiple Mex67 molecules to direct rounds of mRNP remodeling by Dbp5.

Another possible function for FG domains during mRNP remodeling is to specify which RNA binding proteins are removed during the remodeling process (Figure III.11B). Mex67 and Nab2 are *bona fide* targets for Dbp5 remodeling *in vivo* (LUND and GUTHRIE 2005; TRAN et al. 2007), and other proteins, such as the Cap-binding protein (Cbp20/80 in yeast) and presumably the poly(A)$^+$ binding protein Pab1 are retained on the mRNA (reviewed in SCHOENBERG and MAQUAT 2012) (Figure III.11Biii). DEAD-box proteins bind RNA in a sequence-independent manner via the phosphate backbone of polynucleotide chain (reviewed in RUSSELL *et al.* 2013). While other DEAD-box proteins

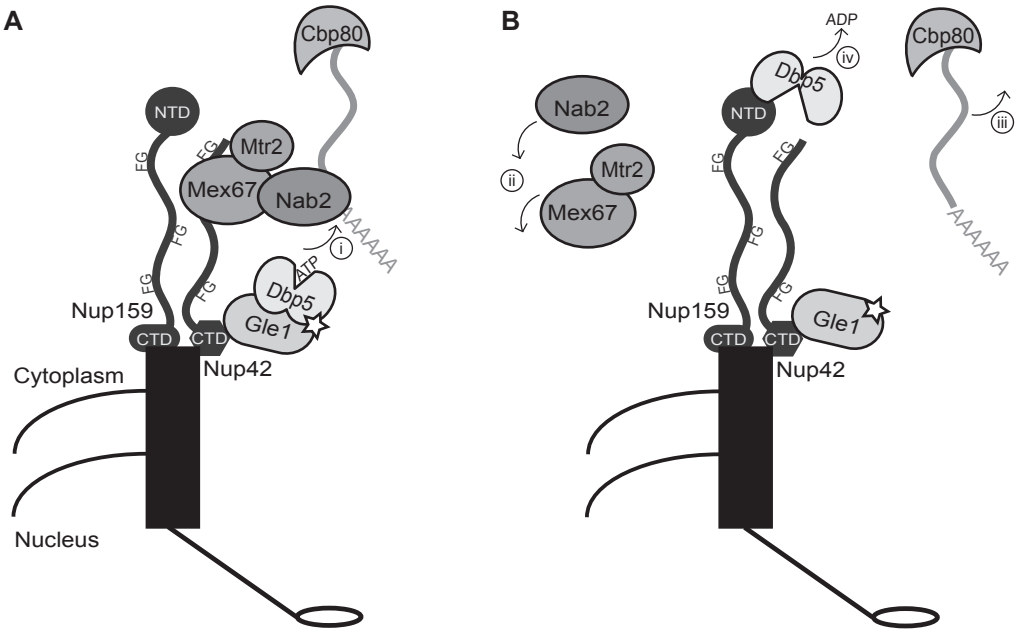

Figure III.11. Schematic diagram for model by which FG Domains on the cytoplasmic face of the NPC recruit exporting mRNPs for remodeling by Gle1-activated Dbp5. (A) Mex67-Mtr2 mediate export of mature mRNPs and the dimer is bound to the transcript via adaptors such as the poly(A)$^{+}$ binding protein Nab2. At the cytoplasmic face of the NPC, the Nup42 and Nup159 FG domains bind Mex67-Mtr2 to bring the mRNP in close proximity to Dbp5. Gle1 stimulates Dbp5 ATP loading, and (i) Dbp5 binds the RNA to trigger remodeling. Dbp5 might also be a constituent of the exporting mRNP. (B) Coincident with ATP hydrolysis, Dbp5 remodels specific proteins such as Nab2 and Mex67 off the mRNP. (ii) These proteins are then recycled into the nucleus for additional rounds of mRNA export. (iii) The mRNP, still bound to other mRNA binding proteins such as Cbp80, is free for cytoplasmic functions. (iv) The Nup159 NTD facilitates ADP release from Dbp5, allowing additional rounds of mRNP remodeling. It is unknown where the Nup159 NTD is localized relative to its CTD in vivo.

contain extensions that direct their activity toward specific substrates, Dbp5 does not (TIEG and KREBBER 2013). Indeed, Dbp5 can remodel non-physiological targets such as Pab1 from a model poly(A)$^+$ substrate *in vitro* (TRAN et al. 2007). Therefore, it is tempting to speculate that the FG domains provide a mechanism for dictating the *in vivo* removal of specific mRNP proteins during mRNA export. In this way, the specificity for remodeling is not conferred by RNA sequence or direct protein recognition of the RNA-binding protein to be removed, but is achieved by spatial proximity between the FG domain (binding the TR) and the remodeling factors: thus, dictated by the NPC structure (Figure III.11Ai). As such, the FG domains at the NPC cytoplasmic face would function to confer specificity to the mRNP remodeling mechanism.

During mRNA export cycles, an alternate function for FG domains at the NPC cytoplasmic face might be to bind Mex67 after it is removed from the RNP and facilitate efficient transport back into the nucleus for additional export events (Figure III.11Bii). This “recycling” of Mex67 would be an indirect function for FG domains in mRNP remodeling. However, our data indicates a direct role in mRNP remodeling due to an accumulation of Nab2 on poly(A)$^+$ RNA when the FG domains are deleted. Moreover, the *nab2-C437S* mutant rescues the cold-sensitivity of the *nup42ΔFG nup159ΔFG* mutant. Additionally, we did not observe increased cytoplasmic Mex67-GFP localization in *nup42ΔFG nup159ΔFG* cells (data not shown).

Our studies uncover an unexpected role for the FG domain of Nup42 in mRNP remodeling. However, it is clear that there is an additional function for the CTD of Nup42: expression of the CTD alone rescues the *hsp* mRNA export in *nup42Δ* cells (STUTZ *et al.* 1995; SAAVEDRA *et al.* 1997; STUTZ *et al.* 1997), and the gle1-FG fusion did

not rescue defects associated with Nup42 CTD (Figure III.10). It has been proposed that the Nup42 CTD is required for anchoring Gle1 to the NPC both during normal growth conditions and during heat shock (STRAHM *et al.* 1999; ROLLENHAGEN *et al.* 2004) and hCG1 is required for steady state human Gle1 localization to the nuclear envelope (KENDIRGI *et al.* 2005). It is also possible that the Nup42 CTD modulates Gle1 stimulation of Dbp5 at the NPC. Overall, it is clear that there are still unresolved steps in this mechanism.

The Dbp5-Gle1 interaction has been compared to the interaction between eIF4A and eIF4G, as the structural rearrangements of the DEAD-box protein (Dbp5 or eIF4A) are similar when the binding partner (Gle1 or eIF4G) interacts (OBERER *et al.* 2005; MONTPETIT *et al.* 2011). eIF4G is considered the major scaffold of the eIF4F translation initiation complex: through multiple interaction partners eIF4G functions to recruit the mRNP to the 40S ribosomal subunit, circularize the transcript, and directly stimulate the ATPase activity of eIF4A to allow structural rearrangements of the mRNP that are necessary for translation (reviewed in ANDREOU and KLOSTERMEIER 2013). Thus, eIF4G plays an important role in coordinating mRNP recruitment to functional interaction partners during translation initiation. We propose that Gle1 is playing a similar role as a scaffold during mRNA export: Nup42 interacts with the mRNP through Mex67 binding to its FG repeats, the Nup42 CTD interacts with Gle1, and Gle1 binds to Dbp5 to regulate its ATPase activity. Thus, recruitment of these factors through distinct interactions effectively increases the likelihood of Dbp5-RNA interaction and thus directs the mRNP remodeling capacity of Dbp5. Furthermore, Gle1 self-association is likely also required for this scaffolding activity (FOLKMANN *et al.* 2013). Together, this work highlights key

mechanisms coupling mRNP export and mRNP remodeling at the cytoplasmic face of the NPC that allow efficient gene expression.

Acknowledgements

The authors gratefully acknowledge D. Görlich for the rabbit anti-Cbp80 antibody and M. Rout for the mouse anti-Nup159 antibody. We also thank members of the Wente laboratory, C. Cole, E. Bowman, and E. Tran for discussions and critical reading of the manuscript. We also thank K. Noble for generating the chicken anti-Nup159-NTD antibody, and R. Dawson, and Y. Zhou for technical assistance. This work was supported by grants from the National Institutes of Health (R37GM051219 [S.R.W.] and training position on T32HD007502 [R.L.A.]).

CHAPTER IV

Discussion and Future Directions

FG function during transport

This work brings the story of Gle1 function full circle. Identified in our lab in a synthetic lethal screen with deletion of the GLFG Nup *NUP100* (MURPHY and WENTE 1996), Gle1's function in mRNP remodeling was subsequently defined (ALCAZAR-ROMAN *et al.* 2006; WEIRICH *et al.* 2006). Uncovering a function for FG domains at the cytoplasmic face of the NPC in mRNP remodeling then links these functions together. More importantly, this work highlights specialized functions of FG domains during transport and emphasizes the complexity of NPC transport. Thus, FG domains do not simply passively contribute to the permeability barrier but are active players in the transport process, likely serving to organize the massive amount of transport that occurs every second.

Additionally, the work described in this thesis uncovers a link between transport and mRNP remodeling, where transport is continuous with release of the mRNA from the NPC. This connection between different steps of mRNA maturation is reminiscent of co-transcriptional recruitment of mRNA export factors (reviewed in RONDON *et al.* 2010). In addition to potentially increasing the efficiency of transcript export and export factor recycling, this connection between steps may be essential to clear the NPC for other transport events. We propose that asymmetric FG domains serve this function for multiple transport pathways. Specifically, Kap95 (importin-β) binds to the FxFG domains of Nup1, Nup2, and Nup60 on the nuclear face of the NPC relatively strongly,

and non-FG domains of Nup1 and Nup2 function in Kap95-Kap60-NLS disassembly and recycling (GILCHRIST *et al.* 2002; GILCHRIST and REXACH 2003; PYHTILA and REXACH 2003). However, it has not been reported whether the FG domains on the nuclear face are important for import cargo disassembly, and future experiments can be aimed at testing this proposal.

We determined that FG domain function in mRNP remodeling is specific, as other FG domains cannot functionally compensate. This leads to the question of what are the sequence requirements for FG function in mRNP remodeling? Nup42 and Nup159 are enriched in FG repeats and SAFGPSFG double repeats (DENNING and REXACH 2007), serine and threonine (S+T) residues. Nup42 is additionally enriched in glutamine and asparagine (Q+N) residues (TERRY and WENTE 2009), suggesting that the type of FG repeat or spacer residues are important. It would be interesting to truncate the FG domains of Nup42 and Nup159 and perform mutagenesis on these sequences to determine what the functional residues of these domains are in mRNP remodeling. The general approach of altering FG domain sequences and assessing viability suffers from the potential that alterations result in pleiotropic defects in transport. Defects in multiple transport pathways could arise either by direct use of FG domains by different transport receptors or because lack of release of a cargo from the NPC could block transport of other molecules. However, performing these experiments on the Nup42 or Nup159 FG domains in the context of *rat8-2 nup42ΔFG nup159ΔFG* biases the results toward identifying sequences important for mRNP remodeling specifically, since loss of these FG domains alone (*nup42ΔFG nup159ΔFG*) has little growth defect. Subsequent biochemical experiments can be used to test whether

Mex67-Mtr2 binding or other biophysical properties of the FG domains are affected in altered FG domains.

A related question is how different transport pathways are defined in the NPC. A possible way to address this question is to identify the FG binding sites of transport factors in the NPC. Although experimentally challenging due to redundancy and flexibility in the NPC, this may be possible by introducing an unnatural amino acid such as *p*-benzoyl-L-phenylalanine or *p*-azido-L-phenylalanine in an FG binding pocket of TAP-tagged Kaps or Mex67 (CHIN *et al.* 2003). Both Kap95 (importin-β) and Mex67 contain hydrophobic residues at the FG binding interface that could be replaced by these unnatural amino acids (HOBEIKA *et al.* 2009; LIU and STEWART 2005). Control experiments would be required to ensure normal transport is not compromised under these conditions. Irradiation with UV_{360} or UV_{254} would crosslink interacting proteins, followed by cell lysis and purification of the TAP-tagged and crosslinked proteins, protease treatment, and mass-spec analysis. Then, targeted alteration of the distinct FG repeats uncovered can be used to test whether these specific binding sites are required for transport and whether the different FG requirements previously uncovered represent binding sites during transport (TERRY and WENTE 2007). The ideal context for these experiments is Δ*N*Δ*C nup100*Δ*GLFG nup145*Δ*GLFG*, where the Goldberg lab collaborated with ours to show that the Kap121 transport pathway within the NPC is altered when its preferred FG domains are deleted (FISEROVA *et al.* 2010). It would be interesting to test whether deletion of specific FG binding sites affects transport or other FG domains compensate for loss of preferred interaction sites.

mRNP remodeling specificity at the NPC

One of the major questions of mRNA export is how specific proteins are removed during mRNP remodeling by Dbp5 at the NPC. Mex67-Mtr2 and Nab2 are *bona fide* targets for removal (LUND and GUTHRIE 2005; TRAN *et al.* 2007), but several others retain RNA association. For example, Pab1 is a poly-A binding protein that associates with RNA in the nucleus and functions in the cytoplasm to circularize the transcript during translation and protect it from degradation (WELLS *et al.* 1998). Thus, how Nab2 is remodeled but Pab1 isn't, even though both are poly-A binding proteins, is unknown.

Because the DEAD-box protein core binds RNA in a sequence-independent manner, activity is usually targeted by amino- or carboxy-terminal extensions or associated binding proteins (reviewed in FAIRMAN-WILLIAMS *et al.* 2010). Dbp5 contains only a small non-essential amino-terminal helix that likely does not provide this function. Rather, it is likely targeted to function at local RNA regions through its interaction partners. However, it is unresolved whether the Dbp5 interaction with RNA for remodeling at the NPC occurs in the nucleus or at the cytoplasmic face of the NPC. For example, Dbp5 accumulates in the nucleus of mRNA export mutants (HODGE *et al.* 1999), it can be visualized on exporting Balbiani ring mRNPs using immuno-EM (ZHAO *et al.* 2002), and it can be enriched with Yra1-containing mRNPs (OEFFINGER *et al.* 2007). Potentially, there is a factor that inhibits Dbp5 ATPase activity to lock it in association with RNA, similar to eIF4AIII in the EJC (PALACIOS *et al.* 2004; SHIBUYA *et al.* 2004; BALLUT *et al.* 2005). In this case, Dbp5 could be loaded at specific sites on a transcript in the nucleus such that these sites are targeted for remodeling once the transcript reaches the cytoplasmic face of the NPC. In this case, the same Dbp5

molecule that is loaded onto a transcript in the nucleus would function at the NPC. It is also possible that Dbp5 has separate nuclear, NPC, and cytoplasmic functions. Dbp5 and Gle1 play a role in translation initiation (GROSS *et al.* 2007; BOLGER *et al.* 2008; BOLGER and WENTE 2011) and may also function in transcription (ESTRUCH *et al.* 2012), but whether the same Dbp5 molecule associates with transcripts for these distinct functions is unknown. Therefore, Dbp5 may be guided to remodel RNA through interaction partners in the nucleus, cytoplasm, and/or at the NPC.

To begin to analyze whether Dbp5 binding to RNA in the nucleus is required for remodeling at the NPC, a mutant of *DBP5* encoding a protein that does not enter the nucleus could be tested for remodeling capacity at the NPC. Although Dbp5 shuttles between the nucleus and cytoplasm (HODGE *et al.* 1999), an NLS has not been defined. An alternate to modifying the Dbp5 NLS is to fuse Dbp5 to Nup159 such that the Dbp5 activity is restricted to the cytoplasmic face of the NPC. Control experiments would be required to determine that this Dbp5-Nup159 fusion is stably localized to the NPC, and subsequent experiments could determine whether this localization is sufficient for mRNP remodeling. A positive result would suggest that factors at the NPC are sufficient for directing Dbp5 activity for specific remodeling.

There are several possible models for how Dbp5 mRNP remodeling removes specific proteins at the NPC. First, interaction partners at the NPC may guide Dbp5 to interact with specific regions of the transcript for remodeling. Second, the structure of the mRNP may be such that Dbp5 only interacts with exposed regions of RNA for remodeling. Third, it is possible that the way a protein interacts with RNA dictates whether it is remodeled. Potentially, RNA binding proteins that are not removed interact

with the RNA backbone, masking the Dbp5 interaction surface. Fourth, RNA binding affinity may dictate whether a protein is remodeled. However, Pab1 and Nab2 have comparable affinity for RNA (Pab1: K_d=7nm (GORLACH *et al.* 1994), Nab2: K_d=10.5nm (HECTOR *et al.* 2002) for poly-A_{25}), and Pab1 is removed upon by Dbp5 mRNP remodeling *in vitro*, suggesting that simple inherent RNA binding protein-RNA interactions do not dictate remodeling specificity. Finally, it also remains a possibility that Dbp5 remodeling non-discriminately removes proteins *in vivo*, but only those that are quickly re-imported do not re-associate with the mRNA.

To determine whether removal of a protein upon Dbp5 mRNP remodeling is determined in *cis* (i.e. a property of Nab2 targets it for remodeling), a fusion between Nab2 and Pab1 should be generated and tested for remodeling. Subcellular localization could provide an initial readout of removal from the mRNP: if the protein is not removed, it is likely to remain on the mRNA in the cytoplasm and exhibit pan-cellular localization at steady-state; if it is removed, it may be re-imported and have a nuclear localization at steady state. Control experiments would be required to determine that the removed protein shuttles out of the nucleus in an mRNA export dependent manner. Because Nab2 has been fairly well characterized, the fusion protein could then be truncated to determine which domains of Nab2 are responsible for directing removal upon Dbp5 mRNP remodeling. It is possible that remaining on mRNA is a dominant trait, and the fusion is not removed, in which case Pab1 could be truncated to determine what regions are responsible for cytoplasmic localization.

A major shortcoming in the understanding of mRNP remodeling is a lack in knowledge of which proteins are removed upon Dbp5 mRNP remodeling. Although

Mex67 and Nab2 have been identified, whether other proteins are also targeted is unknown. This knowledge would be beneficial for further analysis of how specific proteins are removed. One approach for analyzing which proteins are remodeled would be to test candidate proteins for whether they are removed prior to or following export. For example, the THO components are localized to the nucleus at steady state, suggesting they do not associate with cytoplasmic mRNPs. To test whether they are removed after mRNA export, their localization can be assessed using the *nup49-313* strain which prevents nuclear import (LEE *et al.* 1996). An increased cytoplasmic signal suggests removal during Dbp5 mRNP remodling at the NPC, like Nab2, or removal during the pioneer round of translation, like Cbp80. It is possible that if these components are removed during Dbp5 mRNP remodeling, they, at least in part, constitute the link between defects in mRNA export affecting earlier steps in mRNA biogenesis.

Although our study uncovered a function for the Nup159 and Nup42 FG domains in mRNP remodeling, the molecular function has not been determined. We hypothesize that this function may be in determining which proteins are removed by Dbp5 mRNP remodeling. In theory, the only proteins that should be targeted for removal at this step of mRNA biogenesis are those that function in mRNA export. Therefore, our current model is that FG domains at the cytoplasmic face of the NPC bind Mex67-Mtr2, positioning the mRNP near Gle1 and Dbp5 for remodeling. This hypothesis can be tested in a few different ways. First, if binding to FG domains targets a protein for removal, then removal should be induced by fusing a protein that is not normally removed to FG binding domains of Mex67 or Mtr2. Cellular localization combined with

biochemical analysis of association with cytoplasmic mRNA could be used to assess removal from cytoplasmic mRNPs. However, it is possible that a single FG binding domain is not sufficient to target the protein for remodeling. As an alternate approach, it could be tested whether localizing the Gle1-FG fusion to the nucleus results in premature mRNP remodeling and Mex67-Mtr2 removal and an mRNA export defect.

mRNP assembly

A larger unknown is how mRNPs are dynamically assembled. Perhaps the best understood RNPs are mature ribosomes or small RNPs such as telomerase and the signal recognition particle, largely because they form a single canonical structure which can be easily biochemically characterized. However, the dynamic nature of RNP biology, including snRNPs during mRNA splicing and ribosome subunit assembly has added challenges to our understanding of these processes. Understanding mRNP maturation provides an additional challenge because mRNPs are a diverse species. Defined by the presence of a poly-A tail and 5' cap, transcripts differ in sequence, length, splicing, secondary structure, protein repertoire, and ncRNA association. Thus, our understanding of RNP biogenesis come from global studies, including high-throughput sequencing and proteomics, and altering processes thought to affect all mRNP species, but also from reductionist approaches that seek to understand how a single transcript matures or how individual proteins affect global mRNA biogenesis. Indeed, some have defined the mRNP proteome using modern state-of-the art techniques (BALTZ *et al.* 2012; CASTELLO *et al.* 2012; KWON *et al.* 2013; MITCHELL *et al.* 2013). Despite this huge increase in data related to mRNP biogenesis, our

understanding of the process is still far from complete. For example, our understanding of the contribution of each of the proteins of the mRNP proteome to mRNA function and their dynamic occupancy on transcripts is lacking.

A new approach developed by the Michael Rout lab is to purify a single transcript using the MS2-coat protein system under cryogenic conditions to maintain mRNP composition (personal communication). A similar approach has been used to identify associating miRNAs for individual transcripts (YOON *et al.* 2012) and the HIV RNA-associating proteome (KULA *et al.* 2011). This reductionist approach could be combined with state-of-the-art techniques to better understand mRNP assembly of an individual transcript. For example, an individual mRNP can be purified at different stages in maturation biochemically or using mutants that block export and remodeling to identify which proteins are remodeled at the NPC. Furthermore, addition of photo-reactive nucleosides, crosslinking, and secondary purification of RNA binding proteins (PAR-CLIP (HAFNER *et al.* 2010) or CRAC (TUCK and TOLLERVEY 2013)) can be performed after isolation of an individual transcript to map the binding sites for each protein on an individual transcript. Finally, visualization of biochemically purified mRNP structure by single-particle electron microscopy before and after mRNP remodeling *in vivo* will demonstrate whether remodeling by Dbp5 globally alters mRNA structure.

Other functions for Gle1 and Dbp5

A remaining question is what are the molecular functions for Gle1 and Dbp5 during translation and possibly during mRNA biogenesis in the nucleus. Why is the same protein used for multiple steps during gene expression? Does Dbp5 remodeling

remove proteins from mRNPs in the nucleus and during translation termination, and how are these proteins targeted? It is likely that Dbp5 evolved to function at multiple mRNP biogenesis steps because its ATPase cycle is suited for protein removal. Dbp5 is a poor RNA helicase (TSENG *et al.* 1998), and is instead specialized to function as an mRNP remodeler of single-stranded RNA (TRAN *et al.* 2007). Additionally, whereas mRNP remodeling by another DEAD-box protein, Ded1, only requires ATP binding (BOWERS *et al.* 2006), remodeling by Dbp5 is mediated by ATP hydrolysis or ADP binding (TRAN *et al.* 2007). This likely indicates distinct structural mechanisms of remodeling, and Dbp5 is targeted by binding partners for each of these processes. One approach to explore Dbp5 function at other steps in gene expression is to identify interacting partners in the nucleus or cytoplasm. Previous attempts to uncover novel binding partners using yeast-two-hybrid were unsuccessful (K. Noble, personal communication). Dbp5 accumulates in the nucleus of *mex67-5* mutants, possibly being trapped in a step of mRNA biogenesis. This mutant can be used to purify Dbp5-TAP and potential nuclear-associating proteins for identification by mass-spectroscopy. An alternative approach is to use BioID to identify closely associating proteins, where Dbp5 or Gle1 can be fused a promiscuous biotin ligase for subsequent purification using streptavidin-coated beads (ROUX *et al.* 2013). Additionally, PAR-CLIP or CRAC can be used to uncover Dbp5 binding sites on RNA at each of these steps in the mRNP lifecycle. Finally, many proteins that are removed by DEAD-box proteins can be identified as suppressors of temperature-sensitive or cold-sensitive DEAD-box mutants, and a *NAB2* mutation partially rescues a *DBP5* mutant (TRAN *et al.* 2007). Therefore, a

genetic suppression screen might be an approach to identify proteins removed by Dbp5 at the NPC or elsewhere.

Regulation of Remodeling

Finally, based on work in *S.c.*, mammalian cell culture, and zebrafish, it has been proposed the Gle1 and/or Dbp5 activity is generally required for gene expression. However, it remains to be tested whether different transcripts have differential requirements for remodeling. Furthermore, based on proteomic data across a variety of cell types, hGle1 and hDbp5 have distinct expression patterns across tissues and during disease (WILHELM *et al.* 2014). Additionally, hGle1 and hDbp5 protein levels are increased during eIF4E oncogene overexpression (CULJKOVIC-KRALJACIC *et al.* 2012). Therefore, it would be interesting to further explore requirements during development and disease and how these factors are regulated at the mRNA and protein level. Finally, based on the requirement for IP_6 in this process, it remains to be determined if shifting inositol levels during cell responses to signaling affect mRNA export or translation.

Appendix A:

Analysis of Gle1 Oligomer Structure and *in vivo* Requirements

Introduction

hGle1 has been casually linked to the developmentally fatal disease, Lethal Congenital Contracture Syndrome 1 (LCCS1), and the causative mutation results in an altered splice site with the addition of three residues, PFQ, into the amino-terminal coiled coil region of hGle1 (NOUSIAINEN *et al.* 2008). For a time, the molecular basis for this disease remained undefined because, while functions had been assigned to other parts of the protein, this region of Gle1 had been previously uncharacterized. In *S.c.*, this domain is essential, and the homologous region of hGle1 can functionally compensate (WATKINS *et al.* 1998), suggesting a conserved function between *S.c.* and human Gle1. Recently, it was found that the predicted Gle1 coiled-coil domain self-associates *in vitro* to promote the formation of large oligomeric disks that are ~26nm in diameter (FOLKMANN *et al.* 2013). Furthermore, self-association was found to be essential for mRNA export but not for the roles of Gle1 in translation initiation and termination. However, it is unclear why Gle1 self-association is specifically required during mRNA export. *In vitro*, the carboxy-terminus of Gle1 is sufficient for stimulation of Dbp5 ATPase activity (FOLKMANN *et al.* 2013). Additionally, based on FRET analysis of Gle1-Gle1 interaction, hGle1 self-associates to a similar extent in the cytoplasm and at the NE rim (FOLKMANN *et al.* 2013). Finally, both hGle1A and hGle1B contain the amino-terminal coiled-coil region, indicating that distinct functionality of the two isoforms

is not attributable to self-association. We therefore, took several approaches to analyze the function of Gle1 self-association during mRNA export in *S. cerevisiae*.

Testing for Nup42 and Dbp5 competition in binding to Gle1

Results

It is possible Gle1 self-association is required during mRNA export specifically to allow interaction with multiple, overlapping binding partners. Specifically, Andrew Folkmann hypothesized that the Nup42 binding site on Gle1 overlaps with the Dbp5 binding site, competing for its interaction, and both the Nup42 and Dbp5 interactions with Gle1 are important during mRNA export. The *S.c.* $Gle1_{244\text{-}538}^{H337R}$-$Dbp5_{91\text{-}482}^{L327V}$ structure displays two interfaces between Gle1 and Dbp5, where a relatively strong interaction occurs at the amino-terminus of $Gle1_{244\text{-}538}^{H337R}$ and carboxy-terminal RecA domain of $Dbp5_{91\text{-}482}^{L327V}$, and a weaker interaction occurs at the carboxy-terminal helix of $Gle1_{244\text{-}538}^{H337R}$ and the amino-terminal RecA domain of $Dbp5_{91\text{-}482}^{L327V}$ (Figure A.1A) (MONTPETIT *et al.* 2011). These interfaces closely resemble the interaction between eIF4G and eIF4A, where the binding of eIF4A-CTD to eIF4G is stronger (K_D ~70uM) than eIF4A-NTD to eIF4G (to weak to measure), but full-length eIF4A binds stronger to eIF4G than eIF4A-CTD (MARINTCHEV *et al.* 2009). Importantly, both of these interfaces are required for mRNA export as alterations of either result in an mRNA export defect *in vivo* and decreased Gle1 stimulation of Dbp5 ATPase activity *in vitro* (DOSSANI *et al.* 2009; MONTPETIT *et al.* 2011). Specifically, altering uncharged residues in the Gle1 carboxy-terminal helix to aspartic acid ($Gle1^{VAI>DDD}$) completely abolishes the ability of Gle1 to stimulate Dbp5 ATPase activity (MONTPETIT *et al.* 2011).

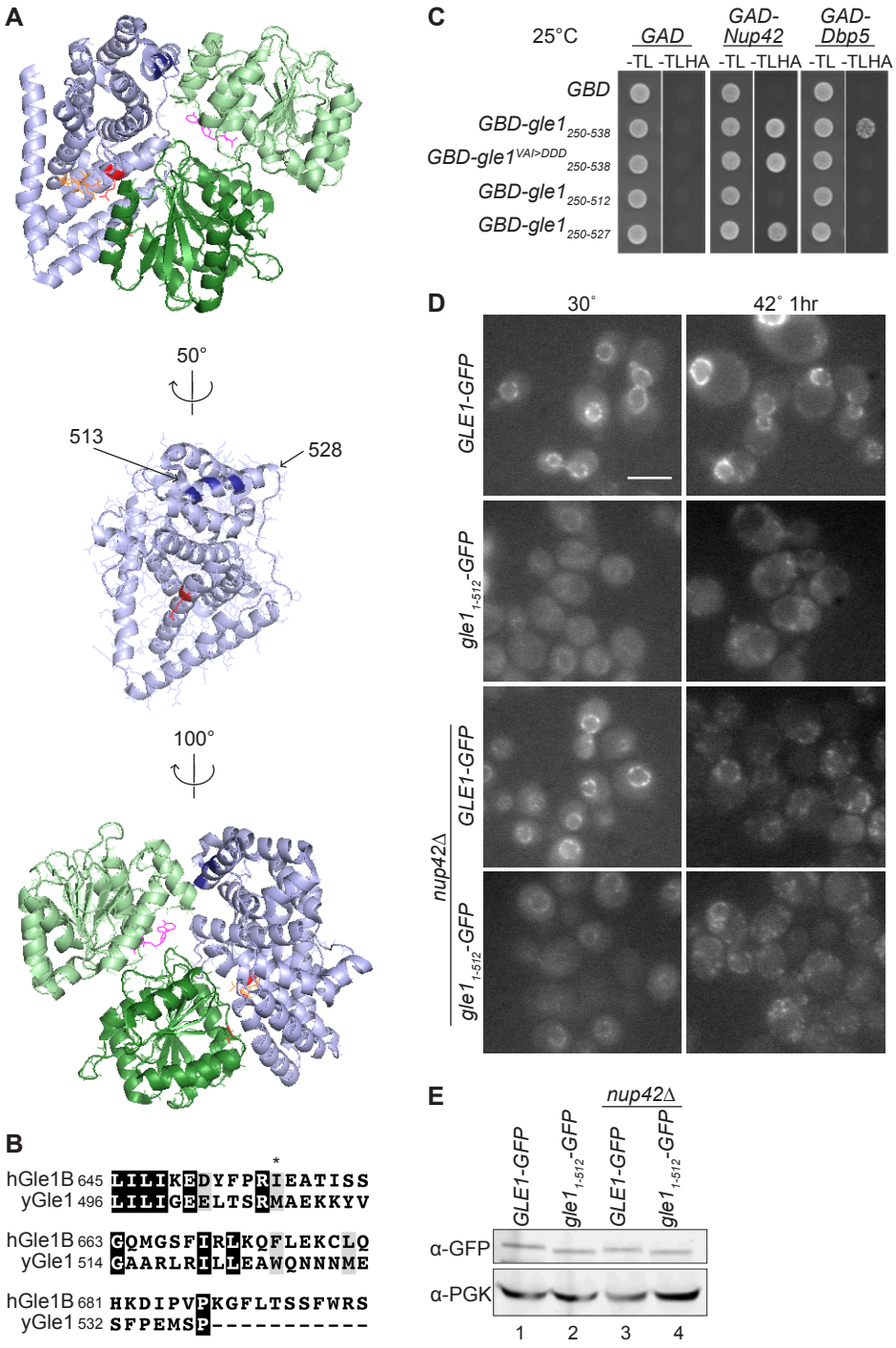
A
50°
513
528
100°
B
hGle1B 645 LILIKEDYFPRIEATISS
yGle1 496 LILIGEELTSRMAEKKYV
hGle1B 663 GQMGSFIRLKQFLEKCLQ
yGle1 514 GAARLRILLEAWQNNNME
hGle1B 681 HKDIPVPKGFLTSSFWRS
yGle1 532 SFPEMSP----------
C
25°C
GAD
GAD-Nup42
GAD-Dbp5
-TL -TLHA -TL -TLHA -TL -TLHA
GBD
GBD-gle1250-538
GBD-gle1VAI>DDD250-538
GBD-gle1250-512
GBD-gle1250-527
D
30˚
42˚ 1hr
GLE1-GFP
gle11-512-GFP
nup42Δ
GLE1-GFP
gle11-512-GFP
E
nup42Δ
GLE1-GFP
gle11-512-GFP
GLE1-GFP
gle11-512-GFP
α-GFP
α-PGK
1 2 3 4

Figure A.1. The carboxy-terminal helix of Gle1 is required for interaction with Nup42. (A) Gle1 and Dbp5 bind at two interfaces. Crystal structure of $Dbp5_{91\text{-}482}^{L327V}$ (green; NTD, light green; CTD, dark green) complexed with $Gle1_{244\text{-}538}^{H337R}$ (blue)(PDB 3RRM (MONTPETIT *et al.* 2011)). ADP, purple; IP_6, orange; GOF mutations ($Gle1^{H337R}$, $Dbp5^{L327V}$), red; $Gle1^{VAI}$, dark blue. Arrows indicate start of carboxy-terminal helix (residue 513) and carboxy-terminal unstructured region (residue 528). (B) Alignment of hGle1B and yGle1. hGle1B and yGle1 protein sequences were aligned using Clustal Omega (SIEVERS and HIGGINS 2014). Asterisk indicates start of 43 unique residues not found in hGle1A, sufficient for interaction with hCG1 (KENDIRGI *et al.* 2005). (C) Deletion of the carboxy-terminal helix of Gle1 results in loss of Nup42 interaction. *GAD* (CP84), *GAD-NUP42*, (pSW486), or *GAD-Dbp5* (pSW1249) and *GBD* (CP86), *GBD-gle1*$_{250\text{-}538}$ (pSW480), *GBD-*$^{gle1VAI>DDD}_{250\text{-}538}$ (pSW4019), *GBD-gle1*$_{250\text{-}512}$ (pSW4083), *GBD-gle1*$_{250\text{-}528}$ (pSW4084) were co-transformed into the reporter yeast strain PJ69-4A (YOL99). Strains were grown to mid-log phase in -Trp-Leu media, spotted onto -Trp-Leu or -Trp-Leu-His-Ade, and grown at 25°C. (D) Deletion of the carboxy-terminal helix results in mislocalization of Gle1. *GLE1-GFP* (CP228) or *gle1*$_{1\text{-}512}$*-GFP* (pSW3785) were transformed into wt (YOL183) or *nup42Δ* (NULL236) mutants. Strains were grown to mid-log phase at 30°C and kept at 30°C or shifted to 42°C for 1hr, and live cells were visualized by widefield fluorescence. Scale bar=5um. (E) *gle1-GFP* constructs are expressed at similar levels. Strains from Figure A.1D were grown to mid-log phase, and equal OD_{600} units of cell numbers were collected by centrifugation, re-suspended in SDS loading buffer, lysed by vortexing with glass beads, and boiled 5min. Lysates were then resolved by SDS-PAGE and blotted with anti-GFP (AOL106), and anti-yPgk1 (AOL30).

hGle1B contains a 43 residue carboxy-terminal extension not found in hGle1A, and this extension is necessary and sufficient to mediate interaction with the carboxy-terminal (non-FG) end of hCG1, the *S.c.* Nup42 homologue (KENDIRGI *et al.* 2005). We identified the *S.c.* Gle1 homologous residues using Clustal Omega (SIEVERS and HIGGINS 2014), and mapping these residues onto the Gle1-Dbp5 structure demonstrates that they overlap with the carboxy-terminal helix of Gle1 that forms the weak Dbp5 interface (Figure A.1B). Because this interface is important for Gle1 stimulation of Dbp5, we proposed that Nup42 competes with Gle1 binding to Dbp5 and/or disrupts Gle1 stimulation of Dbp5 ATPase activity. Potentially Gle1 self-association allows one Gle1 promoter to interact with the NPC while another stimulates Dbp5, or potentially Gle1 interaction with Nup42 is regulated by its interaction with Dbp5. Importantly, Gle1 interacts with Nup42 at the NPC, thus potentially explaining why Gle1 self-association is required for mRNA export specifically. Finally, the Gle1-Nup42 interaction is important in positioning the Nup42 FG domain in close proximity to Dbp5 for mRNP remodeling, and genetic interactions between *S.c. gle1*^{PFQ} mutants and deletion of *NUP42* are bypassed by tethering the FG domain of Nup42 to Gle1 (Chapter III), linking Gle1 self-association with Nup42 function.

First, we tested whether the carboxy-terminal helix of yGle1, which is homologous to the 43-residue extension in hGle1B, is required for the Gle1-Nup42 interaction. Gle1 and Nup42 have a robust reported yeast-two-hybrid interaction (STRAHM *et al.* 1999), and we used this method to assess Gle1-Nup42 binding with Gle1 truncations, using Gle1-Dbp5 as a control. We either deleted the entire carboxy-terminal helix and remaining unstructured carboxy-terminal unstructured region (GBD-

Gle1$_{250\text{-}512}$), or only the unstructured region (GBD-Gle1$_{250\text{-}527}$) in a Gal4 DNA binding domain fusion (GBD). Deletion of the carboxy-terminal helix disrupted the Gle1-Nup42 interaction, but Gle1$^{VAI>DDD}_{250\text{-}538}$ only disrupted the interaction with Dbp5, suggesting that these residues are not important for the Nup42 interaction (Figure A.1C). Attempts to assess expression level either using a Gle1 antibody, GBD antibody, or by cloning in a myc tag were unsuccessful, so it remains a possibility that the altered yeast-two-hybrid interaction is due to decreased expression.

Although deletion of *NUP42* does not result in Gle1 mislocalization at most temperatures, Gle1 accumulates in cytoplasmic foci in *nup42Δ* mutants after heat shock at 42°C (ROLLENHAGEN *et al.* 2004). Therefore, we expected that deletion of the region in Gle1 responsible for this interaction would have the same result. Indeed, gle1$_{1\text{-}512}$-GFP accumulated in cytoplasmic foci after shifting to 42°C for 1hr in wt cells, but Gle1-GFP localization was not changed (Figure A.1D). All mutants had similar expression levels (Figure A.1E), suggesting that the carboxy-terminal helix may be responsible for the Gle1-Nup42 interaction.

Because the carboxy-terminal helix of Gle1 is important for interaction with both Nup42 and Dbp5, we tested whether Nup42 and Dbp5 compete for binding to Gle1. One experimental difficulty with this assay is the weak/transient nature of the Gle1-Dbp5 interaction, and in the tested conditions, Dbp5 bound to Nup42 when present at high concentrations, making interpretation of binding difficult (the implications of the Dbp5-Nup42 interaction have not been explored). First, with MBP-Gle1$_{241\text{-}538}$ (MBP-Gle1C) on beads, Dbp5 was added at a non-saturating concentration, and GST-Nup42$_{365\text{-}430}$ (GST-Nup42C) was titrated up to 50-fold excess. Although Nup42 interaction with

Gle1C was evident (asterisk, lane 12-15), there were no decreases in Dbp5 interaction as determined by western blotting (Figure A.2A). Importantly, this concentration was in the linear range of the Dbp5 antibody (data not shown). Based on this experimental set-up, it is difficult to assess whether the same Gle1 molecule is interacting with Dbp5 and Nup42, so we used a different approach. Gain of function alterations in Gle1 (H337R) and Dbp5 (L327V) bind much more strongly and have previously been used in structural studies (MONTPETIT *et al.* 2011). We thus used these alterations to analyze whether Dbp5 can compete Nup42 off of Gle1. With GST-Nup42C on beads, MBP-Gle1C^{H337R} was titrated to find the concentration of half-maximal binding (Figure A.2B, asterisk indicated concentration used in subsequent experiments). Using this Gle1 concentration, Dbp5^{L327V} was added in the presence or absence of saturating IP_6 and AMP-PNP. If Dbp5 competes for binding to Gle1, it was expected that less Gle1 would bind GST-Nup42 beads. MBP-Gle1C^{H337R} bound to GST-Nup42C beads at similar levels (Figure A.2C, lanes 14). Additionally, under these conditions, Dbp5^{L327V} did not bind to GST-Nup42C beads alone, suggesting that its interaction is mediated through Gle1 and that there is no observable competition between Dbp5 and Nup42 for interaction with Gle1. MBP-Gle1C$^{H337R, VAI>DDD}$ bound to Dbp5^{L327V} at similar levels (compare lane 13 & 14), indicating that the interaction is likely mediated through the stronger interface, and no binding was observed in the absence of nucleotide, demonstrating that the Gle1-Dbp5 interaction was specific (lanes 15 & 16). Finally, addition of H_6-Nup159$_{1-387}$ (H_6-Nup159NTD) resulted in a tetrameric complex (Figure A.2D, lanes 16 & 18), and no changes were evident with the addition of different nucleotides (lanes 19-21).

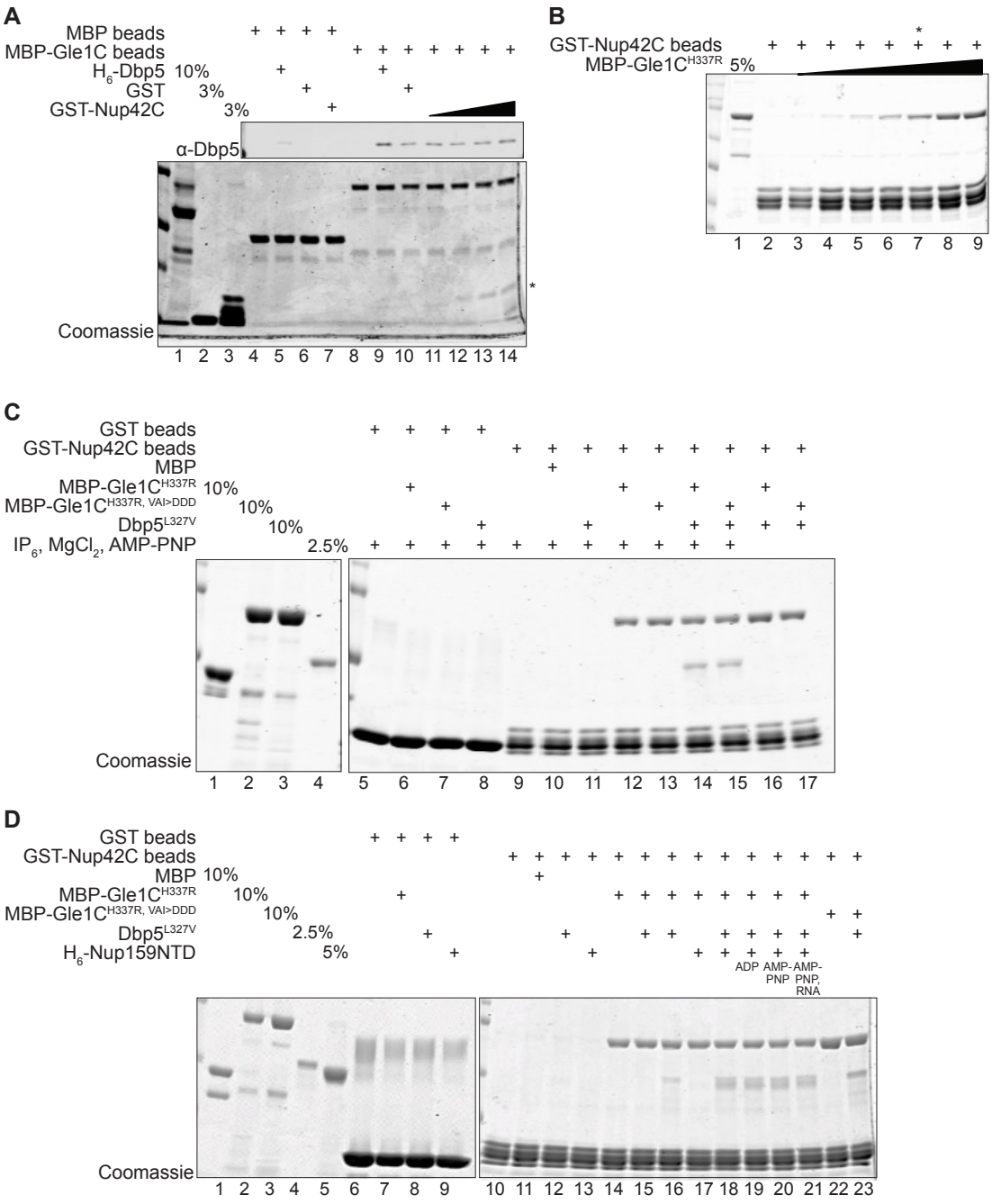
A
MBP beads
MBP-Gle1C beads
H6-Dbp5 10%
GST 3%
GST-Nup42C 3%
α-Dbp5
Coomassie
1 2 3 4 5 6 7 8 9 10 11 12 13 14
B
GST-Nup42C beads
MBP-Gle1CH337R 5%
1 2 3 4 5 6 7 8 9
C
GST beads
GST-Nup42C beads
MBP
MBP-Gle1CH337R 10%
MBP-Gle1CH337R, VAI>DDD 10%
Dbp5L327V 10%
IP6, MgCl2, AMP-PNP 2.5%
Coomassie
1 2 3 4 5 6 7 8 9 10 11 12 13 14 15 16 17
D
GST beads
GST-Nup42C beads
MBP 10%
MBP-Gle1CH337R 10%
MBP-Gle1CH337R, VAI>DDD 10%
Dbp5L327V 2.5%
H6-Nup159NTD 5%
ADP
AMP-PNP
AMP-PNP, RNA
Coomassie
1 2 3 4 5 6 7 8 9 10 11 12 13 14 15 16 17 18 19 20 21 22 23

Figure A.2. Nup42 and Dbp5 do not compete for interaction with Gle1 in soluble binding assays.
(A) Dbp5 binding to Gle1 does not decrease in the presence of Nup42C. 3uM His_6-Dbp5 (CP454) was incubated with MBP (CP30) or MBP-$Gle1_{241-538}$ (pSW3335) beads (at 170nM) for 4 hours at 4°C in the presence of 9.6uM GST (CP183), 1:3 fold dilutions of GST-$Nup42_{365-430}$ (CP3875) up to 9.6uM, or buffer alone in buffer A (20mM HEPES pH7.5, 145mM NaCl, 5mM KCl) +20uM IP_6 +50uM AMP-PNP +4.5mM $MgCl_2$. Samples were washed once with buffer A +IP_6, AMP-PNP, $MgCl_2$, transferred to a new tube with a small hole, and washed two more times by spinning buffer through the hole. Bound proteins were eluted with Magic Buffer ~10' at RT and spun into a new tube. 50% of each sample was resolved with SDS-PAGE and either stained with Coomassie or probed with Dbp5 antibody (ASW42). (B) Titrating Gle1 binding to GST-Nup42C. MBP-$Gle1_{241-538}^{H337R}$ (pSW4054) was incubated at 1:2 dilutions with GST-$Nup42_{365-430}$ beads (at 2.2uM) up to 6.2uM as in A. Samples were washed as in A, resolved on SDS-PAGE, and stained with Coomassie. The starred sample indicates half-maximal binding (1.55uM) and the concentration of MBP-$Gle1_{241-538}^{H337R}$ used in C. (C) Dbp5 does no compete Gle1 off Nup42. GST-$Dbp5^{L327V}$ (pSW3937) was purified using glutathione resin, the GST tag was cut overnight with Factor Xa, followed by removal of the tag by ion exchange chromatography. 1.5uM MBP-$Gle1_{241-538}^{H337R}$ or MBP-$Gle1_{241-538}^{H337R,VAI>DDD}$ (pSW4055) were incubated with GST or GST-$Nup42_{365-430}$ beads (at 2.2uM) in the presence of 2.8uM $Dbp5^{L327V}$ or buffer as in A. Control samples without IP_6, AMP-PNP, or $MgCl_2$ were included to test specificity of the Gle1-Dbp5 interaction. Samples were washed as in A, resolved on SDS-PAGE, and stained with Coomassie. Dbp5 binding in the presence of Gle1 indicates that it does not compete with Nup42 for binding to Gle1, as competition would result in reduced Gle1 binding to GST-Nup42 beads. (D) Nup159, Dbp5, Gle1, and Nup42 form a quartenary complex. Binding experiments were conducted as in C in the presence of 2.8uM His_6-$Nup159_{1-387}$ (pSW3458) or buffer. Nucleotides were added to indicated samples at 50uM.

The soluble binding assay is limited by the fact that the Gle1-Dbp5 interaction is mediated by two interfaces. Potentially, Nup42 impedes interaction at the weak Gle1-Dbp5 interface, where it is predicted to bind, but Gle1 and Dbp5 can still bind at the stronger interface. Additionally, the gain-of-function alterations are located at the stronger interface, and Gle1$^{VAI>DDD}$ alterations do not disrupt the Gle1-Dbp5 interaction when combined with the gain-of-function alterations (MONTPETIT *et al.* 2011, Figure A.2C). However, the interaction at the weaker interface is required for Gle1 to stimulate Dbp5 ATPase activity (MONTPETIT *et al.* 2011). Therefore, we tested whether titration of Nup42 impacts Gle1 stimulation of Dbp5 ATPase activity using an enzyme-coupled kinetic colorimetric ATPase assay (NOBLE *et al.* 2011). Using a concentration of Gle1 that is half-maximal for stimulation of Dbp5 ATPase activity (Figure A.3A, asterisk indicates 250nM Gle1, 200nM Gle1 was used for subsequent experiments), GST-Nup42C was pre-incubated with Gle1C for 1hr and then Dbp5 and ATP were added to start the timecourse. In parallel, using the same buffers and additional proteins that are in the colorimetric ATPase assay, the same concentration of MBP-Gle1C beads were incubated with GST-Nup42C for an hour to ensure they are interacting under the tested conditions. Even in the presence of the highest GST-Nup42C concentration, where the interaction with Gle1 was clear (Figure A.3B, lane 10, asterisk), Gle1C stimulated the Dbp5 ATPase activity to a similar extent as with no Nup42 present (Figure A.3C). GST-Nup42C had no effect on Dbp5 ATPase activity in the absence of Gle1. It is possible that the Gle1-Nup42 interaction is transient, and the binding interface may overlap with the Dbp5 interface, but this result suggests that Nup42 does not inhibit the Gle1-Dbp5 interaction. Additionally, because the readout for

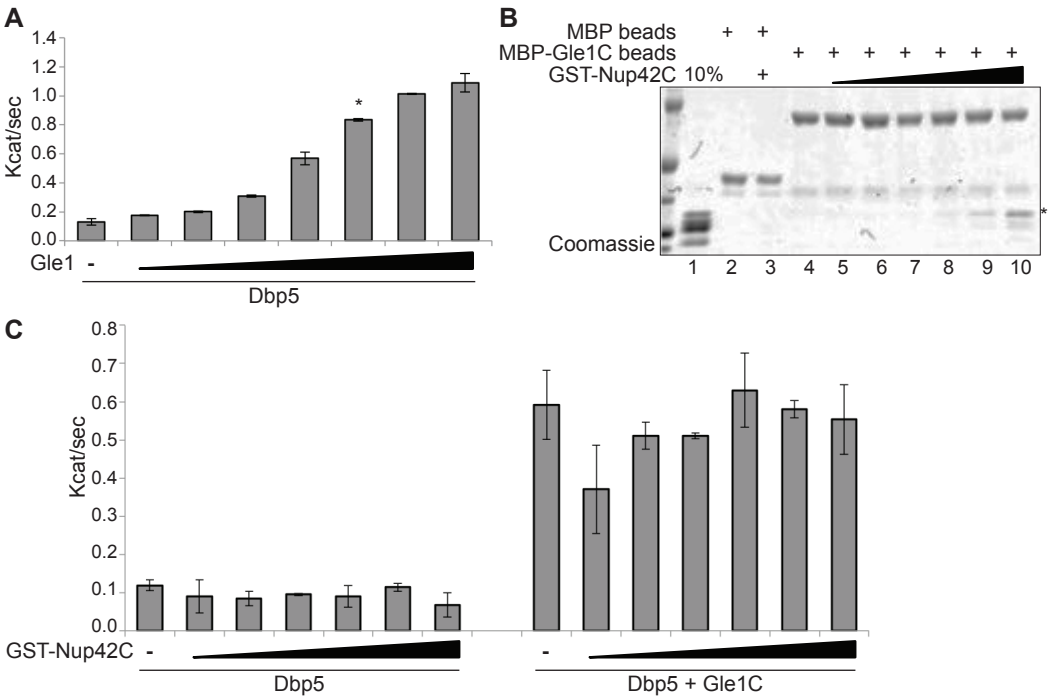

Figure A.3. Nup42 does not reduce Gle1 stimulation of Dbp5 ATPase activity.
(A) Titrating Gle1 stimulation of Dbp5 ATPase activity. Colorimetric enzyme-coupled ATPase rate assays were performed as in (NOBLE *et al.* 2011). 500nM Dbp5 was incubated in ATPase buffer (10mM HEPES pH7.5, 45mM NaCl, 2mM $MgCl_2$, 1uM poly$(A)_{25}$, 1mM DTT, 1U SUPERasin (Ambion), and 100nM IP_6). $Gle1_{241-538}$ was added in 1:2 dilutions up to 1uM, and reactions were started with the addition of 1mM ATP:$MgCl_2$, and OD340 was recorded every 20sec. (B) Nup42C binds Gle1 in ATPase buffer conditions. 200nM MBP-$Gle1_{241-538}$ or MBP beads were incubated with 1:3 fold dilutions of GST-$Nup42_{365-430}$ up to 5.6uM for 1hr in ATPase buffer. Samples were washed as in Figure A.2A, resolved on SDS-PAGE, and stained with Coomassie. (C) Nup42C does not compete with Gle1 for stimulation of Dbp5 ATPase activity. 200nM $Gle1_{241-538}$ was incubated with 1:3 fold dilutions of GST-$Nup42_{365-430}$ up to 5.6uM for 1hr in ATPase buffer. 500nM Dbp5 was added with 1mM ATP:$MgCl_2$ to start the reaction as in Figure A.2E.

the colorimetric assay is coupled with other enzymes, it is possible that the additional steps required to observe the Dbp5 ATPase assay don't reflect the possible inhibition by Nup42. This is unlikely, however, because ADP production is the rate-limiting step under the conditions tested, and half-maximal Gle1 stimulation is evident, indicating that inhibition or enhancement of Gle1 function is within the range of the experimental conditions used.

Discussion

Although truncation analysis suggested that Nup42 may interact with a region of Gle1 responsible for Dbp5 ATPase stimulation, further biochemical analysis indicated that these interactions are not competitive. It is possible that truncated Gle1 does not fold correctly, and deletion studies do not accurately indicate the Nup42 binding site on Gle1. Structural analysis of the Gle1-Nup42 or hGle1B-hCG1 interaction should provide additional insight into the nature of this interface. The minimal region of Nup42 that interacts with Gle1 is only 75 residues long, but this region is predicted to be largely unfolded except for a small predicted helix (PsiPred, data not shown), and it is highly proteolytically sensitive (see input in Figure A.2A and elutions in A.2C and A.2D). Therefore, the next approach should be to narrow down what region of Nup42 interacts with Gle1, possibly using yeast-two-hybrid analysis for subsequent crystallization trials. Additionally, whether the same or a distinct region is required for Nup42 anchoring at the NPC may provide some insight into how either Gle1 or Nup42 localize to the NPC, since additional binding partners have not been characterized.

It remains to be determined what the function of Gle1 self-association during mRNA export is. We hypothesize that multiple Gle1 promoters are required for

simultaneous/rapid activation of Dbp5 for the removal of multiple Mex67-Mtr2 molecules from the mRNP. As outlined in Chapter I, it is unknown how many Mex67-Mtr2 molecules are bound to each mRNP, how many adaptors mediate this interaction, and whether different transcripts have a distinct number of Mex67-Mtr2 dimers bound. It is thought that the long mRNPs require multiple Mex67-Mtr2 dimers to allow efficient export of the large RNP complex, and thus, multiple remodeling events would be required for removal of these transport receptors. Additionally, how Dbp5 contacts the mRNP and whether unfruitful mRNP remodeling events occur before the mRNP successfully escapes the NPC is unknown. Despite the lack of understanding of mRNP remodeling events, it is likely that multiple rounds of mRNP remodeling are required for each transcript. Additionally, it is unknown what is remodeled by Dbp5 and Ded1 during translation, but potentially this process does not require removal of multiple proteins that coat the mRNP. Thus, the complex remodeling that occurs at the NPC may explain the specific requirement for Gle1 self-association for this process. It is possible that shorter transcripts that may contain fewer Mex67-Mtr2 molecules might differentially require Gle1 self-association for remodeling and export.

Structural analysis of Gle1 oligomeric disks

Results

Although we reported that Gle1 self associates to form large oligomeric disks *in vitro* (FOLKMANN *et al.* 2013), several questions remain regarding the details of this structure. First, how are Gle1 disks organized: where are the Dbp5/hDbp5, Nup42/hCG1, hNup155 binding sites? Uncovering where these proteins are bound

relative to the Gle1 disk impacts how this structure might affect mRNA export. For example, if Dbp5 is located in the center of the disk, it might imply that the mRNA exports by threading through the middle of the Gle1 disks. Additionally, although the PFQ mutants were demonstrated to have altered Gle1 disk morphology and altered nucleocytoplasmic shuttling *in vivo*, it was not determined how this change in disk structure affects Gle1 function at the NPC. Thus, we sought to further analyze Gle1 oligomeric disk structure.

First, an unanswered question is whether Gle1 forms oligomeric disk structures *in vivo*. The best approach to answer this question is to analyze Gle1 self-association *in vivo*. Potentially, the ever-increasing resolution capable in fluorescent microscopy techniques may be able to assess Gle1-Gle1 associations *in vivo*, the best resolution capabilities are still 20-30nm (TOOMRE and BEWERSDORF 2010), which is larger than the size of a Gle1 disc. Therefore, Gle1 was purified from cells under cryogenic conditions. This revealed the presence of disk-like structures that were ~15nm in size (range: 10-25nm) (Figure A.4A). Although it is possible that these structures spontaneously formed following cell lysis, this result suggests that Gle1 may self-associate to form slightly smaller oligomeric disks *in vivo*. Gle1 purification was assessed by western blotting (Figure A.4B), but because co-purifying/contaminating proteins were not determined by coomassie staining or performing mass spectroscopic analysis, it is unknown whether the disk structures may come from other proteins. As a control, gle1Δcc-TAP would be expected not to form disks. Potentially, co-purifiying Dbp5 and exporting mRNPs will uncover how mRNA contacts Gle1 oligomeric disks during export.

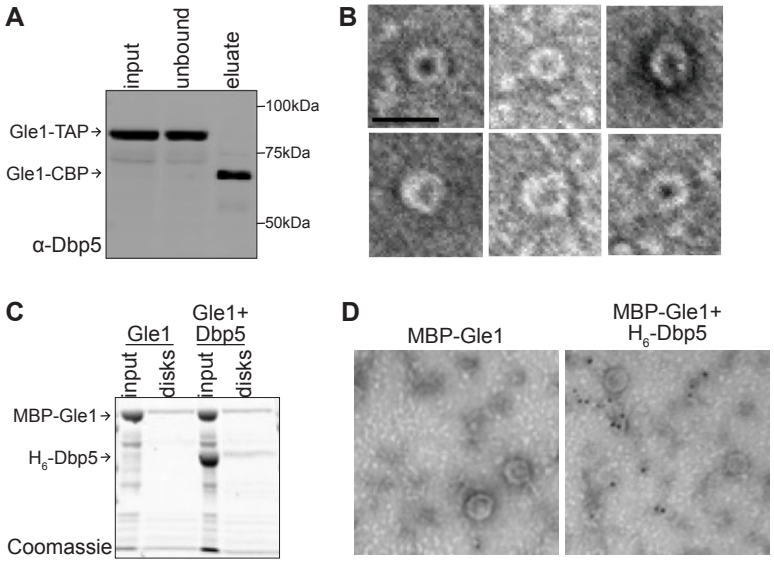

Figure A.4. Exploration of Gle1 disk structure.
(A) Gle1 purified from cells forms disks. 1L cultures *GLE1-TAP* (YOL309) were grown to mid-log phase, centrifuged 10min 4krpm, resuspended in lysis buffer (20 mM HEPES pH 7.4, 1.2% PVP-40), centrifuged again, and rapidly frozen by pressing through a syringe into liquid N_2, which was then decanted. Frozen cells were lysed using a planetary ball mill at cryogenic temperature. Lysate was resuspended in binding buffer (20mM HEPES pH 7.4, 110mM KOAc, 500mM NaCl, 2mM $MgCl_2$, 1% NP-40 with protease inhibitors determined in (ALBER *et al.* 2007) to only co-purify with Nup42) and incubated with IgG sepharose (GE) 1hr at 4°C. Beads were washed 3x with TEV cleavage buffer (20mM HEPES pH7.4, 150mM NaCl, 0.1% NP-40, 0.5mM EDTA, 1mM DTT), and cleaved 1.5hr at 16° with TEV. Cleaved protein was diluted in buffer A, adsorbed to carbon-coated copper grids, stained with uranyl-formate, and visualized using a FEI Morgigani electron microscope at 22000x magnification. Scale bar=25nm. (B) Gle1 samples from 3A. Samples from 3A were combined with 6x SDS loading buffer, resolved by SDS-PAGE and blotted using α-Gle1 (ASW 43.2) antibodies. (C) Dbp5 co-elutes in the void of S200 in the presence of Gle1. Purified MBP-Gle1^{H337R} (pSW3984, 5.5uM) was incubated with His$_6$-Dbp5^{L327V} (pSW4017, 8.0uM) or buffer in buffer A +50uM IP_6 +250uM AMP-PNP for 30 minutes and size exclusion chromatography with an S200 column (GE Healthcare) was used to isolate Gle1 disks. The void fraction was collected, resolved with SDS-PAGE, and Coomassie stained. (D) Ni-NTA-5nm gold does not label Dbp5-Gle1 disks. MBP-Gle1^{H337R} and His$_6$-Dbp5^{L327V} disks were purified as in Figure A.3C. Samples were diluted in buffer A +AMP-PNP and IP_6, adsorbed onto carbon-coated copper grids, incubated with 1:50 5nm Ni-NTA-Nanogold (Nanoprobes) for 5min in buffer A +40mM imidizole +AMP-PNP and IP_6, stained with uranyl-formate, and visualized using a FEI Morgigani electron microscope at 22000x magnification.

Next, using recombinant proteins, we sought to determine where Dbp5 and potentially other binding partners associate with Gle1 oligomeric disks. Although His_6-$Dbp5^{L327V}$ was found in the void fraction only in the presence of MBP-$Gle1^{H337R}$ (indicating specific interaction with Gle1 disks) (Figure A.4C), no obvious difference in density was observed on Gle1 disks (data not shown). To specifically label His_6-$Dbp5^{L327V}$, samples were incubated with 5nm Ni-NTA-nanogold. Although binding of 5nm Ni-NTA-nanogold to grids was higher in the presence of His_6-$Dbp5^{L327V}$, no gold particles were found labeling Gle1 disks (Figure A.4D). Thus, the gold labeling was non-specific (perhaps the Dbp5-Gle1 interface blocks the His_6 residues), Dbp5 does not bind Gle1 disks specifically, or the Dbp5-Gle1 interface was lost in the time course of the labeling.

Discussion

Typically, averaging thousands of particles imaged by electron microscopy provides high-resolution 3D structures of macromolecular structures. However, particle averaging requires homogenous samples in one or a very few conformations. Thus, the formation of different sized disk particles makes it difficult to obtain higher resolution structures of Gle1 by particle averaging. Using sucrose gradients to separate different sized Gle1 particles were unsuccessful. However, EM tomography may provide both higher resolution of Gle1 particles and generate a 3D model of Gle1 disk structure. Additionally, co-expression of Gle1 and Dbp5 may aid in their interaction.

Self-association requirements for Gle1

Results

It was reported that Gle1 dimerization via the GCN4 dimeric coiled-coil is sufficient to partially rescue Gle1 function in cells (FOLKMANN *et al.* 2013). However, because Gle1 self-associates into large disks *in vitro*, it remained a possibility that promoting higher-order oligomerization would further restore Gle1 function. Additionally, because the organization of endogenous self-association was undetermined, we sought to test whether parallel or antiparallel dimerization is required *in vivo*. Therefore, we tested a set of coiled-coil domains for complementation of Gle1 function. Using the Gcn4 coiled-coil as a template, the Alber lab mutagenized key hydrophobic residues at the intermolecular interface to generate a series of parallel dimer, trimer, and tetramer coiled-coils, and the Gle1 coiled-coil domain was replaced with these constructs (HARBURY *et al.* 1993). Additionally, this domain was replaced with the coiled-coil of ProPAt, which forms and intermolecular anti-parallel coiled coil (HILLAR *et al.* 2003). We analyzed the complementation of *gle1-4* temperature sensitivity with each of these constructs. Interestingly, although all dimers, parallel or antiparallel, rescued, higher order oligomers did not (Figure A.5A). GFP-tagged constructs were generated to assess localization and expression level. All chimeric proteins were expressed at similar levels (Figure A.5C), and all were diffusely localized with no clear accumulation at the nuclear rim (Figure A.5B).

Discussion

It remains to be determined whether all constructs self-associate as expected; *in vitro* analysis of these constructs using size-exclusion chromatography or analytical

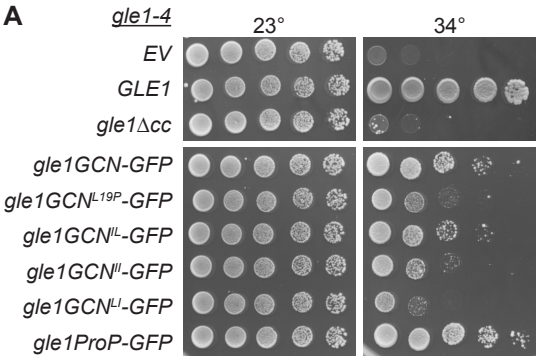
A
gle1-4
23°
34°
EV
GLE1
gle1Δcc
gle1GCN-GFP
gle1GCN^L19P-GFP
gle1GCN^IL-GFP
gle1GCN^II-GFP
gle1GCN^LI-GFP
gle1ProP-GFP

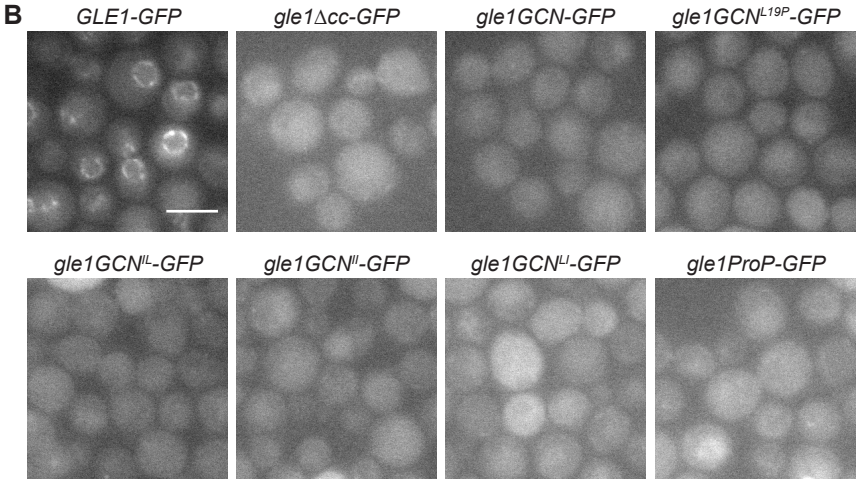
B
GLE1-GFP
gle1Δcc-GFP
gle1GCN-GFP
gle1GCN^L19P-GFP
gle1GCN^IL-GFP
gle1GCN^II-GFP
gle1GCN^LI-GFP
gle1ProP-GFP

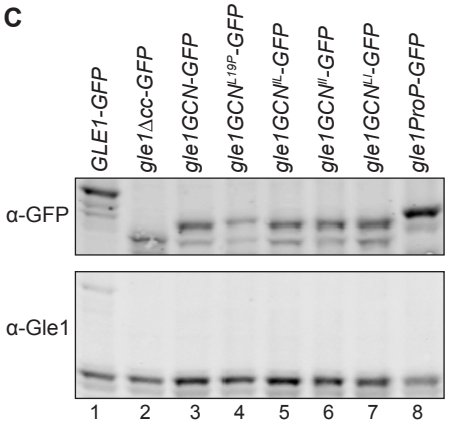
C
GLE1-GFP
gle1Δcc-GFP
gle1GCN-GFP
gle1GCN^L19P-GFP
gle1GCN^IL-GFP
gle1GCN^II-GFP
gle1GCN^LI-GFP
gle1ProP-GFP
α-GFP
α-Gle1
1
2
3
4
5
6
7
8

Figure A.5. Heterologous dimerization, but not higher order oligomerization partially rescues Gle1 loss of function.
(A) Dimerization partially restores Gle1 functionality. *EV* (CP25), *GLE1/LEU* (pSW399), *gle1Δcc/LEU* (pSW4125), and *gle1-coiled-coil chimeras/LEU* (pSW4126-4131) were transformed to *gle1-4* (SWY4209). Strains were grown to mid-log phase and 5-fold serially diluted on -Leu at the indicated temperatures. (B) Gle1 coiled-coil chimeric proteins are diffusely localized. *GLE1-GFP/LEU*, *gle1Δcc-GFP/LEU*, and *gle1-coiled-coil chimeras-GFP/LEU* were transformed to wt (SWY 2284). Samples were grown to mid-log phase, collected, re-suspended in synthetic complete media, and live cells were imaged with widefield microscopy. (B) Gle1 coiled-coil chimeric proteins are similarly expressed. *GLE1-GFP/LEU*, *gle1Δcc-GFP/LEU*, and *gle1-coiled-coil chimeras-GFP/LEU* were transformed to wt (SWY 2284). Samples were grown to mid-log phase, and equal OD_{600} units of cell numbers were collected by centrifugation. Cells were re-suspended in Magic buffer, lysed by vortexing with glass beads, and boiled 5min. Samples were resolved by SDS-PAGE and blotted with anti-GFP (AOL106) and anti-Gle1 (ASW 43.2).

ultracentrifugation should determine the oligomeric state. Furthermore, it is possible that different levels of self-association impact Gle1 function in translation. Rescue of double mutants should uncover different functionality of these Gle1 constructs.

Finally, and perhaps most interestingly, how the coiled-coil domain of Gle1 interacts to form particles that are not only so large, but also diverse in size, is a major unanswered question. Scanning electron microscopic analysis of NPCs from *S.c.* isolated after high pressure freezing uncovered a cytoplasmic basket-like structure at a subset of NPCs (FISEROVA *et al.* 2014). Potentially, flexibility in Gle1 self-association is required for the dynamic organization of cytoplasmic filaments to form this structure. It would be interesting to observe how this structure changes in the presence of the Gle1 coiled coil chimeras.

Appendix B:

Dbp5 Remodels Mex67 from the 60S Ribosomal Subunit

Introduction

Ribosome subunit assembly and export from the nucleus has many similarities to mRNA biogenesis and export. Both exist as RNPs: RNAs coated with associated proteins. Similar to mRNP assembly and maturation, ribosomal subunits undergo coordinated steps of transcription, RNA cleavage (the majority of ribosomal RNA is transcribed as one RNA molecule that is then cleaved to form the 25S and 5.8 S RNAs of the 60S and 18S RNA of the 40S), RNA modification (methylation and pseudo-uridylation instead of polyadenylation and 5' capping), association of binding proteins (> 200 transient and ~80 permanent), and only fully matured subunits export for function in the cytoplasm (reviewed in PANSE and JOHNSON 2010). Indeed, in *S. cerevisiae*, the large 60S subunits (and possibly the small 40S subunits (FAZA *et al.* 2012) even share the mRNA export receptor, Mex67-Mtr2 (YAO *et al.* 2007). Utilization of a common export receptor for ribosome and mRNP export likely evolved to coordinate these processes. It is unknown how Mex67-Mtr2 is removed from ribosomal subunits after export through the NPC.

Unlike most mRNPs, ribosomal subunits also utilize additional transport receptors for export: the 40S subunit is exported by Crm1 and 60S is exported by Crm1 in addition to the non-Kap-related export factors Arx1 and Ecm1 (reviewed in PANSE and JOHNSON 2010). The mammalian homologue of Arx1, Ebp1, has also been suggested to be an export receptor for 60S subunits (BRADATSCH *et al.* 2007). Crm1, Mex67-Mtr2,

and Arx1 associate stoichometrically with the 60S subunit, demonstrating that multiple export factors coincidentally associate with one ribosomal particle (BRADATSCH *et al.* 2012). It has been proposed that having multiple transport receptors provides multiple checkpoints for proper 60S assembly (HUNG *et al.* 2008). It is also possible that use of diverse transport receptors allows for interaction with distinct subsets of FG domains within the NPC, thus increasing the efficiency of export for this large (~20nm at the narrowest point for the mature *S. cerevisiae* 60S subunit, not taking into account additional mass for transport receptor) mRNP cargo. Single deletion of *ARX1*, *ECM1*, or the region of Mex67 responsible for 60S export is not strictly lethal, however, loss of these export factors may slow ribosome export enough to provide more time for nuclear maturation.

The fact that ribosomal subunits utilize the Mex67-Mtr2 dimer for export raises the question of whether removal of these factors is required for translation functionality. Experiments detailing the post-export maturation process for 60S subunits have demonstrated that cytoplasmic maturation steps, wherein other trans-acting factors are removed and permanent functional 60S proteins are added, are required before the subunit is competent for translation. Crm1 associates with 60S particles through the NES of the adaptor protein Nmd3 (HO *et al.* 2000b; GADAL *et al.* 2001). Like other Kap export complexes, Ran-GTP binds Crm1 coincidentally with the Nmd3 NES for export, and upon GTP hydrolysis in the cytoplasm, Ran-GDP and Nmd3 dissociate from Crm1. Once in the cytoplasm, Rpl10 binds to a region of the 60S subunit adjacent to Nmd3 and recruits the cytoplasmic GTPase, Lsg1 (HEDGES *et al.* 2005; WEST *et al.* 2005). GTP hydrolysis promotes release of Nmd3 from 60S (SENGUPTA *et al.* 2010). This step

is essential for 60S-40S subunit joining during translation as Nmd3 blocks this interaction site, thus providing a checkpoint for 60S subunit maturation before functionality (SENGUPTA *et al.* 2010).

Additionally, Arx1, another 60S export receptor, must be removed for 60S function. Instead of containing HEAT repeats characteristic of Kaps, Arx1 is structurally related to methionine aminopeptidases which function to remove the N-terminal methionine on nascent polypeptides (BRADATSCH *et al.* 2007). However, instead of exhibiting amiopeptidase activity, the central cavity of Arx1 binds FG repeats. Arx1 binds to 60S subunits near the exit tunnel, and has been suggested to both inhibit binding of functional methionine aminopeptidases (inhibit functionality) and function as a checkpoint to ensure formation of a proper binding site before nuclear exit (BRADATSCH *et al.* 2012; GREBER *et al.* 2012). Once the 60S subunit exits to the cytoplasm, the zinc finger protein Rei1 functions in removal Arx1 (HUNG and JOHNSON 2006). Therefore another function for the multiple 60S export factors is likely to inhibit different ribosome functions until the particle is fully mature.

This raises the question of whether Mex67-Mtr2 serves a similar function, but it remains unknown where on ribosomal subunits Mex67-Mtr2 associates. It has been proposed that Mex67-Mtr2 can directly bind structured RNA of the ribosome. Vertebrate TAP-p15 directly binds and exports the structured CTE RNA for export (GRUTER *et al.* 1998; BRAUN *et al.* 1999). However, the regions of Mex67-Mtr2 proposed to bind 60S subunits (positively charged loops within the middle NTF2-like region) are not conserved in TAP-p15 (YAO *et al.* 2007) and are independent of the N-terminal RNA recognition and leucine rich domains demonstrated to be responsible for CTE-mediated

export (BRAUN *et al.* 1999). The Mex67-Mtr2 dimer has been demonstrated to bind the ribosomal 5S RNA *in vitro*, and the 5S RNA is somewhat exposed at the surface of the ribosome (Figure B.1). Regardless of how Mex67-Mtr2 associates with ribosomal particles, removal of these proteins is essential for recycling of the transport receptor is essential to allow additional rounds of both ribosome and mRNP export.

It is undetermined how Mex67-Mtr2 is removed from ribosomal particles. We have hypothesized that, similar to removal of Mex67-Mtr2 from mRNPs, Dbp5 in conjunction with Gle1-IP_6 remodel the dimer from the ribosome. In a candidate screen for factors involved in 60S export, the Silver lab published that the *rat8-2 (dbp5)* mutant accumulates ribosomes in the nucleus, suggesting that Dbp5 may play a direct role in ribosome export (STAGE-ZIMMERMANN *et al.* 2000). Therefore, we took a variety of approaches to determine whether Dbp5 and Gle1 function in removal of Mex67 from 60S subunits. Additionally, we analyzed the requirement of FG domains in the ribosome export process.

Results

As a first approach to explore the role of Dbp5 in ribosome export, the *DBP5* allele, *rat8-2* was tested for synthetic genetic interactions with mutants of ribosome export factors, *ecm1Δ*, *arx1Δ*, *mex67* ribosome export mutants, or *nmd3* NES and temperature-sensitive alleles. No obvious growth defects were observed when *rat8-2 (dbp5)* was combined with *ecm1Δ*, *arx1Δ* (data not shown). *rat8-2* displayed mildly enhanced growth defects when combined with *nmd3AAA* (Figure B.2A). Interestingly, expression of *mex67Δloop*, in which the interaction between Mex67 and the 60S

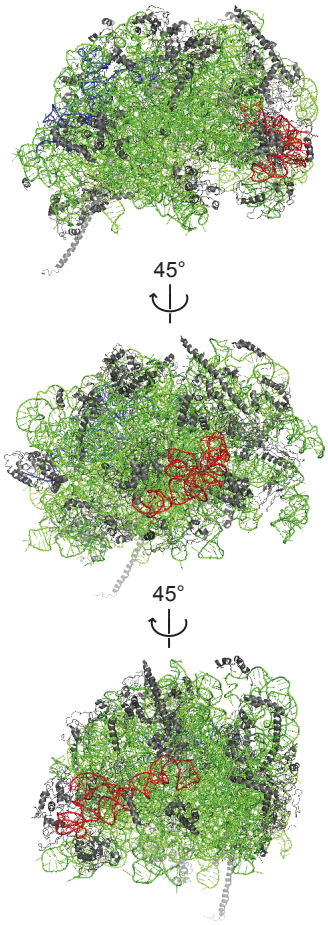

Figure B1. 5S RNA is on surface of the 60S subunit.
Structure of mature *S.c.* 60S subunit from (BEN-SHEM *et al.* 2010) colorized to indicate protein (grey), 25S RNA (green), 5.8S RNA (blue), and 5S RNA (red).

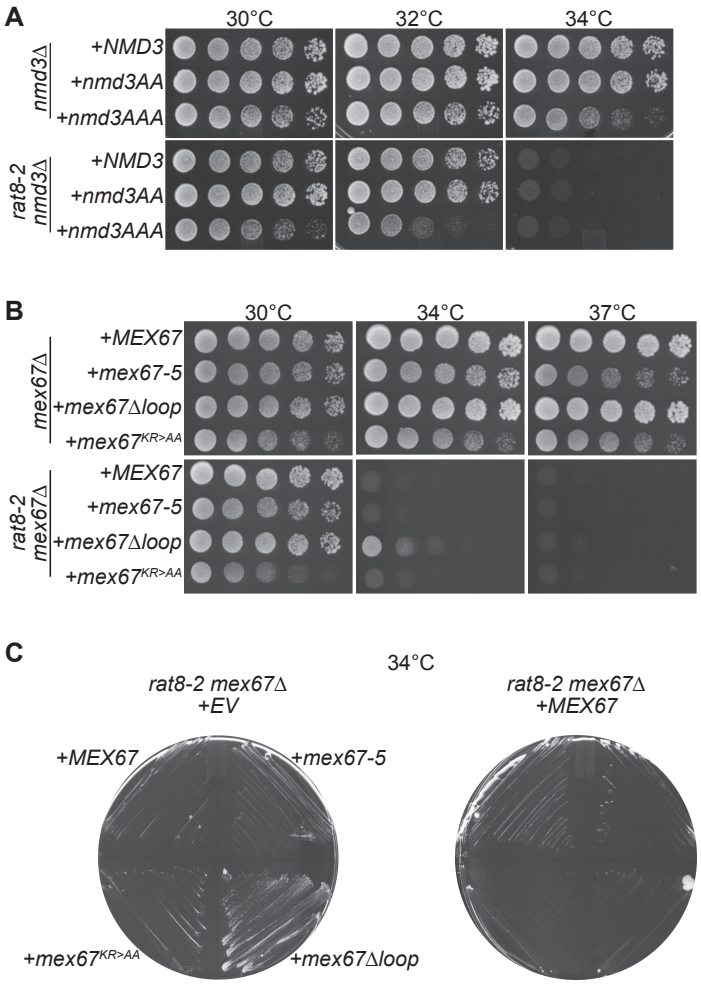

Figure B2. *DBP5* mutants exhibit synthetic genetic interactions with 60S export mutants. (A) *rat8-2 (dbp5)* is synthetically sick with an *nmd3* NES mutant. Indicated strains (YOL675 and SWY 4917 transformed with CP3609-3611 and shuffled on 5-FOA) were grown to mid-log phase and 5-fold serially diluted on YPD at the indicated temperatures. (B) *mex67Δloop*, which has reduced 60S association, partially rescues *rat8-2* growth defects. Indicated strains (SWY4758-4765) were grown to mid-log phase and 5-fold serially diluted on YPD at the indicated temperatures. (C) The *mex67Δloop* growth rescue is recessive. Indicated strains (SWY4760, SWY4764) were transformed with empty vector (EV, CP37) or *MEX67/CEN/URA* (CP3141), struck on -Ura, and grown at 34°.

subunit is abrogated, partially rescued the growth defect of *rat8-2* (Figure B.2B). However, *mex67KR>AA*, where Mex67 interaction with 60S is completely disrupted, did not rescue *rat8-2* growth defects. Thus, reducing the interaction between Mex67 and 60S partially bypasses the requirement for Dbp5 in Mex67 removal. Importantly, this growth rescue was recessive, as expression of *MEX67* in addition to *mex67Δloop* did not allow growth rescue of *rat8-2*, suggesting that the growth rescue was not due to biasing the pool of Mex67 toward mRNA export (Figure B.2C). Therefore, these genetic results suggest that Dbp5 may function in the removal of Mex67 from the 60S ribosomal subunit. It remains to be tested if *nmd3* or *mex67* mutants have growth defects with *gle1-4* or *ipk1Δ*.

We next tested whether Dbp5 function is required for 60S ribosome subunit export. Although it was previously reported that the *dbp5 rat8-2* mutant accumulates the 60S ribosome reporter Rpl11-GFP (STAGE-ZIMMERMANN *et al.* 2000) at the restrictive temperature, we were unable to observe nuclear accumulation of multiple 60S reporters after shifting *rat8-2* mutants to the restrictive temperature over a time scale of 0-120 min. Furthermore, expression of the dominant negative *DBP5* mutant, $DBP5^{R369G}$, also did not result in 60S nuclear accumulation of Rpl25-GFP, although a robust mRNA export defect was observed with this mutant (data not shown). We therefore tested whether ribosome subunits have delayed export when nuclear ribosome biosynthesis is increased. In this assay, cells are grown to saturation, where ribosome biosynthesis is inhibited, and then diluted to early log phase which drastically stimulates ribosome biogenesis. After dilution of saturated cultures for growth for 4hrs at 25°, robust nuclear accumulation of Rpl5-GFP was observed (Figure B.3A). Polysome profiling or analysis

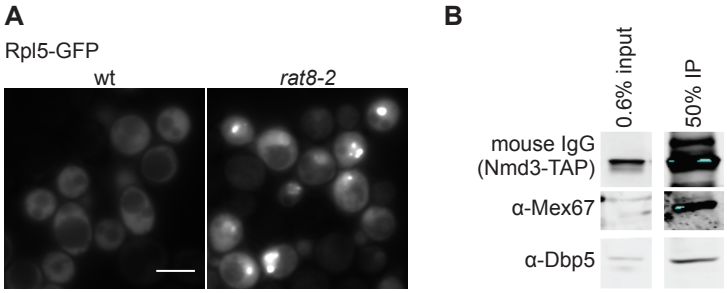

Figure B3. Dbp5 functions in 60S subunit export.
(A) *rat8-2 (dbp5)* accumulates the 60S subunit reporter Rpl5-GFP in the nucleus. Indicated strains (wt, YOL182; *rat8-2* YOL115) carrying the *RPL5-GFP* reporter plasmid (CP3728) were grown overnight to saturation at 25° in –Leu dropout media. The following day, strains were diluted to OD_{600}=0.2 and grown for an additional 4 hrs at 25°. Strains were imaged by live cell fluorescence. Scale bar=5μm. (B) Dbp5 associates with exporting 60S subunits. 1L *NMD3-TAP* (YOL769) was grown at 30° in YPD to mid-log phase. Cells were then centrifuged 10 min 4krpm, resuspended in lysis buffer (20 mM HEPES [pH 7.4], 1.2% PVP-40), centrifuged again, and rapidly frozen by pressing through a syringe into liquid N_2, which was then decanted. Frozen cells were lysed using a planetary ball mill at cryogenic temperature. Lysate was resuspended in 60S binding buffer (50 mM Tris-HCl, 150 mM NaCl, 5 mM $MgCl_2$, 2mM beta mercaptoethanol, 0.05% Tween 20) and incubated with IgG sepharose (GE) 2hrs at 4°. Beads were washed 3x with 60S buffer, and bound proteins were boiled with SDS loading buffer. Input and enriched fractions were separated by SDS-PAGE and blotted using mouse IgG (AOL 122), α-Mex67 (ASW 52), and α-Dbp5 (ASW 42) antibodies.

of additional 60S reporters will be required to determine whether Rpl5-GFP accumulation is reflective of whole 60S subunit nuclear accumulation. However, the robust accumulation of Rpl5-GFP suggests that, Dbp5 functions in ribosome export, and it is likely that combined mRNA export defects prevent nuclear accumulation of ribosome subunits using other assays. It remains to be determined whether *mex67Δloop* rescues the 60S export defect and/or the mRNA export defect.

If Dbp5 plays a direct role in 60S export, it should associate with exporting subunits. Although this interaction may be transient, an RNAse sensitive Dbp5 interaction with Mex67-associated mRNPs has been uncovered (LUND and GUTHRIE 2005; OEFFINGER *et al.* 2007). Using a rapid freezing and cryo-lysis technique that was previously demonstrated to preserve mRNP-associated proteins (OEFFINGER *et al.* 2007), exporting 60S subunits were purified from wt cells using Nmd3-TAP. In addition to enriching for Mex67, the purified fraction was shown to also contain Dbp5 (Figure B.3B). It remains to be determined whether this interaction is RNAse sensitive and whether mRNPs were also isolated by this procedure (by blotting for mRNA-associated proteins such as the cap-binding protein Cbp80 or the poly-A binding protein Nab2). Furthermore, immunoprecipitations of 60S particles at different stages of biogenesis will determine whether the Dbp5 association occurs specifically during export as has been determined for the Mex67-Mtr2 association.

It has been proposed that Mex67-Mtr2 directly binds to structured RNA within the 60S subunit since binds the 5S RNA *in vitro* as determined by electromobility mobility shift assay (EMSA) (YAO *et al.* 2007). Dbp5 is able to remodel Nab2 (TRAN *et al.* 2007) and Mex67-Mtr2 (K. Noble, personal communication) from unstructured poly$(A)_{25}$ RNA,

but it is unknown if Dbp5 can remodel substrates off structured RNA. We therefore attempted a similar biochemical assay to determine whether Dbp5 remodels Mex67-Mtr2 from 5S RNA. Using the previously published assay conditions, titration of Mex67-Mtr2 with *in vitro* transcribed 5S RNA resulted in slower-migrating bands, indicating binding of one or more Mex67-Mtr2 molecules (Figure B.4A). However, addition of Dbp5-ADP did not clearly remodel Mex67-Mtr2 from the 5S RNA and instead resulted in an smeary EtBr staining and staining in the well that was present with Dbp5 alone (Figure B.4B, lanes 3-5, 12). Boiling the sample after incubation resolved the smeared and shifted bands, indicating that Dbp5 did not degrade the 5S RNA (Figure B.4B, lanes 9-11). In a parallel assay, Dbp5-ADP remodeled Nab2 off ^{32}P-poly(A)$_{25}$ RNA, positively demonstrating enzyme activity (Figure B.4C, lane 7). In addition radiographic detection of RNA and different concentrations of proteins, the buffer conditions between the two experiments are also different. Importantly, Mex67-Mtr2 titration with 5S RNA in our published poly(A) remodeling buffer (TRAN *et al.* 2007) resulted in only a single slower migrating band, indicating saturation of 5S binding with a single binding site (Figure B.4D). Thus, due to contaminating EtBr signal by Dbp5, potential non-specific binding of Mex67 and Dbp5 to 5S RNA in other buffer conditions, the next approach should be to ^{32}P-label *in vitro* transcribed 5S RNA, perform the remodeling assay using the poly(A) buffer where Dbp5 has been published to be active, and detect migration by radiography.

Although Dbp5 may remodel Mex67-Mtr2 from 5S RNA *in vitro*, it is unknown how Mex67 interacts with 60S subunits and whether the *in vitro* remodeling assay is relevant *in vivo*. We therefore designed a strategy to purify exporting or nascently

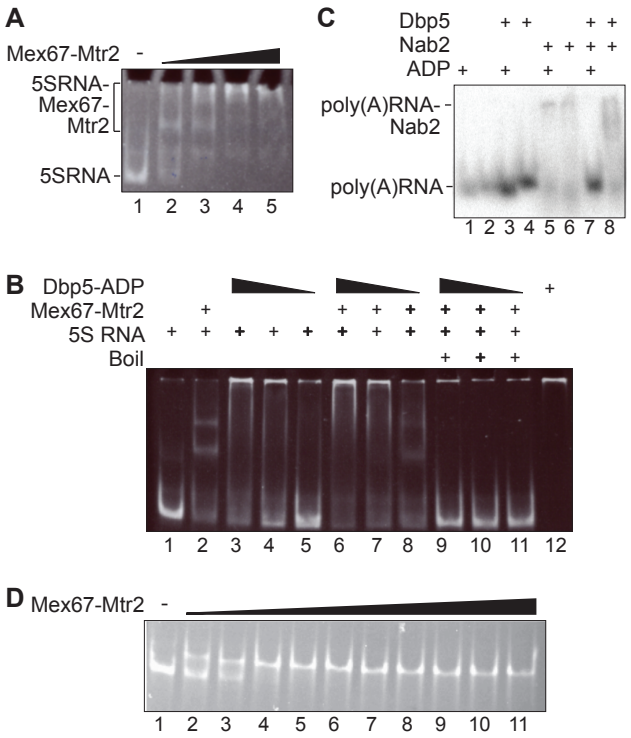

Figure B4. Testing whether Dbp5 remodels Mex67 from 5S RNA *in vitro*.
(A) Mex67 binds 5S RNA *in* vitro. DNA encoding 5S RNA was PCR-amplified (from pSW3557 using oligos 1603&2858), and 1.0 ug was used in an *in vitro* transcription reaction (MegaScript) and treated with DNAse. 150ng (190nM) 5S RNA was incubated with 300-1200nM affinity purified H_6-Mex67-Mtr2 for 30min at RT in 5S binding buffer (20 mM HEPES [pH 7.4], 100 mM KCl, 10 mM NaCl, 4 mM $MgCl_2$, 0.2 mM EDTA, 20% glycerol, 1 mM DTT, 0.5% NP-40). Samples were resolved on a 6% acrylamide gel in 0.5x TBE. The gel was stained with 1:20,000 EtBr 20min and visualized under UV light. "-" indicates sample with no Mex67-Mtr2 added. (B) 150ng 5S RNA was incubated with 300nM H_6-Mex67-Mtr2 5min at RT followed by addition of 300-1200nM Dbp5 + 500nM ADP for 20min at RT. Samples were resolved on a 6% acrylamide gel in 0.5x TBE. The gel was stained with 1:20,000 EtBr 20min and visualized under UV light. (C) Dbp5 remodels Nab2 from poly(A) RNA. As in (TRAN *et al.* 2007), oligo$(A)_{25}$ RNA (Dharmacon) was ^{32}P 5' end labeled with T4 PNK (NEB). 1nM radiolabeled RNA was incubated with 250nM affinity purified Nab2 for 10' at 30° in poly(A) remodeling buffer (20 mM HEPES [pH 7.5], 100 mM NaCl, 3 mM $MgCl_2$, and 10% w/v glycerol). 500nM Dbp5 and 500nM ADP were added to the reaction and incubated for 30' at 30°. Samples were resolved on a 4% acrylamide gel and detected by autoradiography. (D) 150ng 5S RNA was incubated with 300nM-3mM H_6-Mex67-Mtr2 for 20min at 30° in poly(A) remodeling buffer. Samples were resolved on a 6% acrylamide gel in 0.5x TBE. The gel was stained with 1:20,000 EtBr 20min and visualized under UV light.

exported 60S subunits (using Nmd3-TAP and Lsg1-TAP, respectively) from wt and *rat8-2* mutants to assay Mex67 association. Rpl11 was also GFP tagged for use as a control for relative 60S subunit enrichment. From these strains, ribosomes can be purified using the above-described cryo-lysis method and relative Mex67 association determined by immunoblotting. If Dbp5 functions in Mex67 removal from 60S subunits, it is expected that there will be increased Mex67 associated in *rat8-2* mutants. After shifting to 37° for 1 hr, cells were frozen and lysed. Nmd3-TAP was immunoprecipitated, and bound proteins were analyzed by Western blotting. Quantification of enriched protein by densitometry demonstrated that the level of Mex67 enriched with Nmd3 was not different in wt and *rat8-2* strains (Figure B.5). However, it is possible that experimental procedures, including a temperature shift rather than shifting from saturated cultures and pulling down Nmd3-TAP rather than a different 60S protein, must be changed to observe Mex67 accumulation on 60S subunits.

Our lab previously demonstrated that specific FG domains are required for mRNA export from the nucleus (TERRY and WENTE 2007). We wanted to analyze whether 60S subunit export also requires a subsets of FG domains. Several *ΔFG* mutants were analyzed for localization of the Rpl5-GFP reporter after temperature shift or dilution from saturation over a long time course. Although the positive control *xpo1-1* resulted in nuclear accumulation after dilution from saturation, no clear nuclear accumulation was observed in any *ΔFG* mutant analyzed (Figure B.6). Several strains resulted in very large cells, as has been previously observed, suggesting that the strains are very sick, likely due to the other reported transport defects (TERRY and WENTE 2007). Alternate methods of analyses such as polysome profiling may be required to

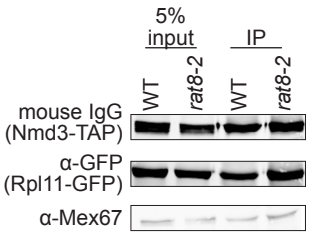

Figure B5. Mex67 does not accumulate on 60S subunits in *rat8-2* after temperature shift.
1L cultures *NMD3-TAP RPL11-GFP* (SWY4855 +CP3022) and *NMD3-TAP RPL11-GFP rat8-2* (SWY4854 +CP3022) were grown to mid-log phase, centrifuged 10 min 4krpm, resuspended in lysis buffer (20 mM HEPES [pH 7.4], 1.2% PVP-40), centrifuged again, and rapidly frozen by pressing through a syringe into liquid N_2, which was then decanted. Frozen cells were lysed using a planetary ball mill at cryogenic temperature. Lysate was resuspended in 60S binding buffer (50 mM Tris-HCl, 150 mM NaCl, 5 mM $MgCl_2$, 2mM beta mercaptoethanol, 0.05% Tween 20) and incubated with IgG sepharose (GE) 2hrs at 4°. Beads were washed 3x with 60S buffer, and bound proteins were boiled with SDS loading buffer. Input and enriched fractions were separated by SDS-PAGE and blotted using mouse IgG (AOL 122), α-Mex67 (ASW 52), and α-GFP (AOL 106) antibodies.

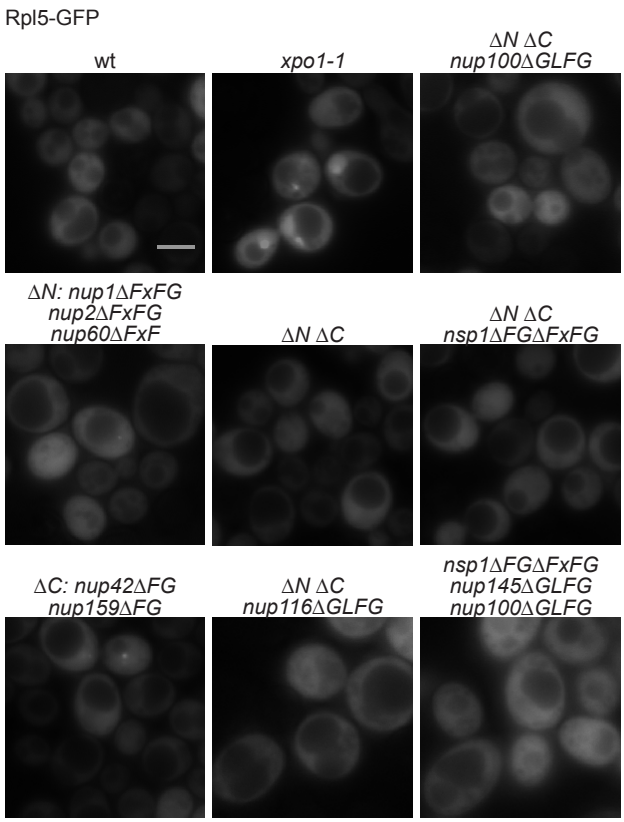

Figure B6. Indicated FG mutants do not accumulate the 60S subunit reporter Rpl5-GFP in the nucleus.
Strains (wt, SWY2284; *xpo1-1*, SWY4318; *ΔN*, SWY2896; *ΔC*, SWY2856; *ΔNΔC*, SWY3041; *ΔNΔCnup116ΔGLFG*, SWY3603; *ΔNΔCnup100ΔGLFG*, SWY3042; *ΔNΔCnsp1ΔFGΔFxFG*, SWY3062; *nsp1ΔFGΔFxFG nup145ΔGLFG nup100ΔGLFG*, SWY3005) carrying the *RPL5-GFP* reporter plasmid (CP3728) were grown overnight to saturation at 25° in –Leu dropout media. The following day, strains were diluted to OD_{600}=0.2 and grown for an additional 2-12 hrs at 25°. Strains were imaged by live cell fluorescence; images shown are 9 hours growth after dilution and representative of all time points. Scale bar=5μm.

definitively assess ribosome export, but these results suggest that ribosome export is not inhibited in the tested *ΔFG* mutants.

Discussion

The above genetic and cell biological data suggest that Dbp5 may function in removal of Mex67-Mtr2 from 60S subunits. However, it is possible that the Dbp5 function in 60S is not through removal of Mex67. Over half of the DEAD-box proteins in humans have been characterized or are predicted to function in ribosome maturation (LINDER and JANKOWSKY 2011). It is possible that, through interaction with a ribosomal protein or ribosome assembly factor, that Dbp5 is recruited to play a role in other steps of 60S maturation. It is also possible that the Dbp5 function in mRNA export plays an indirect role in 60S particle formation. In this case, transcripts of factors required for 60S biogenesis are not efficiently exported in *DBP5* mutants, the factors are thus not translated, and 60S biogenesis is slowed or halted. Further analysis of altered protein interaction with 60S subunits will determine what protein interactions are altered in *DBP5* mutants. Furthermore, purification of 60S subunits at different points of biogenesis should indicate at what steps Dbp5 is associated with these particles.

If Dbp5 does indeed function in removal of Mex67-Mtr2 from 60S particles, how is Mex67 specifically targeted? We speculated in Chapter III and IV that the Nup42 and Nup159 FG domains function in mRNP remodeling by positioning the mRNP and specifically Mex67 in close proximity to Gle1 and Dbp5 for removal. This could also be the mechanism of remodeling specificity of Mex67-Mtr2 for the 60S ribosomal subunit. However, there are several distinctions for the mechanism of Mex67-Mtr2 remodeling

from 60S subunits. It was proposed that Mex67-Mtr2 can directly bind structured ribosomal RNA for export (YAO *et al.* 2007). However, this hasn't been demonstrated for fully formed 60S subunits. It is possible that, like mRNPs, Mex67-Mtr2 associates with 60S subunits via an adaptor protein. Recent advances in ribosome subunit purification and structural determination by high-resolution single particle cryo-electron microscopy can be used to resolve how Mex67-Mtr2 associates with ribosomal subunits. Indeed, purification of Alb1-TAP-associated exporting 60S subunits has revealed extra density not found in mature cytoplasmic subunits that may correspond to Mex67-Mtr2 (BRADATSCH *et al.* 2012). However, it is possible that Mex67-Mtr2 binds multiple exposed RNA regions and it is averaged out in analysis. Despite how Mex67-Mtr2 binds the 60S subunit, a mechanism must exist for these proteins to be specifically removed after export.

If, indeed, Mex67-Mtr2 directly associates with ribosomal RNA, how is recruitment regulated? Is this surface only exposed once the subunit has fully matured in the nucleus? Purification of 60S subunits at distinct stages of maturation demonstrated that Mex67 only associates with exporting subunit (YAO *et al.* 2007). Therefore, an interesting question of how this export receptor is recruited and bound to 60S remains.

We hypothesize that the large subunit requires multiple distinct transport receptors to enhance interaction of this large cargo with FG domains. To analyze which of these FG domains are required for 60S export, we tested several FG mutants from our collection for 60S ribosome accumulation in the nucleus. However, we did not uncover a clear 60S export defect in the tested *ΔFG* mutants. We speculate that the

redundant use of FG domains by the multiple export receptors precludes nuclear accumulation of 60S subunits in the FG mutants we tested. Potentially deletion of a 60S transport receptor in addition to deletion of FG domains will uncover which FG domains are utilized by other transport factors the 60S subunit. Others have generated Nmd3-Mex67 fusions that bypass the requirement for Crm1 in 60S export (LO and JOHNSON 2009). Potentially this fusion can be used to determine whether 60S subunits have a more limited use of FG domains during export. Furthermore, this tool may be useful in determining whether a feature of Mex67 is sufficient for removal of the protein by Dbp5 or another factor (i.e. does the fusion bypass the requirement for Lsg1 in Nmd3 removal?).

Despite the unanswered question of whether Dbp5 remodels Mex67 from 60S subunits, it is clear that there are several parallels between mRNP and ribosome subunit export. In this project, we aimed to relate information known about mRNP export to test whether similarities exist for 60S particle export. However, it is possible that details of ribosome maturation can also be used to draw hypotheses about mRNP maturation. For example, during ribosome biogenesis, distinct steps in the maturation pathway can be distinguished through purification of transiently associating proteins and analyzing co-enriched proteins. This process has also been approached for mRNP biogenesis (OEFFINGER *et al.* 2007), but the heterogeneous nature of transcripts purified under these conditions makes it difficult to determine a model maturation pathway similar to what is being explored for ribosomal subunits. Therefore, purification of a single transcript at distinct stages of development should inform the pathway transcripts take during maturation, although this is technically much more difficult.

An exciting concept that has emerged upon study of ribosome maturation is the existence of numerous checkpoints wherein ribosome functionality is both tested and inhibited until the particles are fully mature. This is reminiscent of the pioneer round of translation for mRNPs where the integrity of a transcript is “tested” before protein is translated. In this process, the nuclear mRNA cap is replaced with cytoplasmic eIF4E (ISHIGAKI *et al.* 2001). Are there other similar protein exchanges wherein early associating proteins are replaced in the cytoplasm? If so, the model of co-transciptional recruitment of proteins for cytoplasmic function may be only one mechanism for mature mRNP assembly. Overall, the conceptual parallels between mRNP and ribosome RNP biogenesis and maturation are both interesting and informative.

Appendix C:

Role of Bop3 in mRNA Export

The majority of this work was done in collaboration with Alania Willet and Nathan McDonald, rotation students who worked with me.

Introduction

As the function of several factors involved in mRNA export has begun to be teased out, several labs have begun to uncover post-translational modifications (PTMs) of these factors and how these modifications affect the regulation of export. For example, as mentioned in Chapter I, Yra1 is mono-ubiquitylated by Tom1, and this modification causes release of Yra1 from the transcript before it enters the NPC (IGLESIAS *et al.* 2010). Additionally, several hnRNP proteins are phosphorylated, and this PTM affects their association with cytoplasmic mRNPs after export (GILBERT *et al.* 2001; WINDGASSEN and KREBBER 2003).

One PTM that has been associated with NPCs and nucleocytoplasmic transport is the small ubiquitin-like modification, SUMO. SUMO conjugation to target proteins was identified in the Blobel lab while studying proteins from the NE that bind Ran (identified as a covalent attachment to RanGAP1 and called GMP1—GAP-modifying protein1) (MATUNIS *et al.* 1996). Subsequently, the Melchior lab found that this modification was required for the RanBP2/Nup358 to interact with RanGAP1 (MAHAJAN *et al.* 1997). SUMO, similar to ubiquitin, is covalently linked to lysines in target proteins, and a cascade of E1, E2, and E3 enzymes are required for this process (reviewed in HOCHSTRASSER 2009; WANG and DASSO 2009). In the case of Nups, RanBP2 functions

as a SUMO E3 with the E2 Ubc9 to modify RanGAP1 for their tight association (MATUNIS *et al.* 1998; PICHLER *et al.* 2002), and the RanBP2-Ubc9-RabGAP1-SUMO complex likely modifies other substrates during their trafficking (WERNER *et al.* 2012).

Although *S. cerevisiae* has SUMO-1 and RanGAP1 homologues (Smt3 and Rna1, respectively; there are three SUMO orthologues in mammals), there is no RanBP2/Nup358 homologue. Despite this, there have been several hints in *S. cerevisiae* literature that SUMO/Smt3 modification impacts nucleocytoplasmic transport, particularly mRNP export. First, the Smt3 protease, Ulp1 interacts with NPCs at the nuclear basket (ZHAO *et al.* 2004b). Importantly, Ulp1 localization is dependent on Mlp1/2 and Nup60 and is involved in mRNP export surveillance, similar to Mlp1/2 (ZHAO *et al.* 2004b; LEWIS *et al.* 2007). Interestingly, overexpression of Ulp1 can suppress the growth defect of a *yra1-2* temperature-sensitive mutant, providing and additional link between SUMO/Smt3 modification and mRNA surveillance/export. However, it is unclear what the substrate for this SUMO protease is during mRNA export. Potentially, Yra1 itself could be a substrate, since in a *nup60* null (where the Mlp proteins and Ulp1 are mislocalized), levels of Yra1 accumulate on poly-A^+ RNA (LUND and GUTHRIE 2005). Finally, in a yeast-two-hybrid screen for Ulp1-interacting proteins, Nup42 and Gle1 were identified, although direct interactions were not verified and the consequences of these interactions were not determined (TAKAHASHI *et al.* 2000).

Large-scale screens to identify SUMOylated proteins have found several hnRNP and poly-A binding proteins that are modified (mammalian hnRNPC and hnRNPM (VASSILEVA and MATUNIS 2004), *S.c.* Pbp1 (Pab1 binding protein) (HANNICH *et al.* 2005), *S.c.* Pab1 (PANSE *et al.* 2004)). Potentially, the SUMO modification is involved in

regulating the association between these factors and transcripts. A recent study has identified the THO complex member Hpr1 as a target for SUMOylation and that this modification is required for proper expression of acid-responsive genes (BRETES *et al.* 2014). Furthermore, the authors found decreased THO recruitment to mRNPs in *ulp1* mutants. Finally, studies in *Arabidopsis* demonstrate that the plant homologue of the Mlps (NUA) also regulates SUMOylation of targets and mutants that affect SUMOylation result in nuclear accumulation of mRNA (XU *et al.* 2007; MUTHUSWAMY and MEIER 2011). Therefore, beyond what has already been uncovered, it is likely that SUMOylation plays a role in mRNA export.

Of note, SUMOylation has also been implicated in ribosome subunit export (PANSE *et al.* 2006), progression through the cell cycle (LI and HOCHSTRASSER 1999), regulated transcription of galactose-inducible genes at least in part due to SUMOylation of transcription factors (TEXARI *et al.* 2013), and DNA damage repair and telomere anchoring at the NE (PALANCADE *et al.* 2007). Finally, in proteomic studies to identify SUMOylated substrates, several factors involved in and regulation of chromatin structure and transcription were uncovered (WYKOFF and O'SHEA 2005).

Results and Discussion

One factor that was confirmed as a SUMO target is the nuclear protein Bop3 (PANSE *et al.* 2004). Our lab became interested in the protein as it was identified as a multi-copy suppressor of a *nup42Δ ipk1Δ* double mutant (Figure C.1A). Bop3 is a non-essential gene that was originally identified as a bypass suppressor of a *pam1* deletion strain (Bypassor of Pam 1) (SGD communication: Hu G-Z and Ronne H (2002)). Bop3

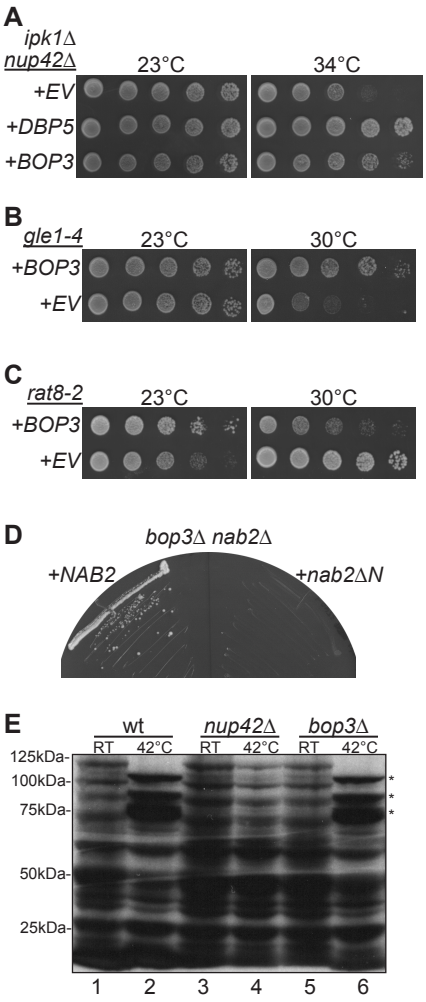

Figure C1. *BOP3* has genetic interactions with mRNA export mutants.
(A) *BOP3* overexpression partially rescues temperature-sensitivity of *ipk1Δ nup42Δ*. *EV* (CP62), *DBP5/LEU/2μ* (CP3010), and *BOP3/LEU/2μ* (pSW3813) were transformed to *ipk1Δ nup42Δ* (SWY2114). Strains were grown to mid-log phase and 5-fold serially diluted on -Leu at the indicated temperatures. (B) *BOP3* overexpression partially rescues temperature-sensitivity of *gle1-4*. *EV* (CP62) and *BOP3/LEU/2μ* (pSW3813) were transformed to *gle1-4* (SWY4209). Strains were grown to mid-log phase and 5-fold serially diluted on -Leu at the indicated temperatures. (C) *BOP3* overexpression has genetic interactions with *rat8-2*. *EV* (CP62) and *BOP3/LEU/2μ* (pSW3813) were transformed to *rat8-2* (YOL115). Strains were grown to mid-log phase and 5-fold serially diluted on -Leu at the indicated temperatures. (D) *bop3Δ* is synthetically lethal with a *nab2* mutant. *bop3Δ nab2Δ* (SWY5121) with a *NAB2/URA* vector was transformed with a *NAB2/CEN* (CP414) or *nab2ΔN/CEN* (CP3098) vector and struck onto 5-FOA at 25°. (E) *bop3Δ* is not essential for heat-shock transcript export. Indicated strains (YOL182, NULL236, NULL507) were grown at 25° to early log phase, kept at 25° or shifted to 42° for 15min, labeled with [^{35}S]methionine for an additional 15 min, and lysed. Lysates were resolved by SDS-PAGE, and proteins were visualized by autoradiography. Asterisks, Hsp proteins induced upon heat shock.

has been identified in a number of screens designed to identify SUMOylated proteins (WOHLSCHLEGEL *et al.* 2004; DENISON *et al.* 2005; HANNICH *et al.* 2005) and confirmed in one (PANSE *et al.* 2004). This modification was demonstrated to be dependent on the SUMO E3 ligase Siz1 (ALBUQUERQUE *et al.* 2013). To identify potential SUMOylated lysines, we input the Bop3 protein sequence into the GPS-SUMO server (ZHAO *et al.* 2014), http://sumosp.biocuckoo.org/). From this predicition software, K53 and K199 were identified as highly likely SUMOylated sites (data not shown). Therefore, it is possible that these sites are SUMOylated and potentially de-SUMOylated by Ulp1 at the NPC.

A *bop3Δ* strain has no apparent growth defects and displays no enhanced growth defects with mRNA export mutants *rat8-2 (dbp5)* and *mex67-5* (data not shown). However, upon exploration of genetic interactions with other mRNA export mutants, it was found that *BOP3* over-expression also rescued the growth defect of *rat8-2 (dbp5)* at 23° (Figure C.1B) and rescued the growth defect of a temperature-sensitive *gle1-4* strain (Figure C.1C) at 30°. Bop3 overexpression did not rescue the cold-sensitive growth defect of *nup42ΔFG nup159ΔFG* (data not shown). Finally, *bop3Δ* was synthetically lethal with *nab2ΔN* (Figure C.1D). Due to the genetic link to *NUP42*, we additionally sought to test whether Bop3 plays a role in heat-shock mRNA export. Using the ^{35}S-methionine pulse assay to label newly-synthesized proteins, a *bop3Δ* mutant displayed expression of heat-shock proteins (Figure C.1E, lane 6). This indicates that Bop3 is not required for export of heat-shock transcripts.

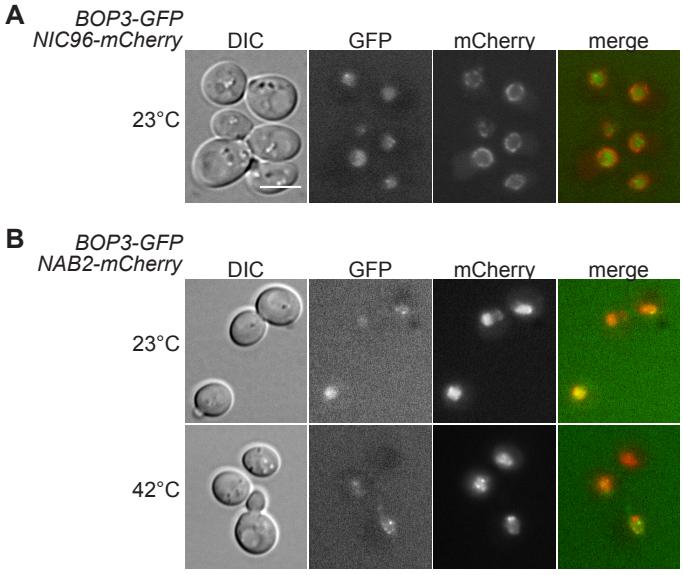

Figure C2. Analyzing Bop3 subcellular localization.
(A) Bop3 is nuclear localized. *BOP3-GFP NIC96-mCherry* (SWY5128) was grown at 23° and live cells were visualized by wide field fluorescence. Scale bar=5μm. (B) Bop3 puncta do not co-localize with Nab2 foci. *BOP3-GFP NAB2-mCherry* (SWY5128) was grown at 23° and kept at 23° or shifted to 42° for 1hr. Live cells were visualized by wide field fluorescence.

Bop3-GFP localizes to the nucleus and is enriched in 1-2 descrete puncta per cell (Figure C.2A). Because Bop3 is enriched in the nuclear compartment and is 44kDa (69kDa including the GFP), it is likely that Bop3 contains an NLS. However prediction software to identify a cNLS or bipartite NLS only displayed low-confidence predicted NLSs that did not meet the threshold for NLS prediciton (NAKAI and HORTON 1999; KOSUGI *et al.* 2009; NGUYEN BA *et al.* 2009; MEHDI *et al.* 2011; LIN and HU 2013). Nab2 localizes to 1-2 nuclear foci upon heat shock at 42° (CARMODY *et al.* 2010). However, the Bop3 foci displayed little to no overlap with these foci after shifting to 42° (Figure C.2B). The subcellular localization of Bop3, nonetheless, indicates that Bop3 likely plays a nuclear function.

We next analyzed whether the predicted structure or mammalian homologues give any insight into Bop3 function. Performing a BLAST search for similar human protein sequences did not result in any significant homologous proteins. Proteins often lack significant sequence homology but can share structural homology with other proteins. We therefore searched for predicted structural homology PSI-pred, where Bop3 emerged as the only member of the protein family (pfam) DUF2722, DUF meaning domain of unknown function (MARCHLER-BAUER *et al.* 2013). Due to the lack of predicted structural homology with other proteins, we analyzed predicted protein disorder using DISOPRED3 (JONES and COZZETTO 2014). This program predicted that the vast majority of Bop3 is disordered with a small amount of predicted helical content.

The multicopy suppression of mRNA export mutants suggests that Bop3 functions in mRNA biogenesis or export. In order to attempt to determine the function of this protein we have designed a strain to perform a traditional synthetic lethal screen

using colony sectoring as a readout. This strain is *ade2Δ ade3Δ bop3::KAN*^{R} (SWY5192) and contains a *BOP3/URA3/ADE3* vector (pSW3815). Analysis of untreated strains results in 100% sectoring on colonies or restruck colonies that didn't originally sector (data not shown). It is likely that mutants that are synthetically lethal with *bop3Δ* will provide insight into Bop3 function.

In several high-throughput studies, Bop3 has been linked to cell cycle-dependent phosphorylation by Cdc28/Cdk1 with the Cln2 cyclin (active at late G1 phase of the cell cycle) (UBERSAX *et al.* 2003; KOIVOMAGI *et al.* 2011; KOIVOMAGI *et al.* 2013). Furthermore, phosphorylation of S231 during the M-phase of the cell cycle was identified in a mass-spec analysis (PhosphoGRID and BODENMILLER *et al.* 2010), and S144 contains the MAPK/CDK SP consensus site. These links between mRNA export and cell cycle regulation provided through Bop3 hint at potential global regulation of mRNA export throughout the cell cycle.

Based on genetic interactions we hypothesize that Bop3 may function in mRNA maturation or export. The fact that this protein has very little characterization, while potentially exciting, also makes it difficult to determine its function. That a *bop3Δ* strain has no growth defect but suppresses mRNA export mutants is reminiscent of *GFD1*, whose function in mRNA export is also still undetermined. The most exciting aspect of this protein is the very convincing evidence that it is post-translationally modified, both by SUMOylation and phosphorylation. An important next step is connecting the PTMs to mRNA export rescue. Thus, first, SUMOylation must be demonstrated in our hands, and an assay to confirm phosphorylation should be developed. A first approach to repeat the reported SUMO footprinting assay (PANSE *et al.* 2004) with Bop3 was

unsuccessful, but this was most likely due to experimental error. Next, predicted SUMOylated and phosphorylated sites should me altered and analyzed for the ability to multicopy suppress mRNA export mutants.

There are several straightforward unanswered questions about Bop3. First, how is Bop3 imported and is nuclear localization required for its function? Although we could not uncover a putative NLS, it is likely that Bop3 is actively imported, since it accumulates against a concentration gradient in the nucleus. Potentially Bop3 contains a non-cannonical NLS, or it is also possible that though an NLS-containing binding protein, Bop3 imports by "piggy backing". Second, does Bop3 shuttle out of the nucleus, and is the potential shuttling dependent on mRNA export (i.e. does Bop3 export on mRNPs)? This can be easily answered by performing a classic heterokaryon assay or by analyzing Bop3 localization in a *nup49-313* mutant in which protein import is specifically inhibited at the restrictive temperature (DOYE *et al.* 1994; LEE *et al.* 1996). Overall, study of Bop3 is likely to provide additional insight into how mRNA export is regulated through various PTMs.

REFERENCES

ABRUZZI, K. C., S. LACADIE and M. ROSBASH, 2004 Biochemical analysis of TREX complex recruitment to intronless and intron-containing yeast genes. Embo J **23:** 2620-2631.

ADAMS, R. L., and S. R. WENTE, 2013 Uncovering nuclear pore complexity with innovation. Cell **152:** 1218-1221.

AGUILERA, A., and H. GAILLARD, 2014 Transcription and recombination: when RNA meets DNA. Cold Spring Harb Perspect Biol **6**.

AITCHISON, J. D., and M. P. ROUT, 2012 The yeast nuclear pore complex and transport through it. Genetics **190:** 855-883.

ALBER, F., S. DOKUDOVSKAYA, L. M. VEENHOFF, W. ZHANG, J. KIPPER *et al.*, 2007 The molecular architecture of the nuclear pore complex. Nature **450:** 695-701.

ALBUQUERQUE, C. P., G. WANG, N. S. LEE, R. D. KOLODNER, C. D. PUTNAM *et al.*, 2013 Distinct SUMO ligases cooperate with Esc2 and Slx5 to suppress duplication-mediated genome rearrangements. PLoS Genet **9:** e1003670.

ALCAZAR-ROMAN, A. R., T. A. BOLGER and S. R. WENTE, 2010 Control of mRNA export and translation termination by inositol hexakisphosphate requires specific interaction with Gle1. J Biol Chem **285:** 16683-16692.

ALCAZAR-ROMAN, A. R., E. J. TRAN, S. GUO and S. R. WENTE, 2006 Inositol hexakisphosphate and Gle1 activate the DEAD-box protein Dbp5 for nuclear mRNA export. Nat Cell Biol **8:** 711-716.

ALEXANDROV, A., D. COLOGNORI and J. A. STEITZ, 2011 Human eIF4AIII interacts with an eIF4G-like partner, NOM1, revealing an evolutionarily conserved function outside the exon junction complex. Genes Dev **25:** 1078-1090.

ALLEN, N. P., L. HUANG, A. BURLINGAME and M. REXACH, 2001 Proteomic analysis of nucleoporin interacting proteins. J Biol Chem **276:** 29268-29274.

ANDERSEN, C. B., L. BALLUT, J. S. JOHANSEN, H. CHAMIEH, K. H. NIELSEN *et al.*, 2006 Structure of the exon junction core complex with a trapped DEAD-box ATPase bound to RNA. Science **313:** 1968-1972.

ANDERSON, J. T., S. M. WILSON, K. V. DATAR and M. S. SWANSON, 1993 NAB2: a yeast nuclear polyadenylated RNA-binding protein essential for cell viability. Mol Cell Biol **13:** 2730-2741.

ANDREOU, A. Z., and D. KLOSTERMEIER, 2013 The DEAD-box helicase eIF4A: paradigm or the odd one out? RNA Biol **10:** 19-32.

ANDREOU, A. Z., and D. KLOSTERMEIER, 2014 eIF4B and eIF4G jointly stimulate eIF4A ATPase and unwinding activities by modulation of the eIF4A conformational cycle. J Mol Biol **426:** 51-61.

BACHI, A., I. C. BRAUN, J. P. RODRIGUES, N. PANTE, K. RIBBECK *et al.*, 2000 The C-terminal domain of TAP interacts with the nuclear pore complex and promotes export of specific CTE-bearing RNA substrates. RNA **6:** 136-158.

BAEJEN, C., P. TORKLER, S. GRESSEL, K. ESSIG, J. SODING *et al.*, 2014 Transcriptome maps of mRNP biogenesis factors define pre-mRNA recognition. Mol Cell **55:** 745-757.

BAIERLEIN, C., A. HACKMANN, T. GROSS, L. HENKER, F. HINZ *et al.*, 2013 Monosome formation during translation initiation requires the serine/arginine-rich protein Npl3. Mol Cell Biol **33:** 4811-4823.

BALLUT, L., B. MARCHADIER, A. BAGUET, C. TOMASETTO, B. SERAPHIN *et al.*, 2005 The exon junction core complex is locked onto RNA by inhibition of eIF4AIII ATPase activity. Nat Struct Mol Biol **12:** 861-869.

BALTZ, A. G., M. MUNSCHAUER, B. SCHWANHAUSSER, A. VASILE, Y. MURAKAWA *et al.*, 2012 The mRNA-bound proteome and its global occupancy profile on protein-coding transcripts. Mol Cell **46:** 674-690.

BARBOSA, I., N. HAQUE, F. FIORINI, C. BARRANDON, C. TOMASETTO *et al.*, 2012 Human CWC22 escorts the helicase eIF4AIII to spliceosomes and promotes exon junction complex assembly. Nat Struct Mol Biol **19:** 983-990.

BATISSE, J., C. BATISSE, A. BUDD, B. BOTTCHER and E. HURT, 2009 Purification of nuclear poly(A)-binding protein Nab2 reveals association with the yeast transcriptome and a messenger ribonucleoprotein core structure. J Biol Chem **284:** 34911-34917.

BAYLISS, R., S. W. LEUNG, R. P. BAKER, B. B. QUIMBY, A. H. CORBETT *et al.*, 2002a Structural basis for the interaction between NTF2 and nucleoporin FxFG repeats. Embo J **21:** 2843-2853.

BAYLISS, R., T. LITTLEWOOD and M. STEWART, 2000 Structural basis for the interaction between FxFG nucleoporin repeats and importin-beta in nuclear trafficking. Cell **102:** 99-108.

BAYLISS, R., T. LITTLEWOOD, L. A. STRAWN, S. R. WENTE and M. STEWART, 2002b GLFG and FxFG nucleoporins bind to overlapping sites on importin-beta. J Biol Chem **277:** 50597-50606.

BEDNENKO, J., G. CINGOLANI and L. GERACE, 2003 Importin beta contains a COOH-terminal nucleoporin binding region important for nuclear transport. J Cell Biol **162:** 391-401.

BELTZ, G. A., and S. J. FLINT, 1979 Inhibition of HeLa cell protein synthesis during adenovirus infection. Restriction of cellular messenger RNA sequences to the nucleus. J Mol Biol **131:** 353-373.

BEN-EFRAIM, I., and L. GERACE, 2001 Gradient of increasing affinity of importin beta for nucleoporins along the pathway of nuclear import. J Cell Biol **152:** 411-417.

BEN-SHEM, A., L. JENNER, G. YUSUPOVA and M. YUSUPOV, 2010 Crystal structure of the eukaryotic ribosome. Science **330:** 1203-1209.

BERNSTEIN, P., S. W. PELTZ and J. ROSS, 1989 The poly(A)-poly(A)-binding protein complex is a major determinant of mRNA stability in vitro. Mol Cell Biol **9:** 659-670.

BILOKAPIC, S., and T. U. SCHWARTZ, 2012 3D ultrastructure of the nuclear pore complex. Curr Opin Cell Biol **24:** 86-91.

BLOBEL, G., 1985 Gene gating: a hypothesis. PNAS **82:** 8527-8529.

BODENMILLER, B., S. WANKA, C. KRAFT, J. URBAN, D. CAMPBELL *et al.*, 2010 Phosphoproteomic analysis reveals interconnected system-wide responses to perturbations of kinases and phosphatases in yeast. Sci Signal **3:** rs4.

BOLGER, T. A., A. W. FOLKMANN, E. J. TRAN and S. R. WENTE, 2008 The mRNA export factor Gle1 and inositol hexakisphosphate regulate distinct stages of translation. Cell **134:** 624-633.

BOLGER, T. A., and S. R. WENTE, 2011 Gle1 is a multifunctional DEAD-box protein regulator that modulates Ded1 in translation initiation. J Biol Chem **286:** 39750-39759.

BONO, F., J. EBERT, E. LORENTZEN and E. CONTI, 2006 The crystal structure of the exon junction complex reveals how it maintains a stable grip on mRNA. Cell **126:** 713-725.

BOWERS, H. A., P. A. MARONEY, M. E. FAIRMAN, B. KASTNER, R. LUHRMANN *et al.*, 2006 Discriminatory RNP remodeling by the DEAD-box protein DED1. RNA **12:** 903-912.

BRADATSCH, B., J. KATAHIRA, E. KOWALINSKI, G. BANGE, W. YAO *et al.*, 2007 Arx1 functions as an unorthodox nuclear export receptor for the 60S preribosomal subunit. Mol Cell **27:** 767-779.

BRADATSCH, B., C. LEIDIG, S. GRANNEMAN, M. GNADIG, D. TOLLERVEY *et al.*, 2012 Structure of the pre-60S ribosomal subunit with nuclear export factor Arx1 bound at the exit tunnel. Nat Struct Mol Biol **19:** 1234-1241.

BRAUN, I. C., A. HEROLD, M. RODE, E. CONTI and E. IZAURRALDE, 2001 Overexpression of TAP/p15 heterodimers bypasses nuclear retention and stimulates nuclear mRNA export. J Biol Chem **276:** 20536-20543.

BRAUN, I. C., E. ROHRBACH, C. SCHMITT and E. IZAURRALDE, 1999 TAP binds to the constitutive transport element (CTE) through a novel RNA-binding motif that is sufficient to promote CTE-dependent RNA export from the nucleus. Embo J **18:** 1953-1965.

BRENNAN, C. M., I. E. GALLOUZI and J. A. STEITZ, 2000 Protein ligands to HuR modulate its interaction with target mRNAs in vivo. J Cell Biol **151:** 1-14.

BRETES, H., J. O. ROUVIERE, T. LEGER, M. OEFFINGER, F. DEVAUX *et al.*, 2014 Sumoylation of the THO complex regulates the biogenesis of a subset of mRNPs. Nucleic Acids Res **42:** 5043-5058.

BRICKNER, D. G., S. AHMED, L. MELDI, A. THOMPSON, W. LIGHT *et al.*, 2012 Transcription factor binding to a DNA zip code controls interchromosomal clustering at the nuclear periphery. Dev Cell **22:** 1234-1246.

BRICKNER, D. G., I. CAJIGAS, Y. FONDUFE-MITTENDORF, S. AHMED, P. C. LEE *et al.*, 2007 H2A.Z-mediated localization of genes at the nuclear periphery confers epigenetic memory of previous transcriptional state. PLoS Biol **5:** e81.

BROCKMANN, C., S. SOUCEK, S. I. KUHLMANN, K. MILLS-LUJAN, S. M. KELLY *et al.*, 2012 Structural basis for polyadenosine-RNA binding by Nab2 Zn fingers and its function in mRNA nuclear export. Structure **20:** 1007-1018.

BUCHWALD, G., S. SCHUSSLER, C. BASQUIN, H. LE HIR and E. CONTI, 2013 Crystal structure of the human eIF4AIII-CWC22 complex shows how a DEAD-box protein is inhibited by a MIF4G domain. Proc Natl Acad Sci U S A **110:** E4611-4618.

BUCHWALTER, A. L., Y. LIANG and M. W. HETZER, 2014 Nup50 is required for cell differentiation and exhibits transcription-dependent dynamics. Mol Biol Cell **25:** 2472-2484.

BURNS, L. T., and S. R. WENTE, 2014 Casein kinase II Regulation of the Hot1 Transcription Factor Promotes Stochastic Gene Expression. J Biol Chem.

CABAL, G. G., A. GENOVESIO, S. RODRIGUEZ-NAVARRO, C. ZIMMER, O. GADAL *et al.*, 2006 SAGA interacting factors confine sub-diffusion of transcribed genes to the nuclear envelope. Nature **441:** 770-773.

CAPELSON, M., Y. LIANG, R. SCHULTE, W. MAIR, U. WAGNER *et al.*, 2010 Chromatin-bound nuclear pore components regulate gene expression in higher eukaryotes. Cell **140:** 372-383.

CARMODY, S. R., E. J. TRAN, L. H. APPONI, A. H. CORBETT and S. R. WENTE, 2010 The mitogen-activated protein kinase Slt2 regulates nuclear retention of non-heat shock mRNAs during heat shock-induced stress. Mol Cell Biol **30:** 5168-5179.

CARUTHERS, J. M., E. R. JOHNSON and D. B. MCKAY, 2000 Crystal structure of yeast initiation factor 4A, a DEAD-box RNA helicase. Proc Natl Acad Sci U S A **97:** 13080-13085.

CASOLARI, J. M., C. R. BROWN, D. A. DRUBIN, O. J. RANDO and P. A. SILVER, 2005 Developmentally induced changes in transcriptional program alter spatial organization across chromosomes. Genes Dev **19:** 1188-1198.

CASOLARI, J. M., C. R. BROWN, S. KOMILI, J. WEST, H. HIERONYMUS *et al.*, 2004 Genome-wide localization of the nuclear transport machinery couples transcriptional status and nuclear organization. Cell **117:** 427-439.

CASTELLO, A., B. FISCHER, K. EICHELBAUM, R. HOROS, B. M. BECKMANN *et al.*, 2012 Insights into RNA biology from an atlas of mammalian mRNA-binding proteins. Cell **149:** 1393-1406.

CHAVEZ, S., and A. AGUILERA, 1997 The yeast HPR1 gene has a functional role in transcriptional elongation that uncovers a novel source of genome instability. Genes Dev **11:** 3459-3470.

CHAVEZ, S., T. BEILHARZ, A. G. RONDON, H. ERDJUMENT-BROMAGE, P. TEMPST *et al.*, 2000 A protein complex containing Tho2, Hpr1, Mft1 and a novel protein, Thp2, connects transcription elongation with mitotic recombination in Saccharomyces cerevisiae. Embo J **19:** 5824-5834.

CHEN, J. Y., L. STANDS, J. P. STALEY, R. R. JACKUPS, JR., L. J. LATUS *et al.*, 2001 Specific alterations of U1-C protein or U1 small nuclear RNA can eliminate the requirement of Prp28p, an essential DEAD box splicing factor. Mol Cell **7:** 227-232.

CHEN, Y., J. P. POTRATZ, P. TIJERINA, M. DEL CAMPO, A. M. LAMBOWITZ *et al.*, 2008 DEAD-box proteins can completely separate an RNA duplex using a single ATP. Proc Natl Acad Sci U S A **105:** 20203-20208.

CHENG, Z., J. COLLER, R. PARKER and H. SONG, 2005 Crystal structure and functional analysis of DEAD-box protein Dhh1p. RNA **11:** 1258-1270.

CHIN, J. W., T. A. CROPP, J. C. ANDERSON, M. MUKHERJI, Z. ZHANG *et al.*, 2003 An expanded eukaryotic genetic code. Science **301:** 964-967.

CHO, A. R., K. J. YANG, Y. BAE, Y. Y. BAHK, E. KIM *et al.*, 2009 Tissue-specific expression and subcellular localization of ALADIN, the absence of which causes human triple A syndrome. Exp Mol Med **41:** 381-386.

CIUFO, L. F., and J. D. BROWN, 2000 Nuclear export of yeast signal recognition particle lacking Srp54p by the Xpo1p/Crm1p NES-dependent pathway. Curr Biol **10:** 1256-1264.

COHEN, S., S. AU and N. PANTE, 2011 How viruses access the nucleus. Biochim Biophys Acta **1813:** 1634-1645.

COLLINS, R., T. KARLBERG, L. LEHTIO, P. SCHUTZ, S. VAN DEN BERG *et al.*, 2009 The DEXD/H-box RNA helicase DDX19 is regulated by an {alpha}-helical switch. J Biol Chem **284:** 10296-10300.

CONTI, E., C. W. MULLER and M. STEWART, 2006 Karyopherin flexibility in nucleocytoplasmic transport. Curr Opin Struct Biol **16:** 237-244.

COOK, A. G., N. FUKUHARA, M. JINEK and E. CONTI, 2009 Structures of the tRNA export factor in the nuclear and cytosolic states. Nature **461:** 60-65.

CULJKOVIC, B., I. TOPISIROVIC, L. SKRABANEK, M. RUIZ-GUTIERREZ and K. L. BORDEN, 2006 eIF4E is a central node of an RNA regulon that governs cellular proliferation. J Cell Biol **175:** 415-426.

CULJKOVIC-KRALJACIC, B., A. BAGUET, L. VOLPON, A. AMRI and K. L. BORDEN, 2012 The oncogene eIF4E reprograms the nuclear pore complex to promote mRNA export and oncogenic transformation. Cell Rep **2:** 207-215.

D'ANGELO, M. A., J. S. GOMEZ-CAVAZOS, A. MEI, D. H. LACKNER and M. W. HETZER, 2012 A change in nuclear pore complex composition regulates cell differentiation. Dev Cell **22:** 446-458.

DABAUVALLE, M. C., B. SCHULZ, U. SCHEER and R. PETERS, 1988 Inhibition of nuclear accumulation of karyophilic proteins in living cells by microinjection of the lectin wheat germ agglutinin. Exp Cell Res **174:** 291-296.

DANEHOLT, B., 2001 Assembly and transport of a premessenger RNP particle. Proc Natl Acad Sci U S A **98:** 7012-7017.

DAVIS, L. I., and G. BLOBEL, 1987 Nuclear pore complex contains a family of glycoproteins that includes p62: glycosylation through a previously unidentified cellular pathway. Proc Natl Acad Sci U S A **84:** 7552-7556.

DEGRASSE, J. A., K. N. DUBOIS, D. DEVOS, T. N. SIEGEL, A. SALI *et al.*, 2009 Evidence for a shared nuclear pore complex architecture that is conserved from the last common eukaryotic ancestor. Mol Cell Proteomics **8:** 2119-2130.

DEL CAMPO, M., and A. M. LAMBOWITZ, 2009 Structure of the Yeast DEAD box protein Mss116p reveals two wedges that crimp RNA. Mol Cell **35:** 598-609.

DEL PRIORE, V., C. HEATH, C. SNAY, A. MACMILLAN, L. GORSCH *et al.*, 1997 A structure/function analysis of Rat7p/Nup159p, an essential nucleoporin of Saccharomyces cerevisiae. J Cell Sci **110 (Pt 23):** 2987-2999.

DEL PRIORE, V., C. A. SNAY, A. BAHR and C. N. COLE, 1996 The product of the Saccharomyces cerevisiae RSS1 gene, identified as a high-copy suppressor of the rat7-1 temperature-sensitive allele of the RAT7/NUP159 nucleoporin, is required for efficient mRNA export. Mol Biol Cell **7:** 1601-1621.

DELEON, D. V., K. H. COX, L. M. ANGERER and R. C. ANGERER, 1983 Most early-variant histone mRNA is contained in the pronucleus of sea urchin eggs. Dev Biol **100:** 197-206.

DENISON, C., A. D. RUDNER, S. A. GERBER, C. E. BAKALARSKI, D. MOAZED *et al.*, 2005 A proteomic strategy for gaining insights into protein sumoylation in yeast. Mol Cell Proteomics **4:** 246-254.

DENNING, D. P., S. S. PATEL, V. UVERSKY, A. L. FINK and M. REXACH, 2003 Disorder in the nuclear pore complex: the FG repeat regions of nucleoporins are natively unfolded. Proc Natl Acad Sci U S A **100:** 2450-2455.

DENNING, D. P., and M. F. REXACH, 2007 Rapid evolution exposes the boundaries of domain structure and function in natively unfolded FG nucleoporins. Mol Cell Proteomics **6:** 272-282.

DENNING, D. P., V. UVERSKY, S. S. PATEL, A. L. FINK and M. REXACH, 2002 The Saccharomyces cerevisiae nucleoporin Nup2p is a natively unfolded protein. J Biol Chem **277:** 33447-33455.

DERMODY, J. L., J. M. DREYFUSS, J. VILLEN, B. OGUNDIPE, S. P. GYGI *et al.*, 2008 Unphosphorylated SR-like protein Npl3 stimulates RNA polymerase II elongation. PLoS One **3:** e3273.

DOMA, M. K., and R. PARKER, 2007 RNA quality control in eukaryotes. Cell **131:** 660-668.

DOMINGUEZ-SANCHEZ, M. S., S. BARROSO, B. GOMEZ-GONZALEZ, R. LUNA and A. AGUILERA, 2011 Genome instability and transcription elongation impairment in human cells depleted of THO/TREX. PLoS Genet **7:** e1002386.

DOSSANI, Z. Y., C. S. WEIRICH, J. P. ERZBERGER, J. M. BERGER and K. WEIS, 2009 Structure of the C-terminus of the mRNA export factor Dbp5 reveals the interaction surface for the ATPase activator Gle1. Proc Natl Acad Sci U S A **106:** 16251-16256.

DOSTIE, J., and G. DREYFUSS, 2002 Translation is required to remove Y14 from mRNAs in the cytoplasm. Curr Biol **12:** 1060-1067.
DOYE, V., R. WEPF and E. C. HURT, 1994 A novel nuclear pore protein Nup133p with distinct roles in poly(A)+ RNA transport and nuclear pore distribution. Embo J **13:** 6062-6075.
DUNCAN, K., J. G. UMEN and C. GUTHRIE, 2000 A putative ubiquitin ligase required for efficient mRNA export differentially affects hnRNP transport. Curr Biol **10:** 687-696.
EGLOFF, S., M. DIENSTBIER and S. MURPHY, 2012 Updating the RNA polymerase CTD code: adding gene-specific layers. Trends Genet **28:** 333-341.
ENCODE, 2012 An integrated encyclopedia of DNA elements in the human genome. Nature **489:** 57-74.
ENENKEL, C., 2014 Nuclear transport of yeast proteasomes. Biomolecules **4:** 940-955.
ESTRUCH, F., and C. N. COLE, 2003 An early function during transcription for the yeast mRNA export factor Dbp5p/Rat8p suggested by its genetic and physical interactions with transcription factor IIH components. Mol Biol Cell **14:** 1664-1676.
ESTRUCH, F., C. HODGE, N. GOMEZ-NAVARRO, L. PEIRO-CHOVA, C. V. HEATH *et al.*, 2012 Insights into mRNP biogenesis provided by new genetic interactions among export and transcription factors. BMC Genet **13:** 80.
FAHRENKROG, B., B. MACO, A. M. FAGER, J. KOSER, U. SAUDER *et al.*, 2002 Domain-specific antibodies reveal multiple-site topology of Nup153 within the nuclear pore complex. J Struct Biol **140:** 254-267.
FAIRMAN, M. E., P. A. MARONEY, W. WANG, H. A. BOWERS, P. GOLLNICK *et al.*, 2004 Protein displacement by DExH/D "RNA helicases" without duplex unwinding. Science **304:** 730-734.
FAIRMAN-WILLIAMS, M. E., U. P. GUENTHER and E. JANKOWSKY, 2010 SF1 and SF2 helicases: family matters. Curr Opin Struct Biol **20:** 313-324.
FAN, J. S., Z. CHENG, J. ZHANG, C. NOBLE, Z. ZHOU *et al.*, 2009 Solution and crystal structures of mRNA exporter Dbp5p and its interaction with nucleotides. J Mol Biol **388:** 1-10.
FAZA, M. B., Y. CHANG, L. OCCHIPINTI, S. KEMMLER and V. G. PANSE, 2012 Role of Mex67-Mtr2 in the nuclear export of 40S pre-ribosomes. PLoS Genet **8:** e1002915.
FEATHERSTONE, C., M. K. DARBY and L. GERACE, 1988 A monoclonal antibody against the nuclear pore complex inhibits nucleocytoplasmic transport of protein and RNA in vivo. J Cell Biol **107:** 1289-1297.
FELDHERR, C. M., E. KALLENBACH and N. SCHULTZ, 1984 Movement of a karyophilic protein through the nuclear pores of oocytes. J Cell Biol **99:** 2216-2222.
FINLAY, D. R., D. D. NEWMEYER, T. M. PRICE and D. J. FORBES, 1987 Inhibition of in vitro nuclear transport by a lectin that binds to nuclear pores. J Cell Biol **104:** 189-200.
FISCHER, T., K. STRASSER, A. RACZ, S. RODRIGUEZ-NAVARRO, M. OPPIZZI *et al.*, 2002 The mRNA export machinery requires the novel Sac3p-Thp1p complex to dock at the nucleoplasmic entrance of the nuclear pores. Embo J **21:** 5843-5852.
FISEROVA, J., S. A. RICHARDS, S. R. WENTE and M. W. GOLDBERG, 2010 Facilitated transport and diffusion take distinct spatial routes through the nuclear pore complex. J Cell Sci **123:** 2773-2780.
FISEROVA, J., M. SPINK, S. A. RICHARDS, C. SAUNTER and M. W. GOLDBERG, 2014 Entry into the nuclear pore complex is controlled by a cytoplasmic exclusion zone containing dynamic GLFG-repeat nucleoporin domains. J Cell Sci **127:** 124-136.

FLOER, M., and G. BLOBEL, 1999 Putative reaction intermediates in Crm1-mediated nuclear protein export. J Biol Chem **274:** 16279-16286.
FOLKMANN, A. W., S. E. COLLIER, X. ZHAN, ADITI, M. D. OHI *et al.*, 2013 Gle1 functions during mRNA export in an oligomeric complex that is altered in human disease. Cell **155:** 582-593.
FOLKMANN, A. W., K. N. NOBLE, C. N. COLE and S. R. WENTE, 2011 Dbp5, Gle1-IP6 and Nup159: a working model for mRNP export. Nucleus **2:** 540-548.
FORMAN-KAY, J. D., and T. MITTAG, 2013 From sequence and forces to structure, function, and evolution of intrinsically disordered proteins. Structure **21:** 1492-1499.
FORWOOD, J. K., A. LANGE, U. ZACHARIAE, M. MARFORI, C. PREAST *et al.*, 2010 Quantitative structural analysis of importin-β flexibility: paradigm for solenoid protein structures. Structure **18:** 1171-1183.
FREY, S., and D. GORLICH, 2007 A saturated FG-repeat hydrogel can reproduce the permeability properties of nuclear pore complexes. Cell **130:** 512-523.
FREY, S., and D. GORLICH, 2009 FG/FxFG as well as GLFG repeats form a selective permeability barrier with self-healing properties. Embo J **28:** 2554-2567.
FREY, S., R. P. RICHTER and D. GORLICH, 2006 FG-rich repeats of nuclear pore proteins form a three-dimensional meshwork with hydrogel-like properties. Science **314:** 815-817.
FRIBOURG, S., I. C. BRAUN, E. IZAURRALDE and E. CONTI, 2001 Structural basis for the recognition of a nucleoporin FG repeat by the NTF2-like domain of the TAP/p15 mRNA nuclear export factor. Mol Cell **8:** 645-656.
FRIBOURG, S., and E. CONTI, 2003 Structural similarity in the absence of sequence homology of the messenger RNA export factors Mtr2 and p15. EMBO Rep **4:** 699-703.
GADAL, O., D. STRAUSS, J. KESSL, B. TRUMPOWER, D. TOLLERVEY *et al.*, 2001 Nuclear export of 60s ribosomal subunits depends on Xpo1p and requires a nuclear export sequence-containing factor, Nmd3p, that associates with the large subunit protein Rpl10p. Mol Cell Biol **21:** 3405-3415.
GALL, J. G., 1954 Observations on the nuclear membrane with the electron microscope. Exp Cell Res **7:** 197-200.
GALY, V., O. GADAL, M. FROMONT-RACINE, A. ROMANO, A. JACQUIER *et al.*, 2004 Nuclear retention of unspliced mRNAs in yeast is mediated by perinuclear Mlp1. Cell **116:** 63-73.
GILBERT, W., and C. GUTHRIE, 2004 The Glc7p nuclear phosphatase promotes mRNA export by facilitating association of Mex67p with mRNA. Mol Cell **13:** 201-212.
GILBERT, W., C. W. SIEBEL and C. GUTHRIE, 2001 Phosphorylation by Sky1p promotes Npl3p shuttling and mRNA dissociation. RNA **7:** 302-313.
GILCHRIST, D., B. MYKYTKA and M. REXACH, 2002 Accelerating the rate of disassembly of karyopherin.cargo complexes. J Biol Chem **277:** 18161-18172.
GILCHRIST, D., and M. REXACH, 2003 Molecular basis for the rapid dissociation of nuclear localization signals from karyopherin alpha in the nucleoplasm. J Biol Chem **278:** 51937-51949.
GOFFEAU, A., B. G. BARRELL, H. BUSSEY, R. W. DAVIS, B. DUJON *et al.*, 1996 Life with 6000 genes. Science **274:** 546, 563-547.
GOMEZ-GONZALEZ, B., M. GARCIA-RUBIO, R. BERMEJO, H. GAILLARD, K. SHIRAHIGE *et al.*, 2011 Genome-wide function of THO/TREX in active genes prevents R-loop-dependent replication obstacles. Embo J **30:** 3106-3119.

GONZALEZ-AGUILERA, C., C. TOUS, B. GOMEZ-GONZALEZ, P. HUERTAS, R. LUNA *et al.*, 2008 The THP1-SAC3-SUS1-CDC31 complex works in transcription elongation-mRNA export preventing RNA-mediated genome instability. Mol Biol Cell **19:** 4310-4318.

GORLACH, M., C. G. BURD and G. DREYFUSS, 1994 The mRNA poly(A)-binding protein: localization, abundance, and RNA-binding specificity. Exp Cell Res **211:** 400-407.

GORLICH, D., R. KRAFT, S. KOSTKA, F. VOGEL, E. HARTMANN *et al.*, 1996 Importin provides a link between nuclear protein import and U snRNA export. Cell **87:** 21-32.

GORLICH, D., and U. KUTAY, 1999 Transport between the cell nucleus and the cytoplasm. Annu Rev Cell Dev Biol **15:** 607-660.

GORLICH, D., and I. W. MATTAJ, 1996 Nucleocytoplasmic transport. Science **271:** 1513-1518.

GORSCH, L. C., T. C. DOCKENDORFF and C. N. COLE, 1995 A conditional allele of the novel repeat-containing yeast nucleoporin RAT7/NUP159 causes both rapid cessation of mRNA export and reversible clustering of nuclear pore complexes. J Cell Biol **129:** 939-955.

GRANT, R. P., D. NEUHAUS and M. STEWART, 2003 Structural basis for the interaction between the Tap/NXF1 UBA domain and FG nucleoporins at 1A resolution. J Mol Biol **326:** 849-858.

GREBER, B. J., D. BOEHRINGER, C. MONTELLESE and N. BAN, 2012 Cryo-EM structures of Arx1 and maturation factors Rei1 and Jjj1 bound to the 60S ribosomal subunit. Nat Struct Mol Biol **19:** 1228-1233.

GREEN, D. M., K. A. MARFATIA, E. B. CRAFTON, X. ZHANG, X. CHENG *et al.*, 2002 Nab2p is required for poly(A) RNA export in Saccharomyces cerevisiae and is regulated by arginine methylation via Hmt1p. J Biol Chem **277:** 7752-7760.

GROSS, T., A. SIEPMANN, D. STURM, M. WINDGASSEN, J. J. SCARCELLI *et al.*, 2007 The DEAD-box RNA helicase Dbp5 functions in translation termination. Science **315:** 646-649.

GRUNWALD, D., and R. H. SINGER, 2010 In vivo imaging of labelled endogenous beta-actin mRNA during nucleocytoplasmic transport. Nature **467:** 604-607.

GRUTER, P., C. TABERNERO, C. VON KOBBE, C. SCHMITT, C. SAAVEDRA *et al.*, 1998 TAP, the human homolog of Mex67p, mediates CTE-dependent RNA export from the nucleus. Mol Cell **1:** 649-659.

GUAN, T., R. H. KEHLENBACH, E. C. SCHIRMER, A. KEHLENBACH, F. FAN *et al.*, 2000 Nup50, a nucleoplasmically oriented nucleoporin with a role in nuclear protein export. Mol Cell Biol **20:** 5619-5630.

HAFNER, M., M. LANDTHALER, L. BURGER, M. KHORSHID, J. HAUSSER *et al.*, 2010 Transcriptome-wide identification of RNA-binding protein and microRNA target sites by PAR-CLIP. Cell **141:** 129-141.

HALLS, C., S. MOHR, M. DEL CAMPO, Q. YANG, E. JANKOWSKY *et al.*, 2007 Involvement of DEAD-box proteins in group I and group II intron splicing. Biochemical characterization of Mss116p, ATP hydrolysis-dependent and -independent mechanisms, and general RNA chaperone activity. J Mol Biol **365:** 835-855.

HANNICH, J. T., A. LEWIS, M. B. KROETZ, S. J. LI, H. HEIDE *et al.*, 2005 Defining the SUMO-modified proteome by multiple approaches in Saccharomyces cerevisiae. J Biol Chem **280:** 4102-4110.

HARBURY, P. B., T. ZHANG, P. S. KIM and T. ALBER, 1993 A switch between two-, three-, and four-stranded coiled coils in GCN4 leucine zipper mutants. Science **262:** 1401-1407.

HARMS, U., A. Z. ANDREOU, A. GUBAEV and D. KLOSTERMEIER, 2014 eIF4B, eIF4G and RNA regulate eIF4A activity in translation initiation by modulating the eIF4A conformational cycle. Nucleic Acids Res **42:** 7911-7922.

HAYAKAWA, A., A. BABOUR, L. SENGMANIVONG and C. DARGEMONT, 2012 Ubiquitylation of the nuclear pore complex controls nuclear migration during mitosis in S. cerevisiae. J Cell Biol **196:** 19-27.

HECTOR, R. E., K. R. NYKAMP, S. DHEUR, J. T. ANDERSON, P. J. NON *et al.*, 2002 Dual requirement for yeast hnRNP Nab2p in mRNA poly(A) tail length control and nuclear export. Embo J **21:** 1800-1810.

HEDGES, J., M. WEST and A. W. JOHNSON, 2005 Release of the export adapter, Nmd3p, from the 60S ribosomal subunit requires Rpl10p and the cytoplasmic GTPase Lsg1p. Embo J **24:** 567-579.

HENN, A., M. J. BRADLEY and E. M. DE LA CRUZ, 2012 ATP utilization and RNA conformational rearrangement by DEAD-box proteins. Annu Rev Biophys **41:** 247-267.

HILBERT, M., F. KEBBEL, A. GUBAEV and D. KLOSTERMEIER, 2011 eIF4G stimulates the activity of the DEAD box protein eIF4A by a conformational guidance mechanism. Nucleic Acids Res **39:** 2260-2270.

HILLAR, A., B. TRIPET, D. ZOETEWEY, J. M. WOOD, R. S. HODGES *et al.*, 2003 Detection of alpha-helical coiled-coil dimer formation by spin-labeled synthetic peptides: a model parallel coiled-coil peptide and the antiparallel coiled coil formed by a replica of the ProP C-terminus. Biochemistry **42:** 15170-15178.

HILLEREN, P., T. MCCARTHY, M. ROSBASH, R. PARKER and T. H. JENSEN, 2001 Quality control of mRNA 3'-end processing is linked to the nuclear exosome. Nature **413:** 538-542.

HO, A. K., T. X. SHEN, K. J. RYAN, E. KISELEVA, M. A. LEVY *et al.*, 2000a Assembly and preferential localization of Nup116p on the cytoplasmic face of the nuclear pore complex by interaction with Nup82p. Mol Cell Biol **20:** 5736-5748.

HO, J. H., G. KALLSTROM and A. W. JOHNSON, 2000b Nmd3p is a Crm1p-dependent adapter protein for nuclear export of the large ribosomal subunit. J Cell Biol **151:** 1057-1066.

HOBEIKA, M., C. BROCKMANN, F. GRUESSING, D. NEUHAUS, G. DIVITA *et al.*, 2009 Structural requirements for the ubiquitin-associated domain of the mRNA export factor Mex67 to bind its specific targets, the transcription elongation THO complex component Hpr1 and nucleoporin FXFG repeats. J Biol Chem **284:** 17575-17583.

HOCHSTRASSER, M., 2009 Origin and function of ubiquitin-like proteins. Nature **458:** 422-429.

HODGE, C. A., H. V. COLOT, P. STAFFORD and C. N. COLE, 1999 Rat8p/Dbp5p is a shuttling transport factor that interacts with Rat7p/Nup159p and Gle1p and suppresses the mRNA export defect of xpo1-1 cells. Embo J **18:** 5778-5788.

HODGE, C. A., E. J. TRAN, K. N. NOBLE, A. R. ALCAZAR-ROMAN, R. BEN-YISHAY *et al.*, 2011 The Dbp5 cycle at the nuclear pore complex during mRNA export I: dbp5 mutants with defects in RNA binding and ATP hydrolysis define key steps for Nup159 and Gle1. Genes Dev **25:** 1052-1064.

HOLT, G. D., C. M. SNOW, A. SENIOR, R. S. HALTIWANGER, L. GERACE *et al.*, 1987 Nuclear pore complex glycoproteins contain cytoplasmically disposed O-linked N-acetylglucosamine. J Cell Biol **104:** 1157-1164.

HUANG, Y., R. GATTONI, J. STEVENIN and J. A. STEITZ, 2003 SR splicing factors serve as adapter proteins for TAP-dependent mRNA export. Mol Cell **11:** 837-843.

HULSMANN, B. B., A. A. LABOKHA and D. GORLICH, 2012 The permeability of reconstituted nuclear pores provides direct evidence for the selective phase model. Cell **150:** 738-751.

HUNG, N. J., and A. W. JOHNSON, 2006 Nuclear recycling of the pre-60S ribosomal subunit-associated factor Arx1 depends on Rei1 in Saccharomyces cerevisiae. Mol Cell Biol **26:** 3718-3727.

HUNG, N. J., K. Y. LO, S. S. PATEL, K. HELMKE and A. W. JOHNSON, 2008 Arx1 is a nuclear export receptor for the 60S ribosomal subunit in yeast. Mol Biol Cell **19:** 735-744.

IGLESIAS, N., E. TUTUCCI, C. GWIZDEK, P. VINCIGUERRA, E. VON DACH *et al.*, 2010 Ubiquitin-mediated mRNP dynamics and surveillance prior to budding yeast mRNA export. Genes Dev **24:** 1927-1938.

IOVINE, M. K., J. L. WATKINS and S. R. WENTE, 1995 The GLFG repetitive region of the nucleoporin Nup116p interacts with Kap95p, an essential yeast nuclear import factor. J Cell Biol **131:** 1699-1713.

ISHIGAKI, Y., X. LI, G. SERIN and L. E. MAQUAT, 2001 Evidence for a pioneer round of mRNA translation: mRNAs subject to nonsense-mediated decay in mammalian cells are bound by CBP80 and CBP20. Cell **106:** 607-617.

JACKSON, R. J., 2013 The current status of vertebrate cellular mRNA IRESs. Cold Spring Harb Perspect Biol **5**.

JANI, D., S. LUTZ, E. HURT, R. A. LASKEY, M. STEWART *et al.*, 2012 Functional and structural characterization of the mammalian TREX-2 complex that links transcription with nuclear messenger RNA export. Nucleic Acids Res **40:** 4562-4573.

JAO, L. E., B. APPEL and S. R. WENTE, 2012 A zebrafish model of lethal congenital contracture syndrome 1 reveals Gle1 function in spinal neural precursor survival and motor axon arborization. Development **139:** 1316-1326.

JENSEN, T. H., K. PATRICIO, T. MCCARTHY and M. ROSBASH, 2001 A block to mRNA nuclear export in S. cerevisiae leads to hyperadenylation of transcripts that accumulate at the site of transcription. Mol Cell **7:** 887-898.

JIMENO, S., A. G. RONDON, R. LUNA and A. AGUILERA, 2002 The yeast THO complex and mRNA export factors link RNA metabolism with transcription and genome instability. Embo J **21:** 3526-3535.

JOHNSON, S. A., G. CUBBERLEY and D. L. BENTLEY, 2009 Cotranscriptional recruitment of the mRNA export factor Yra1 by direct interaction with the 3' end processing factor Pcf11. Mol Cell **33:** 215-226.

JONES, D. T., and D. COZZETTO, 2014 DISOPRED3: precise disordered region predictions with annotated protein-binding activity. Bioinformatics.

JOVANOVIC-TALISMAN, T., J. TETENBAUM-NOVATT, A. S. MCKENNEY, A. ZILMAN, R. PETERS *et al.*, 2009 Artificial nanopores that mimic the transport selectivity of the nuclear pore complex. Nature **457:** 1023-1027.

KALLEHAUGE, T. B., M. C. ROBERT, E. BERTRAND and T. H. JENSEN, 2012 Nuclear retention prevents premature cytoplasmic appearance of mRNA. Mol Cell **48:** 145-152.

KALVERDA, B., H. PICKERSGILL, V. V. SHLOMA and M. FORNEROD, 2010 Nucleoporins directly stimulate expression of developmental and cell-cycle genes inside the nucleoplasm. Cell **140:** 360-371.

KAMINSKI, T., J. P. SIEBRASSE and U. KUBITSCHECK, 2013 A single molecule view on Dbp5 and mRNA at the nuclear pore. Nucleus **4:** 8-13.

KATAHIRA, J., K. STRASSER, A. PODTELEJNIKOV, M. MANN, J. U. JUNG *et al.*, 1999 The Mex67p-mediated nuclear mRNA export pathway is conserved from yeast to human. Embo J **18:** 2593-2609.

KATO, M., T. W. HAN, S. XIE, K. SHI, X. DU *et al.*, 2012 Cell-free formation of RNA granules: low complexity sequence domains form dynamic fibers within hydrogels. Cell **149:** 753-767.

KELLY, S. M., and A. H. CORBETT, 2009 Messenger RNA export from the nucleus: a series of molecular wardrobe changes. Traffic **10:** 1199-1208.

KENDIRGI, F., D. M. BARRY, E. R. GRIFFIS, M. A. POWERS and S. R. WENTE, 2003 An essential role for hGle1 nucleocytoplasmic shuttling in mRNA export. J Cell Biol **160:** 1029-1040.

KENDIRGI, F., D. J. REXER, A. R. ALCAZAR-ROMAN, H. M. ONISHKO and S. R. WENTE, 2005 Interaction between the shuttling mRNA export factor Gle1 and the nucleoporin hCG1: a conserved mechanism in the export of Hsp70 mRNA. Mol Biol Cell **16:** 4304-4315.

KIM, V. N., N. KATAOKA and G. DREYFUSS, 2001 Role of the nonsense-mediated decay factor hUpf3 in the splicing-dependent exon-exon junction complex. Science **293:** 1832-1836.

KISTLER, A. L., and C. GUTHRIE, 2001 Deletion of MUD2, the yeast homolog of U2AF65, can bypass the requirement for sub2, an essential spliceosomal ATPase. Genes Dev **15:** 42-49.

KOHLER, A., and E. HURT, 2007 Exporting RNA from the nucleus to the cytoplasm. Nat Rev Mol Cell Biol **8:** 761-773.

KOIVOMAGI, M., M. ORD, A. IOFIK, E. VALK, R. VENTA *et al.*, 2013 Multisite phosphorylation networks as signal processors for Cdk1. Nat Struct Mol Biol **20:** 1415-1424.

KOIVOMAGI, M., E. VALK, R. VENTA, A. IOFIK, M. LEPIKU *et al.*, 2011 Dynamics of Cdk1 substrate specificity during the cell cycle. Mol Cell **42:** 610-623.

KONIG, J., K. ZARNACK, G. ROT, T. CURK, M. KAYIKCI *et al.*, 2010 iCLIP reveals the function of hnRNP particles in splicing at individual nucleotide resolution. Nat Struct Mol Biol **17:** 909-915.

KOSSEN, K., F. V. KARGINOV and O. C. UHLENBECK, 2002 The carboxy-terminal domain of the DExDH protein YxiN is sufficient to confer specificity for 23S rRNA. J Mol Biol **324:** 625-636.

KOSSEN, K., and O. C. UHLENBECK, 1999 Cloning and biochemical characterization of Bacillus subtilis YxiN, a DEAD protein specifically activated by 23S rRNA: delineation of a novel sub-family of bacterial DEAD proteins. Nucleic Acids Res **27:** 3811-3820.

KOSUGI, S., M. HASEBE, M. TOMITA and H. YANAGAWA, 2009 Systematic identification of cell cycle-dependent yeast nucleocytoplasmic shuttling proteins by prediction of composite motifs. Proc Natl Acad Sci U S A **106:** 10171-10176.

KRAEMER, D., R. W. WOZNIAK, G. BLOBEL and A. RADU, 1994 The human CAN protein, a putative oncogene product associated with myeloid leukemogenesis, is a nuclear pore complex protein that faces the cytoplasm. Proc Natl Acad Sci U S A **91:** 1519-1523.

KRAEMER, D. M., C. STRAMBIO-DE-CASTILLIA, G. BLOBEL and M. P. ROUT, 1995 The essential yeast nucleoporin NUP159 is located on the cytoplasmic side of the nuclear pore complex and serves in karyopherin-mediated binding of transport substrate. J Biol Chem **270:** 19017-19021.

KRESS, T. L., N. J. KROGAN and C. GUTHRIE, 2008 A single SR-like protein, Npl3, promotes pre-mRNA splicing in budding yeast. Mol Cell **32:** 727-734.
KUBITSCHECK, U., D. GRUNWALD, A. HOEKSTRA, D. ROHLEDER, T. KUES *et al.*, 2005 Nuclear transport of single molecules: dwell times at the nuclear pore complex. J Cell Biol **168:** 233-243.
KUERSTEN, S., S. P. SEGAL, J. VERHEYDEN, S. M. LAMARTINA and E. B. GOODWIN, 2004 NXF-2, REF-1, and REF-2 affect the choice of nuclear export pathway for tra-2 mRNA in C. elegans. Mol Cell **14:** 599-610.
KULA, A., J. GUERRA, A. KNEZEVICH, D. KLEVA, M. P. MYERS *et al.*, 2011 Characterization of the HIV-1 RNA associated proteome identifies Matrin 3 as a nuclear cofactor of Rev function. Retrovirology **8:** 60.
KWON, S. C., H. YI, K. EICHELBAUM, S. FOHR, B. FISCHER *et al.*, 2013 The RNA-binding protein repertoire of embryonic stem cells. Nat Struct Mol Biol **20:** 1122-1130.
LABOKHA, A. A., S. GRADMANN, S. FREY, B. B. HULSMANN, H. URLAUB *et al.*, 2013 Systematic analysis of barrier-forming FG hydrogels from Xenopus nuclear pore complexes. Embo J **32:** 204-218.
LANE, C. M., I. CUSHMAN and M. S. MOORE, 2000 Selective disruption of nuclear import by a functional mutant nuclear transport carrier. J Cell Biol **151:** 321-332.
LAURELL, E., K. BECK, K. KRUPINA, G. THEERTHAGIRI, B. BODENMILLER *et al.*, 2011 Phosphorylation of Nup98 by multiple kinases is crucial for NPC disassembly during mitotic entry. Cell **144:** 539-550.
LE HIR, H., D. GATFIELD, E. IZAURRALDE and M. J. MOORE, 2001 The exon-exon junction complex provides a binding platform for factors involved in mRNA export and nonsense-mediated mRNA decay. Embo J **20:** 4987-4997.
LEE, M. S., M. HENRY and P. A. SILVER, 1996 A protein that shuttles between the nucleus and the cytoplasm is an important mediator of RNA export. Genes Dev **10:** 1233-1246.
LEJEUNE, F., Y. ISHIGAKI, X. LI and L. E. MAQUAT, 2002 The exon junction complex is detected on CBP80-bound but not eIF4E-bound mRNA in mammalian cells: dynamics of mRNP remodeling. Embo J **21:** 3536-3545.
LEWIS, A., R. FELBERBAUM and M. HOCHSTRASSER, 2007 A nuclear envelope protein linking nuclear pore basket assembly, SUMO protease regulation, and mRNA surveillance. J Cell Biol **178:** 813-827.
LI, S. J., and M. HOCHSTRASSER, 1999 A new protease required for cell-cycle progression in yeast. Nature **398:** 246-251.
LIANG, Y., T. M. FRANKS, M. C. MARCHETTO, F. H. GAGE and M. W. HETZER, 2013 Dynamic association of NUP98 with the human genome. PLoS Genet **9:** e1003308.
LIBRI, D., K. DOWER, J. BOULAY, R. THOMSEN, M. ROSBASH *et al.*, 2002 Interactions between mRNA export commitment, 3'-end quality control, and nuclear degradation. Mol Cell Biol **22:** 8254-8266.
LIGHT, W. H., D. G. BRICKNER, V. R. BRAND and J. H. BRICKNER, 2010 Interaction of a DNA zip code with the nuclear pore complex promotes H2A.Z incorporation and INO1 transcriptional memory. Mol Cell **40:** 112-125.
LIGHT, W. H., J. FREANEY, V. SOOD, A. THOMPSON, A. D'URSO *et al.*, 2013 A conserved role for human Nup98 in altering chromatin structure and promoting epigenetic transcriptional memory. PLoS Biol **11:** e1001524.

LIKER, E., E. FERNANDEZ, E. IZAURRALDE and E. CONTI, 2000 The structure of the mRNA export factor TAP reveals a cis arrangement of a non-canonical RNP domain and an LRR domain. Embo J **19:** 5587-5598.
LIM, R. Y., B. FAHRENKROG, J. KOSER, K. SCHWARZ-HERION, J. DENG *et al.*, 2007 Nanomechanical basis of selective gating by the nuclear pore complex. Science **318:** 640-643.
LIN, J. R., and J. HU, 2013 SeqNLS: nuclear localization signal prediction based on frequent pattern mining and linear motif scoring. PLoS One **8:** e76864.
LINDER, P., and E. JANKOWSKY, 2011 From unwinding to clamping - the DEAD box RNA helicase family. Nat Rev Mol Cell Biol **12:** 505-516.
LINDSAY, M. E., K. PLAFKER, A. E. SMITH, B. E. CLURMAN and I. G. MACARA, 2002 Npap60/Nup50 is a tri-stable switch that stimulates importin-alpha:beta-mediated nuclear protein import. Cell **110:** 349-360.
LIU, F., A. PUTNAM and E. JANKOWSKY, 2008 ATP hydrolysis is required for DEAD-box protein recycling but not for duplex unwinding. Proc Natl Acad Sci U S A **105:** 20209-20214.
LIU, F., A. A. PUTNAM and E. JANKOWSKY, 2014 DEAD-box helicases form nucleotide-dependent, long-lived complexes with RNA. Biochemistry **53:** 423-433.
LIU, S. M., and M. STEWART, 2005 Structural basis for the high-affinity binding of nucleoporin Nup1p to the Saccharomyces cerevisiae importin-beta homologue, Kap95p. J Mol Biol **349:** 515-525.
LO, K. Y., and A. W. JOHNSON, 2009 Reengineering ribosome export. Mol Biol Cell **20:** 1545-1554.
LONG, J. C., and J. F. CACERES, 2009 The SR protein family of splicing factors: master regulators of gene expression. Biochem J **417:** 15-27.
LORD, C. L. , B. L. TIMNEY, M. P. ROUT, S. R. WENTE, 2015 Altering nuclear pore complex function impacts longevity and mitochondrial function in *S. cerevisiae*. J Cell Biol. *in press*.
LORSCH, J. R., and D. HERSCHLAG, 1998a The DEAD box protein eIF4A. 1. A minimal kinetic and thermodynamic framework reveals coupled binding of RNA and nucleotide. Biochemistry **37:** 2180-2193.
LORSCH, J. R., and D. HERSCHLAG, 1998b The DEAD box protein eIF4A. 2. A cycle of nucleotide and RNA-dependent conformational changes. Biochemistry **37:** 2194-2206.
LOSCHBERGER, A., S. VAN DE LINDE, M. C. DABAUVALLE, B. RIEGER, M. HEILEMANN *et al.*, 2012 Super-resolution imaging visualizes the eightfold symmetry of gp210 proteins around the nuclear pore complex and resolves the central channel with nanometer resolution. J Cell Sci **125:** 570-575.
LOWE, A. R., J. J. SIEGEL, P. KALAB, M. SIU, K. WEIS *et al.*, 2010 Selectivity mechanism of the nuclear pore complex characterized by single cargo tracking. Nature **467:** 600-603.
LUND, M. K., and C. GUTHRIE, 2005 The DEAD-box protein Dbp5p is required to dissociate Mex67p from exported mRNPs at the nuclear rim. Mol Cell **20:** 645-651.
LUND, M. K., T. L. KRESS and C. GUTHRIE, 2008 Autoregulation of Npl3, a yeast SR protein, requires a novel downstream region and serine phosphorylation. Mol Cell Biol **28:** 3873-3881.
LUO, M. J., and R. REED, 1999 Splicing is required for rapid and efficient mRNA export in metazoans. Proc Natl Acad Sci U S A **96:** 14937-14942.

LUPU, F., A. ALVES, K. ANDERSON, V. DOYE and E. LACY, 2008 Nuclear pore composition regulates neural stem/progenitor cell differentiation in the mouse embryo. Dev Cell **14:** 831-842.

LUTHRA, R., S. C. KERR, M. T. HARREMAN, L. H. APPONI, M. B. FASKEN *et al.*, 2007 Actively transcribed GAL genes can be physically linked to the nuclear pore by the SAGA chromatin modifying complex. J Biol Chem **282:** 3042-3049.

MA, J., A. GORYAYNOV, A. SARMA and W. YANG, 2012 Self-regulated viscous channel in the nuclear pore complex. Proc Natl Acad Sci U S A **109:** 7326-7331.

MA, J., Z. LIU, N. MICHELOTTI, S. PITCHIAYA, R. VEERAPANENI *et al.*, 2013a High-resolution three-dimensional mapping of mRNA export through the nuclear pore. Nat Commun **4:** 2414.

MA, J., and W. YANG, 2010 Three-dimensional distribution of transient interactions in the nuclear pore complex obtained from single-molecule snapshots. Proc Natl Acad Sci U S A **107:** 7305-7310.

MA, W. K., S. C. CLOUTIER and E. J. TRAN, 2013b The DEAD-box protein Dbp2 functions with the RNA-binding protein Yra1 to promote mRNP assembly. J Mol Biol **425:** 3824-3838.

MAHAJAN, R., C. DELPHIN, T. GUAN, L. GERACE and F. MELCHIOR, 1997 A small ubiquitin-related polypeptide involved in targeting RanGAP1 to nuclear pore complex protein RanBP2. Cell **88:** 97-107.

MAIMON, T., N. ELAD, I. DAHAN and O. MEDALIA, 2012 The human nuclear pore complex as revealed by cryo-electron tomography. Structure **20:** 998-1006.

MALLAM, A. L., M. DEL CAMPO, B. GILMAN, D. J. SIDOTE and A. M. LAMBOWITZ, 2012 Structural basis for RNA-duplex recognition and unwinding by the DEAD-box helicase Mss116p. Nature **490:** 121-125.

MALLAM, A. L., I. JARMOSKAITE, P. TIJERINA, M. DEL CAMPO, S. SEIFERT *et al.*, 2011 Solution structures of DEAD-box RNA chaperones reveal conformational changes and nucleic acid tethering by a basic tail. Proc Natl Acad Sci U S A **108:** 12254-12259.

MARCHLER-BAUER, A., C. ZHENG, F. CHITSAZ, M. K. DERBYSHIRE, L. Y. GEER *et al.*, 2013 CDD: conserved domains and protein three-dimensional structure. Nucleic Acids Res **41:** D348-352.

MARFATIA, K. A., E. B. CRAFTON, D. M. GREEN and A. H. CORBETT, 2003 Domain analysis of the Saccharomyces cerevisiae heterogeneous nuclear ribonucleoprotein, Nab2p. Dissecting the requirements for Nab2p-facilitated poly(A) RNA export. J Biol Chem **278:** 6731-6740.

MARINTCHEV, A., K. A. EDMONDS, B. MARINTCHEVA, E. HENDRICKSON, M. OBERER *et al.*, 2009 Topology and regulation of the human eIF4A/4G/4H helicase complex in translation initiation. Cell **136:** 447-460.

MASON, P. B., and K. STRUHL, 2005 Distinction and relationship between elongation rate and processivity of RNA polymerase II in vivo. Mol Cell **17:** 831-840.

MASUDA, S., R. DAS, H. CHENG, E. HURT, N. DORMAN *et al.*, 2005 Recruitment of the human TREX complex to mRNA during splicing. Genes Dev **19:** 1512-1517.

MATSUURA, Y., A. LANGE, M. T. HARREMAN, A. H. CORBETT and M. STEWART, 2003 Structural basis for Nup2p function in cargo release and karyopherin recycling in nuclear import. Embo J **22:** 5358-5369.

MATSUURA, Y., and M. STEWART, 2005 Nup50/Npap60 function in nuclear protein import complex disassembly and importin recycling. Embo J **24:** 3681-3689.
MATUNIS, M. J., E. COUTAVAS and G. BLOBEL, 1996 A novel ubiquitin-like modification modulates the partitioning of the Ran-GTPase-activating protein RanGAP1 between the cytosol and the nuclear pore complex. J Cell Biol **135:** 1457-1470.
MATUNIS, M. J., J. WU and G. BLOBEL, 1998 SUMO-1 modification and its role in targeting the Ran GTPase-activating protein, RanGAP1, to the nuclear pore complex. J Cell Biol **140:** 499-509.
MCCRACKEN, S., N. FONG, K. YANKULOV, S. BALLANTYNE, G. PAN *et al.*, 1997 The C-terminal domain of RNA polymerase II couples mRNA processing to transcription. Nature **385:** 357-361.
MEHDI, A. M., M. S. SEHGAL, B. KOBE, T. L. BAILEY and M. BODEN, 2011 A probabilistic model of nuclear import of proteins. Bioinformatics **27:** 1239-1246.
MEINEL, D. M., C. BURKERT-KAUTZSCH, A. KIESER, E. O'DUIBHIR, M. SIEBERT *et al.*, 2013 Recruitment of TREX to the transcription machinery by its direct binding to the phospho-CTD of RNA polymerase II. PLoS Genet **9:** e1003914.
METTENLEITER, T. C., F. MULLER, H. GRANZOW and B. G. KLUPP, 2013 The way out: what we know and do not know about herpesvirus nuclear egress. Cell Microbiol **15:** 170-178.
MILLER, A. L., M. SUNTHARALINGAM, S. L. JOHNSON, A. AUDHYA, S. D. EMR *et al.*, 2004 Cytoplasmic inositol hexakisphosphate production is sufficient for mediating the Gle1-mRNA export pathway. J Biol Chem **279:** 51022-51032.
MILLER, O. L., JR., and B. R. BEATTY, 1969 Visualization of nucleolar genes. Science **164:** 955-957.
MITCHELL, S. F., S. JAIN, M. SHE and R. PARKER, 2013 Global analysis of yeast mRNPs. Nat Struct Mol Biol **20:** 127-133.
MONTPETIT, B., N. D. THOMSEN, K. J. HELMKE, M. A. SEELIGER, J. M. BERGER *et al.*, 2011 A conserved mechanism of DEAD-box ATPase activation by nucleoporins and InsP6 in mRNA export. Nature **472:** 238-242.
MOORE, M. J., 2005 From birth to death: the complex lives of eukaryotic mRNAs. Science **309:** 1514-1518.
MOORE, M. S., and G. BLOBEL, 1994 Purification of a Ran-interacting protein that is required for protein import into the nucleus. Proc Natl Acad Sci U S A **91:** 10212-10216.
MOR, A., S. SULIMAN, R. BEN-YISHAY, S. YUNGER, Y. BRODY *et al.*, 2010 Dynamics of single mRNP nucleocytoplasmic transport and export through the nuclear pore in living cells. Nat Cell Biol **12:** 543-552.
MULLER-MCNICOLL, M., and K. M. NEUGEBAUER, 2013 How cells get the message: dynamic assembly and function of mRNA-protein complexes. Nat Rev Genet **14:** 275-287.
MURPHY, R., and S. R. WENTE, 1996 An RNA-export mediator with an essential nuclear export signal. Nature **383:** 357-360.
MUTHUSWAMY, S., and I. MEIER, 2011 Genetic and environmental changes in SUMO homeostasis lead to nuclear mRNA retention in plants. Planta **233:** 201-208.
NAKAI, K., and P. HORTON, 1999 PSORT: a program for detecting sorting signals in proteins and predicting their subcellular localization. Trends Biochem Sci **24:** 34-36.
NATALIZIO, B. J., and S. R. WENTE, 2013 Postage for the messenger: designating routes for nuclear mRNA export. Trends Cell Biol **23:** 365-373.

NEUMANN, N., D. LUNDIN and A. M. POOLE, 2010 Comparative genomic evidence for a complete nuclear pore complex in the last eukaryotic common ancestor. PLoS One **5:** e13241.
NGUYEN BA, A. N., A. POGOUTSE, N. PROVART and A. M. MOSES, 2009 NLStradamus: a simple Hidden Markov Model for nuclear localization signal prediction. BMC Bioinformatics **10:** 202.
NIESSING, D., S. HUTTELMAIER, D. ZENKLUSEN, R. H. SINGER and S. K. BURLEY, 2004 She2p is a novel RNA binding protein with a basic helical hairpin motif. Cell **119:** 491-502.
NOBLE, K. N., E. J. TRAN, A. R. ALCAZAR-ROMAN, C. A. HODGE, C. N. COLE *et al.*, 2011 The Dbp5 cycle at the nuclear pore complex during mRNA export II: nucleotide cycling and mRNP remodeling by Dbp5 are controlled by Nup159 and Gle1. Genes Dev **25:** 1065-1077.
NOBLE, S. M., and C. GUTHRIE, 1996 Identification of novel genes required for yeast pre-mRNA splicing by means of cold-sensitive mutations. Genetics **143:** 67-80.
NOUSIAINEN, H. O., M. KESTILA, N. PAKKASJARVI, H. HONKALA, S. KUURE *et al.*, 2008 Mutations in mRNA export mediator GLE1 result in a fetal motoneuron disease. Nat Genet **40:** 155-157.
OBERER, M., A. MARINTCHEV and G. WAGNER, 2005 Structural basis for the enhancement of eIF4A helicase activity by eIF4G. Genes Dev **19:** 2212-2223.
OEFFINGER, M., K. E. WEI, R. ROGERS, J. A. DEGRASSE, B. T. CHAIT *et al.*, 2007 Comprehensive analysis of diverse ribonucleoprotein complexes. Nat Methods **4:** 951-956.
OKADA, C., E. YAMASHITA, S. J. LEE, S. SHIBATA, J. KATAHIRA *et al.*, 2009 A high-resolution structure of the pre-microRNA nuclear export machinery. Science **326:** 1275-1279.
OLSSON, M., S. SCHEELE and P. EKBLOM, 2004 Limited expression of nuclear pore membrane glycoprotein 210 in cell lines and tissues suggests cell-type specific nuclear pores in metazoans. Exp Cell Res **292:** 359-370.
ORI, A., N. BANTERLE, M. ISKAR, A. ANDRES-PONS, C. ESCHER *et al.*, 2013 Cell type-specific nuclear pores: a case in point for context-dependent stoichiometry of molecular machines. Mol Syst Biol **9:** 648.
PALACIOS, I. M., D. GATFIELD, D. ST JOHNSTON and E. IZAURRALDE, 2004 An eIF4AIII-containing complex required for mRNA localization and nonsense-mediated mRNA decay. Nature **427:** 753-757.
PALANCADE, B., X. LIU, M. GARCIA-RUBIO, A. AGUILERA, X. ZHAO *et al.*, 2007 Nucleoporins prevent DNA damage accumulation by modulating Ulp1-dependent sumoylation processes. Mol Biol Cell **18:** 2912-2923.
PANSE, V. G., U. HARDELAND, T. WERNER, B. KUSTER and E. HURT, 2004 A proteome-wide approach identifies sumoylated substrate proteins in yeast. J Biol Chem **279:** 41346-41351.
PANSE, V. G., and A. W. JOHNSON, 2010 Maturation of eukaryotic ribosomes: acquisition of functionality. Trends Biochem Sci **35:** 260-266.
PANSE, V. G., D. KRESSLER, A. PAULI, E. PETFALSKI, M. GNADIG *et al.*, 2006 Formation and nuclear export of preribosomes are functionally linked to the small-ubiquitin-related modifier pathway. Traffic **7:** 1311-1321.
PANTE, N., and M. KANN, 2002 Nuclear pore complex is able to transport macromolecules with diameters of about 39 nm. Mol Biol Cell **13:** 425-434.
PARK, H. Y., H. LIM, Y. J. YOON, A. FOLLENZI, C. NWOKAFOR *et al.*, 2014 Visualization of dynamics of single endogenous mRNA labeled in live mouse. Science **343:** 422-424.

PARKER, R., 2012 RNA degradation in Saccharomyces cerevisae. Genetics **191:** 671-702.
PASCUAL-GARCIA, P., C. K. GOVIND, E. QUERALT, B. CUENCA-BONO, A. LLOPIS *et al.*, 2008 Sus1 is recruited to coding regions and functions during transcription elongation in association with SAGA and TREX2. Genes Dev **22:** 2811-2822.
PATEL, S. S., B. J. BELMONT, J. M. SANTE and M. F. REXACH, 2007 Natively unfolded nucleoporins gate protein diffusion across the nuclear pore complex. Cell **129:** 83-96.
PATEL, S. S., and M. F. REXACH, 2008 Discovering novel interactions at the nuclear pore complex using bead halo: a rapid method for detecting molecular interactions of high and low affinity at equilibrium. Mol Cell Proteomics **7:** 121-131.
PAULILLO, S. M., E. M. PHILLIPS, J. KOSER, U. SAUDER, K. S. ULLMAN *et al.*, 2005 Nucleoporin domain topology is linked to the transport status of the nuclear pore complex. J Mol Biol **351:** 784-798.
PETERS, R., 2009 Translocation through the nuclear pore: Kaps pave the way. Bioessays **31:** 466-477.
PICHLER, A., A. GAST, J. S. SEELER, A. DEJEAN and F. MELCHIOR, 2002 The nucleoporin RanBP2 has SUMO1 E3 ligase activity. Cell **108:** 109-120.
POWRIE, E. A., D. ZENKLUSEN and R. H. SINGER, 2011 A nucleoporin, Nup60p, affects the nuclear and cytoplasmic localization of ASH1 mRNA in S. cerevisiae. RNA **17:** 134-144.
PREKER, P. J., and C. GUTHRIE, 2006 Autoregulation of the mRNA export factor Yra1p requires inefficient splicing of its pre-mRNA. RNA **12:** 994-1006.
PREKER, P. J., K. S. KIM and C. GUTHRIE, 2002 Expression of the essential mRNA export factor Yra1p is autoregulated by a splicing-dependent mechanism. RNA **8:** 969-980.
PUTNAM, A. A., and E. JANKOWSKY, 2013 AMP sensing by DEAD-box RNA helicases. J Mol Biol **425:** 3839-3845.
PYHTILA, B., and M. REXACH, 2003 A gradient of affinity for the karyopherin Kap95p along the yeast nuclear pore complex. J Biol Chem **278:** 42699-42709.
QUIMBY, B. B., S. W. LEUNG, R. BAYLISS, M. T. HARREMAN, G. THIRUMALA *et al.*, 2001 Functional analysis of the hydrophobic patch on nuclear transport factor 2 involved in interactions with the nuclear pore in vivo. J Biol Chem **276:** 38820-38829.
RABUT, G., V. DOYE and J. ELLENBERG, 2004 Mapping the dynamic organization of the nuclear pore complex inside single living cells. Nat Cell Biol **6:** 1114-1121.
RAICES, M., and M. A. D'ANGELO, 2012 Nuclear pore complex composition: a new regulator of tissue-specific and developmental functions. Nat Rev Mol Cell Biol **13:** 687-699.
RAY, B. K., T. G. LAWSON, J. C. KRAMER, M. H. CLADARAS, J. A. GRIFO *et al.*, 1985 ATP-dependent unwinding of messenger RNA structure by eukaryotic initiation factors. J Biol Chem **260:** 7651-7658.
RAYALA, H. J., F. KENDIRGI, D. M. BARRY, P. W. MAJERUS and S. R. WENTE, 2004 The mRNA export factor human Gle1 interacts with the nuclear pore complex protein Nup155. Mol Cell Proteomics **3:** 145-155.
RIBBECK, K., and D. GORLICH, 2001 Kinetic analysis of translocation through nuclear pore complexes. Embo J **20:** 1320-1330.
RIBBECK, K., and D. GORLICH, 2002 The permeability barrier of nuclear pore complexes appears to operate via hydrophobic exclusion. Embo J **21:** 2664-2671.
RIBBECK, K., G. LIPOWSKY, H. M. KENT, M. STEWART and D. GORLICH, 1998 NTF2 mediates nuclear import of Ran. Embo J **17:** 6587-6598.

RODRIGUEZ-NAVARRO, S., T. FISCHER, M. J. LUO, O. ANTUNEZ, S. BRETTSCHNEIDER *et al.*, 2004 Sus1, a functional component of the SAGA histone acetylase complex and the nuclear pore-associated mRNA export machinery. Cell **116:** 75-86.

RODRIGUEZ-NAVARRO, S., and E. HURT, 2011 Linking gene regulation to mRNA production and export. Curr Opin Cell Biol **23:** 302-309.

RODRIGUEZ-NAVARRO, S., K. STRASSER and E. HURT, 2002 An intron in the YRA1 gene is required to control Yra1 protein expression and mRNA export in yeast. EMBO Rep **3:** 438-442.

ROGERS, G. W., JR., A. A. KOMAR and W. C. MERRICK, 2002 eIF4A: the godfather of the DEAD box helicases. Prog Nucleic Acid Res Mol Biol **72:** 307-331.

ROGERS, G. W., JR., N. J. RICHTER and W. C. MERRICK, 1999 Biochemical and kinetic characterization of the RNA helicase activity of eukaryotic initiation factor 4A. J Biol Chem **274:** 12236-12244.

ROLLENHAGEN, C., C. A. HODGE and C. N. COLE, 2004 The nuclear pore complex and the DEAD box protein Rat8p/Dbp5p have nonessential features which appear to facilitate mRNA export following heat shock. Mol Cell Biol **24:** 4869-4879.

ROLOFF, S., C. SPILLNER and R. H. KEHLENBACH, 2013 Several phenylalanine-glycine motives in the nucleoporin Nup214 are essential for binding of the nuclear export receptor CRM1. J Biol Chem **288:** 3952-3963.

RONDON, A. G., S. JIMENO and A. AGUILERA, 2010 The interface between transcription and mRNP export: from THO to THSC/TREX-2. Biochim Biophys Acta **1799:** 533-538.

ROSSLER, O. G., A. STRAKA and H. STAHL, 2001 Rearrangement of structured RNA via branch migration structures catalysed by the highly related DEAD-box proteins p68 and p72. Nucleic Acids Res **29:** 2088-2096.

ROTH, K. M., M. K. WOLF, M. ROSSI and J. S. BUTLER, 2005 The nuclear exosome contributes to autogenous control of NAB2 mRNA levels. Mol Cell Biol **25:** 1577-1585.

ROUT, M. P., J. D. AITCHISON, M. O. MAGNASCO and B. T. CHAIT, 2003 Virtual gating and nuclear transport: the hole picture. Trends Cell Biol **13:** 622-628.

ROUT, M. P., J. D. AITCHISON, A. SUPRAPTO, K. HJERTAAS, Y. ZHAO *et al.*, 2000 The yeast nuclear pore complex: composition, architecture, and transport mechanism. J Cell Biol **148:** 635-651.

ROUT, M. P., and S. R. WENTE, 1994 Pores for thought: nuclear pore complex proteins. Trends Cell Biol **4:** 357-365.

ROUX, K. J., D. I. KIM and B. BURKE, 2013 BioID: a screen for protein-protein interactions. Curr Protoc Protein Sci **74:** Unit 19 23.

RUSSELL, R., I. JARMOSKAITE and A. M. LAMBOWITZ, 2013 Toward a molecular understanding of RNA remodeling by DEAD-box proteins. RNA Biol **10:** 44-55.

SAAVEDRA, C., K. S. TUNG, D. C. AMBERG, A. K. HOPPER and C. N. COLE, 1996 Regulation of mRNA export in response to stress in Saccharomyces cerevisiae. Genes Dev **10:** 1608-1620.

SAAVEDRA, C. A., C. M. HAMMELL, C. V. HEATH and C. N. COLE, 1997 Yeast heat shock mRNAs are exported through a distinct pathway defined by Rip1p. Genes Dev **11:** 2845-2856.

SABRI, N., P. ROTH, N. XYLOURGIDIS, F. SADEGHIFAR, J. ADLER *et al.*, 2007 Distinct functions of the Drosophila Nup153 and Nup214 FG domains in nuclear protein transport. J Cell Biol **178:** 557-565.

SANGEL, P., M. OKA and Y. YONEDA, 2014 The role of Importin-betas in the maintenance and lineage commitment of mouse embryonic stem cells. FEBS Open Bio **4:** 112-120.

SANTOS-PEREIRA, J. M., M. L. GARCIA-RUBIO, C. GONZALEZ-AGUILERA, R. LUNA and A. AGUILERA, 2014a A genome-wide function of THSC/TREX-2 at active genes prevents transcription-replication collisions. Nucleic Acids Res **42:** 12000-12014.

SANTOS-PEREIRA, J. M., A. B. HERRERO, S. MORENO and A. AGUILERA, 2014b Npl3, a new link between RNA-binding proteins and the maintenance of genome integrity. Cell Cycle **13:** 1524-1529.

SANTOS-ROSA, H., H. MORENO, G. SIMOS, A. SEGREF, B. FAHRENKROG *et al.*, 1998 Nuclear mRNA export requires complex formation between Mex67p and Mtr2p at the nuclear pores. Mol Cell Biol **18:** 6826-6838.

SAVAS, J. N., B. H. TOYAMA, T. XU, J. R. YATES, 3RD and M. W. HETZER, 2012 Extremely long-lived nuclear pore proteins in the rat brain. Science **335:** 942.

SCARCELLI, J. J., S. VIGGIANO, C. A. HODGE, C. V. HEATH, D. C. AMBERG *et al.*, 2008 Synthetic genetic array analysis in Saccharomyces cerevisiae provides evidence for an interaction between RAT8/DBP5 and genes encoding P-body components. Genetics **179:** 1945-1955.

SCHLEICHER, K. D., S. L. DETTMER, L. E. KAPINOS, S. PAGLIARA, U. F. KEYSER *et al.*, 2014 Selective transport control on molecular velcro made from intrinsically disordered proteins. Nat Nanotechnol **9:** 525-530.

SCHMITT, C., C. VON KOBBE, A. BACHI, N. PANTE, J. P. RODRIGUES *et al.*, 1999 Dbp5, a DEAD-box protein required for mRNA export, is recruited to the cytoplasmic fibrils of nuclear pore complex via a conserved interaction with CAN/Nup159p. Embo J **18:** 4332-4347.

SCHOCH, R. L., L. E. KAPINOS and R. Y. LIM, 2012 Nuclear transport receptor binding avidity triggers a self-healing collapse transition in FG-nucleoporin molecular brushes. Proc Natl Acad Sci U S A **109:** 16911-16916.

SCHOENBERG, D. R., and L. E. MAQUAT, 2012 Regulation of cytoplasmic mRNA decay. Nat Rev Genet **13:** 246-259.

SCHUTZ, P., M. BUMANN, A. E. OBERHOLZER, C. BIENIOSSEK, H. TRACHSEL *et al.*, 2008 Crystal structure of the yeast eIF4A-eIF4G complex: an RNA-helicase controlled by protein-protein interactions. Proc Natl Acad Sci U S A **105:** 9564-9569.

SEGREF, A., K. SHARMA, V. DOYE, A. HELLWIG, J. HUBER *et al.*, 1997 Mex67p, a novel factor for nuclear mRNA export, binds to both poly(A)+ RNA and nuclear pores. Embo J **16:** 3256-3271.

SENGOKU, T., O. NUREKI, A. NAKAMURA, S. KOBAYASHI and S. YOKOYAMA, 2006 Structural basis for RNA unwinding by the DEAD-box protein Drosophila Vasa. Cell **125:** 287-300.

SENGUPTA, J., C. BUSSIERE, J. PALLESEN, M. WEST, A. W. JOHNSON *et al.*, 2010 Characterization of the nuclear export adaptor protein Nmd3 in association with the 60S ribosomal subunit. J Cell Biol **189:** 1079-1086.

SHEPARD, P. J., and K. J. HERTEL, 2009 The SR protein family. Genome Biol **10:** 242.

SHERMAN, F., FINK, G. R., HICKS, J. B., AND COLD SPRING HARBOR LABORATORY., 1986 *Laboratory course manual for methods in yeast genetics*. Cold Spring Harbor Laboratory, New York, N.Y.

SHIBUYA, T., T. O. TANGE, N. SONENBERG and M. J. MOORE, 2004 eIF4AIII binds spliced mRNA in the exon junction complex and is essential for nonsense-mediated decay. Nat Struct Mol Biol **11:** 346-351.

SHOWMAN, R. M., D. E. WELLS, J. ANSTROM, D. A. HURSH and R. A. RAFF, 1982 Message-specific sequestration of maternal histone mRNA in the sea urchin egg. Proc Natl Acad Sci U S A **79:** 5944-5947.

SIDDIQUI, N., and K. L. BORDEN, 2012 mRNA export and cancer. Wiley Interdiscip Rev RNA **3:** 13-25.

SIEVERS, F., and D. G. HIGGINS, 2014 Clustal Omega, accurate alignment of very large numbers of sequences. Methods Mol Biol **1079:** 105-116.

SINGH, G., A. KUCUKURAL, C. CENIK, J. D. LESZYK, S. A. SHAFFER *et al.*, 2012 The cellular EJC interactome reveals higher-order mRNP structure and an EJC-SR protein nexus. Cell **151:** 750-764.

SMITH, A., A. BROWNAWELL and I. G. MACARA, 1998 Nuclear import of Ran is mediated by the transport factor NTF2. Curr Biol **8:** 1403-1406.

SMITH, A. E., B. M. SLEPCHENKO, J. C. SCHAFF, L. M. LOEW and I. G. MACARA, 2002 Systems analysis of Ran transport. Science **295:** 488-491.

SNAY-HODGE, C. A., H. V. COLOT, A. L. GOLDSTEIN and C. N. COLE, 1998 Dbp5p/Rat8p is a yeast nuclear pore-associated DEAD-box protein essential for RNA export. Embo J **17:** 2663-2676.

SOOD, V., and J. H. BRICKNER, 2014 Nuclear pore interactions with the genome. Curr Opin Genet Dev **25:** 43-49.

SPEESE, S. D., J. ASHLEY, V. JOKHI, J. NUNNARI, R. BARRIA *et al.*, 2012 Nuclear envelope budding enables large ribonucleoprotein particle export during synaptic Wnt signaling. Cell **149:** 832-846.

STAGE-ZIMMERMANN, T., U. SCHMIDT and P. A. SILVER, 2000 Factors affecting nuclear export of the 60S ribosomal subunit in vivo. Mol Biol Cell **11:** 3777-3789.

STALEY, J. P., and C. GUTHRIE, 1998 Mechanical devices of the spliceosome: motors, clocks, springs, and things. Cell **92:** 315-326.

STORY, R. M., H. LI and J. N. ABELSON, 2001 Crystal structure of a DEAD box protein from the hyperthermophile Methanococcus jannaschii. Proc Natl Acad Sci U S A **98:** 1465-1470.

STRAHM, Y., B. FAHRENKROG, D. ZENKLUSEN, E. RYCHNER, J. KANTOR *et al.*, 1999 The RNA export factor Gle1p is located on the cytoplasmic fibrils of the NPC and physically interacts with the FG-nucleoporin Rip1p, the DEAD-box protein Rat8p/Dbp5p and a new protein Ymr 255p. Embo J **18:** 5761-5777.

STRASSER, K., J. BASSLER and E. HURT, 2000 Binding of the Mex67p/Mtr2p heterodimer to FXFG, GLFG, and FG repeat nucleoporins is essential for nuclear mRNA export. J Cell Biol **150:** 695-706.

STRASSER, K., and E. HURT, 2000 Yra1p, a conserved nuclear RNA-binding protein, interacts directly with Mex67p and is required for mRNA export. Embo J **19:** 410-420.

STRASSER, K., and E. HURT, 2001 Splicing factor Sub2p is required for nuclear mRNA export through its interaction with Yra1p. Nature **413:** 648-652.

STRASSER, K., S. MASUDA, P. MASON, J. PFANNSTIEL, M. OPPIZZI *et al.*, 2002 TREX is a conserved complex coupling transcription with messenger RNA export. Nature **417:** 304-308.

STRAUSS, E. J., and C. GUTHRIE, 1991 A cold-sensitive mRNA splicing mutant is a member of the RNA helicase gene family. Genes Dev **5:** 629-641.

STRAWN, L. A., T. SHEN, N. SHULGA, D. S. GOLDFARB and S. R. WENTE, 2004 Minimal nuclear pore complexes define FG repeat domains essential for transport. Nat Cell Biol **6:** 197-206.

STRAWN, L. A., T. SHEN and S. R. WENTE, 2001 The GLFG regions of Nup116p and Nup100p serve as binding sites for both Kap95p and Mex67p at the nuclear pore complex. J Biol Chem **276:** 6445-6452.

STUTZ, F., A. BACHI, T. DOERKS, I. C. BRAUN, B. SERAPHIN *et al.*, 2000 REF, an evolutionary conserved family of hnRNP-like proteins, interacts with TAP/Mex67p and participates in mRNA nuclear export. RNA **6:** 638-650.

STUTZ, F., J. KANTOR, D. ZHANG, T. MCCARTHY, M. NEVILLE *et al.*, 1997 The yeast nucleoporin rip1p contributes to multiple export pathways with no essential role for its FG-repeat region. Genes Dev **11:** 2857-2868.

STUTZ, F., M. NEVILLE and M. ROSBASH, 1995 Identification of a novel nuclear pore-associated protein as a functional target of the HIV-1 Rev protein in yeast. Cell **82:** 495-506.

SUN, C., G. FU, D. CIZIENE, M. STEWART and S. M. MUSSER, 2013 Choreography of importin-alpha/CAS complex assembly and disassembly at nuclear pores. Proc Natl Acad Sci U S A **110:** E1584-1593.

SUN, Y., E. ATAS, L. M. LINDQVIST, N. SONENBERG, J. PELLETIER *et al.*, 2014 Single-molecule kinetics of the eukaryotic initiation factor 4AI upon RNA unwinding. Structure **22:** 941-948.

SVITKIN, Y. V., A. PAUSE, A. HAGHIGHAT, S. PYRONNET, G. WITHERELL *et al.*, 2001 The requirement for eukaryotic initiation factor 4A (elF4A) in translation is in direct proportion to the degree of mRNA 5' secondary structure. RNA **7:** 382-394.

TADDEI, A., G. VAN HOUWE, F. HEDIGER, V. KALCK, F. CUBIZOLLES *et al.*, 2006 Nuclear pore association confers optimal expression levels for an inducible yeast gene. Nature **441:** 774-778.

TAKAHASHI, Y., J. MIZOI, E. A. TOH and Y. KIKUCHI, 2000 Yeast Ulp1, an Smt3-specific protease, associates with nucleoporins. J Biochem **128:** 723-725.

TAN-WONG, S. M., H. D. WIJAYATILAKE and N. J. PROUDFOOT, 2009 Gene loops function to maintain transcriptional memory through interaction with the nuclear pore complex. Genes Dev **23:** 2610-2624.

TEPLOVA, M., L. WOHLBOLD, N. W. KHIN, E. IZAURRALDE and D. J. PATEL, 2011 Structure-function studies of nucleocytoplasmic transport of retroviral genomic RNA by mRNA export factor TAP. Nat Struct Mol Biol **18:** 990-998.

TERRY, L. J., E. B. SHOWS and S. R. WENTE, 2007 Crossing the nuclear envelope: hierarchical regulation of nucleocytoplasmic transport. Science **318:** 1412-1416.

TERRY, L. J., and S. R. WENTE, 2007 Nuclear mRNA export requires specific FG nucleoporins for translocation through the nuclear pore complex. J Cell Biol **178:** 1121-1132.

TERRY, L. J., and S. R. WENTE, 2009 Flexible gates: dynamic topologies and functions for FG nucleoporins in nucleocytoplasmic transport. Eukaryot Cell **8:** 1814-1827.

TETENBAUM-NOVATT, J., L. E. HOUGH, R. MIRONSKA, A. S. MCKENNEY and M. P. ROUT, 2012 Nucleocytoplasmic transport: a role for nonspecific competition in karyopherin-nucleoporin interactions. Mol Cell Proteomics **11:** 31-46.

TEXARI, L., G. DIEPPOIS, P. VINCIGUERRA, M. P. CONTRERAS, A. GRONER *et al.*, 2013 The nuclear pore regulates GAL1 gene transcription by controlling the localization of the SUMO protease Ulp1. Mol Cell **51:** 807-818.

THEISSEN, B., A. R. KAROW, J. KOHLER, A. GUBAEV and D. KLOSTERMEIER, 2008 Cooperative binding of ATP and RNA induces a closed conformation in a DEAD box RNA helicase. Proc Natl Acad Sci U S A **105:** 548-553.

TIEG, B., and H. KREBBER, 2013 Dbp5 - from nuclear export to translation. Biochim Biophys Acta **1829:** 791-798.

TIMNEY, B. L., J. TETENBAUM-NOVATT, D. S. AGATE, R. WILLIAMS, W. ZHANG *et al.*, 2006 Simple kinetic relationships and nonspecific competition govern nuclear import rates in vivo. J Cell Biol **175:** 579-593.

TOOMRE, D., and J. BEWERSDORF, 2010 A new wave of cellular imaging. Annu Rev Cell Dev Biol **26:** 285-314.

TOPISIROVIC, I., N. SIDDIQUI, V. L. LAPOINTE, M. TROST, P. THIBAULT *et al.*, 2009 Molecular dissection of the eukaryotic initiation factor 4E (eIF4E) export-competent RNP. Embo J **28:** 1087-1098.

TORETSKY, J. A., and P. E. WRIGHT, 2014 Assemblages: functional units formed by cellular phase separation. J Cell Biol **206:** 579-588.

TOYAMA, B. H., J. N. SAVAS, S. K. PARK, M. S. HARRIS, N. T. INGOLIA *et al.*, 2013 Identification of long-lived proteins reveals exceptional stability of essential cellular structures. Cell **154:** 971-982.

TRAN, E. J., Y. ZHOU, A. H. CORBETT and S. R. WENTE, 2007 The DEAD-box protein Dbp5 controls mRNA export by triggering specific RNA:protein remodeling events. Mol Cell **28:** 850-859.

TSENG, S. S., P. L. WEAVER, Y. LIU, M. HITOMI, A. M. TARTAKOFF *et al.*, 1998 Dbp5p, a cytosolic RNA helicase, is required for poly(A)+ RNA export. Embo J **17:** 2651-2662.

TUCK, A. C., and D. TOLLERVEY, 2013 A transcriptome-wide atlas of RNP composition reveals diverse classes of mRNAs and lncRNAs. Cell **154:** 996-1009.

UBERSAX, J. A., E. L. WOODBURY, P. N. QUANG, M. PARAZ, J. D. BLETHROW *et al.*, 2003 Targets of the cyclin-dependent kinase Cdk1. Nature **425:** 859-864.

VASSILEVA, M. T., and M. J. MATUNIS, 2004 SUMO modification of heterogeneous nuclear ribonucleoproteins. Mol Cell Biol **24:** 3623-3632.

VON MOELLER, H., C. BASQUIN and E. CONTI, 2009 The mRNA export protein DBP5 binds RNA and the cytoplasmic nucleoporin NUP214 in a mutually exclusive manner. Nat Struct Mol Biol **16:** 247-254.

WALDE, S., and R. H. KEHLENBACH, 2010 The Part and the Whole: functions of nucleoporins in nucleocytoplasmic transport. Trends Cell Biol **20:** 461-469.

WANG, S., Y. HU, M. T. OVERGAARD, F. V. KARGINOV, O. C. UHLENBECK *et al.*, 2006 The domain of the Bacillus subtilis DEAD-box helicase YxiN that is responsible for specific binding of 23S rRNA has an RNA recognition motif fold. RNA **12:** 959-967.

WANG, Y., and M. DASSO, 2009 SUMOylation and deSUMOylation at a glance. J Cell Sci **122:** 4249-4252.

WARNER, J. R., 1999 The economics of ribosome biosynthesis in yeast. Trends Biochem Sci **24:** 437-440.

WATKINS, J. L., R. MURPHY, J. L. EMTAGE and S. R. WENTE, 1998 The human homologue of Saccharomyces cerevisiae Gle1p is required for poly(A)+ RNA export. Proc Natl Acad Sci U S A **95:** 6779-6784.

WEIRICH, C. S., J. P. ERZBERGER, J. M. BERGER and K. WEIS, 2004 The N-terminal domain of Nup159 forms a beta-propeller that functions in mRNA export by tethering the helicase Dbp5 to the nuclear pore. Mol Cell **16:** 749-760.

WEIRICH, C. S., J. P. ERZBERGER, J. S. FLICK, J. M. BERGER, J. THORNER *et al.*, 2006 Activation of the DExD/H-box protein Dbp5 by the nuclear-pore protein Gle1 and its coactivator InsP6 is required for mRNA export. Nat Cell Biol **8:** 668-676.

WELLINGER, R. E., F. PRADO and A. AGUILERA, 2006 Replication fork progression is impaired by transcription in hyperrecombinant yeast cells lacking a functional THO complex. Mol Cell Biol **26:** 3327-3334.

WELLS, S. E., P. E. HILLNER, R. D. VALE and A. B. SACHS, 1998 Circularization of mRNA by eukaryotic translation initiation factors. Mol Cell **2:** 135-140.

WENTE, S. R., and G. BLOBEL, 1993 A temperature-sensitive NUP116 null mutant forms a nuclear envelope seal over the yeast nuclear pore complex thereby blocking nucleocytoplasmic traffic. J Cell Biol **123:** 275-284.

WENTE, S. R., and M. P. ROUT, 2010 The nuclear pore complex and nuclear transport. Cold Spring Harb Perspect Biol **2:** a000562.

WERNER, A., A. FLOTHO and F. MELCHIOR, 2012 The RanBP2/RanGAP1*SUMO1/Ubc9 complex is a multisubunit SUMO E3 ligase. Mol Cell **46:** 287-298.

WEST, M., J. B. HEDGES, A. CHEN and A. W. JOHNSON, 2005 Defining the order in which Nmd3p and Rpl10p load onto nascent 60S ribosomal subunits. Mol Cell Biol **25:** 3802-3813.

WILHELM, M., J. SCHLEGL, H. HAHNE, A. MOGHADDAS GHOLAMI, M. LIEBERENZ *et al.*, 2014 Mass-spectrometry-based draft of the human proteome. Nature **509:** 582-587.

WINDGASSEN, M., and H. KREBBER, 2003 Identification of Gbp2 as a novel poly(A)+ RNA-binding protein involved in the cytoplasmic delivery of messenger RNAs in yeast. EMBO Rep **4:** 278-283.

WINDGASSEN, M., D. STURM, I. J. CAJIGAS, C. I. GONZALEZ, M. SEEDORF *et al.*, 2004 Yeast shuttling SR proteins Npl3p, Gbp2p, and Hrb1p are part of the translating mRNPs, and Npl3p can function as a translational repressor. Mol Cell Biol **24:** 10479-10491.

WINZELER, E. A., D. D. SHOEMAKER, A. ASTROMOFF, H. LIANG, K. ANDERSON *et al.*, 1999 Functional characterization of the S. cerevisiae genome by gene deletion and parallel analysis. Science **285:** 901-906.

WOHLSCHLEGEL, J. A., E. S. JOHNSON, S. I. REED and J. R. YATES, 3RD, 2004 Global analysis of protein sumoylation in Saccharomyces cerevisiae. J Biol Chem **279:** 45662-45668.

WU, H., D. BECKER and H. KREBBER, 2014 Telomerase RNA TLC1 shuttling to the cytoplasm requires mRNA export factors and is important for telomere maintenance. Cell Rep **8:** 1630-1638.

WYKOFF, D. D., and E. K. O'SHEA, 2005 Identification of sumoylated proteins by systematic immunoprecipitation of the budding yeast proteome. Mol Cell Proteomics **4:** 73-83.

XU, D., A. FARMER and Y. M. CHOOK, 2010 Recognition of nuclear targeting signals by Karyopherin-beta proteins. Curr Opin Struct Biol **20:** 782-790.

XU, X. M., A. ROSE, S. MUTHUSWAMY, S. Y. JEONG, S. VENKATAKRISHNAN *et al.*, 2007 NUCLEAR PORE ANCHOR, the Arabidopsis homolog of Tpr/Mlp1/Mlp2/megator, is involved in mRNA export and SUMO homeostasis and affects diverse aspects of plant development. Plant Cell **19:** 1537-1548.

YAMADA, J., J. L. PHILLIPS, S. PATEL, G. GOLDFIEN, A. CALESTAGNE-MORELLI *et al.*, 2010 A bimodal distribution of two distinct categories of intrinsically disordered structures with separate functions in FG nucleoporins. Mol Cell Proteomics **9:** 2205-2224.

YANG, Q., M. DEL CAMPO, A. M. LAMBOWITZ and E. JANKOWSKY, 2007 DEAD-box proteins unwind duplexes by local strand separation. Mol Cell **28:** 253-263.

YANG, Q., and E. JANKOWSKY, 2005 ATP- and ADP-dependent modulation of RNA unwinding and strand annealing activities by the DEAD-box protein DED1. Biochemistry **44:** 13591-13601.

YANG, W., J. GELLES and S. M. MUSSER, 2004 Imaging of single-molecule translocation through nuclear pore complexes. Proc Natl Acad Sci U S A **101:** 12887-12892.

YANG, W., and S. M. MUSSER, 2006 Nuclear import time and transport efficiency depend on importin beta concentration. J Cell Biol **174:** 951-961.

YAO, W., D. ROSER, A. KOHLER, B. BRADATSCH, J. BASSLER *et al.*, 2007 Nuclear export of ribosomal 60S subunits by the general mRNA export receptor Mex67-Mtr2. Mol Cell **26:** 51-62.

YARBROUGH, M. L., M. A. MATA, R. SAKTHIVEL and B. M. FONTOURA, 2014 Viral subversion of nucleocytoplasmic trafficking. Traffic **15:** 127-140.

YOON, J. H., S. SRIKANTAN and M. GOROSPE, 2012 MS2-TRAP (MS2-tagged RNA affinity purification): tagging RNA to identify associated miRNAs. Methods **58:** 81-87.

YORK, J. D., A. R. ODOM, R. MURPHY, E. B. IVES and S. R. WENTE, 1999 A phospholipase C-dependent inositol polyphosphate kinase pathway required for efficient messenger RNA export. Science **285:** 96-100.

YOUNG, C. L., S. KHOSHNEVIS and K. KARBSTEIN, 2013 Cofactor-dependent specificity of a DEAD-box protein. Proc Natl Acad Sci U S A **110:** E2668-2676.

ZEITLER, B., and K. WEIS, 2004 The FG-repeat asymmetry of the nuclear pore complex is dispensable for bulk nucleocytoplasmic transport in vivo. J Cell Biol **167:** 583-590.

ZEMP, I., and U. KUTAY, 2007 Nuclear export and cytoplasmic maturation of ribosomal subunits. FEBS Lett **581:** 2783-2793.

ZENKLUSEN, D., and F. STUTZ, 2001 Nuclear export of mRNA. FEBS Lett **498:** 150-156.

ZENKLUSEN, D., P. VINCIGUERRA, Y. STRAHM and F. STUTZ, 2001 The yeast hnRNP-Like proteins Yra1p and Yra2p participate in mRNA export through interaction with Mex67p. Mol Cell Biol **21:** 4219-4232.

ZENKLUSEN, D., P. VINCIGUERRA, J. C. WYSS and F. STUTZ, 2002 Stable mRNP formation and export require cotranscriptional recruitment of the mRNA export factors Yra1p and Sub2p by Hpr1p. Mol Cell Biol **22:** 8241-8253.

ZHAO, J., S. B. JIN, B. BJORKROTH, L. WIESLANDER and B. DANEHOLT, 2002 The mRNA export factor Dbp5 is associated with Balbiani ring mRNP from gene to cytoplasm. Embo J **21:** 1177-1187.

ZHAO, Q., Y. XIE, Y. ZHENG, S. JIANG, W. LIU *et al.*, 2014 GPS-SUMO: a tool for the prediction of sumoylation sites and SUMO-interaction motifs. Nucleic Acids Res **42:** W325-330.

ZHAO, R., J. SHEN, M. R. GREEN, M. MACMORRIS and T. BLUMENTHAL, 2004a Crystal structure of UAP56, a DExD/H-box protein involved in pre-mRNA splicing and mRNA export. Structure **12:** 1373-1381.

ZHAO, X., C. Y. WU and G. BLOBEL, 2004b Mlp-dependent anchorage and stabilization of a desumoylating enzyme is required to prevent clonal lethality. J Cell Biol **167:** 605-611.